# bio-host glass:

A recycled porous glass foam, developed for bioreceptive applications in the urban environment.

Georgina Giassia

# Acknowledgements

During this very special journey a 'thank you' note, to all the people that have contributed to enrich this experience, expresses my gratitude as a promise for the many new ones to come.

To begin with, I would like to show my deep appreciation to my 1st mentor in this project, Telesilla Bristogianni, who greatly contributed with her expertise to my original vision. I am deeply thankful, for the moments we had together brainstorming about the glass recipes and the findings, together with the coaching sessions for presenting such scientific subjects. Acquiring this deeper knowledge for the world of 'porous glass' would not have been possible without working with her in the Glass lab of TU Delft.

During stressful times, that I would question the feasibility and significance of my own subject, Marcel Bilow was always encouraging and resourceful in suggesting 'other ways to show how smart this idea is and the potential about this project'. Despite the fact that material science took over this thesis, and the part of the product development has yet a long way to go after graduation, I am grateful for the opportunity that he gave me to be seen as an 'expert' during the Bucky lab studio, with the knowledge I acquired by designing and conducting my own experimental process for the very first time on bioreceptive glass foam.

Last but not least in my mentoring team, I would like to give a special thanks to Faidra Oikonomopoulou, who by having the role of the stricter judge in my presentations, made me strengthen my argumentation and belief in my topic. Her work together with Telesilla Bristogianni has been very inspirational for many students in my year, and a driving force to delve deeper into the 'glass world.'

I also thank my fellow lab-mates Isidora Matskidou and Anna-maria Koniari, for being supportive even at our 'darkest' moments and most importantly for making all the hard work enjoyable! This last semester that was everything but normal, would not have been as fun and rewarding as it was in its every single moment, without firstly my flat mates Alex Coelho and Thomas Lindemann, and then all of my friends in Delft and in Athens, for their relentless support, no matter the distance.

Finally, I thank the unseen hero of my life, my mother. Relentlessly, she has supported me to pursue all my dreams and ambitions. I am so grateful for having her as a role model, for how strong and powerful she is and the way she has taught me to move forward no matter the difficulties that may arise.

Georgina Giassia

5382777

Msc Architecture, Urbanism & Building Sciences
(Building Technology track)

Graduation Thesis

Ir Telesilla Bristogianni (1st Mentor)

Dr.-Ing.Marcel Bilow (2nd Mentor)

Dr. Faidra Oikonomopoulou (3rd Mentor)

Delft University of Technology

June 2022

# Abstract

Keywords: glass foam, bioreceptivity, open-porosity, hydraulic properties, wind-driven rain, facade

Dense urbanization increases the demand on the building sector who is responsible, on the one hand for producing large amounts of landfilled glass waste, and on the other for consuming the earth's natural resources and release additional $CO_2$ emissions, for the manufacture of new architectural glass. These unfavorable conditions together with the already apparent effects of climate change, demand resourceful solutions for adaptive and resilient cities, that utilize current waste and require low maintenance and low costs, to be implemented universally.

This, can only be ensured by letting nature to take over. Unexploited urban facades have a key role to provide this new ground that can be colonized by microorganisms, creating a microclimate by forming an outer green layer growing on its own. Aiming this, materials covering our urban facades need to be transformed to porous hosts by retaining rainwater and providing the right environment for bio-growth to take place.

This research aims to discover new ways that unutilized glass waste can be upcycled into bioreceptive applications, that form a promising set of criteria. By shedding light firstly on the specific material properties needed, the method of glass foaming is chosen to be investigated, as the mean to provide an open porous network for retaining water, by incorporating large amounts of waste into its recipe.

An experimental approach has been designed, to explore the parameters related to the mixture, manufacturing process affecting the glass foam's microstructure and potential biofilm formation, by producing a total of 22 samples in the Glass lab in Stevin lab, TU Delft. These specimens were not foamed at once, but gradually being tested first of all, microscopically, to reveal the porosity network and secondly, with a series of quick tests related to their hydraulic performance, providing feedback for the next batch of samples regarding the most promising recipes to be further explored. All the samples were tested for their water absorption, evaporation rate and frosting resistance, while only the higher-scored specimens were put under test for moss-growth and compressive strength.

Apart from the experimental analysis, the next steps towards a product development were also explored by setting the bioreceptive design principles for manufacturing the meso-scale surface. Limitations in adjusting these guidelines to the way glass-foam is produced are addressed with possible solutions as suggestions for further experimentation. In addition, an application catalogue was composed as schematic recommendations to showcase the potential of bio-host glass. Combining this idea to the material science, these applications were also approached from an engineering view to analyze the material properties' specific demands per product. This tool, can prove to be beneficial both in the hands of the future designer and material researcher to have a starting point on what needs to be further developed, depending on the chosen product out of bioreceptive glass-foam.

Taking the most immediately feasible example of a façade tile, based on the findings of the aforementioned analysis, during the last part of this project, a methodology for designing and implementing the new material into the urban environment is proposed. By informing the design of the macro-scale with weather data, precipitation levels can be exploited, in order to provide the maximum water content for the benefit of bioreceptivity.

Therefore, the novelty of this thesis, aspires by providing a holistic approach, based on the knowledge obtained both in the literature review and the conducted experiments, to stir not only bio-growth on our cities, but also innovative thinking and exploration on ways to combat the increasing landfill waste.

# Contents

## 1.1. Introduction

This research focuses on the exploration of an idea for the development of a new product, merely by tackling simultaneously two immense problems that the world faces. Climate change on the one hand and material waste on the other, demand a major change on the way we live, that cannot happen over a night. To combat such problems there are two kinds of solutions: the ones that mitigate the problem and the rest that aids to adjust on the new establishing circumstances.

The great risk human race and natural systems undergo, has been constantly outlined and reported. To name a few examples that illustrate the emergency, according to the Intergovernmental panel on climate change of IPCC across the world, changing precipitation, melting snow and ice, together cause changes to the hydrological systems, meaning that the water resources deteriorate in quantity and quality. In the land areas, negative impacts on crop yields have also been reported together with entire species extinctions leading to an overall land degradation affecting the general balance, together with shifts on migration patterns of species (Field et al., 2014). Thus, the need for implementation of both mitigation and adjusting strategies is explicit by now. Exploring materials that ameliorate the unfavorable urban conditions, by forming a habitable microclimate locally, while at the same time combatting climate change globally, can be an efficient solution part of such strategies. For this reason, the building sector with its vast energy and material consumption as well as waste production, constitutes a meaningful field to take action by applying material innovations that alter the way we think and build.

The emerging term of bioreceptivity in façade cladding materials, even though as a concept exists for more than 25 years now, it was previously seen only as a negative phenomenon. Its direct link to materials' degradation, especially in monumental constructions colonized from microorganisms and plants as time passed by forming ecosystems on their own, has been extensively studied (Gaylarde et al., 2006; Guiamet et al., 2019; Jurado et al., 2014; Mondo et al., 2018; Mustafa & Ahmet, 2015). However, as the need for greening our cities becomes more and more urgent (Croce & Vettorato, 2021), resourceful solutions, such as covering with algae or moss unused opaque surfaces in our urban environment, are growing popularity.

When the value of a new product is being discussed, apart from the application that will define its place in the market, also its environmental impact is of utmost importance. Since, in the past years of industrial evolution, the prevailing linear model of producing and consuming was the only known way, by manufacturing products – selling them – using them until their end of life and then just discarding them in the landfill. Nowadays, to reverse this and establish a circular economy that promotes the use of fewer sources, material stored in the existing products have to be exploited, in order to lower the environmental impact and become independent of volatile markets based on natural resources (Velden, 2020).

Therefore, for this study the driving force for innovation is to create an alternative that is not only sustainable, but also makes use of materials that have no purpose and end up in the landfill. Hence, the importance of defining the potential of already known and widely used construction materials that are repurposed, for bioreceptivity is explicit. In the following sections, first and foremost the problem statement, the objectives of the research, as well as the research question and sub-questions are going to be analyzed. Then, the methodology to approach the complexity of such an issue, from the stage of the concept validation through the argumentation building based on the findings of the literature review, and finally the experimental research to draw conclusions upon the parameters under investigation, is going to be presented. Finally, the results of literature review are going to be organized in two main chapters in immediate relation with the topics answering the research question and sub-questions.

## 1.2. Problem Statement

As briefly mentioned in the introduction, the general problem of climate emergency and accumulative material waste, form the starting point of this study. Both problems are linked to population growth, which by 2050 over 68% will be living in urban megacities, an increase of 2.5 billion people leaving marginal space for green areas. The consequences will be obvious in multiple fields: air & water pollution, extremer temperatures due to the increase of the urban heat island effect stress and extinction of biodiversity (Veeger et al., 2021). Many sources, including the Rotterdam Climate Change Adaptation Strategy (Municipality of Rotterdam, 2013) highlight the importance of growing the green & blue network in big cities, that already suffer from warmer summers and severe rainfalls. This, entails green roofs & facades that contribute to the alleviation of the effects of climate change in multiple levels (Veeger et al., 2021). Hence, engineering bioreceptivity in favor of the urban environment and the building envelope is the chosen focus in this specific research, that answers the aforementioned problems.

But how do we engineer bioreceptivity and what are the optimum characteristics from the material aspect, as well as the environment where it applies? And more importantly, out of what material and in what form or shape, should we manufacture the substrate that hosts the bio-growth, unlocking all the desired benefits for the urban microclimate? Despite the difficulty of these questions at first sight, from the literature review, the conditions for bioreceptivity are thoroughly analysed, for the mere purpose to understand this phenomenon and prevent it, since its negative connotation was prevailing until now. For this reason, it is fully justified why stone is the most researched material, due to its wide application in monumental construction (D'Orazio et al., 2014). Specifically, literature evidence is focused on algae and -cyanobacteria stains on rock surfaces and concrete walls [*(Barberousse et al., 2006)- in France, (Dubosc et al., 2001; Escadeillas et al., 2007; Escadeillas et al., 2009; Miller et al., 2012) - for stone, (Mustafa & Ahmet, 2015)- in Turkey, (Mondo et al., 2018)- in Italy, (Veeger et al., 2021)- bioreceptive concrete manufacture in the Netherlands*], some on lichens colonizing monuments [*(Gaylarde et al., 2006)- on limestone, (Matteucci et al., 2019)- on rock monuments), or fungi [(Tanaca et al., 2011)- on cement, (Somayeh et al., 2017)- on paper*], and a few on clay bricks and mortars [*(D'Orazio et al., 2014; Lubelli et al., 2021)*].

However, about glass – being one of the most commonly-used and preferred materials in construction by architects and designers – there is limited research. This literature gap in combination with experimental research, conducted in the Glass & Transparency department of TUDelft, on casting glass waste, revealing foam structures that have potential for bioreceptivity, form an extremely promising opportunity to investigate this topic even further having the aim to provide a solution that enhances the closed-loop recycling of glass.

Since, the consequential waste production of human activities is one of the focus of discussions in view of the new sustainability goals, waste management experts emphasize the potential of recycling and incineration, to eliminate as much as possible landfilling. Although both of these methods to some extent generate lower-quality products, further testing and experiments can bring new innovations to light (Velden, 2020). Zooming in the glass industry and its waste flow, Europe is responsible for producing glass of approximately one third of the total world - equal in 38 million tons of glass waste every year. Thus, a more sustainable waste management (Anagni et al., 2020) encourage initiatives to change the way we produce glass products today.

Bioreceptive glass can be a valuable solution for tackling major problems both related to mitigating the effects of climate change and combating the rapidly increasing amounts of material waste. The key advantage in this strategy, are the properties for bioreceptivity that are mandatory to be met.

Particularly, hydraulic properties related to open porosity, water absorption and surface roughness in every other recipe scheme for recycling any type of glass would constitute a major limitation and therefore characterized as a flaw. In this case, these undesirable characteristics from already-conducted experimental work are seen as a potential for further investigation for a new application in the building industry that favours bio-growth. Hence, the aim of engineering porosity in the microstructure and surface of the material, produced by waste, can provide a whole new spectrum of fully sustainable applications, not only for the building envelope, but also for the urban environment.

## 1.3. Objectives

The objectives of this research as indicated by the title itself, aim to give a second life on glass products that after their end of life end up in landfill, due to lack of applications for their recycled recipes and form. Therefore, having identified this market niche and by exploiting the criteria for a material to be bioreceptive, this new product should:

- use glass recipes that remain unutilized until today,
- be manufactured by the optimum process regarding the environmental impact (relation of temperature and time),
- constitute a competitive solution, by being more sustainable from other related products,
- be specifically defined on its application potential based on its material properties (compressive strength, durability, etc.).
- be designed for optimum bio-growth,
- be applied with circularity principles ensuring reversibility, or continuous recycling (closed-loop product recycling).

## 1.4. Research question and sub-questions

According to the aforementioned problems and concerns, as well as the demand for new market applications that tackle them, the main research question could be formulated as followed:

**‘How can porous glass be manufactured out of glass waste to obtain bioreceptivity and which are the possible applications for this new product?’**

The research question can be further analyzed to sub-questions derived from:

1) its general concept and feasibility:
    - What is bioreceptivity and what are the general conditions and material properties that characterize a bioreceptive substrate?
    - What type of plants or microorganisms are involved in this phenomenon?
    - Can glass become a bioreceptive material?
2) the assessment of bioreceptivity:
    - How do we assess bioreceptivity?
    - What are the optimum values for green coverage that should the material under experimentation obtain, compared to the other bioreceptive examples?
3) boosting bioreceptivity potential:
    - How can the bioreceptive potential of a substrate be increased?
    - If water absorption and retention is the answer, how can we achieve better hydraulic properties for the material under investigation?
    - If porosity is the answer, what type of porosity is ideal?
4) choosing the right recipe for glass waste and production method:
    - How can we produce this type of porosity in glass foam?
    - What types of glass waste could facilitate the manufacturing of the above porosity?
    - What is the most efficient and environmental-friendly manufacturing method for porous glass?
5) the resulted product:
    - What are the material properties? (density, porosity, compressive strength)
    - What are the limitations based on its properties?
6) the possible applications for this material:
    - What current products could it replace as a better solution?
    - What new applications could it offer?

Compiling all the questions above, it is evident that not all of them can be answered only by the literature review. What is also going to be explained in the methodology afterwards, is that the knowledge coming from the research based on the sources, is going to give feedback for the experiments afterwards, which in turn are going to give tangible answers to the questions described above. Due to the experimental nature of the project and the level of innovation, there is an additional set of sub-questions targeted on the material properties that need to be investigated only through lab-testing.

In detail: How does the water move into foam glass? Does it stay on the surface because of the existence of a closed-pore network? Or can it be sucked deeper into the material by a coarse-pore network, favoring water retention? Is the microstructure of glass composed only from closed pores, rendering water capillarity impossible, or is there a way to modify this property? How can we produce foam glass with open-pore network? In the case we cannot, do glass foams with closed pores present adequate hydraulic properties for bioreceptivity? Can the loss of water capillarity be mitigated with another way? Can the moisture content of certain environments in combination with the surface roughness of the substrate provide a satisfactory combination as an alternative? Is the final product more sustainable than the prevailing ones, like concrete?

## 1.5. Methodology Overview

The methodology that is outlined to be followed for this research is a combination of three research methods. In the first part, during the literature review, knowledge through the gathered information is going to be obtained by answering the sub-questions. Then, certain assumptions are formed related to the research question, which by experimental research are validated. What's more, due to lacking literature sources, in this second part specific sub-questions are answered by comparing the results of the lab experiments. While, in the third and final method, the most promising results of the previous are illustrated in a case-study showing the design and construction implementation of the developed material (Fig. 1).

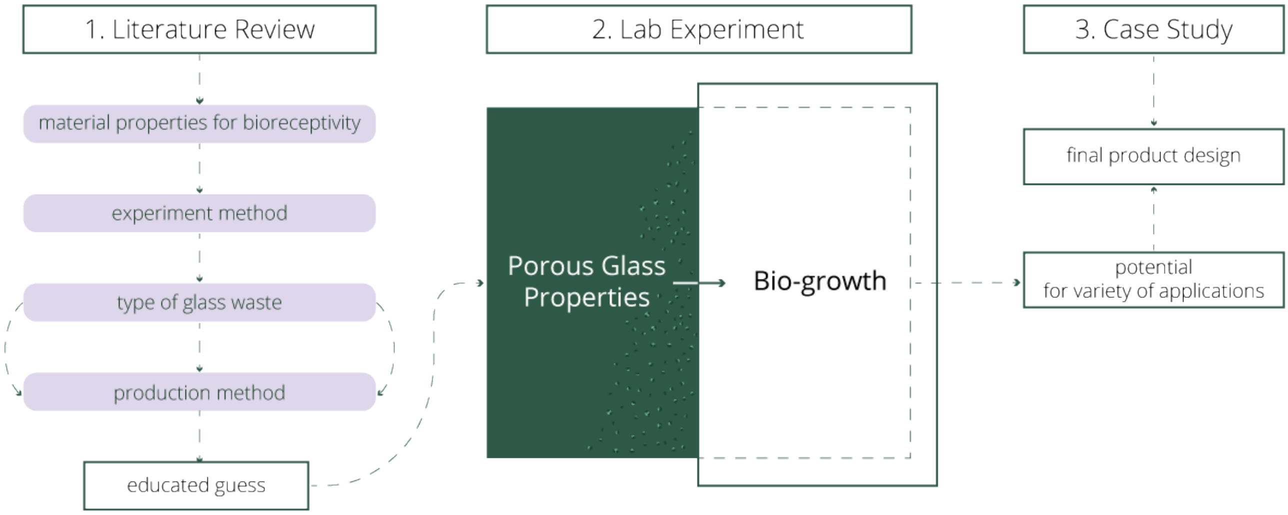


Figure 1. General Flowchart showcasing the connections of the three different methods of research.

During the first part, knowledge is gained in the form of theory that is later being tested for validation. This, focuses on the subjects of: bioreceptivity, learning how to test it, current applications, ways to achieve porosity in glass, unutilized glass waste sources and foam glass production method. Out of this, by identifying the optimum conditions for a bioreceptive material both in the environment and most importantly in the material itself, a detailed list of bioreceptive criteria are created, so as to investigate the way these can be obtained for the new product. Then, from the review of experimental work and current innovations related to glass recycling, evidence is sought to form an educated guess that was also validated through the experimental research. Hence, two very distinctive subjects – bioreceptivity & glass recycling – are investigated, while informing each other for the common goal of being combined.

Inside the lab, first and foremost the production method for porous glass was studied, in regards of three main parameters: (1) the glass recipe (type of waste and additives), (2) the powder/particle size and (3) the temperature for foaming/firing based on the findings from foaming methods and kiln-casting. In the next step, the created samples, were measured for their material properties: (1) density, (2) surface roughness, (3) porosity, (4) water absorption and (5) compressive strength. Then, the most promising set of the samples was tested for bioreceptivity with accelerating the microorganisms' growth in a controlled environment, with adequate water content. Research has shown that an accelerated test can provide results in 25 days, while the regular growth needs at least twice that time (Escadeillas et al., 2007; Escadeillas et al., 2009). By comparing these results, conclusions are drawn for the potential of the material application, mapping its advantages and limitations. Hence, choosing an application to illustrate the effect of a bioreceptive porous glass is mandatory, to address all the possible points of attention or for future research for this new product.

What's more, during the porosity testing from the Figure 3, not only the porosity in terms of density

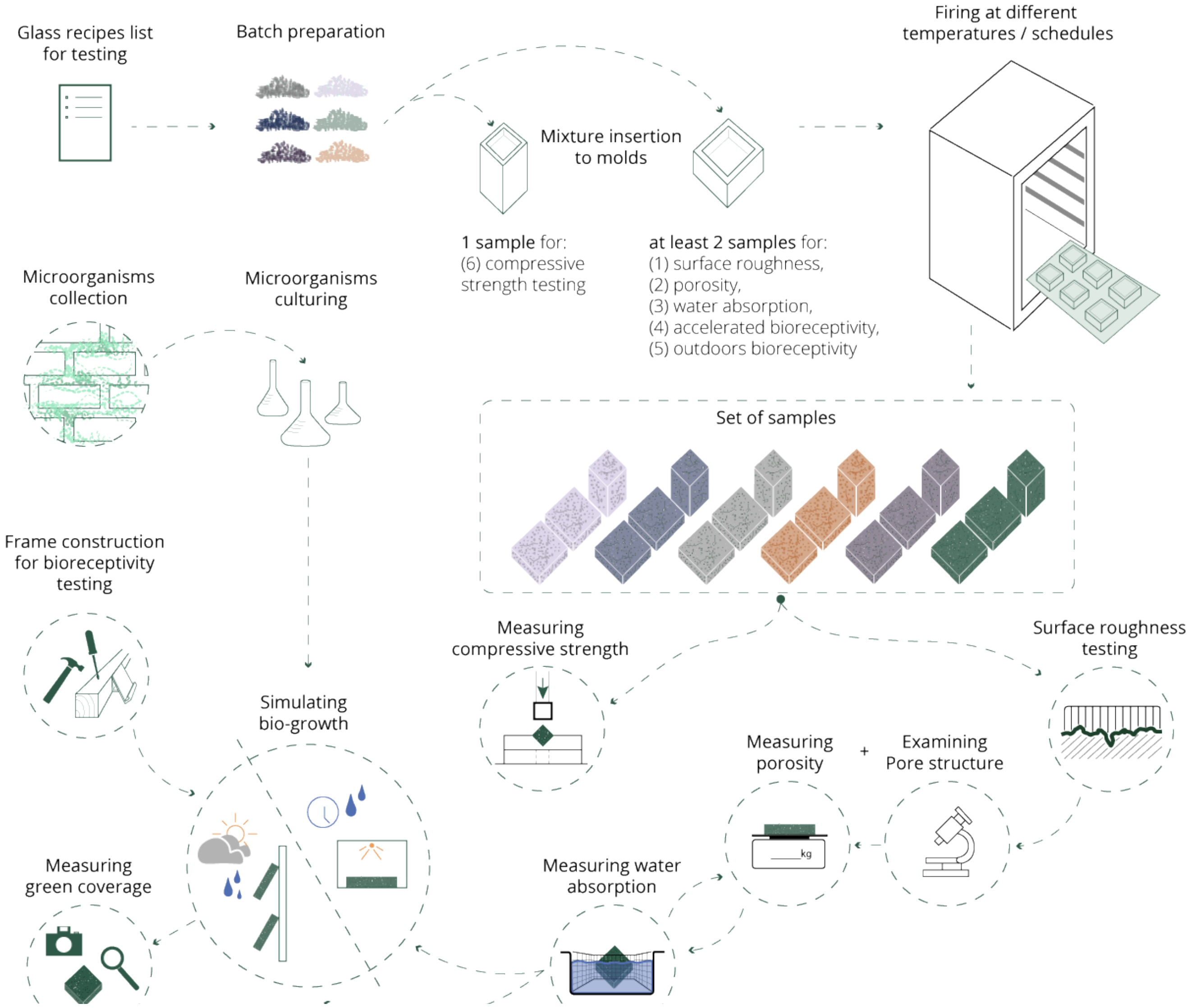


Figure 2. Infographic describing the 2nd part of the methodology – the experimental analysis – where the different samples are going to be tested for their properties and bioreceptivity potential.

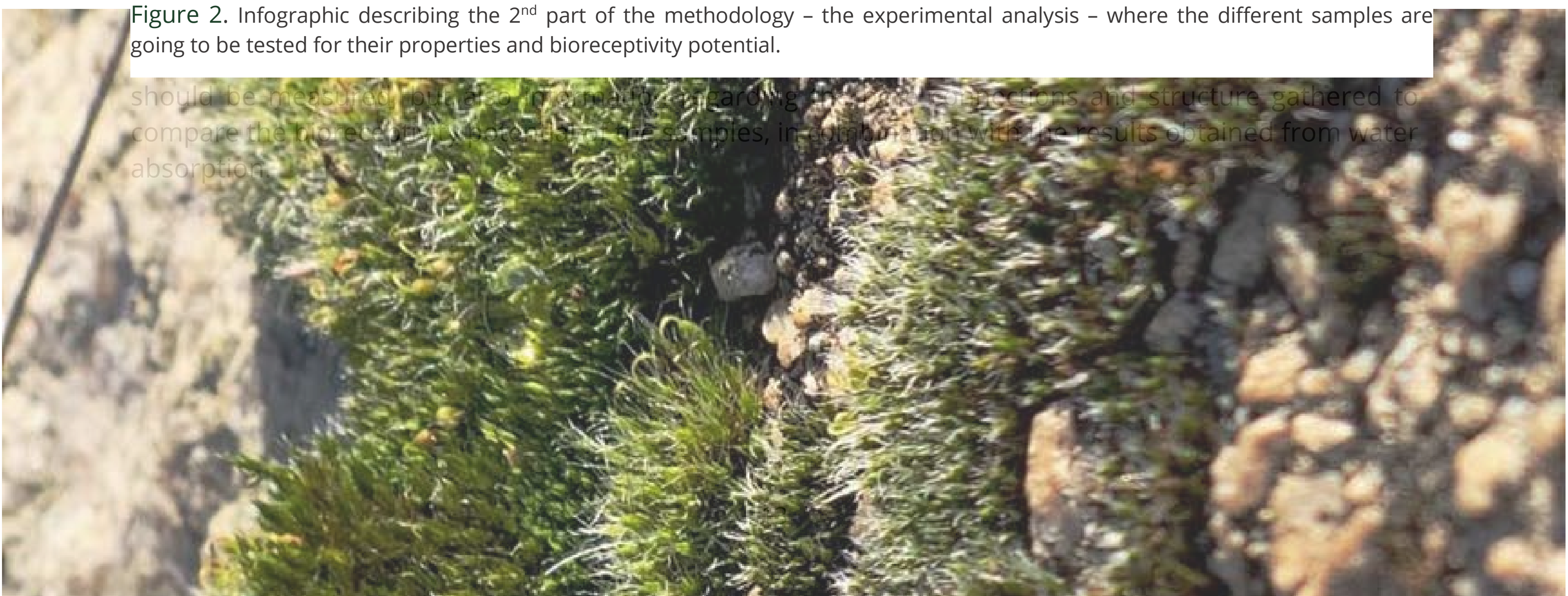

should be measured, but also information regarding the pores' connections and structure gathered to compare the bioreceptivity potential of the samples, in combination with the results obtained from water absorption.

# 2. Literature Research

## 2.1. Global challenge: Climate Change

### 2.1.1. Definition & Benefits of bioreceptivity

In the work of Barberousse H. et al. (2006), it is mentioned that: ''Biofouling of surfaces is a phenomenon which takes place in a large range of ecosystems, either aquatic or terrestrial. The biofilm formed by microorganism colonization will be more or less complex depending on the characteristics of the substratum, and the way it protects itself or is protected.'' In other words, bioreceptivity is a natural phenomenon associated with the 'ability of the material to be colonized by microorganisms' (Guillitte, 1995), when exposed to the environment and under certain criteria which are explained in detail in the following paragraphs. It is interesting to look at the origins of this idea mentioned by Miller et al. (2012), which is related to the term ''susceptibility'', used both in medicine and heritage studies, defining an organism's proneness level to host a multiplying pathogen but without being harmed. Hence, the birth of the term bioreceptivity linked the substrate surface as a host to microorganisms with an ecological meaning

To the above, it must be added that "the totality of material properties contributing to the establishment, anchorage and development of fauna and/or flora" form holistically the concept of bioreceptivity (Guillitte, 1995). When talking about materials used in the building envelope, due to their exposure to the environment, it is crucial to determine the factors that will affect their performance, even if they cannot be fully predicted, so that our designs are informed to the best way possible.

Thus, Guillitte (1995) suggested three types of bioreceptivity to better help understanding this phenomenon. Firstly, the "primary or intrinsic", referred to the earliest form of bio-colonization, secondly, the "secondary bioreceptivity", which is already linked to the microorganisms' growth on decaying materials, and thirdly, the "tertiary bioreceptivity", related to materials that have deteriorated even more and are subjected to maintenance treatments. Apart from these, there are also extrinsic factors, that affect the plants' type and growth. For this reason, in such cases bioreceptivity is characterized as extrinsic or semi-extrinsic, when dust particles or soil are collected either on the material or the biofilm itself, resulting in a multiplying colonized community. For instance, once the microorganisms appear, more and more piling nutrition can be observed by bacteria and fungi, that later on this, can lead to soil accumulation attracting insects and birds, therefore forming new flora and biodiversity. The wind also contributes to this growth by transferring seeds, where depending on the surface geometry or roughness and the gradual appearance of cracks, even rooted sprouts can start developing (Mustafa & Ahmet, 2015).

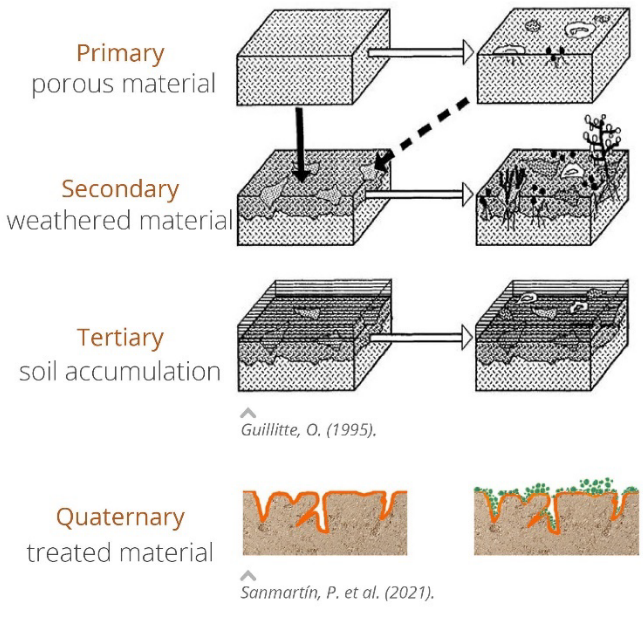


Figure 3. Bioreceptivity types depending on the state of the substrate material. These can all take place as a dynamic process attributed to the natural weathering, as the material deteriorates biofilm takes over with even more species. Image Source: Guillitte O. (1995) & Sanmartin P. et al. (2021).

However, for the scope of this paper that the aim is to study the material properties favoring colonization, the third type of tertiary, followed by extrinsic and semi-extrinsic bioreceptivity describing mainly the deposit of other substances on the material leading even to the growth of higher plants, should not be considered. Because the focus is on how to enhance the biofilm development, by altering the material properties, these exogenous factors, taking place at any possible material with surface impurities, inclination or 'pockets', should be excluded.

As Lubelli B. et al. (2021) mentions such a phenomenon happening on historical buildings and structures, made from masonry, is linked with negative meaning conveyed by the terms "biodeterioration" and "biodegradation". This resonates due to the observed habitation of stress-tolerant organisms, like bacteria, algae, fungi, lichen and mosses that happens naturally in building surfaces which are exposed to the environment. However, as it is mentioned earlier Guillitte (1995) supports, no physical or chemical weathering is happening merely because of microorganisms' colonization, mainly color alterations are observed in different ways depending on the material and also the type of biofilm (Guillitte, 1995). Regarding this, there are many studies investigating specific aspects, in order to reveal the reasons of happening or suggest ways of mitigation, like specific coatings and surface treatments (Toreno et al., 2018; Zhang et al., 2013). A lot of discussion has been raised about monuments' deterioration from the microorganisms' colonization and natural weathering. This increased focus, can also be proven by the bibliometric study, already conducted by (D'Orazio et al., 2014), showing that the main material analyzed until that time, was stone.

However, the ongoing and increasing dispute about the climate change and its repercussions on the urban environment with extreme weather phenomena, has led to the strengthening of the argument for the establishment of a green and blue network. Therefore, the municipality of Rotterdam has included the greening of neighborhoods in the near future goals published in the adaptability and resiliency report by 2030, to combat the rising temperatures and extreme rainfalls. To make this happen, it should be highlighted how important is the cooperation between public and private sector to force this change in the buildings' envelopes, seen as urban settings (Municipality of Rotterdam, 2013). Specifically, green rooftops, facades, and quay walls (Lubelli et al., 2021) promise to make use of unexploited surfaces for this purpose. Recent research sheds light upon the material properties and how we can engineer them to favor biological growth, so we can turn this flaw into an advantage.

Recently, great dispute has been held around the benefits of bioreceptive materials, as a low cost and low maintenance solution (Ottelé, 2021) when compared with other types of green walls and systems. Since, by definition a bioreceptive material is any material that is susceptible to host biological growth. To emphasize the benefits of this phenomenon, evapotranspiration together with the decrease of the surface albedo due to the green layer absorbing and retaining water, are contributing to the mitigation of the Urban Heat Island Effect. Not to mention, specific plants like moss are increasing the thermal insulation, since thermal conductivity is lessened (Aisar et al., 2017).

Another extremely important advantage of bioreceptivity, is the improvement of air quality (Ferrándiz-Mas et al., 2016). During photosynthesis, not only the $CO_2$ sequestration aids to the mitigation of greenhouse gas emissions, but also some airborne pollutants from humankind act as nutrients for these specific types of microorganisms (Veeger et al., 2021). Thus, the whole building envelope could potentially contribute to the alleviation of climate change only by providing green surfaces out of bioreceptive materials. Particularly, the advantages of moss in contrast to vascular plants, in both vertical and inclined roof surfaces, due to its ability to form a more resistant layer to dryer periods and re-bloom, while also providing stormwater management, acoustical, thermal insulated and air-filtration lightweight solutions, with minimum maintenance, have been extensively researched and reported (Aisar et al., 2017; Anderson et al., 2010; Burszta-Adamiak et al., 2019; Kaufman, 2016; Perini et al., 2020).

Thus, taking the above into consideration, introducing a bioreceptive index part of each material identity would be extremely useful (Guillitte, 1995; Miller et al., 2012). By putting in the agenda, the issue of buildings' decaying because of material weathering, this would be helpful for engineers and designers to decide which material should they construct with, depending on their vision and building's needs. Under no circumstances, should the potential of each material to be colonized by microorganisms be neglected or assigned as a problem for the maintenance to take care. Since, the application of preventing coatings which should be frequent in order to be effective, is highly unsustainable(Ferrándiz-Mas et al., 2016). Consequently, bioreceptivity is an inevitable phenomenon, taking place under certain climatic conditions analyzed in the next paragraph, but holds many benefits that should be unlocked.

### 2.1.2. General conditions for a material to be bioreceptive

What does it mean for a material to be bioreceptive, what criteria does it have to meet and in which climates does it thrive, are questions that will be answered in this section. In general, the conditions for the phenomenon of bioreceptivity, can be divided into two main categories: the ones related to the material (Figure 4) and the rest to the environmental parameters (Figure 5).

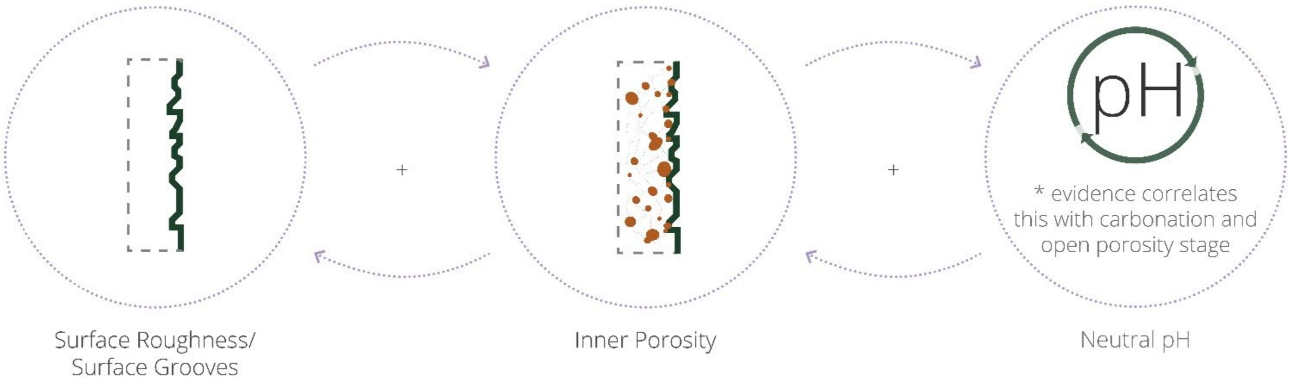


Figure 4. Diagram illustrating material conditions for bioreceptivity. Image Source: Own.

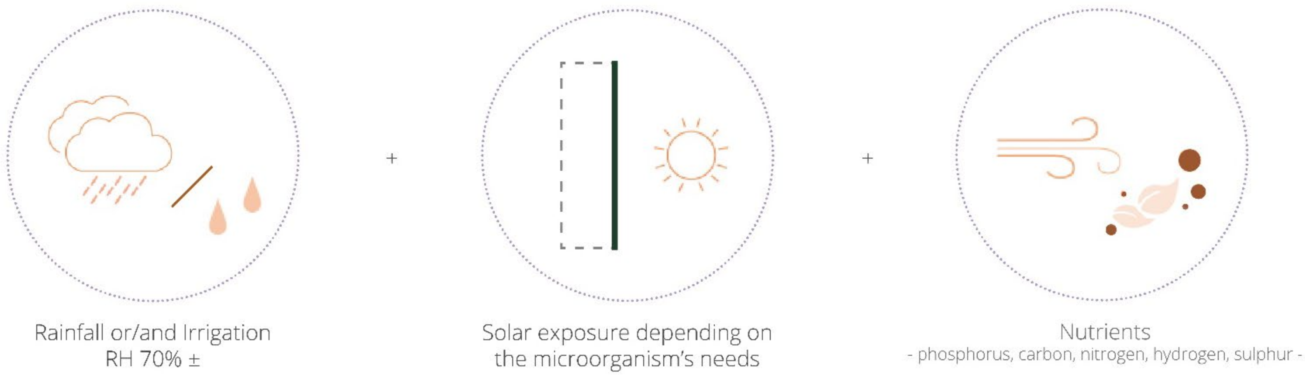


Figure 5. Diagram identifying environmental conditions affecting bioreceptivity. Image Source: Own.

From testing that Barberousse H. et al. (2006) conducted in their research gathering biofilm samples of algae and cyanobacteria located on buildings' facades in France, many factors related to water availability and temperature were found to be of an influence. These are: 'precipitation, hygrometry, thermal amplitude and proximity to the sea and greenery'. Additionally, studying colonization on stone buildings has highlighted the connection to: light for photosynthesis, temperature, wind, atmospheric pollution and lastly, content of airborne microbial contaminants. Especially temperature, is reported to favour the rate of bio-growth in about 23°C. Whereas, extensive solar radiation can turn out to be negative, resulting in quick surface drying (Escadeillas et al., 2007). Linked to all these environmental factors, is also the term 'accessibility' characterized in the paper of Guillitte (1995) as the potential of transferring seeds in various ways. These are: anemochoria, myrmochoria, avichoria etc., ensuring the long-term bioreceptivity. Therefore, the environment similarly to the material itself, has the ability to be bioreceptive, meaning that there is an abundance of means to provide seeds and nutrients, to which the substrate is going to be exposed (Guillitte, 1995).

In addition, other type of parameters are important related to the orientation of the surface, the shading it receives and the permanent capillary humidity. What is frequently observed in the outdoor environment directly connected to the aforementioned, is that in northern facades where solar radiation is not a factor, microflora is lushing even more. Since the water either from the rain or from the moisture environment, is not being evaporated as quickly as in the southern surfaces that the sun reaches, the biofilm grows faster. Thus, out of all the bioreceptive prerequisites that need to be met, water is the most crucial one, for the colonization, diversity, and abundance of organisms (Miller et al., 2012).

Exactly this, is also expressed in the early review of Escadeillas G. et al. (2007) about testing biological stains on concrete walls, that high humidity is the only mandatory condition. Different moisture levels on the substrate, could lead to the growth of different microorganisms. Additionally, even rain and wind on a single wall, creating various conditions, could mean a different set of microbial colonization. This type of data would be interesting to be gathered for distinctive locations, just like Barberousse et al. (2006) did, in order to offer even more insights on the type of climate and microorganisms' match. In their research, the gathered samples from different regions, were characterized by a factor describing the ''micro-humidity'', meaning the conditions created if there is a water leakage from a gutter or just rainwater run-off (Figure 5), but also another one named ''wetness'', depicting how many hours the wall was retained wet from the environment. These two factors were found to affect greatly the growth of cyanobacteria, while algae remained constant in every tested environment (Barberousse et al., 2006).

What's also crucial to mention is, that the characteristics of the climate affect the type of microorganisms that the substratum will host. For instance, it is referred that cyanobacteria were mainly found in Latin America, while in Europe there was also algae dominating in paints, and cyanobacteria were found only on mineral materials. It can be also inferred that certain climate zones favour bioreceptivity to take place naturally, while others will require mechanical support (Guiamet et al., 2019; Jurado et al., 2014).

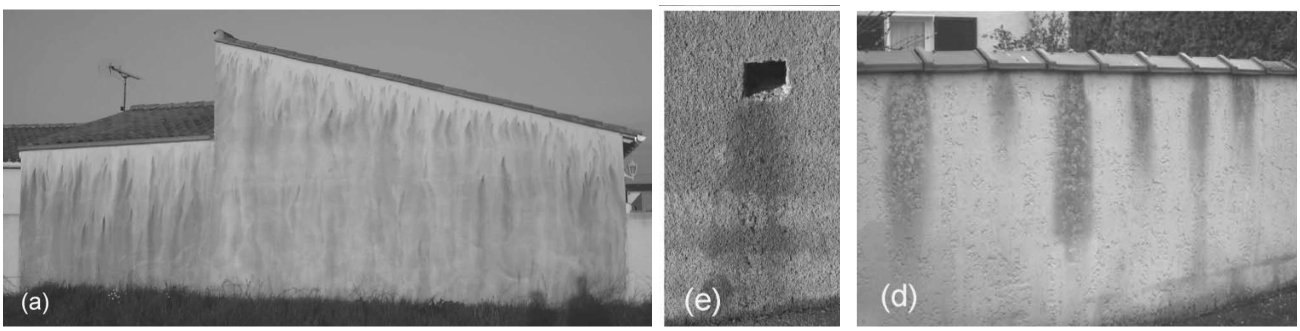


Figure 6. Images of the locations in France of collected samples, showing the different levels of bio-growth on a wall surface depending on the conditions of water content. From left to right: a) on mortar located along the Atlantic coast, extensive red colonisation by Trentepohlia iolithus was found, d & e) from zones of high micro-humidity black stains were collected composed of algae and cyanobacteria.

Image Source: Fig. 2, page 2, (Barberousse et al., 2006)

From the investigations that have primarily been done to examine and prevent the bio-colonization of rocks, since this constitutes the main problem for monumental buildings, there are many interesting points regarding the material properties. Specifically, it is proven that for encouraging biological colonization, firstly the pore space structure, meaning porosity, permeability, and capillarity kinetics, and secondly, the surface roughness matter (Miller et al. 2012). In many literature reports, that aimed to reveal the beneficial for biofouling substrate properties especially concrete walls, findings supported that Chlorophyceae and Cyanophyceae were growing denser where the substrate was more porous (Dubosc A. et al. 2001). Therefore, delving deeper to the porosity[1], a high level of open pores that allow the water to move and transferred throughout the highly porous substrate is reported to create better conditions for water retention and therefore for bioreceptivity, too (Miller et al., 2012; Perini, 2021).

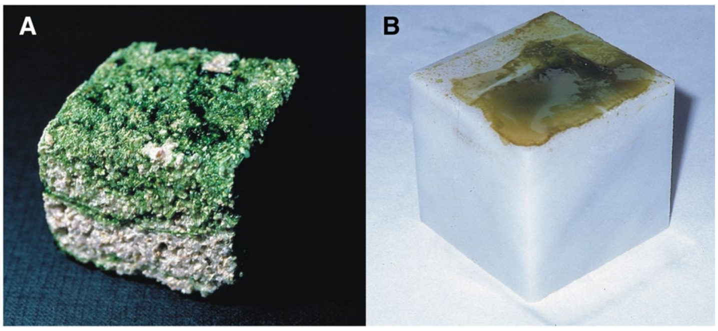


Figure 8. Photographs of experiments on primary bioreceptivity, showing the varying microorganism species promoted on the substrates' properties, affected mainly by surface roughness. From left to right: a) calcarenite, b) marble

Image Source: Fig. 3, page 9, (Miller et al., 2012).

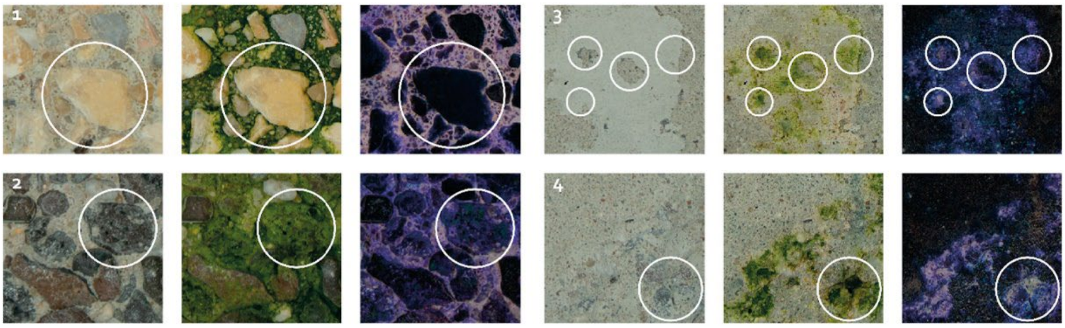


Figure 7. Images of the tested specimens for bio-growth, showing increased green coverage on those that a surface retarded was used. In contrast to the ones that biofilm grew only on surface imperfections or broken corners.

Image Source: Fig. 11, page 15, (Veeger et al., 2021)

Moreover, surface roughness is rendered as the most essential parameter for the microflora attachment. As a property, it describes how irregular is the outer surface and is observed that the rougher it is, the faster it will be colonized. This can be explained by zooming in the micro-texture, where irregularities are of equal or greater size than the microorganisms' cells and seeds, providing many attachment points, sheltered from hydrodynamic forces (Miller et al. 2012). Even, in the lab experiment of Veeger M. et al (2021) where these forces do not apply, again increased surface roughness by the application of a surface retarded, resulted in enhanced bio-growth, as it can observed from the samples in Figure 7. This happened, because the total surface area for the entrapment of the microorganisms is also increased (Veeger et al., 2021). Mustafa & Ahmed (2015) when investigated this property on stone materials, they observed that a high number of voids can lead to high values in the measurements due to irregularities, while a small pore size evenly distributed, results in a smooth surface. Large surface cavities are characterized even more beneficial, since they not only provide wider spaces for microbial attachment, but also moisture can penetrate even deeper in the material. Therefore, surface roughness is mandatory for the anchorage and spread of biological communities on the surface. Then, it is a matter of porosity and water capillarity to retain humidity for the favour of the biofilm growth, that might be spread within the pore system depending on the macroporosity.

[1] In the Appendix, porosity as a material property allowing water to move inside the material, is further analyzed.

Although it is clear from the experiments' findings that higher porosity leads to higher bioreceptivity (Ferrándiz-Mas et al., 2016), there is an upper limit on the pore size of the material. In further detail, when high porosity is mentioned, it can mean two different things that should not be confused. On the one hand, there is the level of porosity in terms of the pore dispersion in the micro-structure, which is mainly the one favouring greatly bioreceptivity, by allowing the water to penetrate deeper into the material and retain it for longer periods of time. On the other hand, high porosity can be linked also, to the diameter of the pore size, which is the parameter that shows constraints, in respect of both minimum and maximum size. This is usually examined through an electron microscope. Specifically, the minimum size could prevent water by capillarity depending on the location, meaning if its closer to the outer surface (Hall & Hoff, 2003). While, for the maximum an upper limit should be characterized, due to the fact that the larger the pore becomes, the quicker the water will be evaporated, allowing only for temporary growth or phototrophic organisms and not permanent establishment (Guillitte and Dreesen, 1995).

Regarding the pH values especially of the surface, it is generally supported that neutral values are promoting bioreceptivity. For instance, in materials such as mortars and concrete, lower pH values have proved to increase the variety and abundance of microorganisms (Francis, 2010; Miller et al., 2012). However, the findings in the experiment of Veeger M. et al (2021) for concrete, showed that pH is not a predominant factor for bioreceptivity to occur, contrary to the common belief. Samples that presented high coverage of biofilm, also had pH values greater than 10. One possible explanation sought for this, is the correlation of the pH with higher porosity and therefore water sorptivity values, due to the carbonation[2] process that is occurring in combination with material weathering. Thus, as time passes and calcite minerals in concrete are being released, the reduction of total porosity might be observed, in contrast to an increase of the pore size, resulting to an overall higher water absorption, but not water retention. Whilst this might not be seen as a positive effect, in environments where there is high water availability, such a case will still be extremely beneficial as higher water quantities will be absorbed without the need of being kept for longer to survive dry periods.

Furthermore, depending on the hosted microorganism specific chemical substances play a significant role. To illustrate, bioreceptivity as a natural phenomenon occurs mainly in materials that are rich in minerals, such as stone or bricks. Algae for example is greatly benefited from nutrients like nitrogen, phosphorus, and sulphur, etc. The source of such elements may derive from the substrate, or from run-off waters and even from ashes in polluted air (Escadeillas G. et al. 2007).

Another example is analysed in the extensive review of Miller et al. (2012), that the salinity of the surface affected the complexity and the types of microorganisms, due to the fact that they were detected high concentrations of halophylic bacteria. What's more, at the experiment of Veeger M et al. (2021), where in contrast to its initial assumptions and references about the favouring of Magnesium Phosphate cement, bio-growth was not larger than the one taking place in the Portland cement. Leading to possible explanations, that the type of biofilm used in the experiment and originally captured from a building with Portland cement, was not the appropriate one, or there were poisonous additives in their ready-to-use cement mixture, preventing a lush green growth. In a personal discussion with him, he also claimed that microorganisms have adaptability mechanisms, since one would expect that on Portland cement no biofilm would thrive, due to higher pH values (Francis, 2010), while in his experimental analysis exactly the opposite was proven.  Apart from this observation, the addition of bone ash shows an impact only at the latest stages of bio-development, implying that as a source of nutrients is being utilized when needed. For example, when the appropriate nutrients are not provided through air or water, then the substrate's chemical composition plays an important role, together by reassuring that no other material ingredient having detrimental effects on plant-growth is contained.

[2] See Glossary for term explanation.

Researchers De Muynck et al. (2009) reported in the work of Miller et. al. (2012), tested the prevention of biological growth on two types of concrete, proving that material attributes are the reason of the development of primary bioreceptivity. By observing the behaviour of the materials, after having applied water repellent coatings and biocides, the different rates of the remaining biofilm were associated with porosity and the existence of organic adjuvants. It was also stressed out, how important is the relationship between the inspection of drying rates correlated with the microorganisms' growth time upon the moment of anchorage.

Overall, out of all the material qualifications for microbial colonization, the most fundamental is the surface roughness combined with moisture/water retention from high open porosity and/or environmental conditions, that under no circumstances allow frosting to occur. Then, chemical composition and abrasion pH are also important, but as secondary factors that may define the type of microorganisms that will thrive on the substrate (Prieto & Silva, 2005).

### 2.1.3. Overview of materials

#### 2.1.3.1. Plants

When analyzing the biological stains created on concrete by microorganisms in the work of Escadeillas et al. (2007), the colonized species can be identified by:

- bacteria: ubiquitous - pioneering microorganisms forming an invisible biofilm, which causes the degradation of the material.

- algae: among the first colonizers - autotrophic [3] organisms that grow on mineral substrates, if the environmental conditions regarding moisture or water availability are appropriate (Dubosc et al., 2001; Escadeillas et al., 2007). Their frequent adhesion on the building surfaces takes place, because they exist in the air in the form of spores, cells or fragments of filaments (Barberousse H. et al. 2006). They will be spotted to follow the rainwater runoff on walls and may have different colored-stains depending on the species (black, green or red).

- fungi: heterotrophic[4] organisms, found both on organic substrates, which they impair by producing acids and living or dead organisms. For their development a very moist environment is needed.

- lichens and mosses: lichens are the result of a fungi and alga symbiosis, by providing the right moisture and organics together. While, mosses are defined as the lower plants, grow after an algal biological layer has formed and are observed in pads (Escadeillas et al., 2007).

Out of these, algae is a pioneer organism, tolerant in many different climatic conditions - seen in arid environments too - and the first one to colonize porous materials. Additionally, extremely resistant and tolerant to unfavorable extrinsic conditions, are the photoautotrophic microorganisms. These are: the green microalgae, cyanobacteria and lichens (Miller et al., 2012). Especially cyanobacteria are reported to be not only one of the first colonizers of stones, but also have been found in abundance in monuments (Prieto & Silva, 2005). Being poikylohydric, meaning that they are capable of adapting their metabolism in relation to their need of water, they are the first to colonize and survive on porous materials in the most arid climates (Miller et al., 2012)

[3] See Glossary for the term definition.

Conducted experiments that gathered samples out of scraped concrete walls in France, have defined that Cyanophyceae cells, which are obvious as black stains, grow inside of a mucilage sheet[5], that aids them to withstand dry seasons, since it preserves water from rain. On the other hand, Chlorophycae which are responsible for green and red stains, need a stable humid environment to develop. For this reason, one can easily observe green stains on wet areas on walls. Regarding the climate and the location, in these experiments, the algae species found in France, were also reported from different researchers in other locations too, drawing the conclusion that certain types of microorganisms are omnipresent and dependent exclusively on humidity and surface conditions (Dubosc A. et al. 2001).

It is stated in the work of Miller et. al. (2012), who reviewed the term of bioreceptivity on stones, that on buildings, communities of different types of biofilms are observed to grow naturally all-together, in compound forms, rather than single species in specific areas. What's more, both in the research of Barberousse H. et al. (2007) and Mustafa & Ahmet (2015) it is explained how starting from the presence of algal and cyanobacteria, if the environmental and surface conditions are suitable, the colonization will evolve with other species, reaching ferns and higher plants. These evidence, can be linked with the previous analysis of the different stages of bioreceptivity by Guillitte (1995), and specifically tertiary, semi-extrinsic and extrinsic, that existing biofilm by accumulating dust and soil creates the conditions for other type of organisms and plants to grow.

Although this is considered as the main difference of the laboratory experiments where usually only one microorganism is tested, evidence from (Guillitte & Dreesen, 1995) has illustrated that also a composition of cyanobacteria, green algae, diatoms, and bryophytes can mimic the bio-colonization that can derive conclusions of the bioreceptive potential of the material. Another used method is to capture phototrophic microorganism mixtures from actual stone monuments, accelerate their growth and testing their colonization to new materials inside the lab (Miller et. al. 2012).

#### 2.1.3.2. Building Materials

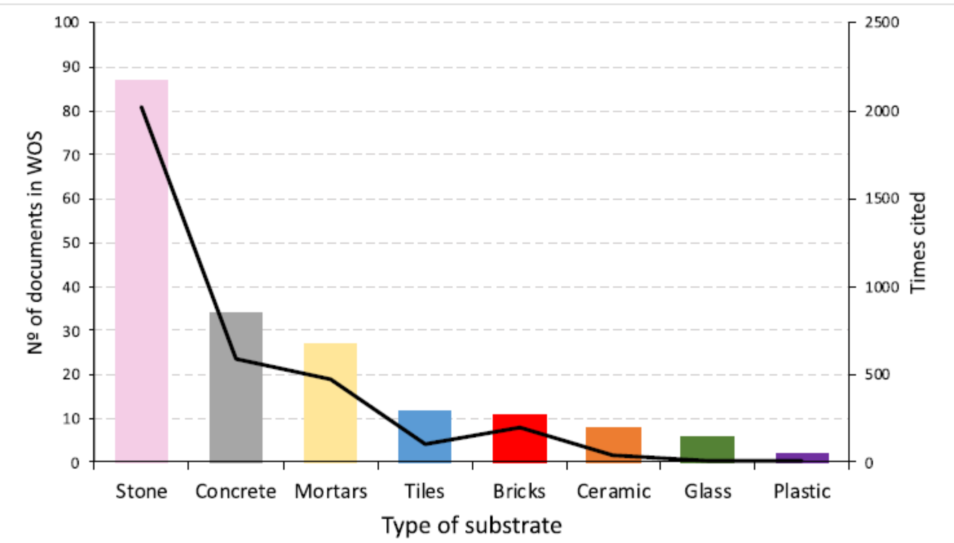


Figure 9. Diagram showing the amount of records in the WOS database combining the term 'bioreceptivity' with keywords related to building materials -accessed on the 19th of November 2020 by the (P. Sanmartín et al., 2021)

Image Source: Fig. 3, page 4, (Sanmartín et al., 2021)

Apart from stone, other common materials that bioreceptivity is examined through lab experiments are mainly concrete, clay bricks with mortars, ETICS and glass through recycled industrial soda-lime bottles and last but not least a variety of different stones. Out of these, the literature focuses greatly on stone and concrete as the findings of the research, measuring the cited records (Figure 8), shows on the

[4,5] See Glossary for term explanation.

research of (Sanmartín et al., 2021). Thus, a gap in the literature can be observed regarding the potential of recycled glass which also constitutes a major problem in the waste management industry. What's more, the building materials presented in this section come from journals exclusively on lab experiments, studying the bio-growth on the aforementioned specific materials either to measure their properties, or the bioreceptive potential by altering specific steps in the recipe or the production method. Thus, the analysis for the materials, in contrast to the plants previously, is based on the investigation of the experiments' findings.

**Stone** stands as one of the most predominant materials for construction in history. Given that it is a natural material, its mineral composition, texture, and microstructure differs, therefore also its mechanical and chemical properties. From these, it is easily concluded that every stone has different resistance to weathering (Miller et. al. 2012). The conditions for observing this phenomenon, as Mustafa & Ahmet (2015) mention are related both to climatic factors and biological impact. Specifically for the stone, that is affected with slow weathering, forming cracks and pores, the developing surface roughness combined with the mineral composition and the surface pH, favors the adhesion of microorganisms transported from the wind and water runoff on the substrate (Miller et al., 2012; Mustafa & Ahmet, 2015). For this reason, defining bioreceptivity as dynamic, with significant stages – analyzed in the first paragraph – in weathering is very accurate by Guillitte (1995).

Thus, microflora takes place at the contact area of the interface between the porous substrate filled with minerals and air. As a result, being exposed in the climatic changes of the seasons, with more and more fluctuations, endolithic colonization on stones is also observed as a better survival mechanism, which obviously contributes even greatly to the substrate's weathering. Specifically, by Miller et. al. (2012), the work of Pohl and Schneider (2002) is mentioned to have identified the depth of endolithic colonization into carbonate rock surfaces, at 150-250μm below, being sheltered from adverse solar radiation.

Korkanç Mustafa, S. A. (2015) by collecting samples from different monuments around the same region, compared how porosity and surface roughness affects the material properties. It was proven through testing, that the higher porosity, water absorption and capillary water absorption meant lower abrasion and compressive strength. Thus, ignimbrites and tuffs presented the most biodegration, while they had the lowest mechanical properties.

Even though, it is observed that microorganisms like algae and mosses are capable of growing on **brick** and stones, the research conducted by Lubelli et. al. (2018) studied the plant colonization of ivy-leaved toadlax and yellow corydalis mainly on the **mortar**, by analyzing brick/mortar combinations. Analyzing only the bricks, smaller-sized pores presented slower water absorption rates. Higher porosity was achieved by lean clay mixtures that have high water content. However, those were the specimens with the lower compressive strength values as expected.

From the findings of this research in the case of the mortars, the factors influencing greatly the porosity are: the binder/aggregate ratio, the grain size distribution of the aggregate and in the ready-to-use mortars the presence of air entraining agents. While for the water absorption rate and the compressive strength, the nature of binder used were also crucial. In detail, the mortars with lime-trass had quicker water absorption when compared to the cement-based ones. Examining the aggregates, gap-graded sand forming coarser pores, in contrast to well-graded sand, showcased higher porosity and faster capillary absorption. Similarly to the bricks, higher porosity ratios presented lower strength.

Another interesting take-away is the increased plant-growth portrayed in the mortar-mixtures containing seeds, while the ones without seeds in their majority, did not have sprouts after the monitoring of 3 months. Only in some samples that had the addition of vermiculite, plants grew. This fact leads to the suggestion, that seeds captured through the wind transfer were extremely favored by this additive, while also it produces higher porosity due to its own pore concentration and volume. What's more, air-lime/trass-based mortars were characterized as the best-performing mix.

From this experiment it is proven that the bricks act as a water storage for the mortar, which through capillarity drain the water and preserve the plant growth. For this reason, higher open porosity and faster water absorption for the bricks play an important role. However, in mortars, attention to cases must be given, that showcase extremely fast absorption with low water retention, since this leads to also rapid drying. Therefore, bioreceptivity was favored in cases with higher rate of capillary absorption, higher porosity and the insertion of vermiculite as a light-weight aggregate forming an intermediary for preserving nutrients for the plants (Lubelli et al., 2021).

Looking into **concrete**, one of the main advantages, is its widespread use in construction which already implies that there could be many applications for its bioreceptive alternative. Moreover, its similar intrinsic characteristics to stone, render its potential for biological colonization highly successful (Veeger et al., 2021) since, as a cement based material it contains organic adjuvants - highly probable to be present in the mixture (Miller et al., 2012).

Veeger M et al. (2021) tested 4 different ways of producing bioreceptive concrete with the goal to reveal the easiest to make, out of commonly used materials. Thus, they chose to start working with Portland cement by modifying its mixture properties to test bioreceptivity. To begin with, by adding blast furnace slag, through accelerated carbonation, they successfully lowered, the mixture's pH. Then, by using a surface retarder on the specimens' surface, the irregularities increased since the aggregate was exposed (Figure 7). Two ways were explored to increase porosity and water capillarity: on the one hand the water/cement factor was enlarged to the maximum allowed by the regulations, as the water evaporation would create more pores and on the other hand, crushed expanded clay was used as an aggregate. The benefits of crushed expanded clay are reported to be numerous, as it is mentioned that it aids especially in relation to water not only to retain it in the produced lightweight concrete, but also it resists freezing. In addition, for its water infiltration properties it is frequently used in hydroponics and aquaponics (wikipedia). Finally, into the concrete mixture an organic addition was tested, containing CaO and $P_2O_5$.

In the study by Dubosc A. et al. (2001) testing different water/cement factors for mortars, microscopic images, by SEM and LVSEM micrographs, shed light upon the reasons that microorganisms prefer areas between the aggregate's particles to grow as seen in the Figure 7. The porosity is higher on the cement paste than on the aggregates' particles. Higher magnification, showed for the Cyanophyceae in Figure 9, unicellar growth of 10μm size, while mineral particles appeared to be hooked in-between (Figure 10) (Dubosc et al., 2001). This explanation, can also be supported from the fact that the samples with the replacement of the regular aggregate with the crushed expanded clay also represented better bioreceptive performance in both types of the used cement, as shown in Figure 11. Since the particles of the expanded clay provided better water retention than the regular aggregates, and bio-growth expanded on top of them, even if not so thick as on the cement.

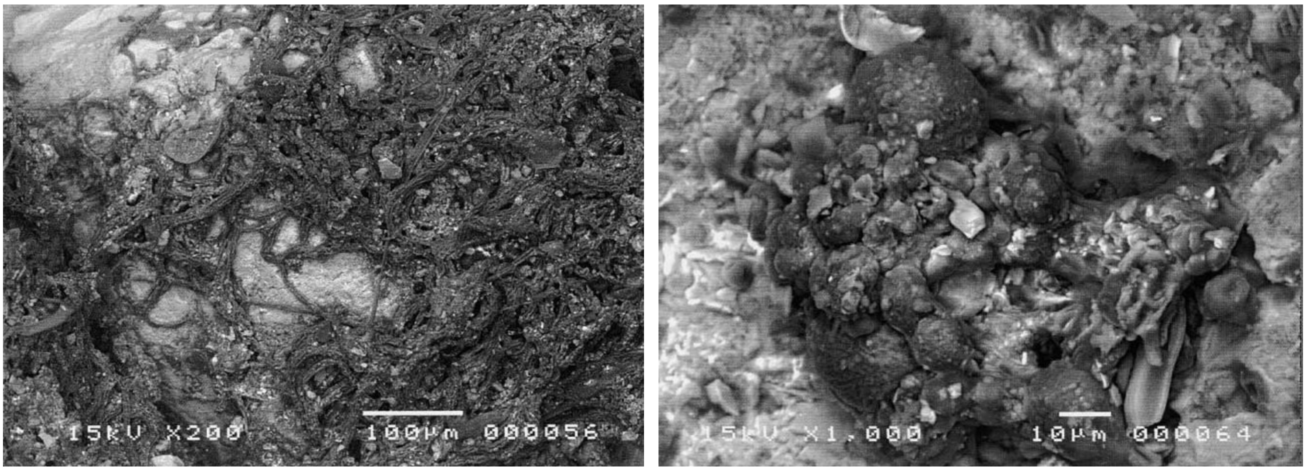


Figure 11. From left to right: a) Image produced by SEM micrograph representing Chlorophyceae on concrete forming a green stain x1000, b) LVSEM micrograph zooming in the black stain formed by Cyanophyceae x1000. Image Source: Fig 5 & 3, page 3 (Dubosc et al., 2001).

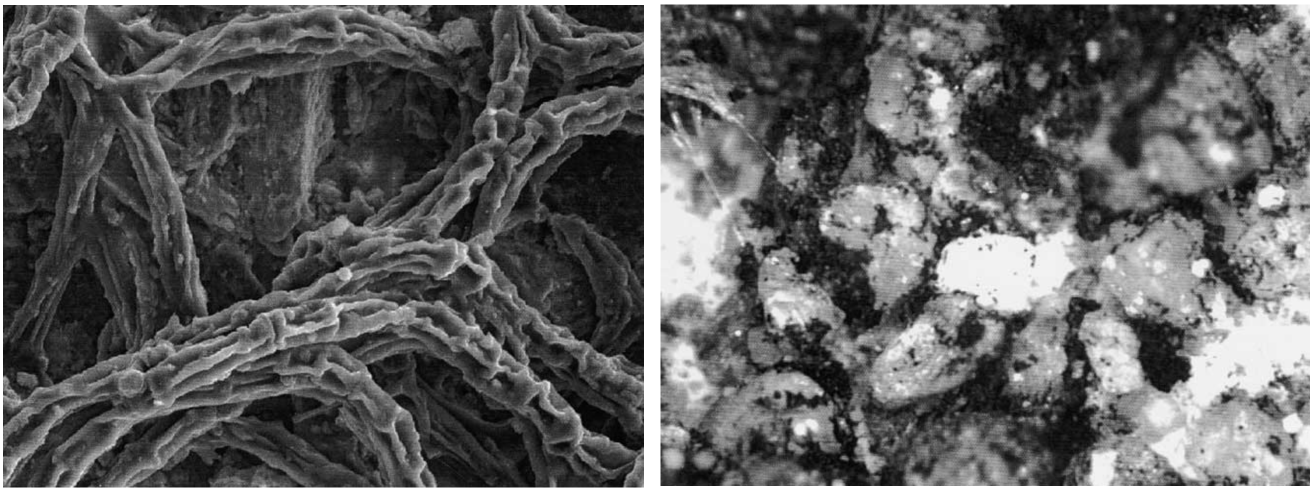

Figure 10. From left to right: a) LVSEM micrograph zooming in the green stain x200, b) Video-microscope micrograph of the black stain x100. Image Source: Fig 4 & 2, page 3 (Dubosc et al., 2001).

From the parameters tested, in contrast to the experiments of Veeger M. et al. (2021), that higher water/cement factor did not have a significant impact, in Dubosc A. et al. (2001) is revealed that the higher the W/C ratio, the higher the porosity, leading to better conditions for colonization. Last but not least, in the additives test of Veeger M. et al. (2021), bone ash as an organic element did not represent effective changes in the material properties of the sample, it did result in long-term accelerated colonization, since in the samples of 8-weeks the coverage was denser.

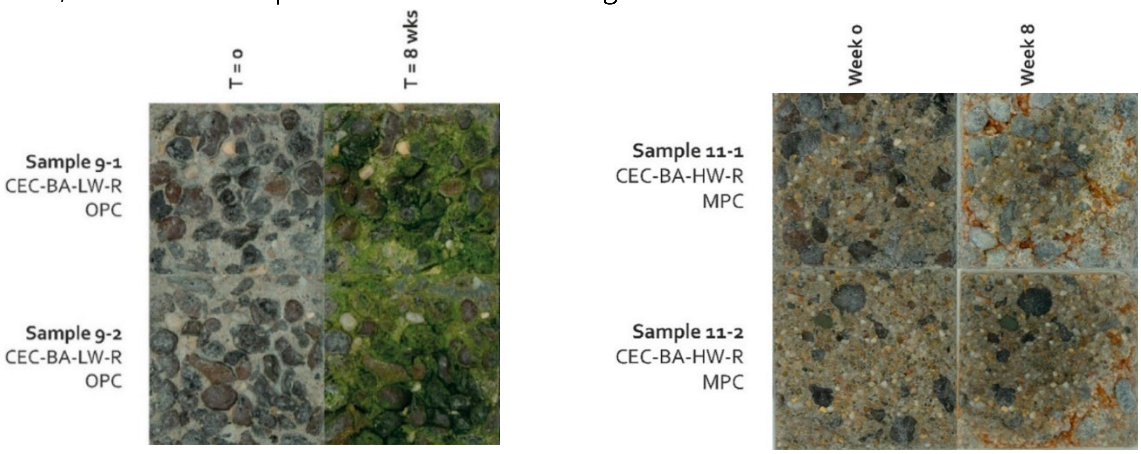


Figure 12. From left to right: a) Samples produced by Portland Cement and Crushed Expanded Clay, Bone Ash with low water/cement ratio showcasing high green coverage, while the observed microorganisms expanded partially also on top of altered the aggregate, b) Mixture with Magnesium Phosphate cement and Crushed Expanded Clay, Bone Ash with high water/cement ratio. Image Source: Fig. 8 & 9, pages 12-14, (Veeger et al., 2021).

## 2.1.4. Overview of applications (bioreceptive & urban greenery)

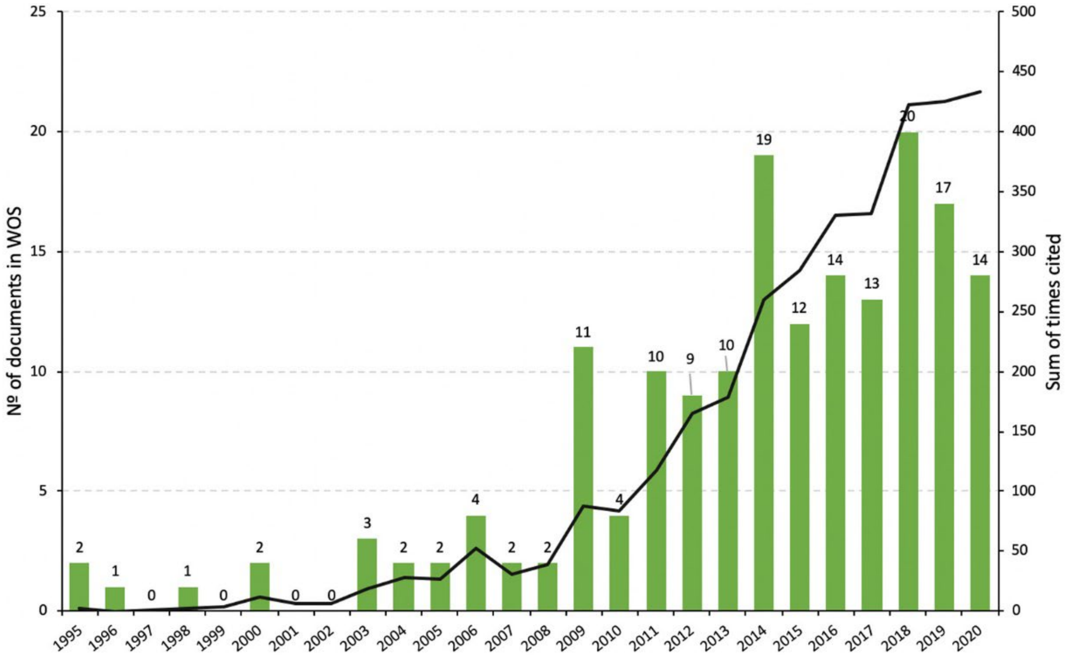


Figure 15. Diagram illustrating how bioreceptivity is not a new concept, but only the recent years has gained reputation. These are the numbers of publications and their citations from 1995 to 2020 from WOS database, accessed 19th November 2020, by (P. Sanmartín et al., 2021).

Image Source: Fig. 1, page 3, (P. Sanmartín et al., 2021)

It is a remarkable fact, that even though bioreceptivity is not a new concept (Figure 12), there are no existing applications on the built environment, apart from a few on experimental or expositional basis, mainly about concrete and mortars. So far, the most published projects have been held academically, in Bartlett - UCL, TUDelft and ISAAC- Barcelona.

Figure 13. Photograph capturing Respyre team checking the wall of application.

Image Source: Facebook page of Amsterdam Institute for Advanced Metropolitan Solutions - AMS Institute, uploaded on 24/06/2021. Retrieved 05/01/2022.

Figure 14. Photograph capturing Respyre team applying the moss mixture.

Image Source: Facebook page of Amsterdam Institute for Advanced Metropolitan Solutions - AMS Institute, uploaded on 24/06/2021. Retrieved 05/01/2022.

Exceptions constitute the team 'Respyre' that has been recently formed and is aiming to build bioreceptive concrete walls in the Netherlands. Promoting the benefits of bioreceptivity for the urban microclimate, this team with young entrepreneurs, studied mainly engineering and supported by professors of TUDelft, Marc Ottelle and Henk Jonkers, they applied their first experiment at the Marineterrein Amsterdam Living Lab, in Amsterdam, together with Delft University of Technology and Wageningen University & Research. Particularly, they have coded the application steps onto existing walls to make the process friendly and easy to install, by (1) checking the wall – (2) covering it with plastic sheet – (3) applying the moss layer, as depicted in the Figure 14 – (4) encapsulating it with another plastic membrane for rapid growth. An interesting point in their work is that they claim to collect moss from old buildings, that is later 'pulverized into powder and mixed with water and nutrients until a porridge-like mixture is formed'. Unfortunately, no published images exist of their first application seven months ago (*Respyre | Advanced Bioreceptive Technology*), (Ponstein), (*Bioreceptive concrete for liveable cities*).

Another innovative work is the project GreenQuays, with the already built small-scaled test in Breda and preparing in the next months to showcase another one in Delft. Many stakeholders cooperated in this project that is aimed to expand in a 175m pilot area in Breda in the coming years. In this project, professors of TU Delft, Koen Mulders (Figure 15) and Barbara Lubelli worked together along with a team, applying their knowledge on masonry and experimental research on bioreceptive mortars and bricks with herbaceous plants, which is also analyzed in the building materials section. In the project of Breda, the aim was to test different combinations in real conditions to assess the plant growth. Interesting and surprising at the same time, was the fact that the greenest coverage appeared on a mortar that was also contaminating the water (Figure 16), therefore this sample was rejected for future considerations of the next projects and another panel that showcased the best compromise was selected.

Figure 16. Koen working on the panels

Image Source: Georgi, B. (03/05/2021). The brickwork story behind GreenQuays. UIA | Urban Innovative Actions. Retrieved 05/01/2022 from https://uia-initiative.eu/en/news/brickwork-story-behind-greenquays

Figure 17. Photograph of the vivid plant growth on the mortar that appeared to contaminate the water. Image by K. Molder.

Image Source: Georgi, B. (03/05/2021). The brickwork story behind GreenQuays. UIA | Urban Innovative Actions. Retrieved 05/01/2022 from https://uia-initiative.eu/en/news/brickwork-story-behind-greenquays

The work of Marcos Cruz investigating bioreceptivity as an example of hydrophilic design is extremely valuable, as he was one of the first ones to publish online his experimental work with 1:1 concrete models, created in partnership6. In these, together with his team, they investigated how to optimize the

[6] Cladding was produced together with Richard Beckett and afterwards with an EPSRC-funded grant 'Computational Seeding of Bioreceptive Materials' until April 2017, porous MPC concrete with biologist Dr Sandra Manso at UPC Barcelona, in the team together with the previous they also were: Dr Chris Leung from Bartlett, Javier Ruiz (computation) and Bill Watts from Max Fordhams LCC, in partnership with Laing O' Rourke. After 2017, a new industrial partnership with Pennine Stone Limited for three pilot projects *Building Greener Cities with Poikilohydric*

design for poikilohydric plants (lichens, algae and moss) growth by creating encapsulating geometries shown in Figure 17, attempting to create a commercial product. The goal of the design was to provide such an optimized surface for 'water catchment', but also a geometry that protects plants from wind, a condition already mentioned in the previous section. To achieve such aims for real conditions, they emphasized the complex aspects of the project that requires to work in three different scales: micro linked to the material composition, meso to the surface and macro to the tectonics of construction. Their first project was constructed as a trial mock-up in September 2020 at the St Anne's Catholic Primary School in South London, made from 32 GRC Limestone concrete panels. In recent research for the next experimental applications, mixes of natural and expanded cork are being investigated as an alternative aggregate. Inspired by the potential of this work, their vision goes far beyond this attempt to produce massive production panels ready-to-use in contemporary constructions. In the future, buildings should be able to grow on their own by bio-colonization forming photosynthetic cities, instead of just providing surfaces as a scaffold for outer growth (Building Greener Cities with Poikilohydric Living Walls).

Figure 18. From left to right: a) The concrete pilot models of 1:1 scale, b) preparing the panel for St Anne's Catholic Primary School, c) samples exhibited in the Meanwhile Wildlife Gardens and Camley Street nature Park in London.

Image Source: website of UCL, Innovation Enterprise, (*Building Greener Cities with Poikilohydric Living Walls*)

### 2.1.5. Assessing Bioreceptivity

#### 2.1.5.1. Experiment: Tools & Methods

From the review of the aforementioned realized experiments, it can be concluded that there are certain material properties that need to be tested, regardless the nature of the material, in order to examine whether these affect the bioreceptivity or in what extent. In detail, these are: (1) chemical composition, strength (compressive and/or flexural-bending), hardness (cracks, falling objects, brittleness), surface roughness, porosity, bug holes (surface bubbles), weight (loads), resistance to weather phenomena (durability) and appearance so that there is potential in this application.

In Table 2, a concentrated analysis of the goal and parameters in the reviewed experiments is presented, while in table 3 their specific steps and methods are shown. Apart from the lab explorations, in the literature review there are various ways referred for measuring the desired material properties and an attempt to concentrate those, follows.

To begin with, porosity can be measured with several ways. The most widely-used methods is through liquid saturation or gas pycnometry, that a liquid such as water, mercury, etc. or gas, fills the pore network until the material's saturation point. It is crucial to mention here, that saturation is not always achieved, since it is difficult for large samples or for a small pore size, which needs long periods of time for the saturating medium to enter. Therefore, it is largely dependent on the network and pore size, and for every material the pumping and immersion times should be adjusted accordingly. Apart from these,

*Living Walls*. UCL. Retrieved 10/01/2022 from https://www.ucl.ac.uk/bartlett/architecture/about-us/innovation-enterprise/building-greener-cities-poikilohydric-living-walls.

in the category of image analysis, is also stereology, where a section of the specimen needs to be made to analyze the quantity and the size of the pores. This, can be done either by counting random points or on a grid assigning values from 0 to 1, whether they fall on solid or on void, or with a line along the surface by calculating the chord lengths of the void areas to the total line length. As evidence has shown, this method is labor-intensive, and most importantly, cannot separate open or closed porosity, thus resulting in approximations of total porosity. Other methods, are linked on the depletion of radiation that provide an estimation of the total porosity by counting all pores. Last but not least, are measurements about the bulk and solid density can also give a good estimation about the total porosity (Hall & Hoff, 2003).

In further detail, the way of measuring the hydraulic properties of the material can vary from researcher to researcher. However, the sequence of measurements in the case of Lubelli et al. (2021) was useful to describe with accuracy the needs of such an approach. This was done in three steps, by measuring the mass of the dry brick, at its saturation point in the atmospheric pressure and lastly, when soaked into the water for one week, its saturated weight, so that density and porosity can be calculated. For the compressive strength, the dimensions, a shape factor according to regulations and standards and the maximum force were needed for the identification of the normalized compressive strength of the masonry unit. The maximum force was measured during a test where a hydraulic jack of 300-ton capacity, pressed the bricks, positioned on a steel plate with a perpendicular force. The same procedure was applied for the mortars, too.

In the example of Veeger M et al. (2021), the material properties were measured in the following way: specimens were dried in 24 h circles in the oven at 37 $^{o}$C, until their weights were identical, in order to certify that they were completely dried to measure their weight. After that, the specimens were soaked again into water for 24 h, to record their weight when they are fully saturated, so that water absorption can be measured. Additionally, the specimens were dried again with the same process, measuring their weight in 1, 2, 4, 8 and 24 h, so as to draw conclusions for their water retention capabilities.

| Experiment / Application | Researcher / Constructor | Material | Objective | Additives | Experiment's Samples | Microorganisms Tested | Experiment Method | Positive Results | Considerations | Suggestions for Applications | Points for further research |
|---|---|---|---|---|---|---|---|---|---|---|---|
| Bioreceptive Concrete | Veeger M et al. (2021) | Concrete | To produce a bioreceptive concrete out of the most commonly-used materials | (1) Portland Cement (2) blastfurnace slag to reduce pH (3) surface retarder to reveal the aggregate (4) increased the water/cement factor (wcf) for higher porosity - max factor 0.6 per regulations (5) crushed expanded clay as an aggregate for higher porosity (6) organic material (10%) containing mainly CaO & P2O5 | Each mixture 4 specimens tested of size: 50×50×30mm. 2 of them for bioreceptivity & the other 2 for material properties. +2 extra mixtures were prepared with another concrete to act as reference | Biofilm collected from the faculty building of Architecture and the Built Environment in Delft, containing algae. Then, it was kept with optimal growing conditions in an Erlenmeyer containing BG11 liquid growth medium. | After the samples' biofouling, they were kept in a container with distilled water right underneath the sampled surface for 8 weeks. | (1) Simple materials used (2) Changes in the hydraulic properties of the material have the highest impact (3) Increasing the surface roughness by applying a surface retarder led to greater green coverage (4) Addition of bone ash enhanced bio-growth at a later stage as a source of nutrients. (5) Cruched Expanded Clay has inherent bioreceptivity, leading to the expansion of the biofilm even on top of it, when used as an aggregate. | (1) The influence of a lower pH is not mandatory once the hydraulic properties are sufficient. (2) Magnesium Phosphate cement did not host increased bio-growth as expected. | Superficial layer on top of regular concrete or as façade cladding Non-structural cases | (1) Durability because of water abrasion - weaker cement- susceptible to freeze/thaw cycles & mechanical abrasion, environmental conditions (2) exact effects on urban environment (3) embedded energy |
| Mortar for masonry walls | Lubelli T. et al. (2021) | Bricks and mortars | To examine biological growth in different mortar and brick combinations | | | ivy-leaved toadlax and yellow corydalis | stacks were positioned with a 20 degrees slope, protected from rain and ground, while water-sprayed regularly | | | | |
| Prevent algal growth by examining the factors tha favor it | Dubosc A. et al. (2001) | Cement Mortar | Algal growth on mortars with different porosities | (1) Portland sement (2) siliceous river sand as aggregate (3) different water/cement ratios: 0.38, 0.5, 0.6, 0.7 (4) only for the 0.38 W/C, superplasticizer & densified silica fume | 3 for each mixture: 12 in total | | | (1) Water/cement ratio increases the porosity (3) microscopic method is appropiate for stain identification | (1) The total thickness was very thin to estimate the effect of open porosity (2) Chlorophyll α used to determine the scraped microorganisms of the original surfaces did not provide acurate results | | The impact of substrate's mineral composition and the material weathering because of the acit production from the algal development |
| Bioreceptive tiles made off sintering granular waste glass | Ferrandiz-Mas V. et al. (2016) | Soda-lime waste glass | To reveal the optimal processing conditions to obtain algae growth | | 110 x 55 x 7-8 mm | algae Chlorella vulgaris | Accelerated bio-growth was formed for the test of 21 days by testing samples both with neutral pH (6.8-7.8) and unconditioned pH. | | | | |
| Moss growing on different substrates | Penini K. (2021) | | | | | | | (1) Most green coverage was observed in the capillary carpet, then for the rest: cement> (2) On vertical surfaces, the water distribution requires attention to achieve a total wetting of the surface (3) The adhesion of moss in vertical surfaces is not always successful, (4) Faster moss development is attained with constant water provision. | | Vertical and horizontal surfaces for residential retrofitting solutions and industrial areas. | (1) Adaptability and survival of moss in real-time conditions in a long-term basis. (2) Quantification of the created ecosystem when moss thrives. |

Table 1. Ongoing summary of the experiments reviewed of different bioreceptive materials, their objectives and considerations that can be used as information for further investigation in the scope of the project. Source: Own

| Researcher | Material | Spacimens Size | Types of plants | Step.01 | Duration.01 | Goal.01 | Step.02 | Duration. 02 | Goal.02 | Step.03 | Duration. 03 | Goal.03 | Step.04 | Duration. 04 | Goal.04 | Step.05 | Goal.05 |
|---|---|---|---|---|---|---|---|---|---|---|---|---|---|---|---|---|---|
| Veeger M et al. (2021) | Concrete | | mix gathered from the Faculty of Architecture, Delft | Soak the concrete samples | 56 weeks | Provide moisture on the sample to host immediately the microorganisms when placed | Grow Biofilm | | | | | | | | | Drop the liquid biofilm on top of the sample surface | To acquire homogeneous bio-growth on the samples |
| Escadeillas G. et al. (2007) | Mortar | 5 x 5 x 1 $cm^3$ | Three-species algae: (1) Chlorhormidium (2)Chlorellachloro-phyceae (3)Chroococcidiopsis cyanophyceae | Soak the mortar samples | 3 days | Provide moisture on the sample to host immediately the microorganisms when placed | Grow Biofilm | 35 days | This period deemed necessary to reach the beginning of the exponential growth | Place samples on top of a 160g vermiculite layer | | "To guarantee the algae mineral supplies" | Dry samples | 2 hours | To absorb easier the algae liquid | Spread 0.2–0.5 ml/25 $cm^2$ of algae on the sample surface using a pipette | To acquire homogeneous bio-grwoth on the samples |
| Escadeillas G. et al. (2007) | Mortar | 5 x 5 x 1 $cm^3$ in 45˚ | Three-species algae: (1)Chlorhormidium (2)Chlorellachloro-phyceae (3)Chroococcidiopsis cyanophyceae | Soak the mortar samples | 3 days | Provide moisture on the sample to host immediately the microorganisms when placed | Grow Biofilm | 35 days | This period deemed necessary to reach the beginning of the exponential growth | - | - | - | - | - | - | Apply constantly, uniform run-off of a BG11 solution inoculated with a mixture of three algae | To simulate the water run-off impact on the bio-growth |
| Dubosc A. et al. (2001) | Mortar | 5 x 5 x 1 $cm^3$ in 45˚ | Algal diaspores | Capture microorganisms by scraping different building surfaces | - | (1) Test the species (2) Quantify them through chlorophyll α test (3) cultivate them for the growth test | Determination of the original concrete conditions of the colonization | - | Preliminary data regarding humidity, surroundings, porosity | Produce the mortars with the different W/C ratio by casting them to the mould | - | Produce different porosity to test the algal growth | Periodic sprinkling with deionized water with minerals containing the algal mixture | 2 months | Quantification of the growth | - | - |

Table 2. Ongoing overview of the different steps in the experiments reviewed for assessing the bioreceptivity potential of different materials. Source: Own

When testing the combinations of bricks and mortars for the masonry wall it is important to also calculate the flexural bond strength. All the specimens were above the lower limit set by Dutch regulations regarding masonry, except for the combinations with the brick presenting the higher porosity. Its compressive and flexural bond strength were below the preferred limits. Thus, aiming to combine the maximum bioreceptivity with mechanical performance, a brick with similar capillary absorption and porosity is suggested to be used, but with better compressive strength. Another solution to this problem can be sought, by designing an external dry-stack masonry system out of polymer. This, would ensure better mechanical strength and in case of a mortar failure due to the impact of the plant roots, the whole construction will not be damaged, as the mortar will mainly act as the plant substrate and not as the brick joint.

To measure the surface roughness there are multiple methods. Veeger M et al. (2021) used a low-tech one, by transforming an image to a black and white bitmap, from a photograph of the negative surface traced by a needle profilometer 0.8mm, and then analyzed it with Matlab. This, produced a ratio of the normal length of the traced surface to its projected one in the surface plane. Another similar way to identify surface roughness is to measure by tracing it, in a handheld comb profilometer (Korkanç Mustafa and Savran Ahmet, 2015). Out of these, the most technologically advanced solution might be the one that Veeger M. et al. (2021) referred to in his journal, whilst did not conduct it due to Covid-19 measures, a White Light Optical Interferometry (WLOI) in Vertical Scanning Interferometry (VSI), that could produce more precise results.

For the pH measurement, a Metrohm 827 pH meter that had been calibrated before was used in the experiment of Veeger M. et al (2021). A sample of 10gr of the material was crushed, grounded in a mortar and pestle, dried, and then distilled water was added into the mixture out of which the pH was determined (Veeger et al., 2021).

Apart from the aforementioned material properties and the way to test them, of utmost importance is also the preparation for the actual test for bioreceptivity, that contains first of all the moistening of the samples. For instance, Veeger M. et al. (2021) soaked the samples into water for 8 weeks, after having them biofouled with a liquid biofilm, which was captured from an actual building and was left for 4 and 6 weeks in an Erlenmeyer containing BG11 liquid growth medium, to develop. Another example is the experiment conducted by Escadeillas G. et al. (2007), where they tested in each sample only one type of inoculum in three different mortar specimens, sizing 5 x 5 x 1 cm3. Specifically, the mortars were soaked in water for 3 days until they reach their saturation prior to the bioreceptivity test. In the case of the test for bricks and mortars by Lubelli et al. (2021), in the half of the mixtures, seeds were included inside.

Typically, in the majority of the experiments reviewed the microorganisms were cultivated before they were located on the surface of the samples, either in the form of drops or just by positioning on top of them. It should be mentioned that the sequence of the steps in Table 3 is chosen by the author of this report for comparing purposes, since it does not influence the outcome as long as they have occurred before the microorganisms' placement on the substrate.

In the case of Escadeillas G. et al. (2007), we have the reference for the optimum conditions to replicate a substrate's colonization in a much shorter period of time with accelerated testing. It is mentioned in the report that full coverage was obtained before 30 days from the chlorophyceae algae species, while in the second experiment with the water run-off simulation after 35 days maximum, from all the species. This was attributed mainly to the matching temperature between 21 to 25°C, which is the optimum for the algae growth, as well as the artificial extensive lighting. Catalytic role in this rapid growth, had also the vermiculite support of the substrate, that was used to reassure that all needed nutrients would be provided so that the biofilm intense coverage would not be limited. Despite that, the two experiments simulating bio growth both in a horizontal and in 45°-tilted position are valuable, crucial is the validity for the potential in horizontal surfaces and the inclination or verticality for simulating the growth on the building envelope. Thus, in real conditions such greenery would be observed after 1 or maybe 2 years, since the environmental conditions regarding moisture, light and wind can neither be predicted, nor stable. Such an experiment, gives valuable feedback in the case a researcher wants to stimulate the exact optimum conditions for plant growth to test the possible potential of the material. However, they should not be taken for granted that they neither correspond to reality, nor they predict long-term bioreceptivity because of the reasons just mentioned.

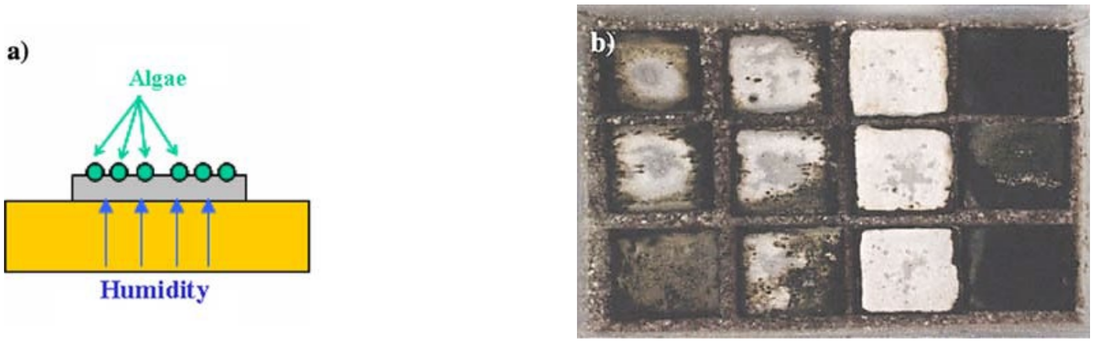


Figure 20. Experiment set-up in horizontal surfaces. Specimens were positioned on top of a vermiculite layer to reassured that all the needed nutrients together with the water content were provided.

Image Source: Fig. 3, page 8, (Escadeillas et al., 2007).

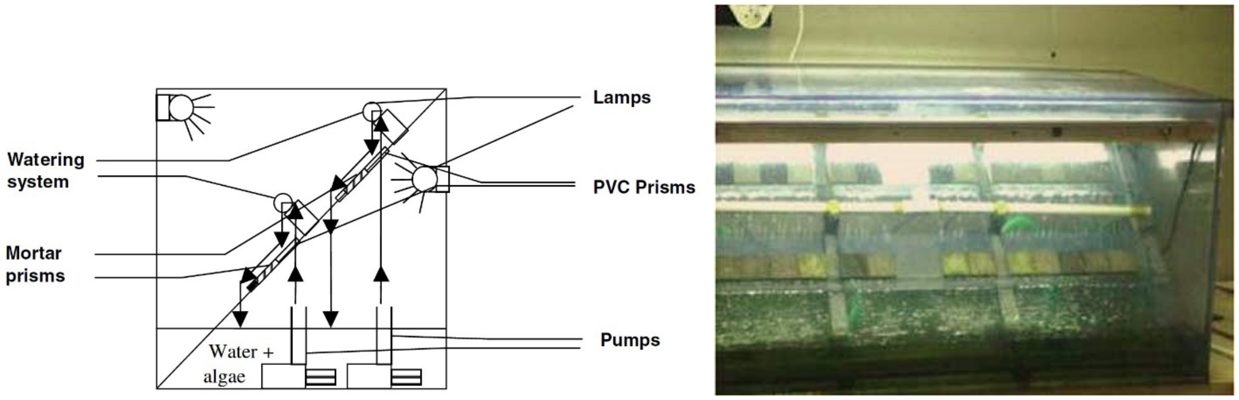


Figure 19. Experiment set-up for accelerated growth in inclination of 45° degrees. The first lamp provides lighting for the specimens, whereas the second for the nutrients and algae contained at the bottom with water being pumped constantly.

Image Source: Fig. 5, page 9, (Escadeillas et al., 2007).

### 2.1.5.2. Bio-growth

Although a variety of testing methods has been reported and is difficult to correlate the results between them as they also vary, the three following methods have been characterized as valid ones for inspecting bioreceptivity on stones.

The first, one of the most-used method to assess the bio-growth, is the quantification and monitoring of the surface cover area with microscopic and image analysis (Miller et al., 2012). According to Escadeillas G. et al. (2009), this is a 'non-destructive' one, along with another one which is to assess how intense is the algae, by spectrophotometry or colorimetry. It is crucial to mention that, after some accuracy tests conducted, it was revealed that for low coverage image analysis is not the most appropriate method to use, since the difficulty in distinguishing the colonized areas is raised. Another point that requires attention is when the surface is moist, therefore 2-3 hours for drying could eliminate color alterations from this reason. Furthermore, approximations for better color identifications can only be conducted if the porosity-bubble distribution on the surface is uniform (Escadeillas et al., 2009).

Then, the third method is to extract chlorophyll α or in vivo chlorophyll α fluorescence and quantify its color (Miller et al., 2012). However, this is reported to be destructive by Escadeillas G. et al. (2009), who conducted these experiments, to measure and identify the most appropriate method for concrete walls. The latter method, together with image analysis are most appropriate when there is also endolithic growth and cannot be observed from image analysis. According to Miller et al. (2012), validating results through experiments rendered appropriate the use of a specific solvent: dimethyl-sulphoxide (DMSO) in chlorophyl α extraction, to quantify the biomass inside the stone specimens. While, the method of in vivo chlorophyll α fluorescence was more suitable with quick results, when determining the epilithic phototrophic colonization.

Other researchers have also obtained ways of assessing the bioreceptivity of materials without growing microorganisms, since these types of experiments take time to achieve results. Specifically, Preto and Silva (2005), by analyzing the open porosity, bulk density, and water absorption by capillarity, they calculated the bioreceptivity of granite, in regards of μg chlorophyll α/cm2, through an equation (Prieto & Silva, 2005).

### 2.1.6. Conclusions

As it was explained in the first section of this chapter, bioreceptivity has many recorded benefits and it's a phenomenon that despite its negative connotation until now, it has a lot to offer if engineered. It can constitute an upcoming solution for the predicted impact of climate change and in accordance to the latest trends in construction, which include minimum maintenance work and costs, durability in various and extreme weather phenomena with a minimum impact in the building loads.

For this to happen, certain criteria have to be met firstly in the environmental conditions and secondly in the micro and macro scale of the material conceived as the substrate. In summary, enough water content and moisture, while depending on the microorganism or plant, sunlight for photosynthesis is also required. Moreover, seeds and nutrients should be provided to form lush flora and fauna, either from the material itself or by the environment via wind or insects.

From the literature review it is important to take into consideration, that depending on the climatic conditions together with the substrate chemical composition, different species of microorganisms can be the colonizers. From the experiments Barberrousse et al. (2016) it can be derived that cyanobacteria are affected more than algae from the water content of the substrate itself, if there is a drainage leakage for example and there is running water flowing on the surface. What's more, the location of the application matters greatly, since it is proven that areas with less direct sun – northern facades – and towards the prevailing winds, which will bring rainfalls – western facades in France – contribute to the formation of local favouring conditions. Similarly, in the experiment of Veeger M. et al. (2021), in the two types of tested concrete, even though the same biofouling mixture was applied, different types of microorganisms thrived. In the Portland cement green stains were developed, while in the Magnesium Phosphate cement, there were red ones observed.

Material properties play the most dominant role to meet optimum bioreceptive conditions once the above environmental circumstances are ensured. The literature review revealed about the substrate properties and mixture, that it should be:

Porous-able to absorb and retain water depending on the dry periods the area of the application experiences, but not susceptible to frosting. This is achieved by a bimodal pore size distribution, containing both coarse and fine pores being connected (open network), where the biggest ones are located on the contact surface creating increased surface roughness and as we go deeper into the section these become even smaller. By this formation, frosting is avoided, while the water is retained since the pores suck the water penetrating deeper into the material, extending the evaporation time needed in drier periods.

Crude with enhanced surface roughness, since it defines the potential of the material developing apart from primary, also terrestrial, and extrinsic bioreceptivity. The continuous anchorage of not only biofilm's cells, but also soil and dust particles result in the formation of a living community on the contact surface of the material to the environment.

Enriched with nutrients such as nitrogen, phosphorus, and sulphur that could be provided either from the substrate or the environment via wind or rain. Bone-ash being a source of organics, in the experiment of Veeger M. et al. (2021) proved to be useful for long-term bioreceptivity, by providing nutrients in due time. Another solution can be the addition of vermiculite, that Lubelli et al. (2021) and Escadeillas et al. (2007) used in their experiments as explained in the previous sections.

Sculpted in such a way that apart from the surface roughness, the geometry of the surface should create 'pockets' facilitating both the entrapment of poikilohydric organisms and water retention.

Apart from these, to define the potential of a bioreceptive product a variety of tests have to be carried out in relation to the aforementioned properties that have to be met. Attention should be paid to the experimental process during each step, since this has to be calibrated with the specific material and specimen size being tested, its limitations and needs. For instance, when capturing biofilm from the environment, the substrate conditions should match with the material under testing, so that jumping to wrong conclusions or assumptions is avoided.

What can be also concluded beyond any doubt from all the lab experiments reviewed is that when examining the potential of a bioreceptive material and the aim is to optimize it, a compromise has to be determined between the mechanical and hydraulic properties. This can be further determined and analyzed based on the scope of every project. Particular solutions of external frames that can be assembled – disassembled providing dry stacking have already been mentioned as alternatives for providing extra support when lush greenery is the paramount concern.

Out of the analysis on this chapter, it is obvious that research is focused mainly on the most-commonly used material currently in construction under one limitation. The noteworthy experiments aim to offer a more sustainable solution by rethinking the already-known elements as they are, either changing their way of production or altering their initial mixture. However, bioreceptive materials or applications have not yet been launched as a construction alternative or a product in the market in the hands of designers and architects. We should firstly consider the reasons behind this problem, since this is such a promising strategy for the mitigation of climate change, and then envision the option that this innovative material is re-manufactured out of landfilled waste, offering a totally new and fully sustainable application.

Towards a net-zero built environment, we ought to re-invent the whole life-cycle of the materials that currently have no purpose at their end-of-usage. Such a case are the various glass sources that are being downcycled or landfilled, while researchers of the Glass & Transparency Group of TUDelft has proven that there is potential of obtaining a closed-loop recycling, analysed in the next chapter. For these reasons, the current project focuses to determine the potential and limitations of a bioreceptive material made by glass waste.

| Product | Commercial product / Research | Substrate Production method | Surface roughness | Total porosity | Open Porosity | Closed Porosity | Pore size d (mm) | Density ρ (kg/m^3) | Sorptivity (g/cm² * s½) | Water absorption | Water retention (after 24h) | Resistance to frosting | pH | Compressive Strength σ (Mpa) | Flexural Strength | Thermal Conductivity λ [mW/m*K] | Type of bioreceptive | Cultivation time on samples | max Green coverage |
|---|---|---|---|---|---|---|---|---|---|---|---|---|---|---|---|---|---|---|---|
| GF | commercial values | | | 70-95 % | - | 85-95 % | | | | | | | | 0.4 - 6 | | 40 - 80 | | | |
| GF | König J. et al. (2020) | powder foaming | - | 94.5 - 95.5 % | 91.2 - 99% | | 0.3 - 1.75 | 116-143 | | - | - | - | - | 0.82 - 1.21 | | 57.2 - 65.6 | - | - | - |
| GF | König J. et al. (2020) | powder foaming | - | 91.3 - 96.2 % | 0 - 8% | 91.3 - 100% | 0.21 - 1.51 | 107–245 | | - | - | - | - | 0.47 - 2.46 | | 37.5 -56.2 | - | - | - |
| GF | Souza et al. (2017) | sintering foam with eggshells as foaming agent | - | (1 wt % EG): 80, (3 wt % EG): 92.5, (6-15 wt % EG): 90-82.5 | | | (1 wt % EG): 0.5-1.8, (3 wt % EG): 1.7 - 8 | (1 wt % EG): 500, (3 wt % EG): 250, (30 wt % EG): 1250 | - | - | - | - | - | (1 wt % EG): 1.3 , (3 wt % EG): 0.2, (6-15 wt % EG): 0.6 - 1.5 | - | (1 wt % EG): 100, (30 wt % EG): 200 | - | - | - |
| GF | Siddika A. et al. (2022) | curing-sintering (with fly ash) | - | 31-90% | | | 0.5 (mean), 0.1-2 | 213-1670 | | - | - | - | - | | | 83-309 | - | - | - |
| GF | Samoilenko & Tatarintseva (2013) | | | | | | 2-3mm (775 °C ) | | | 13-17 % (2.5% foam agent), 5-6 % (1.5 % foam agent) | | | | | | | | | |
| BC | Veeger M et al. (2021) | water content, crushed clay as surface retarder | 1.09 | | 5-25 % | - | 50µm | - | - | 5 - 13 % | 15 - 30 % | - | 10.0-12.2 | - | - | - | indoor | 8 weeks | 43.17% |
| BC | Veeger M et al. (2021) | contrast between bioreceptive and UHP concrete | | | | | | | | | | | | | | | | 8 weeks (full covererage obtained after | |
| BG | Ferrandiz-Mas V. et al. (2016) | sintering glass | - | 33.5±1.2% (680°C), 17.8 ± 1.4%(740°C) | 33.5±1.2% (680°C), 17.8 ± 1.4%(740°C) | | | | after 80 s (8.94 s½), tiles sintered at 680 °C absorbed 1.66 g of water per cm² | (680°C) 0.201 ± 0.004, (740°C) 0.007 ± 0.003 (g/cm²*s^1/2) | | | 7.5 - 9.5 | | 8.8 ± 1.1 Mpa (680°C),19.2 ± 2.0 MPa(740°C) | - | indoor | | - |
| BC | Dubosc A. et al. (2001) | Cement mortars with increased water content to increase porosity | | | 10-22 % | | | | | | | | | | | | indoor, tilted 45° | 8 weeks | 80% (22% porosity) |
| BB | Lubelli T. et al. (2021) | Combinations of mortars with/without seeds with porous bricks | | 31.66 % | 31.66 % | | | 1811 *10³ | | WAC: 418.7 (g/m²sec^1/2), IRA: 3.91 (Kg/m²min) | | | | 10.88 ± 1.38 | | | | | |
| BM | Lubelli T. et al. (2021) | Combinations of mortars with/without seeds with porous bricks | | 19.3-50.6 | 19.3-50.6 | | | 2138 (P:19.3%), 1308 (P:50.6%) | | | | | | 19.5 (P:19.3%), 0.6(P:50.6%) | | | outdoor, regular spraying | 3 months / 18 weeks | |
| ETICS | D' Orazio et al. (2014) | | 13.98 µm | 24.05 % | 24.05 % | | 8.97 - 1.16 µm | | | 0.0038 (kg/m²*sec^1/2) | | - | | - | - | - | indoor, accelerated | 9 weeks (equals to 2 years of natural exposure) | |
| BB | D' Orazio et al. (2014) | molded (FVM) and extruded (FVE) | 9.65µm, 6.49µm | 38.82%, 33.65% | 38.82%, 33.65% | | 1.46, 0.77 - 0.24 µm | | | 0.2293 , 0.0437 (kg/m²*sec^1/2) | | - | | - | - | - | indoor, accelerated | 9 weeks (equals to 2 years of natural | |
| R | Mustafa, K., & Ahmet, S. (2015) | samples from monuments | 1109.98 µm (travertine) | | 3.88 -33.18 %, 3.88-6.10 (travertine), 10.79 (andesite) | | | | | 1.54 - 24.11 %, 1.54-2.56 (travertine), 4.89 (andesite) | | | | 5.74 - 53.00, 39.20-53.00 (travertine), 47.75 (andesite) | | | | | |
| R | Prieto & Silva, 2005 | testing granites intrinsic properties to predict their bioreceptive behavior | | | 11% | | | 24 | | 5% (20 days) | | | | | | | | | |
| BC | Manso S. et al., (2014) | Magnesium phosphate cement | 0.06 ± 0.00 µm | | 2.47 % | | | | | | | | 6.7 | 24.45 ± 1.4 (Ma28-1C) | | | | | |
| BC | Escadeillas G. et al., (2009) | cement mortars accelerated tests | 1.9 % (bubbles) | | 21.6 % | | | | | | | | | 37.9 (M1) | | | indoor, accelerated | 100 days | 80 - 100% |

Table 3. Report of values about material properties on literature. The table aims to provide a guide for comparison for the discovered scores of bio-host glass, in order to assess its value. Source: Own

## 2.2. Local Challenge: Glass Waste

### 2.2.1. The problem of glass waste

Glass is an inert material that can be used in a closed-loop system indefinitely, as it is 100% recyclable (DeBrincat & Babic, 2018). Yet, only the packaging industry is working towards this goal of collecting and recycling 90% of the glass containers by 2030 in EU. One of the latest press releases of the platform 'Close the glass loop', published on the website of the European Container Glass Federation, reveals that in 2019 the average collection of glass packages reached the record rate of 78% (FEVE, 2021). It is evident that the specific industry only, has invested in the glass recovery and recycling, therefore scores the highest percentages. The reason behind this, lies on the fact that contaminated glass cullet cannot be allowed in the food packaging, since it might have a consequence on the products taste or smell (T. Bristogianni et al., 2018), therefore the recycled products can re-enter the loop, by satisfying the required guidelines.

Encouraging as these numbers may seem, what happens with the rest of the glass being produced especially in the building industry, which should be the main focus of architects and engineers? To illustrate the impact of the waste from the specific field, in a scenario where the architectural glass would be collected, dismantled, and recycled by re-melting it in furnaces, the actual number of 1.23 million tonnes of raw materials would be recovered, as well as the avoidance of 230,000 tonnes of excessive carbon emissions produced from new products (DeBrincat & Babic, 2018). In the Netherlands, where outstanding numbers of recycled float glass are achieved between 80-90% in contrast to other countries, only 9% returns in the float glass industry, whereas the rest gets down-cycled to bottles or in insulating products. Such numbers are observed, due to the fact that existing window coatings, adhesives between material components, or other contaminants, not only consist a labor intensive disassembling process, but also the recycled glass cannot meet the austere quality criteria to be exploited again as float glass (Oikonomopoulou, 2019), because the transparency and the risk for breakage is affected.

Together with architectural glass, much more unutilized glass waste sources are included, such as household items, electronic waste, automotive industry waste and industrial / laboratory (T. Bristogianni et al., 2018). Since, every item is linked with a specific glass type, for instance: ceramic glass: kitchen glass, microwave glass disks, borosilicate glass: light bulbs, oven ware, laboratory equipment, lead glass: crystalware, aluminosilicate: mobile phone screens and the list goes on, an appropriate recycling/reusing scheme for these specific glass recipes should be established, so that these items get recycled. Unfortunately, the only method until now, is down-cycling into aggregates for lightweight and insulating concrete, ceramic, or pavement products and into abrasive or foam insulation. Apart of the lacking applications, relevant infrastructure is needed, such as collecting points and recycling plants specifically for these other types of glasses (Oikonomopoulou, 2019).

### 2.2.2. Overview of glass waste sources & experimental work at TU Delft on casting glass waste

In this section, after having indicated the extents of the problem of glass waste, it is deemed imperative to review the possibilities of unexplored glass waste recipes, in terms of sources, current applications and revealing evidence in published experiments that outline the possible paths that could be followed to produce bioreceptive recycled glass. Thus, gaining insight for the manufacturing method is equal to choosing the optimum glass recipe. These two factors affect the resulted material properties, which define the suitability of the product, therefore they are inextricably linked together.

Anagni (2018) analyzes in her thesis the existing uses for glass waste but also the developing research, aiming to provide ways of enabling a closed-recycling loop for this widely-used material. Her work proves the most viable ways to take advantage of it, is by integration into construction applications even for CRTs and LCD products, which are extremely difficult to discard. Specifically, more and more evidence about the advantages of using the glass waste in certain applications is gaining light. These are, firstly in concrete mixtures as glass powder, secondly in ceramics and thirdly as a foam material mainly for insulating products (Giulia, 2018). The reported advantages of replacing fine aggregates in concrete are: the enhancement of mechanical properties of strength, compressive performance, abrasion resistance and especially with CRT waste glass an X-ray radiation shielding. In addition, this solution constitutes a lightweight, un-inflammable alternative since glass has inorganic nature, thus benefitting greatly concretes that have a higher demand for better thermal and acoustical insulation (Bernardo et al., 2010).

Another use for glass foam as Anagni (2018) indicates is the mixture for ceramic materials and bricks, where the main gains are focused on the lowering of sintering temperatures. For instance, "a mixture of 50% pottery and 50% recycled glass has been reported to decrease the temperature from 1230°C to 1050°C", which is a considerable amount. Additionally, compact bricks showcase better mechanical performance, while others with high levels of porosity improved insulating characteristics. Extremely promising for such additions in the ceramic sector, has proved to be CRT glass. Even, the next generation of the latter, the TFT-LCD (Thin-Film Transistor Liquid Crystal Display) is claimed to ameliorate the compressive strength of bricks and water absorption in fired bricks, if it replaces clay up to 30%.

Finally, other types of products under investigation regarding their re-use and recycle, are the glass fibers. Considering that their use has been exponentially increased the latest years it is absolutely mandatory to be able to promote a process that could enable their closed-loop recycling. Currently, there are encouraging studies that separate glass fibers from other materials like polyester resin, through a water-based solvolysis technology in a laboratory experiment and present similar Young's modulus but reduced tensile strength. Therefore, again in this case the open-loop recycling is only feasible, yet (Giulia, 2018).

Although the use of glass can be attractive under multiple aspects and its production is continuously increasing, once employed as a construction element, it is rarely reused or recycled due to the high-quality requirement demanded to the industry of production. Nevertheless, besides its main applications as a 2-dimensional element, the new technology of cast glass has been recognized as a potential mean of glass recycling.

Pioneering work regarding the waste of glass has been conducted by the *Glass & Transparency Group* of TUDelft, and specifically the project Re^3 glass, proving the concept that glass recycled into cast components can absorb through its larger section more impurities than the thin 2-dimensional float glass. Furthermore, by assigning it as a construction element, it provides a wide variety of aesthetical tools for designers (Velden, 2020). As the Figure 22 depicts, the recycling of different sources of waste was examined primarily for their viscosity in working temperatures between 900-1100 °C. In the samples produced by experimentation, cases of crystallization and alterations in colour because of contaminants were discussed, to meet the most appropriate heating temperature and treatment. What’s more, combinations of different types of glasses were also tested in higher temperatures at 900-1450 °C, where the casted blocks did not present cracking during cooling and annealing. These findings are extremely valuable as they suggest a major solution so far for recycling many different glass recipes, by making new components for the building industry, that are reusable or recyclable, since their stacking can be achieved without any adhesives. This is accomplished through a studied interlocking geometry, designed according to glass properties for the maximum reduction of shear forces, while a minimal metal framing support and a dry, colourless interlayer reassures the system’s integrity, even if some blocks fail (Bristogianni et al., 2019).

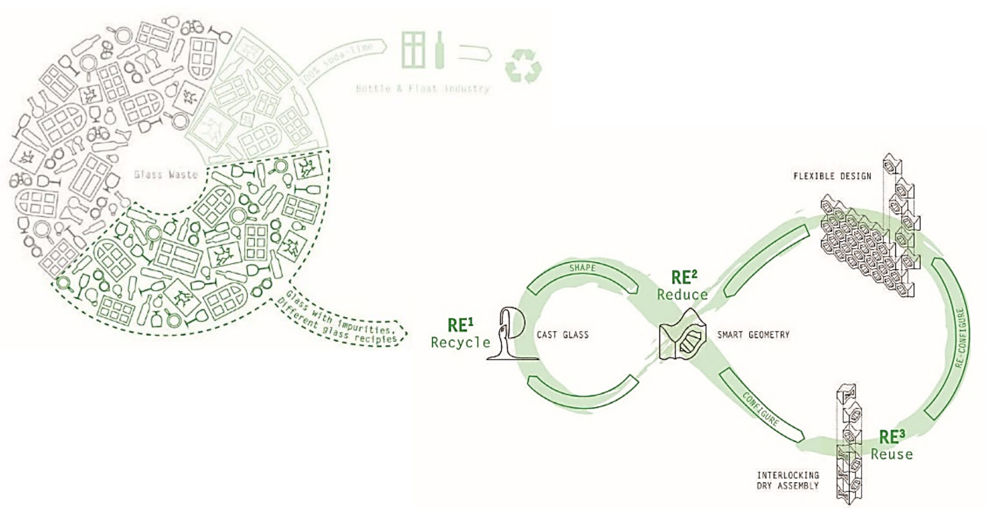


Figure 21. Diagram illustrating the portion of unitilized glass waste that can be exploited through the kiln-casting method in the building industry, by the proposal of Re^3 glass, suggesting a circular use with dry-assembling interlocking components.

Image Source: page 5, (Bristogianni et al., 2019)

Prior to this project, there has been a great number of experimental works published, that piece-by-piece either validated the potential of Re^3 Glass, or showed promising experimental mixtures for our goal of manufacturing porous recycled glass out of unexploited waste.

To start with, Bristogianni T. et al. (2018) analysed the recycling capability of many different glass recipes related to everyday objects, that are currently dumped into the landfill, while also pointing out their constrains on fulfilling the criteria for load-bearing components. In detail, important criteria to compare the results contain the workability, due to the different method these glasses have been initially produced, in combination with lowest working temperatures for energy savings, as well as the overall resistance to crystallization. For the latter, the chemical composition revealed with a Panalytical Axios Max WD-XRF spectrometer, aids to predict or justify certain phenomena, such as the high percentage of lime (CaO), not only leads to crystallization, but also by raising the glass softening temperature which facilitates the automated blowing process for the manufacturing of bottles, it makes casting more difficult. Out of these first experiments, it is evident that the higher the temperature is set in heating, the less crystallized the mixtures become under the top surface, even though in many cases there is entrapment of bubbles observed (Fig 23). While on lower temperatures, porous samples are derived mainly from chemical interaction with the mould (aluminosilicate glass – mobile phone screen with Crystalcast M248 mould), as shown in the Figure 23 (Telesilla Bristogianni et al., 2018).

Figure 22. Images showing the different steps of Alkali-aluminosilicate glass treated, being retrieved from a mobile phone screen. From left to right, before tested, fired at 1250°C and at 1500°C.

Image Source: Fig. 15, page 19 (Telesilla Bristogianni et al., 2018)

Moreover, tested combinations of matching glass recipes present a certain interest, especially the one of distinctive colours, coming from different soda-lime bottles. These mixtures were created to test also various sizes of cullet, both small shards and powder. The resulted specimens even though heated at 970°C, they partially fused with the unique pieces still apparent (Fig 24). Contrary to what was expected due to the similarity of the glass recipes, non-homogenized samples were formed, offering an alternative for creating glass with increased surface roughness and porosity. Even though further investigation is needed in regards of the optimum cullet size especially for bigger-sized samples, the potential of this experiment can be based on the correlation with the sintering technique used to create bioreceptive glass tiles out of soda-lime bottles in the work of Ferrándiz-Mas V. et al. (2016), analyzed in the previous chapter.

Figure 23. Photographs of the produced samples from different coloured glass bottles kiln-cast at 970 °C. From left to right: out of small shards and powder.

Image Source: Fig. 17, page 21, (Telesilla Bristogianni et al., 2018)

Since currently, in the plants dedicated to recycling, borosilicate, crystal and glass ceramic are isolated and eliminated from the collection of soda-lime cullet, the opportunity to exploit these quantities arises. Hence, the work of (Anagni et al., 2020) exploring mixtures of the aforementioned for the purpose of characterizing the suitability for cast components, is extremely valuable. Specifically, the sample of Soda-lime, itself and mixed with Borosilicate, fired in three different temperatures -970 (soda-lime), 1120, and 1200 °C (soda-lime and borosilicate)- exhibited surface roughness through big-sized bubbles, indicated a high level of porosity (Fig. 25). Even though from personal close inspection of the element, these pores do not seem to connect by forming an open-network, examination under microscope is needed to certify this assumption. The results of the performed splitting test, verified that the more porous-lower in density material, the lesser compressive strength it possesses, since the specific piece was split (Fig. 26) with the lowest required maximum Force, out of the total number of samples tested.

Figure 24. Photograph of samples with coded names: (from left to right) S-D01, SB-A01, SB-G01. Indicating the mixtures of soda-lime glass, soda-lime and borosilicate in different firing temperatures: 970, 1120, 1200°C. These samples indicated the highest porosity out of the tested recipes.

Image Source: (Anagni et al., 2020)

Figure 25. Photograph of the element after conducting the splitting experiment. $F_{max}$ (N): 4478,62

Image Source: (Anagni et al., 2020)

Another noteworthy example providing evidence for our scope, that was produced unexpectedly during experimentation is depicted in the Figure 27. In this testing, the main mixture was comprised out of silica plaster and cement, combined with $Al_2O_3$ (>20%) that during firing at 1200°C resulted in a reaction with the mold. The most suitable explanation derived by the glass experts is that the addition of aluminosilicate in combination with the cement, at such a high temperature eradicated in a way of absorbing into its own mass the walls of the mold. However, out of this reaction, an increased surface roughness is formed together with irregular shapes of cavities and pores. Not to mention, the value of this example as it explores the mixing of concrete – which is proven to have a bioreceptive performance – with glass elements as a potential alternative for further exploration. Specifically, (Siddika et al., 2022) mentions that studies focused on examining the recycling of automotive shredder residue as a binder or aggregate in concrete, report that the high expansion possibility from the alkali-silica reaction and low adhesion between these two materials, have led to the conclusion that only around 30% of waste glass is optimum for mixing with cement paste, providing proof for the experiment reported in Figure 27.

Figure 26. Photographs depicting the reacted sample of cement and aluminosilicate and its produced surface roughness and porosity.

Image Source: by Bristogianni T. 2022.

### 2.2.3. Porosity from recycled glass

The starting point of this new bioreceptive material, as concluded from the previous chapter is to obtain inner-porosity and surface roughness, while the research's objective is to use glass waste as a raw material. While porosity and glass are not terms that go together, porosity and foam glass do. As the main product coming from glass that not only generates lower density with a cellular structure, but also in its production method can incorporate waste as the main material, sounds like an ideal solution. If a type of glass waste can be crushed and grinded until the level of a refined powder can serve as the basis of the foam, that combined with foaming agents or other additives can form the final recipe. The most common way of producing it, is by heating the mixture near the melting point, that the agent releases gas forming the bubbles on the interior. When cooled, the mixture solidifies with the remaining voids, offering its light weight and low density.

However, there is one major obstacle that must be investigated further both with literature review and experiments. This, is the uniformly distributed closed pore structure that foam glass as we know it, produces. In principle, its outstanding advantages from the closed-cell porosity, offer thermal and acoustic properties joined with high strength. One critical point in its manufacturing method for insulating applications is the stage that the pores start coalescing in the glass matrix and a non-uniform structure might be resulted. This is avoided with the use of chemical stabilizing agents, rendering its manufacturing method highly unsustainable (Siddika et al., 2022).

Another inspiring method of producing porosity by recycling glass waste shows the research of Ferrándiz-Mas et al. (2016) by sintering crushed soda-lime glass. By adjusting the glass particle size and its distribution, in combination with the re-manufacturing conditions they investigate the relationship controllable porosity and water absorption, which are the main objectives for a bioreceptive material. Due to the sintering method used, the investigation focuses on the correlation of the level of bio-growth with the light transmittance, depending on how porous the resulted samples are by testing different sintering temperatures.

After checking these two methods of producing different types of porosity in recycled glass materials, reviewing the term of a porous material is important to delve deeper into the characteristics that matter for bioreceptivity. Hasanuzzaman M. who investigated the production of porous glasses to study their thermal behavior, mentions in his thesis the following definition for a porous material by International Union of Pure and Applied Chemistry, 'Any solid material which contains caivities, channels or interstices may be regarded as porous, though in a particular context a more restrictive definition may be appropriate' (Hasanuzzaman M., 2013). Apart from the aforementioned ways focused on recycled glass, for new glass mixtures the sol-gel process, and especially for borosilicate glass also the phase separation after leaching of the alkali borosilicate glass system, are mentioned to result in microstructure ranging from 2 to approximately 50 nm pore sizes.

From the findings, it was concluded that the porosity is inversely correlated with the temperature and therefore to light transmittance, since the highest porosity of approximately 33.5% achieved at the sintering temperature of 680°C (Figure 20). Thus, the higher the temperature the denser the material became with lower porosity values, reaching the 17.8% at 740 °C (Figure 20). It is important to mention, that these samples were compared with the porosity produced from mixtures out of Portland cement, in order to provide argumentation for the suitability of this new method for obtaining bio-colonization, compared to porous concrete. Regarding the measured pH of the samples, it was observed that higher porosity was leading to higher pH values, reaching to the conclusion that these samples were allowing more the alkaline leaching ingredients from the glass.

As it was expected, lower sintering temperatures producing higher porosity tiles showcased in general the highest biofilm growth, with the lowest light transmittance. According to the results of the chlorophyl-α extraction, samples sintered at 700°C had the highest values of bioreceptivity up to 11.09 ±0.44 μg per cm$^2$ of tile (Figure 21) (Ferrándiz-Mas et al., 2016).

It is an undeniable fact, that this work presents promising results not only towards the direction of porosity, but also to the bio-colonization as a whole. Specifically, the sintering method can also be correlated with the fusing glass process – analysed in the next paragraphs (Figure 24) – as another way of producing porous glass.

Out of this overview for the different possibilities to provoke porosity in the material's microstructure from recycling glass, encouraging evidence is sought in the treatment of other glass waste sources, excluding crushed soda-lime bottles which have already a closed-recycling loop obtained. Then, focus is given in the production of glass foam and how to overcome the problem of closed-pore network, since this solution could include unlimited choices of unutilized glass waste that can be examined for the glass recipe.

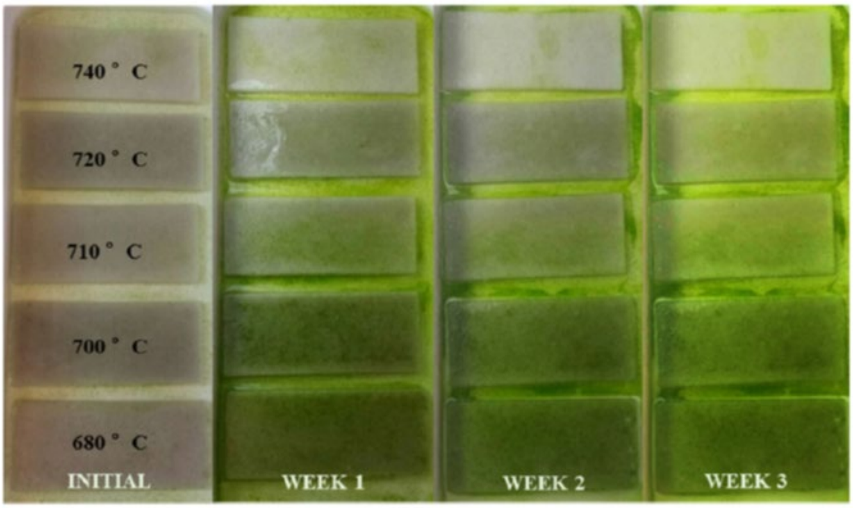


Figure 28. Image of the pH conditioned tiles in the period of 1-2 & 3 weeks of bio-growth of Chlorella Vulgaris. Image Source: Fig. 7, page 8,

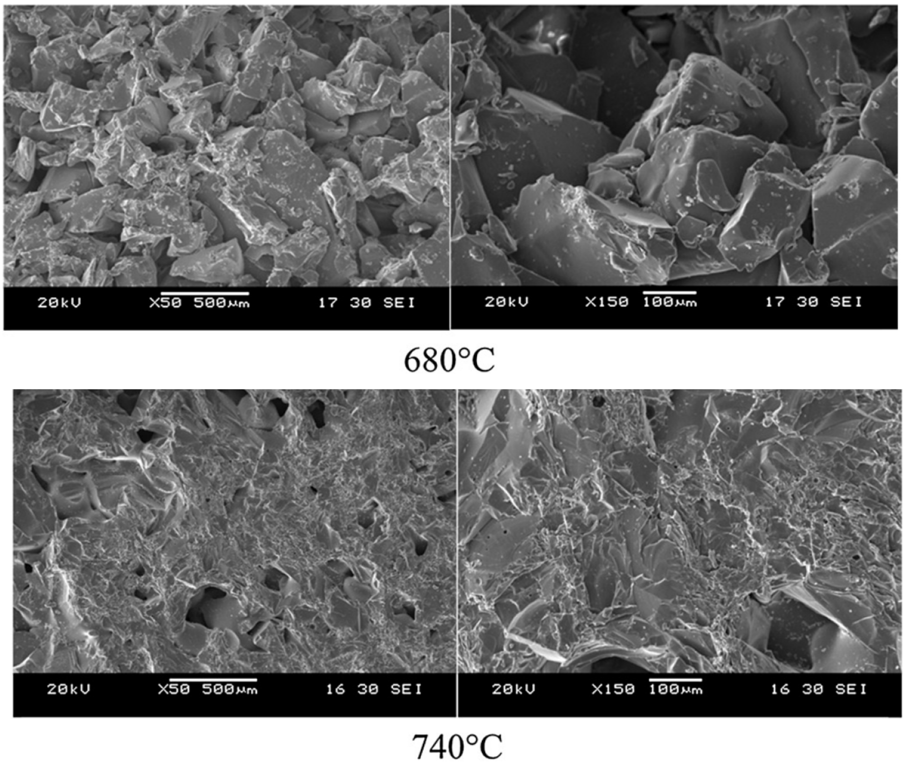


Figure 27. Microscopic images for the sintered samples of 680°C and 740°C, showing the relationship between porosity and temperature. Image Source: Fig. 6, page 7, (Ferrándiz-Mas et al., 2016)

### 2.2.4. Producing foam glass (method – parameters & case-studies)

What makes foam glass worth of investigating its potential as the main material for this new application of bioreceptivity is firstly the fact that its porosity in general is usually around 60% and higher (Souza et al., 2017), while the rest of the analysed materials have around 30% (Lubelli et al., 2021; Veeger et al., 2021), which can also be verified in the findings of Table 4. Secondly, its ability to replace at least 70% of its initial raw material used in the production process with waste (Hesky et al., 2015). The term up-cycling is referring to the introduction of waste in the manufacturing of a new product, however sustainability in terms of produced carbon emissions and cost-effectiveness are dependent merely on the chosen production method. Thus, when discussing such innovations these aspects should also be considered (Siddika et al., 2022).

#### 2.2.4.1. The production method

The method of producing foam glass, or 'cellular glass' from glass batch was discovered in the 1930s by I. I. Kitaigorodskii. It is an extremely useful and promising material due to its unique set of properties: excellent heat insulation behaviour, fire, moisture and frost resistance, low density and ease of instalment or work (Samoilenko & Tatarintseva, 2013). Current uses in the construction industry are focused mainly on the building insulation and on the development as a lightweight and robust additive to concrete mixtures, providing insulation properties. Recent discussions have also focused on the benefits of glass foam for acoustical applications, where open porosity is demanded (König et al., 2020).

Regarding the manufacturing process, among a variety of techniques such as gelcasting, sintering, or replication, foaming and incorporation of foaming agents are the simplest and most preferred ones. During foaming, finely fragmented particles of glass with their additives are heated, and through the gas emission at high temperature, the hot glass is foamed, forming a cellular composition that needs to be slowly annealed and cooled down to a room temperature (Samoilenko & Tatarintseva, 2013). Out of numerous experiments that have been held testing different foaming agents and their ratios combined with different sources of glass, it is proven that the particle size of the foaming agent affects greatly the pore size generated by the foaming decomposition (Bernardo et al., 2010; Souza et al., 2017).

#### 2.2.4.2. Main material

For the glass source used in the glass foam recipe as the main material, in the scientific papers reviewed it was stressed out the importance of recycling wastes. Different kind of glasses were mentioned, with different additives, foaming agents and last but not least different firing schedules according to the goal of the glass foam. For instance, whether open porosity was demanded for acoustical purposes or a closed network for insulation and robustness to be used in the building industry, as a competitive material for the existing commercial ones.

CRT glass both panel and funnel, was investigated as a great source of waste to be recycled, with the addition of eggshells as a foaming agent (Fernandes et al., 2014). By comparing the thermal behaviour of the two types of glasses with the same additive as well as portion, can provide some concrete evidence for which main ingredient to choose, if for example the lowest temperature is an important factor. Out of the thermal behaviour, key aspects to monitor for comparison is the temperature where the sample undergo the maximum shrinkage. According to proof when comparing the two types of CRT glass, -panel and funnel-, the one with the lowest refractoriness presented shrinkage at a lower temperature, while also the expansion trend by releasing air/$CO_2$ was immediate. This, can be justified by lower $SiO_2$ content as well as richer PbO of the funnel, in contrast to the panel that has more BaO.

### 2.2.4.3. Foaming agents

It is important to note that the different production methods can also define the pore structure in both macro and micro scale. In addition, as the choice of foaming agent has already been stressed out, it is important to also distinguish their role: there are the ones that cause foaming by thermal decomposition, meaning that they 'decompose above the glass softening point by releasing gases', and the rest that react with the chemical composition of glass above its softening point when glass's phase change from solid to liquid. Furthermore, they can also be distinguished in two categories, depending on their chemical reaction: 'into the neutralization foaming agents (carbonates, sulphates, etc.) and the 'redox foaming agents' (silicon carbide, silicon nitride, manganese dioxide, carbon etc.) (Hubálková et al., 2017). For glasses that contain hazardous chemicals, and large amounts of heavy metals, it is more suitable to use foaming agents that decompose like carbonates ($Na_2CO_3$,$CaCO_3$, $MgCO_3$,etc), in order to avoid heating processes in higher temperatures as well as the formation of toxic oxides out of the chemical reaction with these metals, that could be easily contaminate in later uses (Fernandes et al., 2014).

In a comparison between the main foaming agents, such as calcite and dolomite, with eggshells, the content of $CaCO_3$ was found crucial, as it was almost equal to their weight loss due to the release of $CO_2$. To this, even the chemical elements of the agents' composition play an important role, since dolomite presented -out of the three- the highest difference in weight (Curve D, in Figure 29) only because magnesium has higher molecular mass than calcium. In addition, the organic content of eggshells helped in their thermal decomposition at lower temperatures (Fernandes et al., 2014). These observations from testing, act as a guideline for predicting the foaming behaviour of the ingredients based on their chemical composition, especially when such elaborate testing and tools are not available.

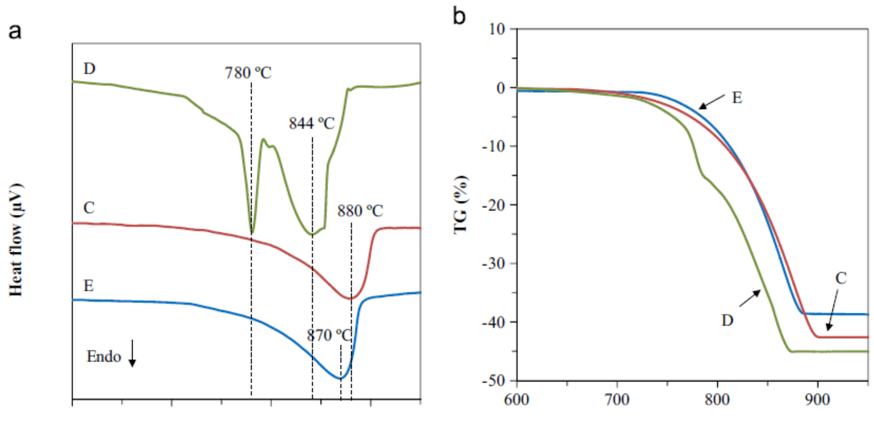


Figure 29. Thermal analysis curves of foaming agents: (a) DTA and (b) TGA, D: domolite, C: Calcite, E: Eggshells, Image Source: Fig.1, Fernandes et al., 2014.

### 2.2.4.4. Microstructure on experimental examples

For controlling the microstructure it is important to note, that the particle size distribution and composition of the glass powder as well as the foaming agent, together with the heating process (rate, temperature, and cooling) define the pore formation and structure. One way to produce various pore sizes, is to vary the particle size of the pore foaming agent used, which can result in a mixed porosity type of not only closed and open, but also a varying combination of those. Regarding the process, heating and cooling time is important, as gravity can prevent the mixture's expansion, since coalescing and pore collapse can be caused by extremely low viscosity. Ultimately, all the above including the pore size, strut (wall) size arrangement and their connections determine the mechanical, thermomechanical and hydraulic properties, of the foam (Hubálková et al., 2017).

For this study, as it was analysed in the first chapters, the manufacturing method of glass foam as well as the recipe are investigated under the lens of achieving the best combination of porosity structure, in size and connection to meet water absorption and retention capabilities that benefit the bio-growth. One of the major problems of this novel experiment is the closed pores in the common glass foam materials, that favour high compressive strength, as well as moisture resistance – properties highly – sought after for thermal insulation applications. For these reasons, combinatorial information in the studied papers elucidates this potential, by further discussing different recipes tested and their production sequence to achieve an open-pore network, with water retention capabilities.

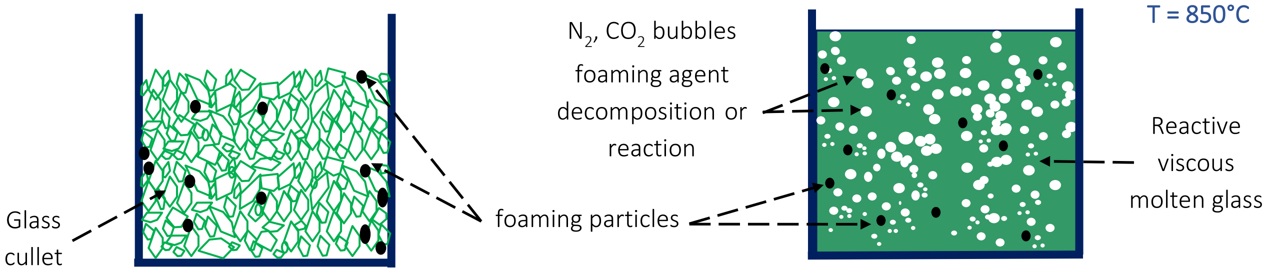


Figure 30. Diagram explaining the formation of foam glass out of glass powder mixed with foaming agent.
Source: (Lebullenger, 2012)

In the reviewed literature there a number of examples, that have studied glass foams, either with mathematical models as a tool to predict the bubble sizes and growth formation, depending on the glass viscosity and surface tension (Fedosov et al., 2018), or because it consists a major problem in the glass melting furnaces (Fedorov & Pilon, 2002). Out of these reports, better knowledge can be obtained not only on the key aspects that influence the pore radius growth during glass foaming, but also in the process itself. It is explained by Fedosov S. et al. (2018), that for mathematical models simulating the bubble expansion, diffusion processes should also be incorporated, since significant role to the porous structure formation has also the 'mass transfer process of glass melt along a pore surface'. Another useful insight is that, for products targeted to be used for insulation with good structural performance – which is the main current application for foam glass-, the goal is to achieve a uniform microstructure in the distribution of pores.

What's more, regarding the manufacturing process, the foaming temperature should be above the softening of glass and simultaneously from the point of gas agent decomposition. In Figure 32 is shown schematically, how the external boundaries of voids are formed while glass is sintered. Thus, to produce a foam with lower density, it is these pores radius that should grow depending on the gas content that determines the pore-forming potential. In further detail for this procedure, dissolved oxygen in the glass volume existing around the pore surface, is the cause that gas is generated, due to its chemical and physical interaction with carbon, CO, or $CO_2$ (Fedosov et al., 2018).

Research on the production method has revealed useful information regarding the importance of the overall recipe in the working temperature decrease of the furnace and the impact of the porosity on the mechanical properties. First and foremost, Samoilenko & Tatarintseva (2013), in their experiments worked with microcalcite instead of the traditional carbon foaming agents, which are reported to be:

soot, coke, anthracite, peat charcoal etc., to lower the foaming temperature, which is generally above 800$^{O}$C. In the Table 5, one can observe all the steps and the parameters tested analytically, as for example the different temperatures tested (725, 750 and 775 °C). Out of these experiments, it was verified that as the foaming temperature or/and the heat-treatment time values raise, the material density gets lower. Similar findings are noted in regards with the foaming agent increase (Samoilenko & Tatarintseva, 2013). However, there is a limitation in the latter, as it is reported that when used in amounts greater than 30wt% of the mixture, the porosity decreases (Souza et al., 2017), or even when it exceeds the quantity of an agent, the material crack and fails.

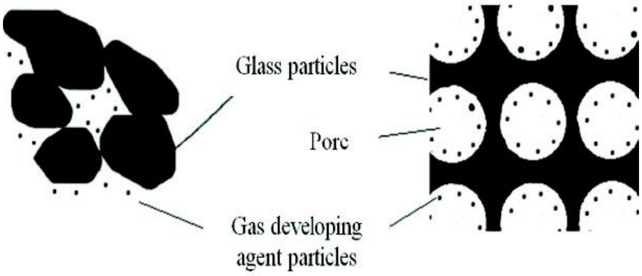


Figure 31. Diagram portraying how pores are formed from the initial state and during the sintering process of glass with the gas agent in the mixture. Pores are spherically depicted, for easier mathematical calculations that allow a 5% error instead of polygonal shapes that increase complexity.

Image Source: Fig. 1, page 2, (Fedosov et al., 2018)

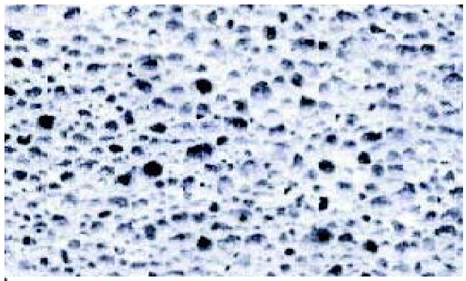

Figure 32. Image showing the final pore matrix after the initial formed pores radius have interacted with each other.

Image Source: Fig. 2, page 3, (Fedosov et al., 2018)

Studying the bubbles' formation during the foaming process that create the pore network in glass foams, the work of Fernandes et al. (2014), is the only one out of the reviewed papers, that addresses the different sizes in microstructure along the specimens, as indicated in Figure 35. Due to the effect, that air bubbles rise inside the mixture and coalescing takes place depending on the foaming time, this density gradient is observed, from the bottom to top. This happens mainly because of the density difference between the tested CRT glasses and air, but also the potential formation of different viscosity flows alongside the glass powder, resulting in such inhomogeneous examples (Fernandes et al., 2014).

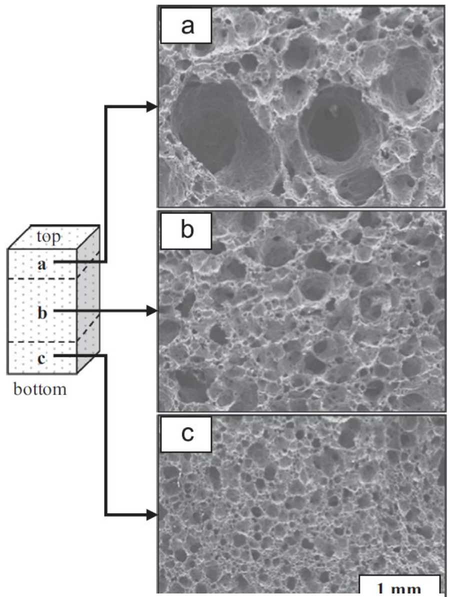


Figure 33. SEM micrograph of a specimen with panel CRT glass, with calcite foamed at 700°C for 15 min, presenting differences in the pore size and network along its height.

Image Source: Fig. 5, Fernandes et al., 2014.

What was striking in the findings of Samoilenko & Tatarintseva (2013), was that the higher the temperature together with the higher heat-treatment time was not only producing larger-sized pores, but also bigger portion of open pores, an effect that also König et al., 2020, based his work upon by producing open and closed-pore glass foams. Specifically, foam-glass produced at 775 °C had lower density, but larger pore size than the other samples, measuring approximately 2-3mm, which are greatly larger than the ones of concrete for example that could have a maximum size of 50μm diameter (Veeger et al., 2021). Out of the reviewed papers for glass foams only a few were investigating the water absorption, with the highest values reported in the mixture of Samoilenko & Tatarintseva (2013), with foaming agent 2.5%, that had a 13-17%, in contrast to lower foaming agent's content of 1.5%, that had 5-6% absorption to the lowest density achieved of 250g/m$^3$. Thus, there is encouraging evidence that even though foam glass structure produces closed pores that do not favour water absorption though capillarity, in this particular case and recipe open pores and water absorption were observed.

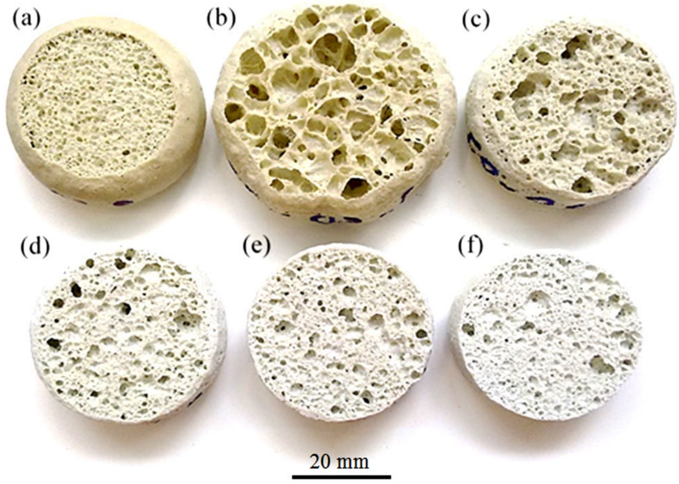


Figure 34. Image showing the porosity, foam expansion and dimensional changes of samples fires at 900 °C / 30 min with different content of eggshells in the mixture, (a) 1 wt%, (b) 3 wt%, (c) 6 wt%, (d) 9 wt%, 12 wt%, ( e) 15 wt% and (f) 30 wt%.

Image Source: Souza et al., 2017.

Shedding more light on the production of open pore glass foams that are studied for acoustical reasons, partial crystallization of the glass during the foaming process is revealed to be the reason for achieving the desirable type of porosity for bioreceptivity. Due to this, glasses that tend to crystallize can be a valuable option for the recipe, whereas in any other applications would be seen as a problem. Through 'heating microscopy' is important to define the optimal foaming temperature for the transition from closed to open pores, with mixtures of low density, always dependent on the glass softening point. In this reviewed study, open porosity was caused by finely milling bottle gas powder, while in other studies it is supported that this effect can also take place with the addition of $TiO_2$. It is stated that, ''the crystalline content increases with the increasing foaming temperature and the decreasing heating rate. However, open porosity should be in balance with the density, thus crystallization rate should be predicted. Specific values of the levels of open porosity are gathered in Table 4, in order to draw conclusions for the value of this research for our goal, by comparing with the measurements from other bioreceptive materials which were investigated in the previous chapters. It is important to keep as a general note, that percentages around 91% for open porosity were obtained, with a pore size larger than 100μm reaching even 2-3mm (König et al., 2020).

Thus, open porosity is observed merely because of crystallization that causes pore walls to break, while instantly the pore size cannot be increased due to overpressure inside the pores. As expected, larger pores and wider distribution lead to lower density. Compressive strength is mainly proved to be affected by the pore size and pore distribution. Therefore, homogeneity is preferred for good mechanical properties. Therefore, by modifying the foaming temperature and heating rate not only the density can be controlled, but also the percentage of an open pore network.

Promising is also the work of Hujova M. et al. (2020), about the formation of glass-ceramic foams from glass waste of Soda-lime and Borosilicate glass, combined with Vitrified Bottom ashes (VBAs). The latter, is a by-product produced from the incineration of mixed municipal waste, consisting at a percentage of 90% from minerals and glass. Even though, the addition of glass waste and especially pharmaceutical helped the foaming process by alkali-activation and then mechanical stirring and sintering, the final products were extremely brittle, followed by a 3.7 (±0.5) MPa compressive strength as the best result (Sample: BSG addition, heated at 900°C) (Hujova et al., 2020). Despite this undesirable property, worth of investigation appears to be not only that all the samples were extremely porous -approximately 70%-, but also that their pore-network was open, which is the property that we seek to engineer for the study of bioreceptive glass foams.

While searching in literature for examples of open porosity, different production methods of glass foams were reviewed. From these, powder foaming was the one chosen mainly because of the evidence found on the paper of König J. et al. (2020), where refined powder of soda-lime glass was used to create open porous foams for acoustical purposes, as aforementioned. Points for further research could include the investigation of which of these methods can provide the most sustainable solution to produce glass foams that meet the requirements of bioreceptivity.

Although there are examples of research that test and discuss the relation of temperature-time to reach the optimal values for the foaming process, since there are many variables that can also have an impact according to the goal of each experiment, each case should be studied critically and not in comparison, if exactly the same ingredients are not used.

| Researcher | Parameter Tested | Main Ingredient(s) | Foaming Agent | Heating Temperature (°C) | Time (min) | Time (min) / Rate | Foaming Temperature (°C) | Time (min) / Rate | Annealing Temperature (°C) | Cooling Temperature (°C) | Time (min) / Rate | Conclusions | Considerations |
|---|---|---|---|---|---|---|---|---|---|---|---|---|---|
| Samoilenko & Tatarintseva (2013) | (1) Foaming agent content (1.5, 2.0, 2.5 wt.%) (2) Foaming Temperature *(725, 750, 775°C) (3) Heat-treatment time (30, 45 and 60min) | - | microcalcite | 20 - 600°C | 120 | 5 K/min | 600 - x* | 1 K/min | 600-200 | 600 | 5 K/min | Lower density samples are produced by increased foaming temperature + prolonged heating-time, that showcased larger pores in size & bigger open pore network, achieving water absorption of 13-17%. | What happens when Density is even lower due to microcalcite quantities larger than 2.5% leading to the increase of the pore size and pores coalesce |
| Hujova M. et al. (2020) | (1) Production of glass-ceramic foams from VBAs with the addition of glass waste, through alkali-activation (2) Mechanical properties (3) Chemical composition | (1) Vitrified bottom ashes (VBAs, mean particle size<75μm) combined with (2) Soda-lime glass (SLG, mean particle size<30μm) or (3) Borosilicate glass (BSG, mean particle size<75μm) | - | developed by suspension with aqueous solution, then mechanical stirring and left at 40°C for 48h | 2880 (48h +) | 10°C/min | 850-1000 | 60 | - | - | 5°C/min | (1) Samples extremely porous (>70%), with mainly open porosity (2) Glass addition aided the production method and lowered the sintering temperature (3) The mixture with Boroscilicate glass **presented the best strength (3.7 ±0.5 MPa) with open porosity.** | (1) Mixtures with only VBA, were too brittle (2) Chromium ions were included in mixtures that sintered in higher temperatures, where in lower values it stayed in the amorphous phase. |
| König J. et al. (2020) | For fully closed porosity foams: (1) synthesis, (2) structure (3) thermal conductivity | Closed porous specimens: (1) CRT panel glass | (2) 0.44 wt% carbon (3) 5.97 wt% Mn3O4, (4) 1.85 wt% potassium phosphate (K3PO4) | | 40 min | 5°C/min | 740-820 | 7 °C/min | 550 °C | to room temp in the furnace | | (1) Density can be controlled by modifying the foaming temperature, (2) Decreasing density decreases thermal conductivity | |
| König J. et al. (2020) | For fully open porosity foams: (1) synthesis, (2) structure (3) thermal conductivity | Open porous specimens: (1) 33 wt%/67 wt% container/flat soda-lime-silica glass) | (2) 0.33 wt% carbon, (3) 4.45 wt% iron(II) oxide Fe2O3, (4) 1.66 wt% calcium hydrogen phosphate (CaHPO4) | 200-600 | 40 min | 5 - 15 °C/min | 840 - 880 | 7 °C/min | 550 °C | to room temp in the furnace | | (1) Partial Crystalization during foaming led to open pore formation. This was triggered by using a finely milled bottles glass powder as the main component. In contrast to other studies, where this was achieved through the addition of $TiO_2$, (2) foaming temp and heating rate control pore size and density, the bigger the size the less dense the material. | compressive strength measured is adequate for load-bearing operations |
| Siddika A. et al. (2022) | (1) Use of car windshields as a raw material for glass foams, (2) Stabilisation of pores in a modified curing-sintering method | automotive vehicles' waste glass | (1) reagent grade calcium car-bonate (CaCO3 with >98% purity) of about 1-3 wt% of the raw mix, (2) Low calcium type Fly ash (to improve the stability of the raw mix) | room - 800 | 10-60 min | 5°C/min | 800 (sintering) | - | - | 800-room | naturally inside the furnace | (1) Open porosity found on samples without Fly ash, (2)Amorphous silica shows high pozzolanic reactivity->car windscreens are suitable for the curing-sintering procees, (3) $Na_2O$ acts as a softening agent, (4) PVB plastic layers can negatively impact foaming process, (5) sintering influences the pore expansion & distribution, (6) increasing sintering time decreased total porosity and open pores turned to closed ones thus higher density, (7) Fly ash aids to pore stability and homogeneity but refrains pore expansion, increases density but lowers thermal conductivity since it leads to more refined pore structures | |
| (Fernandes et al. (2014) | Eggshells as a foaming agent | CRT glass waste (panel & funnel) and eggshells replacing foaming agents | eggshells 3 wt% crushed and dry-milled to 8μm particle sized | | | | 650 - 750 | | | | | | |

Table 4 Overview of foam glass experiments, production parameters and conclusions - considerations for further research.

### 2.2.5. Conclusions (waste for porous glass & production method)

Out of the methods presented for producing porosity from waste glass, foam glass is chosen as the one to be investigated through experimental work. The primary reason that this is decided, is that through the detailed review presented in this chapter, its properties show great potential, that is not yet explored, since currently is only being used as an insulation material, demanding high values of a closed-cellular network. What's more, its ability to integrate glass waste through the form of powder makes it even more promising to be explored under the conditions of bioreceptivity, which embrace its specific characteristics of surface roughness, porosity and low density.

Apart from these, when it comes to sustainability from an energy aspect, the manufacturing method of foam glass also presents certain benefits in comparison to casting glass waste. As it was reported from the already carried out experimental work in the Glass department of TUDelft, in order to recycle different glass recipes higher values of temperatures are needed to obtain products not crystallized, with a good working flow for intricate moulds. Specifically, these temperatures are far above 900°C and in most cases reaching 1120°C, in contrast to the foaming temperatures that reach the optimum around 840°C. In favour of this argument, the sintering method of glass cullet in producing porosity should also be mentioned, that the lower the temperature the more porous the material remains – around 740°C -. However, this process is not chosen to be studied, due to lack of relative equipment and the fact that it produces semi-transparent objects, which is deemed unnecessary for this specific application where the optimum bio-growth is desired, but most importantly because the already tested glass recipe in the experiment of Ferrándiz-Mas V. et al. (2016), uses soda-lime glass - the only type of glass being recycled at the present. While, this thesis aspires to bring a more innovative solution by using other unutilized sources of glass waste.

In combination with the findings of the previous chapter, regarding bioreceptivity and its conditions there is still one remaining question until now, not answered with clarity from the literature review. Whether glass foams can be produced with capillary porosity that provides adequate water absorption and water retention for microorganisms to survive without heavy maintenance, by thriving longtermly on this material than any other substrate.

Encouraging evidence was found in the work of Samoilenko & Tatarintseva (2013), where in the samples rendering unsuitable for building insulation, water absorption and open pores were observed. In addition, Hujova M. et al. (2020) combined another type of waste: VBAs that when combined with borosilicate glass waste, produced highly open porous samples but with very low mechanical strength. However, because the latter example used a different method for foaming, than the most common, further investigation needs to be done to conclude whether these findings can be of a use for this specific study. Finally, the idea of adding another organic material in the mixture, that by the end of the process will on the one hand be eradicated by the high working temperatures, but on the other will have left voids in the microstructure leading to open porosity, will also be considered as a possible solution. For instance, these organic materials could be straws or fur that is used at the present for insulation purposes.

What is most valuable for the specific goal of this project, derived from the conclusions of the literature review, is to firstly analyse and illustrate the potential with tangible measurements of the porosity type and pore characteristics of the glass foams to be tested from different glass recipes out of waste. Particularly this is achieved, through sections studied under the digital microscope, as well as, water absorption and evaporation experiments performed for validity. Such measurements form tangible evidence about the bioreceptive potential of the materials, that explain the findings regarding biofilm formation.

In the case, that the aimed capillary porosity cannot be achieved with glass foam structures, which is an argument that needs more advanced testing methods, than the ones used in this thesis, to be verified, the solution could be derived from the design of the meso-scale addressed in the next sections (Chapter 4). Another possible outcome, based on the literature findings could be that the desirable open-pore structure results in very brittle behaviour or the altered heating schedule creates cracks resulted from stresses developed due to rapid cooling, rendering the material unsuitable for building applications. For such conclusions, the best compromise, depending on the case study and the designer's input, can be found regarding the choice of a less-porous glass-foam, but more robust in its mechanical properties, that by the manipulation of the surface, the final product is able to receive life in a favourable environment.

# 3. Engineering the micro-scale

## 3.1. Experimental criteria for bioreceptive foam glass

The scope of this project is to investigate the maximum bioreceptive potential of the new material that is under testing and compare its efficiency to other ones, which until now are only developed in lab experiments, unfortunately. Since the novelty of this research cannot be fully-advanced, the strategy to reach the set goals will be designed and explained with the knowledge obtained from the experimental process that is going to be realized and presented in the next chapters.

For this, certain criteria are already defined from the analysis of the literature findings. In detail, the experimental process is going to focus on engineering micro-scale of the material for stirring bio-growth. The first one is to investigate for the best fit among the sources of glass waste, which currently end up in the landfill. The parameters to define this suitability are: the capillary porosity leading to primary bioreceptivity, connected to the sample's enhanced surface roughness and the critical brittle behavior that the previous might result.

Therefore, experiments assessing the water absorption and retention capability of the samples aim to reveal the one with the best performance, in order to validate the most suitable porosity network for bio-host glass. For this to be achieved, samples were prepared in batches, so that feedback gained from the tests could be incorporated into the next recipes under examination. Apart from porosity, material's ingredients are crucial to be filtered both for their chemical composition, but also the sample's resulted pH, as these factors might affect the ability for colonization. Not to mention, that final specimens' result should contain phosphorus as a nutrient for the microorganisms, because it is not contained in the air or water (M. Veeger, personal communication, February 25, 2022). Such an example are the eggshells, that are used in a considerable number of experiments, by replacing the foaming agent since they are rich in calcium carbonate by 95% ($CaCO_3$), while the remaining 5% contains calcium phosphate, magnesium carbonate and other soluble and insoluble proteins (Fernandes et al., 2014; Souza et al., 2017).

## 3.2. Experiment Design Set-up

The general experimental set-up is comprised by a series of smaller tests, taking place at a specific sequence, in order to provide valuable feedback regarding the tested values' suitability of the parameters under investigation. Figure 38 illustrates this workflow, where it is evident that after the first group of studies, related to porosity, contact angle and permeability, their results let to the decision of the recipes and manufacturing process for the second batch of samples. Then, in further detail and scientific rigor water absorption and evaporation rate assessment tests were conducted to all the samples, to enumerate their hydraulic performance as the main indicator for their bioreceptive potential. Taking these into consideration, the most promising specimens were tested for their compressive strength to offer tangible evidence for comparison with other developed materials in lab experiments studying biofouling. Similarly, moss-growth was also explored to validate the previous findings and assumptions. The overall goal of this experimental process is to offer evidence to future researchers and designers regarding the material properties and the potential of this new material in the building industry, since glass foams were not explored before under the lens of bioreceptivity

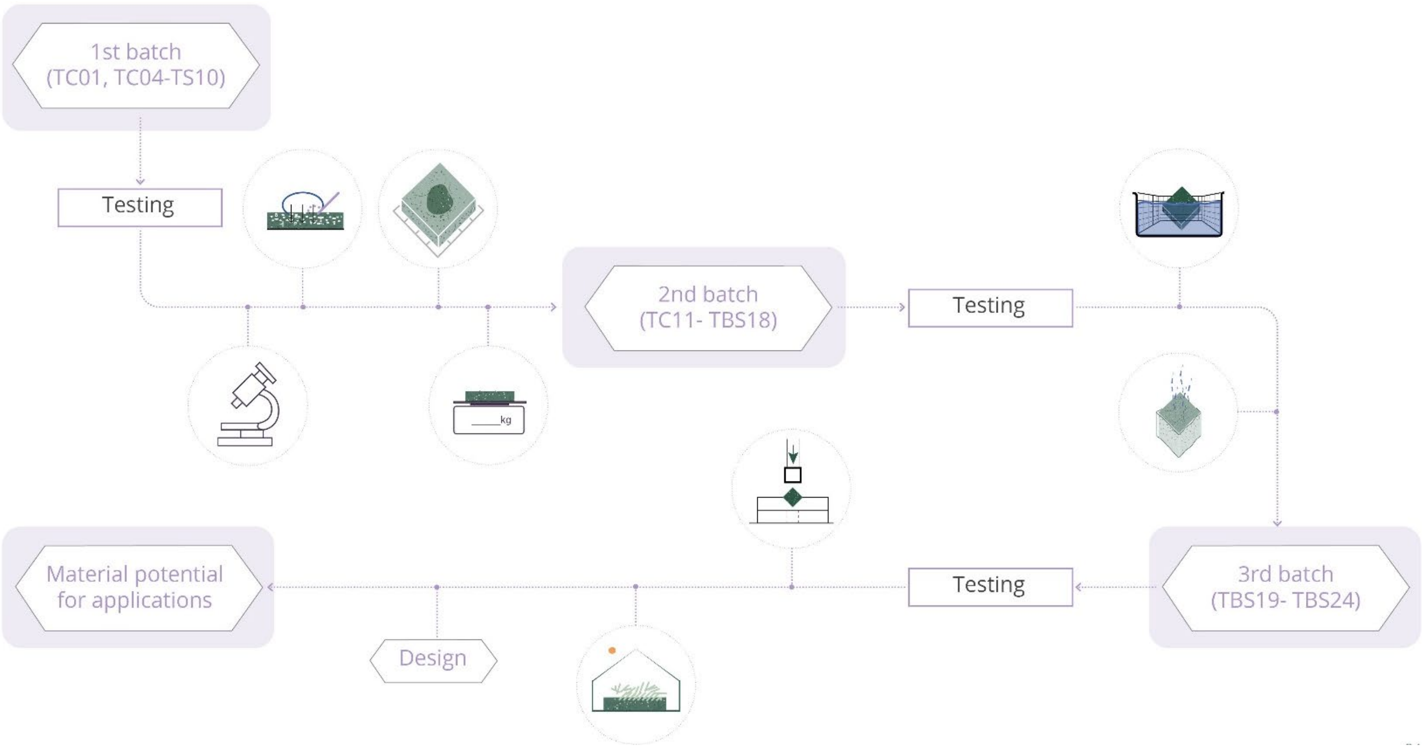

Figure 35. Overall set-up of the experimental process and findings analysis towards the answer of the research question.

### 3.2.1. Tested Parameters

The scope of this research is to produce a series of glass foam samples to compare them for their primary bioreceptivity potential, through analysing their capillary porosity and later on, their strength to assess their potential for the construction industry. The parameters that need to be analysed to reach this outcome are numerous, and can be divided into the ones that affect the main mixture's ingredients, whereas the rest define the manufacturing process, and especially the temperature-time relationship.

#### Mixture's ingredients

The first and foremost element for investigation, as seen in Figure 36 is the glass waste source. Since, the conventional method of manufacturing glass foam is through carbon foaming agents, the different kind of agents, together with their percentages is the second one to be tested. Leading to the third, which is the potential of other additives, depending on the previous ones chosen and their reacting effect. The listed inputs in the three categories are based on the findings of the previous chapters, indicating general suggestions for the topic of this research, however the specific scope was limited to the exploration of only a few inputs that are highlighted in the discussed diagram.

#### Top temperature for foaming

Furthermore, the next set of parameters is related with the optimal temperature-time relation to obtain a product, as described in the paragraph of Experimental criteria for bioreceptive foam glass. These are seen exactly in Figure 37, and their values were chosen based on literature findings together with previous experimentations of *Glass & Transparency Group* of TUDelft, described in the previous chapter. In further detail, higher temperatures for samples based on their mixture's chemical reaction, are expected to lead to more reactive and therefore porous samples. Whereas, for recipes leading to porosity from fused particles lower temperatures were chosen as more beneficial.

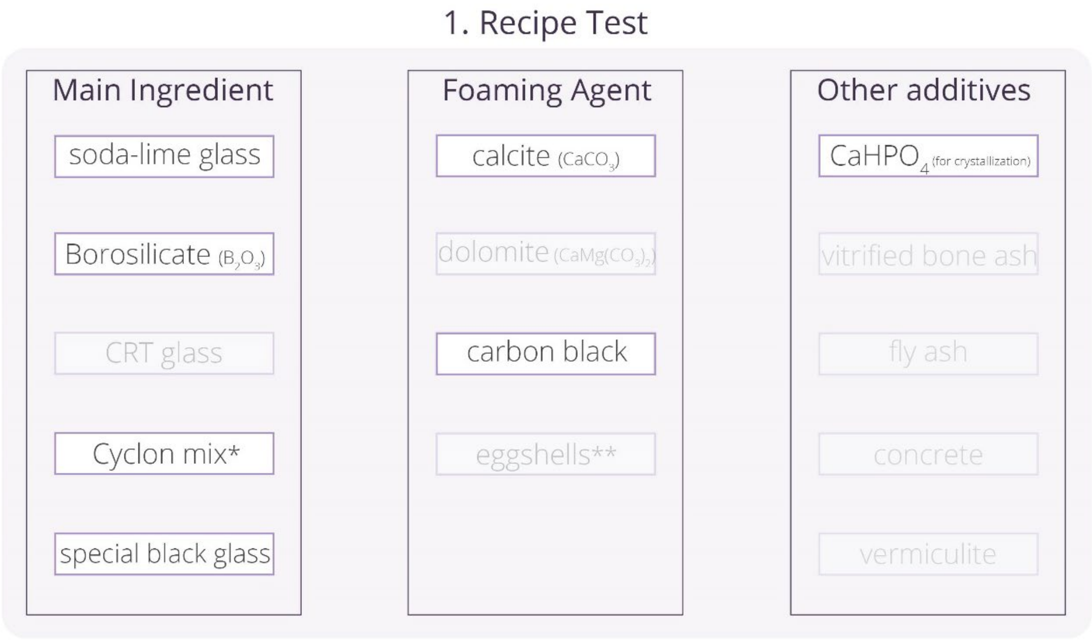


Figure 36. Different parameters related to the mixture's recipe, glass waste-foaming agent-additives. The list of values for each of them are an indication of what can be tested according to literature related both to glass foams and bioreceptivity.
* refer to Appendix_Table 1 for chemical composition.
** 95% contain of $CaCO_3$.

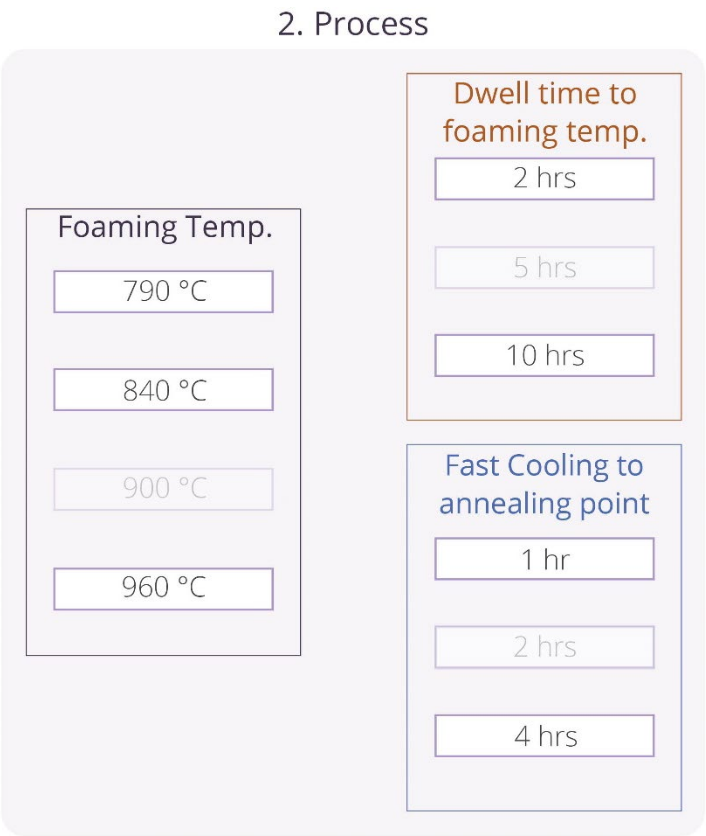


Figure 37. Parameters related to manufacturing process, foaming temperature-heating rate-cooling rate. To these, it should be added the dwelling time, which was not investigated thoroughly. Foaming temperature is always dependant on the main material used, as it should be defined according to the temperature of glass softening. Thus, this set of parameters describe the heating schedule for glass foaming, upon variant results can be achieved.

### Heating & Cooling rate to annealing point

What’s more, the heating rate and the fast cooling rate to annealing point as well as the dwelling time of the at the top temperature are parameters greatly affecting the microstructure of the material. Notwithstanding the limited time of this project and the restrained number of samples produced, this set of parameters was greatly investigated.

### Particle Size

Related to the ingredients, another crucial parameter is the particle size. This, was not conceived as a unique variable on its own from the beginning of the process, instead it was only after the first porosity results under the microscope that revealed the great impact variant sizes either in powder, or in cullet have had in the porosity network. Similarly, the homogeneous mixing can affect the outcome, however this was not feasible to be explored, due to the possibility of mixing the ingredients with only one possible way.

The proposed testing method to obtain results is investigating in the produced samples one parameter at a time, however due to time constraints and project’s broad scope, multiple parameters aimed to be tested resulted in a more dynamic process of selecting the changing variables each time. Hence, extreme cases were firstly being tested, and then middle values for completeness and better-informed guesses for the next steps. Values for each parameter, were being tested in sets of three, in order to obtain a representative range of the different behaviors of the material. For instance, the foaming temperatures obtained in the oven () were: (1) 790°C, (2) 840°C and (3) 960°C.


Figure 38. Overview of the produced samples analysed in Table 5.

| Sample | Recipe description | Main material as 1ST tested parameter | Foaming Agent as 2nd tested parameter | Top Temp. as 3rd tested parameter | Dwell time to top temperature as 4th tested parameter | Cooling rate to annealing point as 5th tested parameter | Cullet size as 6th tested parameter | Mould shape as 7th tested parameter |
|---|---|---|---|---|---|---|---|---|
| **TC01** | Cyclon mix*, no foam. additive, 840°C, slow cool | • | | | | | | |
| **TT02** | Black Glass mix powder, no foam. additive, 840°C, slow cool | • | | | | | | |
| **TT03** | Fiber Glass powder, no foam. additive, 840°C, slow cool | • | | | | | | |
| **TC04** | Cyclon mix* + $CaCO_3$ (10%), 840°C, slow cool | | • | | | | | |
| **TC05** | Cyclon mix* + C + $CaHPO_4$, 840°C, slow cool | | • | | • | • | | |
| **TC06** | Cyclon mix* + C + $CaHPO_4$, 960°C, slow cool | | | • | | | | |
| **TS07** | SLS float powder + C + $CaHPO_4$, 960°C, slow cool | • | • | • | | | | |
| **TBS08** | SLS float powder + Borosilicate cullet + C + $CaHPO_4$, 790°C | • | | • | | • | • | |
| **TC09** | Cyclon mix* + C + $CaHPO_4$, 790°C | | | • | | • | | |
| **TS10** | SLS float powder + C + $CaHPO_4$, 790°C | | | • | | • | | |
| **TC11** | Cyclon mix* + $CaCO_3$ (3%), 840°C | | • | • | | | | |
| **TC12** | Cyclon mix* + $CaCO_3$ (5%), 840°C | | • | • | | | | |
| **TC13** | Cyclon mix* + $CaCO_3$ (10%), 840°C | | | | • | • | | |
| **TC14** | Cyclon mix* + $CaCO_3$ (10%), 840°C | | | | | | | • |
| **TBS15** | SLS float powder + Borosilicate cullet + $CaCO_3$ (5%), 840°C | | • | • | | | • | |
| **TS16** | SLS float glass- 2 particle sizes + $CaCO_3$ (5%), 840°C | | | • | | | • | |
| **TBS17** | SLS float powder + Borosilicate cullet + C + $CaHPO_4$, 790°C | | | | | | | • |
| **TBS18** | SLS float powder + Borosilicate cullet + $CaCO_3$ (5%), 790°C | | | • | | | | |
| **TBS22** | SLS float powder + Borosilicate cullet + C + $CaHPO_4$, 790°C | | | | | | | • |

Table 5. Overall parameters tested in the samples produced. The dot is indicating what is different every time from the similarly-previous tested sample. For example, if a Borosilicate & Soda-lime with a specific cullet range and $CaCO_3$ (5% wt) mixture is foamed initially in 840 °C, for 2hrs with cooling rate in -200 °C and the next mixture of the same exactly recipe, is foamed in 790 °C, with -15 °C, then the two variables changed is the foaming temperature and cooling rate.

* refer to Appendix_Table 1 for exact chemical composition. Cyclon mixture is a by-product of the bottle- recycling industry, containing SLS glass heavily contaminated.

### 3.2.2. Material Recipes

In this section a detailed description regarding what was tested is given. To begin with, the 1st set of samples were designed to obtain a first output among completely different sources of glass waste that remain unexplored and unutilized in the construction industry. These specific main ingredients are shown in Table 6.

After this, there was a series of experiments performed according to the recipe of König et al., (2020) by using soda-lime glass, carbon black, iron (III) oxide and calcium hydrogen phosphate, due to the fact that there was indicated clear evidence for open porosity. The suggested additives, apart from the aforementioned main ingredient, were also mixtured with the Cyclon mix, which was one of the main objectives to be explored as an industrial residue currently disposed in landfills. These specific recipes, were greatly experimented in different heating schedules with the aim to achieve an outcome close to literature. Even though, this was not obtained for reasons analysed in the next sections, great insight was acquired regarding the impact of the other parameters on the foaming process in close relation with the ingredients tested.

To the previous, also the testing of the mixture of Borosilicate cullet (50& wt) with soda-lime glass powder (50% wt) should be added. This type of glass was chosen mainly due to previous deviating results from their initial purpose that showcased porosity (refer to section 2.2.2). In addition, literature findings indicate the high propability for crystallization, which was reported as one of the main reasons for observing open-porosity in glass foams (König et al., 2020).

As a foaming additive calcite was also notably investigated in different percentages (3% - 5% -10%) as one of the prevailing ingredient in the glass foaming industry. Encouraging is the fact, that the replacement of calcite as a raw material has been recently explored by eggshells, which contain high percentages of $CaCO_3$. Therefore, once a recipe with calcite is successful for our experiment, then incorporating more sources of waste would constitute an even sustainable solution.

| Sample | Recipe description | Main Glass waste source | Particle size (μm) | Foaming Additive | Mixture Additive |
|---|---|---|---|---|---|
| **TC01** | 840°C, slow cool | Cyclon mix* | approx. 90 – 2500 (agglomerated particles) | - | Cyclon mix* |
| **TC04** | 840°C, slow cool | Cyclon mix* | approx. 90 – 2500 (agglomerated particles) | $CaCO_3$ (10%) | - |
| **TC05** | 840°C, slow cool | Cyclon mix* | approx. 90 – 2500 (agglomerated particles) | Carbon black (0.33%) | $CaHPO_4$ (1.66%) |
| **TC06** | 960°C, slow cool | Cyclon mix* | approx. 90 – 2500 (agglomerated particles) | Carbon black (0.33%) | $CaHPO_4$ (1.66%) |
| **TS07** | 960°C, slow cool | Soda-lime glass | 50 - 250 | Carbon black (0.33%) | $CaHPO_4$ (1.66%) |
| **TBS08** | 790°C | Borosilicate (50%) + Soda-lime glass (50%) | 200 -1700 (Boro) + 50 – 250 (SL) | Carbon black (0.33%) | $CaHPO_4$ (1.66%) |
| **TC09** | 790°C | Cyclon mix* | approx. 90 – 2500 (agglomerated particles) | Carbon black (0.33%) | $CaHPO_4$ (1.66%) |
| **TS10** | 790°C | Soda-lime glass | 50 - 250 | Carbon black (0.33%) | $CaHPO_4$ (1.66%) |
| **TC11** | 840°C | Cyclon mix* | approx. 90 – 2500 (agglomerated particles) | $CaCO_3$ (3%) | - |
| **TC12** | 840°C | Cyclon mix* | approx. 90 – 2500 (agglomerated particles) | $CaCO_3$ (5%) | - |
| **TC13** | 840°C | Cyclon mix* | approx. 90 – 2500 (agglomerated particles) | $CaCO_3$ (10%) | - |
| **TBS15** | 840°C | Borosilicate (50%) + Soda-lime glass (50%) | 200 -1700 (Boro) + 50 – 250 (SL) | $CaCO_3$ (5%) | - |
| **TS16** | 840°C | Soda-lime glass powder (50%) + cullet (50%) | 200 -1700 (Boro) + 50 – 250 (SL) | $CaCO_3$ (5%) | - |
| **TBS18** | 790°C | Borosilicate (50%) + Soda-lime glass (50%) | 200 -1700 (Boro) + 50 – 250 (SL) | $CaCO_3$ (5%) | - |

Table 6. List with the tested recipes in the produced samples. In the majority of the specimens the total weight used was approximately 250gr.
* refer to Appendix_Table 1 for exact chemical composition. Cyclon is a by-product of the bottle- recycling industry, containing SLS glass heavily contaminated.

| Sample | Recipe description | Heating rate (°C/h) | Top Temp. (°C) | Dwell time to Top temp. (hrs) | Cooling rate to annealing (°C/h) | Cooling time to annealing point (hrs) |
|---|---|---|---|---|---|---|
| **TC01** | Cyclon mix*, no foam. additive | 50 | 840 | 10 | -15 | 4 |
| **TC04** | Cyclon mix* + $CaCO_3$ (10%), | 50 | 840 | 10 | -15 | 4 |
| **TC05** | Cyclon mix* + C + $CaHPO_4$, | 50 | 840 | 2 | -6 | 4 |
| **TC06** | Cyclon mix* + C + $CaHPO_4$, | 50 | 960 | 2 | -6 | 4 |
| **TS07** | SLS float powder + C + $CaHPO_4$, | 50 | 960 | 2 | -6 | 4 |
| **TBS08** | SLS float powder + Borosilicate cullet + C + $CaHPO_4$ | 50 | 790 | 2 | -200 | 1 |
| **TC09** | Cyclon mix* + C + $CaHPO_4$ | 50 | 790 | 2 | -200 | 1 |
| **TS10** | SLS float powder + C + $CaHPO_4$ | 50 | 790 | 2 | -200 | 1 |
| **TC11** | Cyclon mix* + $CaCO_3$ (3%) | 50 | 840 | 2 | -200 | 1 |
| **TC12** | Cyclon mix* + $CaCO_3$ (5%) | 50 | 840 | 2 | -200 | 1 |
| **TC13** | Cyclon mix* + $CaCO_3$ (10%) | 50 | 840 | 2 | -200 | 1 |
| **TBS15** | SLS float powder + Borosilicate cullet | 50 | 840 | 2 | -200 | 1 |
| **TS16** | SLS float glass- 2 particle sizes + $CaCO_3$ (5%) | 50 | 840 | 2 | -200 | 1 |
| **TBS18** | SLS float powder + Borosilicate cullet + $CaCO_3$ (5%) | 50 | 790 | 2 | -200 | 1 |

Table 7. Detailed information about the manufacturing parameters for the tested samples, refer to Table 6 for brief chemical synthesis.

* refer to Appendix_Table 1 for exact chemical composition. Cyclon is a by-product of the bottle- recycling industry, containing SLS glass heavily contaminated.

### 3.2.3. Experimental process

#### Mould & Mixture's preparation for foaming

The aforementioned methodology of exploring the various parameters regarding the type of glass waste as a raw material and its manufacturing process, followed very specific steps and tools for every sample. To exemplify, Crystal-cast mould to withstand furnace temperatures, was prepared per each mixture (Figure 41). This, was an important part of the process, since for every tested sample there was material used that would instantly become waste afterwards, therefore the number of samples were carefully considered. The specific process for making the moulds out of Crystal cast and water is depicted in Figure 41. The mixture's portions have been defined from previous research held in TU Delft's Glass lab. Once poured into the set-up from plywood pieces, after 45 to 60' the mould is ready to be cleaned from clay remnants, to be used into the oven.

Figure 39. Soda-lime crushed cullet turned to powder after 4sec of sieving (Herzog Disk Mill).

Then, the defined tested recipes from Table 6, were manually mixed to obtain homogeneous mixtures without clods. Measured in weight, they were inserted into the moulds and then into the oven, according to the defined heating schedule each time. When the glass source was not provided by the company *Maltha Glass Recycling,* pieces of either float Soda-lime or Borosilicate glass were crushed, sieved and milled as seen in Figure 42 according to the desirable powder or cullet sizes, presented in Table 6.

## Arranging samples for testing

After taken out of the oven the moulds were carefully broken at the corners, so that the sample is released intact. Then, they were photographically documented in Appendix_Table 2, and a cut resulting in two pieces (Figure 40) was made with the saw-cutter in Stevin II, in TU Delft, in order to study their section for more accurate results. For this reason, studied surfaces were also polished (Proverto, Grinding and polishing disk) to clean contamination from the chainsaw & better reveal the microstructure.

In particular, these two shapes were chosen to be used for testing the manufactured materials ,since they better fit in the experimenting requirements. (1) The one, close to a cubic shape had varying dimensions not only because the slices made manually, but also because the samples themselves varied greatly due to shrinkage and volumetric distortion during foaming.

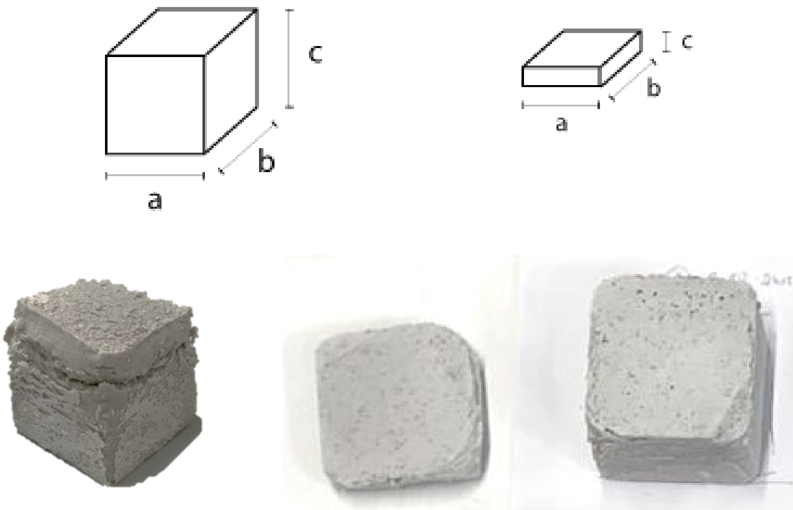


Figure 40. (from left to right) The original moulded shape, and the two shapes obtained after the cut.

This impact is analysed in further detail in the next paragraph *(see 3.3).* (2) The second shape is a slate one, working with the digital microscope (KEYENCE, VHX-7000) and permeability tests.


Figure 41. Photographical documentation about the 'life of a mould' .

## Porosity study

During the microscopical investigation, various pore sizes were measured to obtain the mean value. High-resolution images, were captured and studied in the following paragraphs to draw conclusions, regarding the type of pore network. While, the outer surfaces were investigated to check the differences and identify the possible reaction with the mould.

## Hydraulic Properties investigation

Once the microscopic study is complete for each sample, then the hydraulic performance calculation initiates. As a first step density (ρ) needs to be measured regardless the shrinkage or volumetric distortion examined. Consequently, the method used to measure the density is according to Archimedes laws, since the shapes not perfect cubes.

## Dried-weight calculation

For the second step, the dried weight of the specimens was obtained after their consecutive weight measurements were identical (Figure 42). This happened, by heating them in the oven at 40 °C for 24hrs and then in cycles of 8hrs, at least.

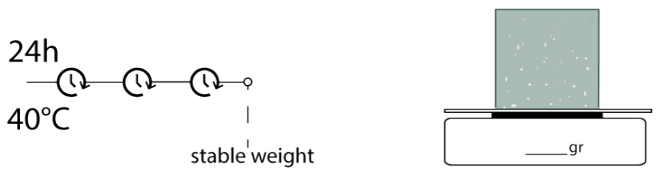


Figure 42. Diagram depicting the steps for reporting the dried weight until there is no difference in two consecutive measurements.

## Contact Angle monitoring

Simultaneously to the previous, the slate-shapes were quickly-studied for their hydrophilic / hydrophobic nature, to use this feedback for the formation of the next recipes. Since, one of the most important conclusions that needed to be drawn, according to studies regarding the water behaviour to porous solids is whether the surface is negatively or neutrally ion-charged (refer to Appendix_Figure 9). To investigate this, a quick test was designed, using the slate cut shape of the original moulded material, by simply dropping one or two water droplets on it and monitor the contact angle they form with its surface.

## Permeability test

In addition, another experiment was designed to assess the permeability of the material (Figure 43). The decision of this was made because other tests measuring the absorbance and evaporation rate, take time to be completed, while the following method was outlined to give rapid feedback for the next steps and recipes to be tested during the ongoing experimental process. Specifically, pipette for dropping water onto the slate surface is needed, together with a grid acting as an elevated base for the sample, allowing the dropped water to replace the air filled inside the pores. Hence, a draft observation by comparing the results between the specimens' permeability can be formed based on the time needed to leave a stain on the bottom surface. For this test, the same amount of water is indicated to be used for all the specimens.

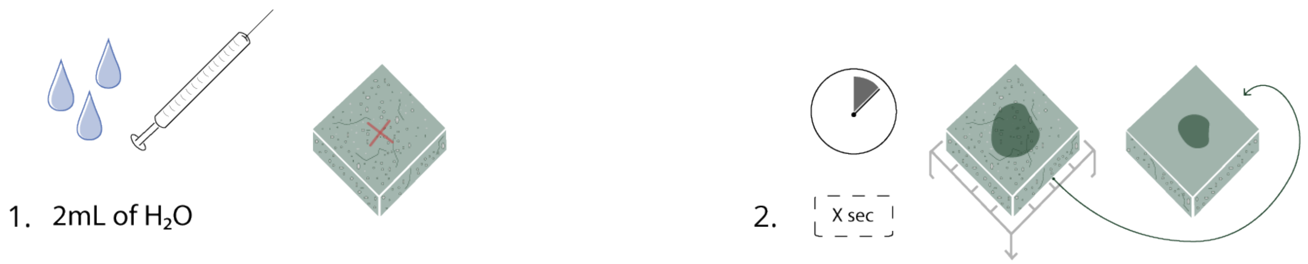


Figure 43. Diagram illustrating the testing process of the permeability test.

## Absorption rate

After the dried weight measurement the cubic shapes, according to literature and a personal conversation with the moisture expert Lubelli B. (on 14/04/2022) opted to be checked for their water absorption rate. A water tank, a supportive grid and a bottle are needed for the first small experimental set-up. When placing the specimens onto the grid, the water needs to be only 2-3mm above their base to allow water absorption by capillary rise from the one surface. An important part of this set-up is firstly to seal the samples from all the sides, apart from the one touching the water, while the bottle positioned upside-down is used due to hydrostatic pressure, to ensure that the water level remains the same during the whole process. This, also acts as an indicator for the amount of water that is absorbed by the specimens during the experiment.

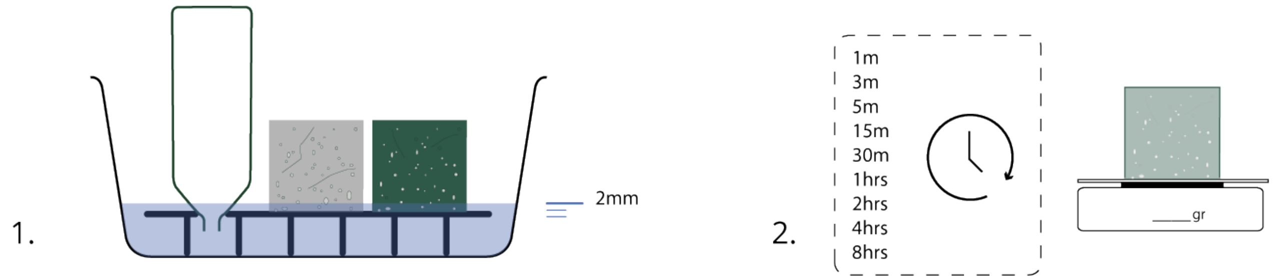


Figure 44. Diagram showing schematically the set-up for the absorption rate test and the time intervals for the measurements to determine the absorption curve.

## Saturation weight

Once the previous was reported, the fully-saturated weight of the specimens ($W_s$) is the next needed measurement. By fully-covering all the samples with water for 24hrs, the saturated weight ($W_s$) is reported. This aims to the calculation of the difference between the dried and the fully-saturated weight to reveal the samples' capacity of absorbing water.

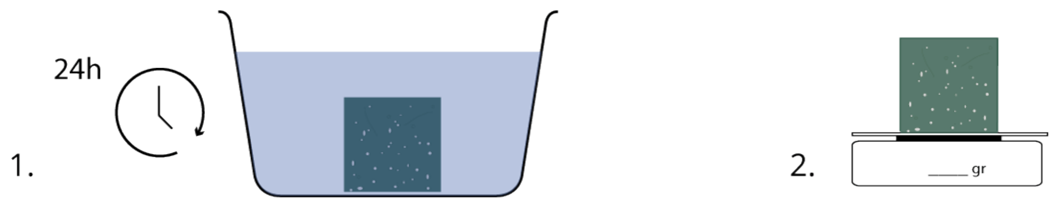


Figure 45. Diagram illustrating the water saturation level measurement.

## Evaporation rate

The evaporation rate test, as the last one to be conducted can also last the longer period of time (Figure 46). According to each material capabilities of retaining water, findings in literature regarding mortars and bricks record slight changes in weight for over a month. Similarly with the previous ones, the specimens should be left with only one uncovered side, so as to calculate the evaporation per unit of area. Then, by leaving them in room temperature, in order to have stable conditions, the weight should be monitored until it approximates the levels of the dried one, not to mention that this might not exactly reached depending to the pore-network size.

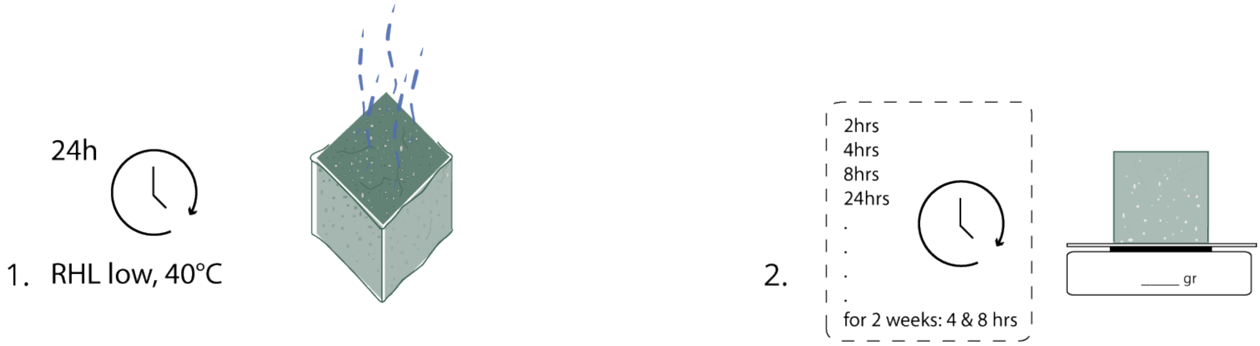


Figure 46. Diagram illustrating the evaporation test process, starting from the full-saturated point, aiming to reach the dried weight levels.

## Susceptibility to Frosting

One of the last conducted material testing is the resistance of the samples against frosting. To quickly gather information for making a rough estimation about their durability for the scope of this project without following specific guidelines instructed in NEN-code, all the specimens were inserted into a freezer two times at different conditions, however at a constant temperature as explained in Figure 50.

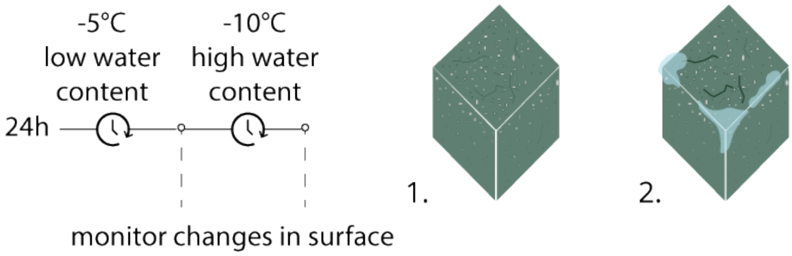


Figure 47. Alternative freezing conditions to test the material's resistance to frosting. These circles should be repeated more times to form an outcome according to material testing guidelines for market products.

## Compressive strength testing

The calculation of the material's strength is only one of a series of tests that should be examined to validate the performance and durability of the open-porous glass foam, in order to be incorporated as a new product into the building industry. Therefore, as a testing on its own does not offer revealing information at such an early stage of experimentation. Despite this, it provides additional tangible evidence for comparison with other materials, such as bricks or cement, that are under investigation for potential bioreceptive solutions. For this mere purpose, it was deemed necessary to choose the recipe with the highest performance on the hydraulic properties test and measure the strength of three new specimens of cubic shape (Figure 40) for statistical accuracy.

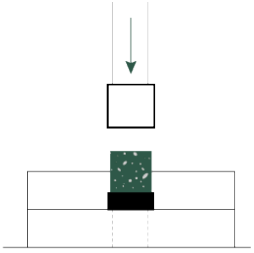

$$f_b^* = F_{max} / l_u \times w_u$$

$F_{max}$ is the maximum force, $l_u$ length, $W_u$ width of the unit.

Figure 48. Diagram for compressive strength and calculations using the maximum force applied on the samples until plastic deformation, conducted with an Istron Machine, microlab in the building of Civil Engineering, TU Delft.

## Moss growth

The most important part of the testing process is the one related to the bio-growth. However, it is also the most unpredictable given the time constraints of this research, since there are a number of factors related to the testing environment affecting the microorganisms growth, without being able to fully control them. These, will be further analysed in the next paragraphs. For this step, tiles were prepared (Figure 38), by applying Tortula muralis following the method illustrated in Figure 52. The needed period for moss growth is between 6 to 8 weeks, even though encouraging evidence can be identified from the 4th week.

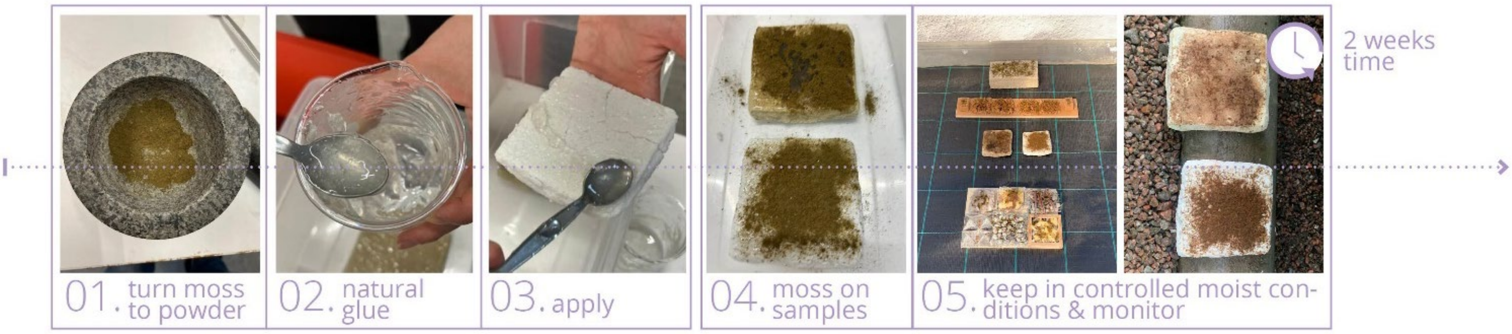


Figure 49. Photographical documentation of the mould application onto the samples (TBS17 & TC14). Firstly, the collected moss is turned to powder into a grinding bowl after being dried. Secondly, by mixing demineralized water and sodium alginate, a natural glue is created, which is applied onto the samples' tested surface to glue the moss powder. Lastly, the moss onto the samples is sprayed with natural water and positioned into the Botanical Garden of Delft, Greenhouse 6 (Kaas 6), to maintain moisture without immediate sunrays. The moss application process was based on previous experience of the TU Delft researcher, Max Veeger.

Image Source: Photographs taken by Dimitrios Ntoupas

The already described process was done in a justified order regarding the water intake and evaporation of the samples. However, since the immediate assessment of the samples' potential was needed, a different sequence was followed. For instance, after calculating the density of the samples, their saturated weight was measured right after drying, already leading to determine their maximum absorbing potential for the next parameters under testing. Nevertheless, this process provided immediate results, higher values of water intake were reported during the adsorption rate test, compared to the full saturation, proving the initial measurement partially not valid. It should be mentioned, that these differences did not alter the scoring of the samples between them, even though notable changes were monitored. Therefore, the assessment for the next batches was luckily based on correct results, but not precise. As a result, the saturation weight measurement was repeated to record the exact numbers for maximum absorption, while the next batch of samples were also being tested under the above described sequence in steps. Overall, each process presents specific advantages and disadvantages, that have to be taken into consideration especially, depending on the goals of each planning.

## 3.3. Experimental Findings

In this section, a detailed description of the conducted experiments and discovered limitations along the process is going to be presented, together with the findings and the specimens' performance during each test.

### 3.3.1. Microstructure

#### 3.3.1.1. Pore network

The samples' microstructure was checked primarily in the microscope and then, the experimental analysis continued by measuring in weight difference the water that is absorbed. The second way aims to give insight on the hydraulic properties rather as an indication of measuring porosity since it cannot be fully accurate, due to the fact that the solids could also be hydrophobic and highly porous, or having closed-cellular structure. The most precise way of measuring porosity is by mercury intrusion, which for the scope of this research was not feasible. As an alternative way of validating porosity Lubelli B. suggested to use water with soap when checking either the contact angle or sinking the samples for 24hrs, in order to decrease the surface tension of water and let it penetrate the open-pore network – if existing – (Personal discussion, on 14/04/2022). However, since the aim is to test the material properties for bioreceptivity, water absorption and water saturation levels were chosen as the most appropriate measures both for porosity validation, but also to investigate the material potential based on the hydraulic behaviour.

For this test, the samples' cut piece of less than 1cm thickness (Figure 40) was used**.** Overall, the analysis presented very interesting findings regarding the specimens' microstructure related both to their particles' different ways of bonding due to their ingredients, but also to their pore sizes and distribution. These results, are concentrated to four main porosity types and their sub-categories expressing differences in ranges and sizes, illustrated in Figure 50, and analysed in Table 8.

In further detail, Porosity Type 01 having two image-expressions, one with almost spherical pores from gas bubbles released when foaming and the other with irregular-shaped ones, produced from the chemical reaction between the ingredients. These two forms of closed-porosity are expressing the same recipe, produced in different temperatures (TS07: 960°C & TS10: 790°C) and cooling rates (TS07: slow cool-4hrs, TS10: fast cool-1hr), as well as from different cullet size, showing that the highest temperature generated a dissimilar structure, with shrunk volume especially towards the point that there is higher pore-concentration revealed in the cut surface (refer to TBS07 in Appendix_Table 2).

Thus, if the temperature rises above the optimal, such as in TS07, then the foam volume collapses due to dropping glass viscosity. The use of Soda-lime refined powder, also showed that the ingredients were better-mixed leading to more homogeneity in the structure, that only the effect of the gas release remained recognizable. What is surprising, is the fact that this recipe was expected to be the most successful, since it was based on the proven example for open-porous glass foams from König J. et al. (2020). However, there are a number of reasons why this did not work, because only the main ingredients and their proportions used were identical. For instance, apart from the powder size that in literature, was very refined, around the size of 20μm, the step of adding iron (III) oxide $Fe_2O_3$ to the recipe was excluded, since glass already contains percentages of it. What's more, the literature samples prior to foaming were homogenized with a planetary ball mill, and then placed into a stainless steel form where they were supressed from a flat surface, before they were inserted to the electric furnace to be heated for foaming. These slight divergences may account for such a different outcome.

## Type 01

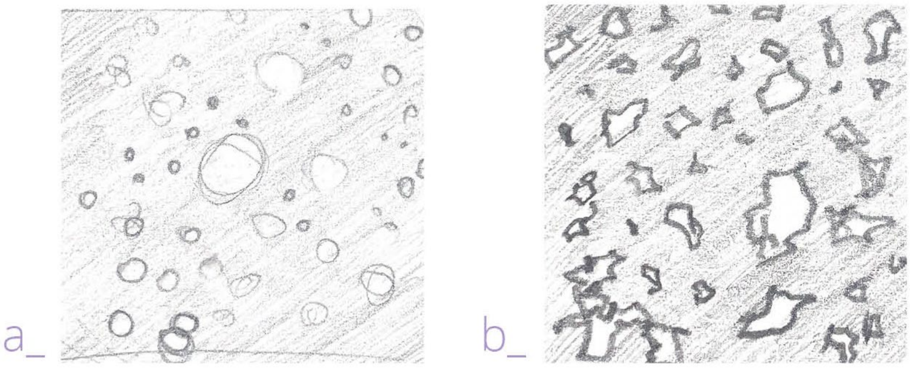


Figure 50. Distinctive microstructure type 01 of closed porosity. Sample TS07 & TS10 both consisted by Soda-lime glass, the first out of refined powder, foamed at 960 °C, while the second out of small cullet ranging between 200-400μm, foamed at 790 °C, showcase a complete different image of porosity and brittleness behaviour.

## Type 02

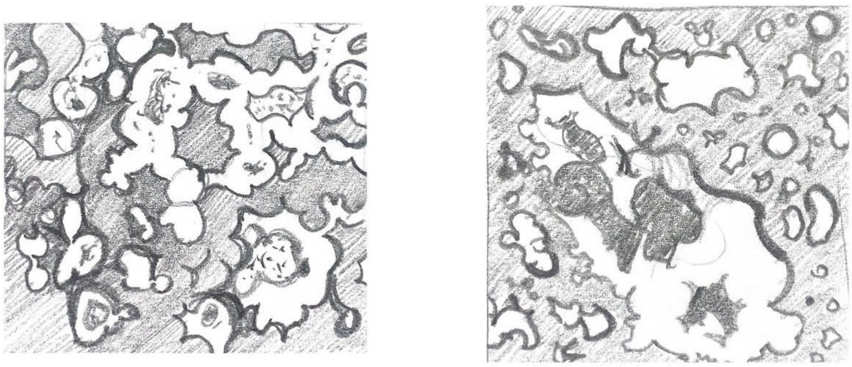

Figure 51. Microstructure types 02 & 03, made from the same Cyclon mixture, but with different foaming additives, contrasting firstly a structure that is closer to typical glass-foams, with vertical open networks, while the second one is revealing a partially fused-granules structure that results in a highly open network with high brittle performance.

## Type 03

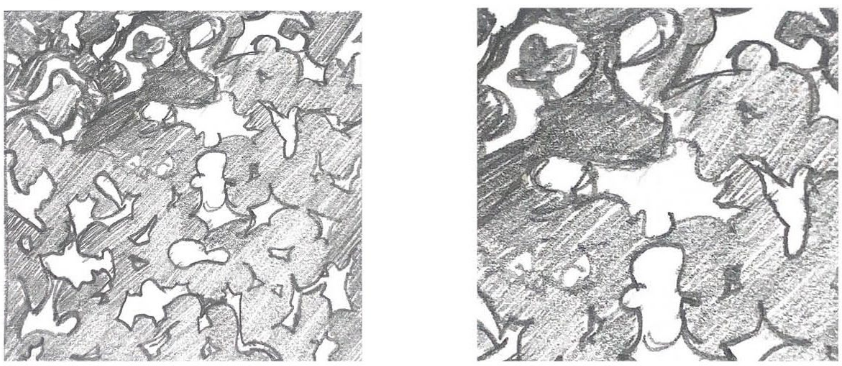

## Type 04

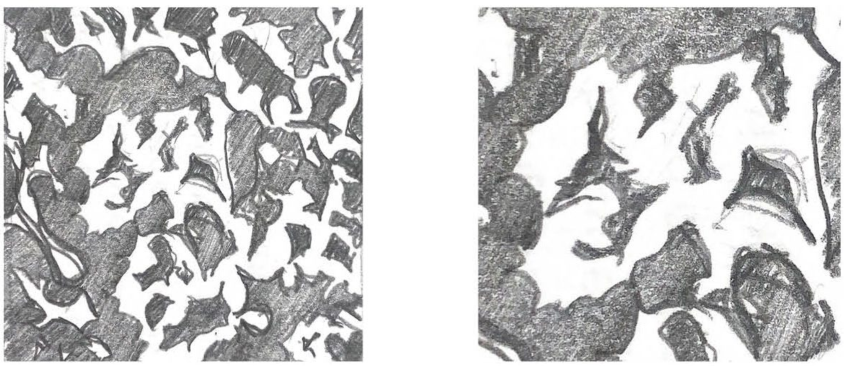

Figure 52. The 4th and last porosity type, characterizing the produced samples of the research,

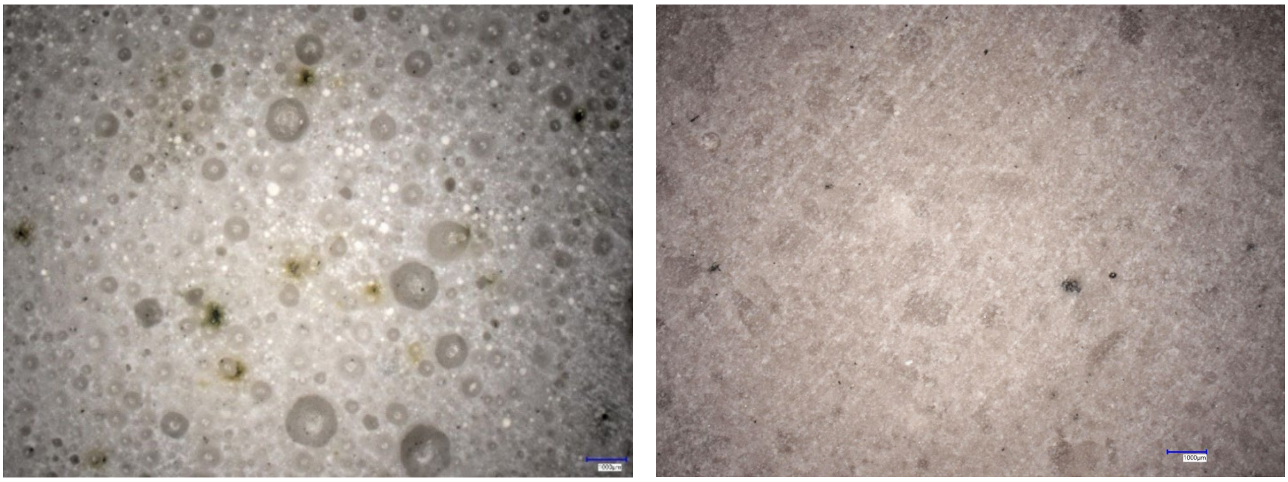

Figure 53. Microscopic images of samples TS07 & TS10, illustrating the two different images of closed porosity represented in Type 01. Images were captured with zoom x20, blue line representing the scale equals with 1000μm.

In contrast to the previous type, the next two – 2 & 3 – are showing evidence of open-porosity as seen in Figure 51, with the peak of permeability identified in microstructure type 03. However, samples linked with these two types present a range of different sizes related, either to pores or wall thickness.

In particular, samples TC01, TC05 and TC09, demonstrate a really similar microstructure going from a less to a more porous outcome. This, is attributed not only to the different temperatures tested but also to the increase of the cooling rate as well as the different foaming additives explored. Specifically, in the case that no foaming agent was used – since Cyclon mix already contains a high percentage of organics – together with the longest cooling period, the least open-porosity was identified (TC01).

Moreover, the common characteristic of these samples is the creation of pore clusters forming bigger groups of an open-pore network, that is mainly identified vertically. This vertical movement can be linked with the origin of pores out of gas bubbles which move upwards. Proof of this can be found in Figure 57, that produced microscopically when studying the vertical cut of the TC05. It is evident that different-sized pores are mainly connected due to the foaming process, creating various paths. This fact is of utmost importance to be especially considered during the later steps of mould design, since this vertical network needs to be connected with the outer surface exposed to environmental conditions.

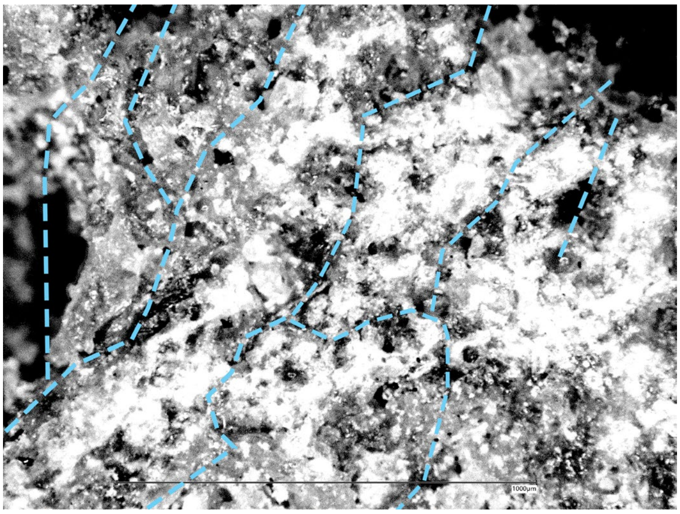

Figure 54. Connection route from the outer surface identified in a microscopic image of TC05, vertically sliced.

To identify the effect of foaming temperature in the mixtures, TC06 has to be taken into account, as it was fired at the highest tested temperature - 960°C and exhibited the greatest pore size range and uneven pore distribution, due to pore-clusters formation. Thus, focusing on the produced porosity of samples in this category, the results shown in Figure 56 - Figure 57, are surprisingly interesting, since it is proven as stated in the literature (König J. et al., 2014), that increasing foaming temperature increases the probability of having open pores, by the effect of certain pores coalesce and pore walls break with the extensive gas release. This phenomenon is also accompanied by the coarsening of the shape and increase in pore-wall thickness that contains other closed ones, since they are of a smaller size. However, it is seen that the merged pores forming the bigger clusters – a characteristic of Type 2 –, are connected mainly vertically and there is a high potential for the horizontally linked ones to be characterized as blind and are reaching the outer surface. Leading to the conclusion of having a distinction between closed and open ones, depending on their size: smaller than approximately 0.1mm have a closed-cell structure, while the larger ones have the potential to be open. In addition, the changes in the heating schedule of decreasing the dwell time, while on the other hand increasing the cooling rate proved to be beneficial, for the gas releases to form larger pores while glass viscosity was low.

Specifically for TC06, it should also be mentioned that a reaction with the mould is obvious, along with greater impact than the rest of the specimens. Not only there were separated granules, mixed with mould particles on the outside, composing a totally different image from the inside, but also significant cracks formed on almost all sides, implying vulnerability for breakage. Although in this sample the largest pore sizes and open network was achieved, it must be thoroughly examined whether the short cooling time, set in the highest tested temperature, results these cracks attributed to internal stresses, created by the low glass viscosity that was forced to quickly cool down. Such results might sieze the sample's potential for further examination, especially if it fails in the frosting test.

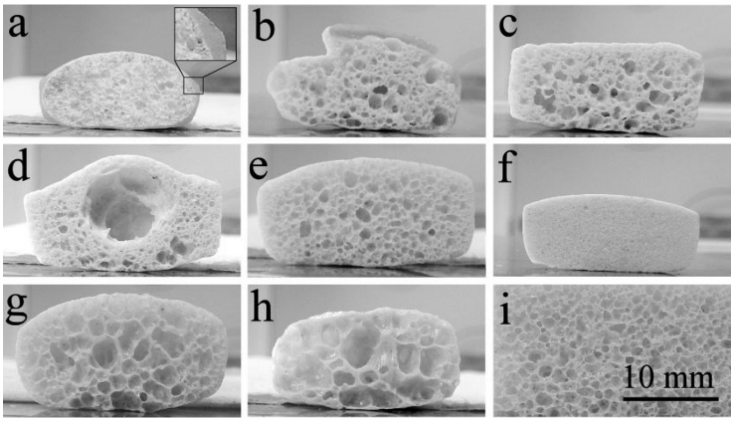


As far as Type 03 is concerned, its formation appears to be very interesting, because tested glass foams in literature with different proportions of $CaCO_3$ presented greatly different structures illustrated in Figure 58.

Figure 55. Study of experimental samples produced by mixing, with 1, 2 and 4 wt% of $CaCO_3$, in different temperatures and milling times.

Image Source: König J. et al., 2014.

When comparing the samples produced with different weight ratios of $CaCO_3$ , a decrease in density is observed as the amount of foaming agent is increasing (Table 7 & Table 13). This phenomenon is justified due to higher $CO_2$ release during foaming that made the samples more porous, when foamed in the same heating schedule. Therefore, sample TC04 which was proven to be promising from the first quick permeability tests analysed in the next paragraphs, cannot be immediately compared since its dwell time was way larger than TC11-TC13. For this reason, only for comparison purposes TC13 was tested with the exact recipe as TC04 had.

Furthermore, from this microscopic analysis it is seen that in the samples with less $CaCO_3$, the solid-pore parts form larger areas, without varying greatly in their open-to-porous overall ratio when comparing the other samples. In further detail, the amount of open space in TC11 can be correlated with TC13 as equal, even though it contains larger areas, but also thicker pore walls defined from the mixture's particles space. From this observation, it can be concluded that the interest for this microstructure lies on the fact that it is not formed out of gas-bubble pores as a typical glass foam, but from the partially fuse of granules together and their residual porosity, clearly examined in Figure 58.

Last but not least, Type 04 even though presents a lot of similarities with Type 03, consists another category because it has been the result of mixing glass powder with small-sized cullet either from the same source of glass or different. Therefore, typical of this porosity structure are all the mixtures that contain Borosilicate glass (50% wt) together with Soda-lime glass powder (50% wt) (Figure 57 & Figure 58), except for TBS18, which follows under the group of Type 3. In this particular case, the temperature of 790°C in combination of $CaCO_3$ that was chosen to be investigated, produced a structure – very similar to sample TC13 –, expressed by larger particles and others closer to powder-size that were not well-bonded into the mixture, resulting to a very brittle behaviour. Therefore, it can be concluded that for such recipes really low temperatures are not beneficial, since the glass particles should at least partially fuse creating a more stable solid matrix that does not come apart on its own. The aforementioned recipes can also be traced in Table 6.

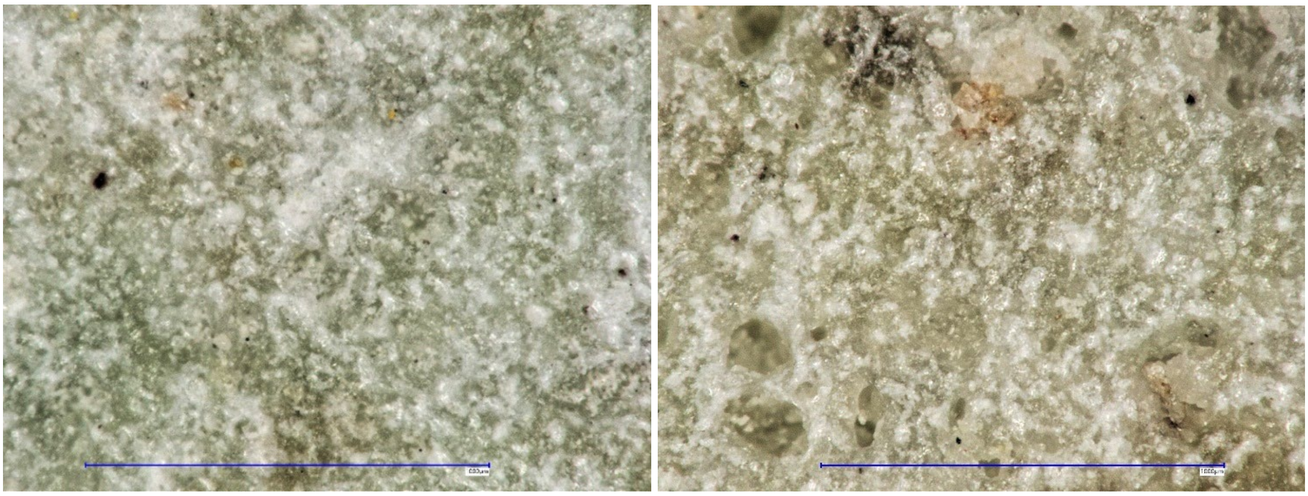

Figure 56. Microscopic images of TC01 & TC05, at the larger zoom x200 in the digital microscope (VHX-7000 series, Keyence located at the Faculty of Architecture), showcasing the crystallized parts of the mixture together with other various ingredients represented with different colours and textures. The effect of foaming agent is evident from the existence of distinctive pore formations of larger sizes in the right image of TC05.

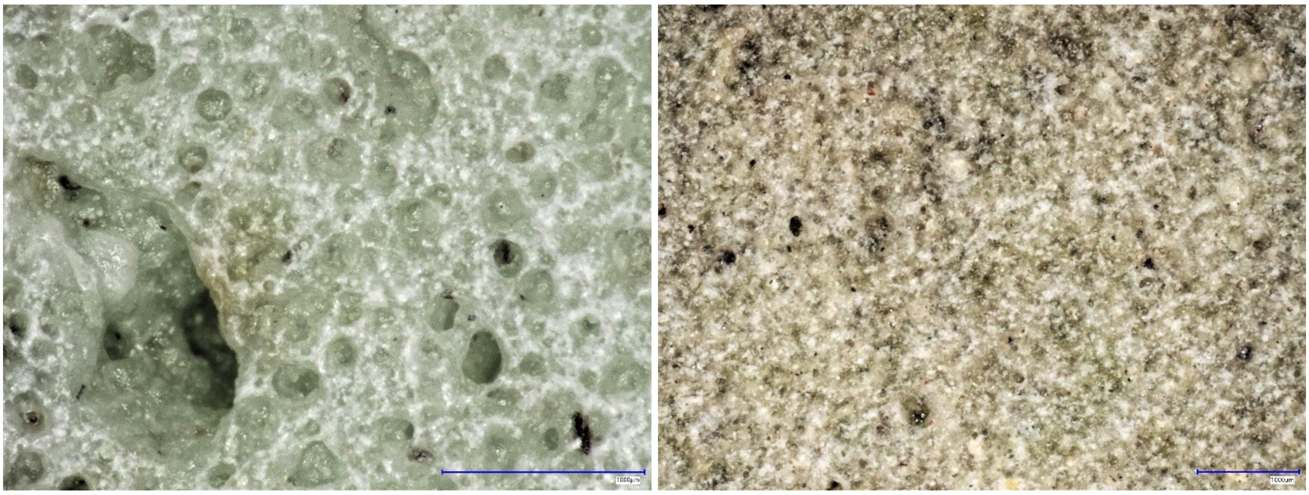

Figure 57. Microscopic images of TC06 & TC09, at different zoom scales (x100 & x50), depicting the effect of higher temperature in the chemical reactions of the additives during foaming. Various kinds of particles are still apparent with different colours.

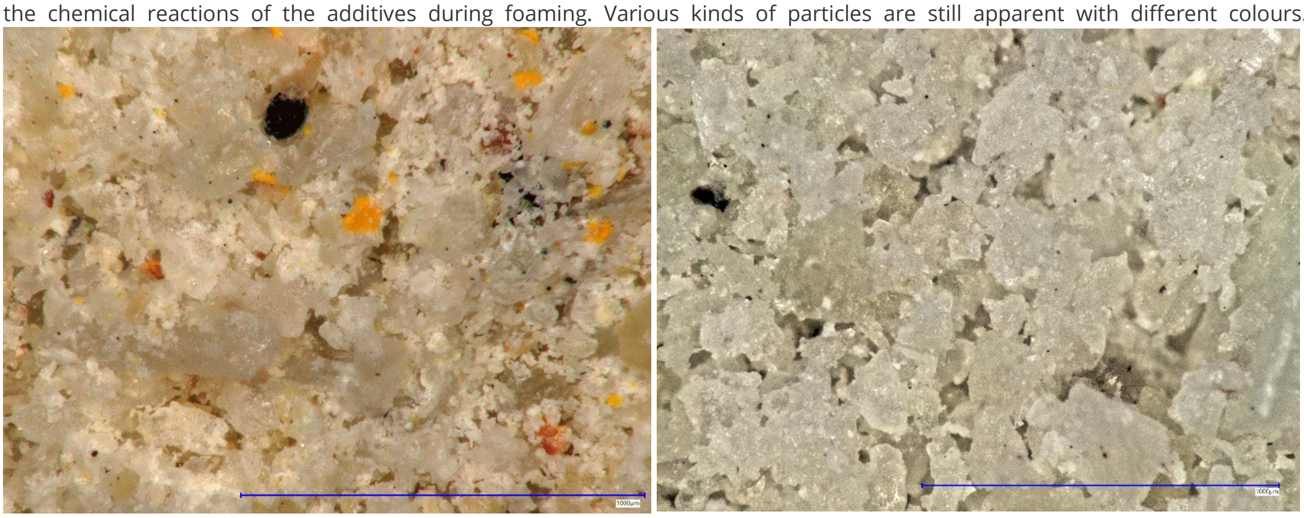

Figure 58. Microscopic images of TC04 & TC13, at different zoom scales (x200 & x150), depicting the range in sizes of the solid-pore matrix due to different percentages of foaming agent (10% & 3%). Yellow-coloured particles captured in TC04 are either contamination for waste in the Cyclon mix or from the saw-cutter in the cutting process in Stevin Lab II, in TU Delft.

From the microscopical analysis, the texture observed in the polished surfaces of Type 4, appears to offer a highly open network through the irregular shapes of pore walls and their remaining voids, at least on the horizontal axis that is investigated. Reactions from the foaming agents are visible, both in the form of gas-bubbles, and also in the shape of dissolved particles by leaving a coarse-shaped void network. As a result, a vertical section would also be meaningful to study to validate whether this structure remains identical or there is a gradient in the ratio of open-to-close pore surfaces. It can be speculated based on the findings of this research until now, that this specific type of porosity will lose its benefit of an open network in higher temperatures, as glass is expected to fuse more, by creating stronger bonds and also reducing the porosity levels.

Despite the fact that sample TS16 seem to comprise a unique category, its microstructure pattern is similar to the one identified in Type 4, but only much larger in scale. For this reason, porosity types are formed by ranges to include different micro-network expressions, since no sample produced in this experimental research is identical. The reactive expansion revealed (refer to Appendix_Table 2 for the photographical documentation) after de-moulding this sample was surprisingly interesting, as the material had no brittle behaviour, even though its shape could be prone to damaging. Overall, the sample had an increasing porosity range towards its upper part that can be justified due to the chemical reaction with $CaCO_3$, by releasing $CO_2$. Its large open pores both in diameter and in depth having a well-bonded structure, can be explained from the main ingredients that was powder and small-sized cullet of Soda-lime glass, mixed with $CaCO_3$. Thus, it can be concluded that the combination of alternate sizes of recycled raw material caused the coarser and varying in shapes and size pores. Again, a higher temperature would reduce its porosity and probably the potential for an open-network, however it would be interesting to test whether the expansion could have been avoided also in a lower temperature. The sample as it is, since its pores are vastly larger than the other samples, it is expected to score low in hydraulic performance targeted for bioreceptivity.

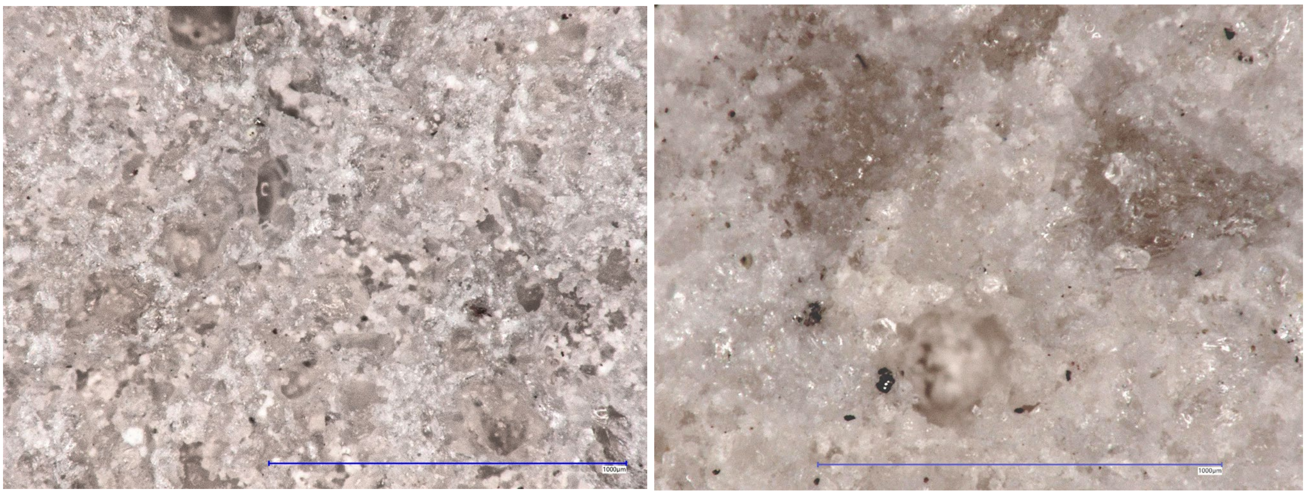

Figure 59. Microscopic images of TBS15 & TBS08, at different zoom scales (x150 & x200), depicting the microstructure type pattern, derived from fused glass-particles together with bubble-like pores implying gas release during the foaming process. The two samples were not produced in identical temperatures (840°C & 790°C) and they were mixed with different foaming additives ($CaCO_3$ & carbon black, $CaHPO_4$), however the particle-size of the main ingredient and the glass waste source seem to be the ones that have defined the microstructure.

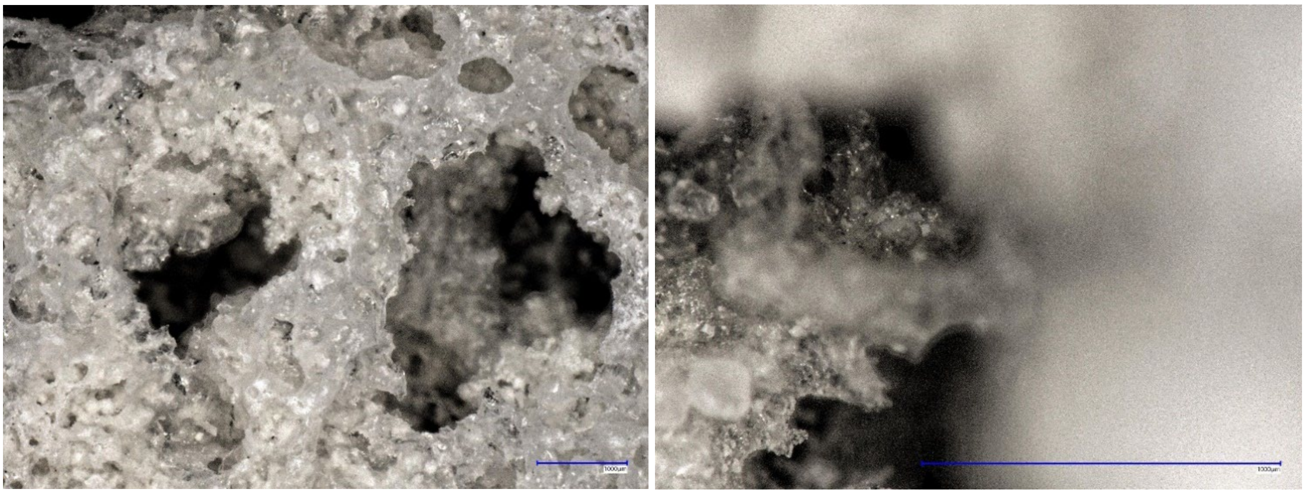

Figure 60. Microscopic images of TS16, at different zoom scales (x50 & x200), revealing the highly porous microstructure formed by the combination of Soda-lime powder & small-sized cullet, which was characterized by expansion during foaming at 840 °C, as seen in the Appendix_Table 02. The resulted pore size range in this mixture was phenomenally large compared to the rest of the samples, mainly due to the expansion effect.

| | **Type 01** | **Type 02** | **Type 03** | **Type 04** |
|---|---|---|---|---|
| Description | Closed porosity created by gas release or chemical reaction | Open porous-network formed by bigger clusters, connected mainly vertically, thick pore walls contain closed pores | Open porous-network, formed by different-sized granules and particles partially fused between them | Highly open-pore network both horizontally and vertically, created by crystallized cullet and foamed glass powder |
| Immediately-characterized samples | TS07 | TC01, TC05, TC09 | TC04, TC13 | TBS08, TBS15 |
| Family-attributed samples | TS10 | TC06 | TC11, TC12, TBS18 | TS16 |
| Corresponding type of bioreceptivity | Tertiary | Secondary | Primary & Secondary | Primary & Secondary |

Table 8. Identified types of porosity and their characterized-samples' microstructures.

#### 3.3.1.2. Pore size

Studying the pore size together with the type of porous-network is an important step for the aim of this research to manufacture the right pore network for microorganisms colonization. After having defined the optimal shape from literature, measuring the pore size is characteristic mainly for glass foams and no other material that has open porosity as an inherent property, such as concrete and mortars. Therefore, due to the fact that there are no recorded values to correlate for optimized bioreceptivity, comparing pore sizes between the obtained samples is a useful parameter for drawing conclusions only in combination with the evaporative test's results.

Although, it is believed that larger pore diameters will lead to rapid evaporation, it is also stated in the previous chapter that bigger pores aid in the capturing of water from the surface as long as they are combined with a fine network to retain it. Therefore, as a general trend pore sizes will contribute to defining the potential of the material based only on the polished surface taken as an example and not on the full depth of the sample. Regarding the last, further studying is needed into the vertical direction with a bigger sampling number for accuracy.

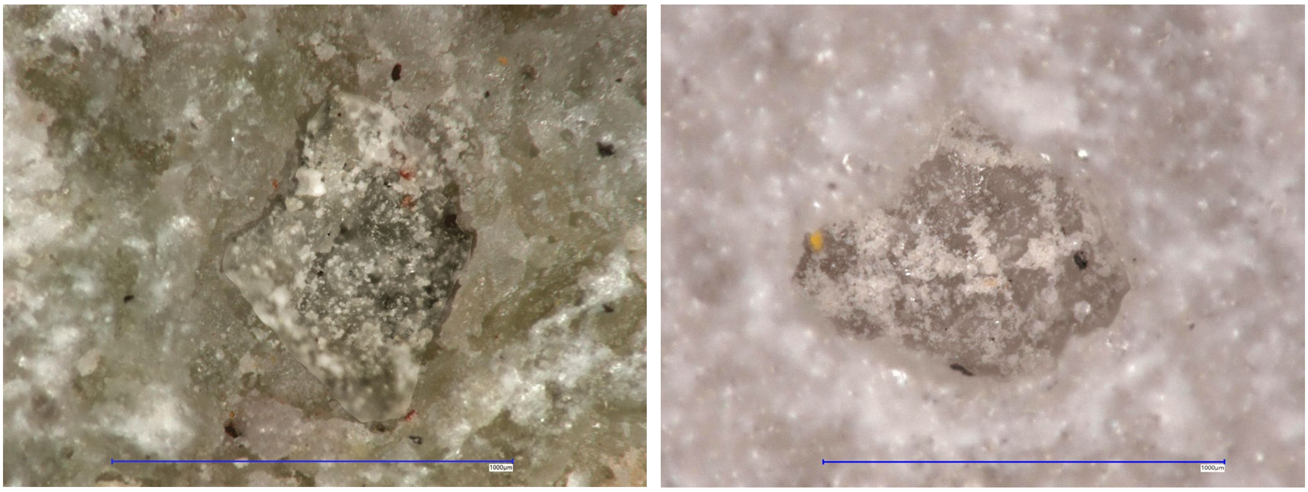

Figure 61. Microscopic image of TC05 (on the left), TS10 (on the right), calibrated to capture the depth of the pore. TC05: Irregular pore size of max dimensions: 613 x 823μm, TS10: 835 x 686μm.

Each type of porosity analysed in the previous paragraph may have a distinctive pore shape or a combination of those, however pore size is irrelevant, since there can be a wide range. Specifically, chart 1 illustrates the findings measured microscopically. As expected, the samples that showcase the highest values are: TC06 and TS16, followed by TS07. These, are assumed to present higher evaporation rates from the beginning of the measurements. Interesting are the results regarding the Cyclon mixes, and specifically the ones with porosity Type 3, whose pore sizes are the residual voids, which can be measured as the distance in perpendicular direction between the solid granules. Out of these, TC04 & TC13 represent the same recipe under the same foaming temperature, while the only difference is the dwelling time in the furnace. Therefore, the difference in their pore size can be justified by the coalesce effect that took place due to the longer period of time that TC04 was left inside the kiln, during which the glass had lower viscosity. Correlating also the Density values described in Table 13, it is proven that this pore merging made TC04 denser.

Apart from these, mixtures that contain Borosilicate glass, made from similar recipes contribute to understanding the impact of lower foaming temperatures, that maintain higher residual porosity. Since the ones heated in 790°C (TBS08 & TBS18), when compared to the samples of 840°C (TBS15), present higher values in similar range lengths.

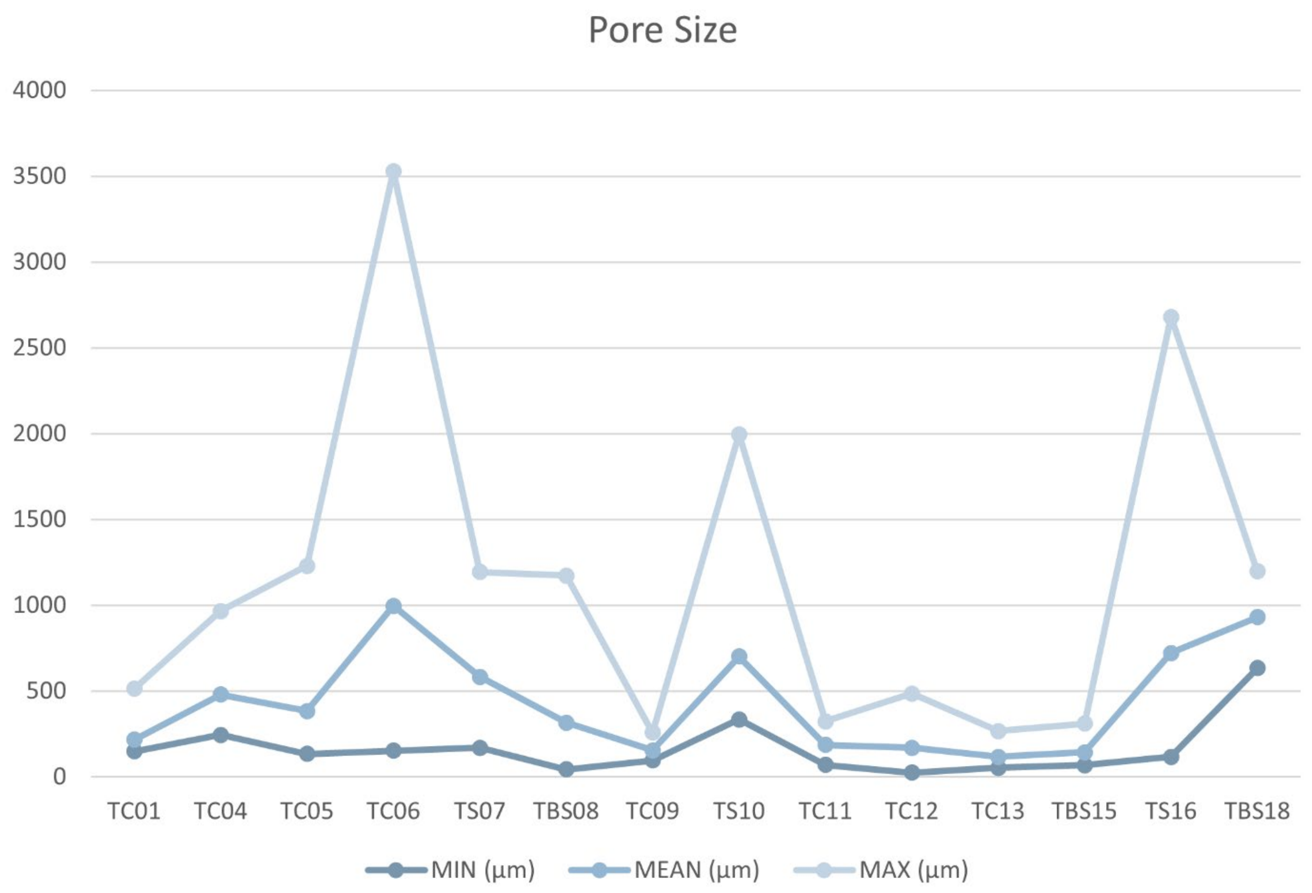


Chart 1. Lined-chart illustrating the pore sizes values of the polished surfaces of the cubic samples that were tested microscopically. Apart from the mean, the greatest range in sizes can be identified in the specimens TC06, TS10 and TS16, showing an uneven pore-distribution.

### 3.3.2. Hydraulic properties

The following paragraphs focus on a series of tests, having as a goal to offer evidence for the water behaviour to the produced glass foam specimens. In particular, evaluating the water absorption and evaporation rate, were experiments carried out based on the literature and other lab experiments. Additionally, some quick assessments were designed as well to verify the potential of the samples against certain obstacles, such as the contact angle proving if the solid is hydrophilic or hydrophobic, then the permeability by revealing the existence of an open-pore network and last but not least testing the material resistance against frost temperatures. The aforementioned processes were planned without high-tech equipment that would give answers with precise measurements, in order to provide a framework for every researcher to quickly assess the potential of his/her idea.

What's more, the sequence that these are presented is not necessarily the one followed. Since, as a first pass/fail test it is crucial to determine the contact angle of the water droplet to the solid surface (refer to Appendix_Figure 9),– even before determining the porosity – for the mere purpose to check if the water will enter the material's pore, or it will be repelled. Therefore, the described necessities led to the conducted workflow presented in Figure 72.

#### 3.3.2.1. Hydrophilic / Hydrophobic surface test

To check this, water droplets were dropped from a close distance of approximately 2.5cm height, onto the surface, and the shaped contact angle or immediate absorption was observed on the spot and through photographs for documentation. For this experimental test, the cut parts of the specimens were used with thickness of approximately 1cm. Regardless of the flatness of the tested surface, when the water was not immediately absorbed, these slices in most cases did not have an even base, leading to the droplets running along the inclination. Despite this fact, important conclusions were drawn regarding the behaviour and the surface tension between the water droplets and the tested solid.

Findings of this test are gathered in Table 9, where the main focus was to reveal the reaction of the water droplet upon touching the specimens' surface, even though accuracy cannot be certified as the human error and subjectivity are high. Figure 64 captures the highest contact angle observed, where the droplet remained on the surface validating the closed-porosity of the solid and therefore, was used as a reference case.

On the one hand in Figure 65, is depicted an interesting effect, represented by a large team of samples, contrary to what was expected for glass foams. The water was soaked immediately without remaining at all on the surface. These samples can be linked with the previous paragraph regarding porosity, with Types 3 & 4. On the other hand, the majority of the tested samples needed at least a second attempt to monitor and verify the if the droplet was forming an angle below or above 90 degrees (Figure 63). After careful consideration, only model TS10, was revealed that it was forming a high contact angle, probably because its mixture contained the highest percentages of Soda-lime glass which is known to be hydrophobic, together with carbon black as a foaming agent. Apart from the ingredients, its closed-porosity aided on the identification of this phenomenon with this low-tech method.

Overall, the findings of this test were encouraging for the potential of the material, since the incorporation of carbon black in the recipes was leading to the assumption that the solids would result in a hydrophobic behaviour. However, its low percentages in combination with organic substances have led to their release through foaming, leaving no doubt that the produced samples did not have a high contact angle. The observed effect of not absorbing directly the water droplets in certain cases during the tested time, can already be justified by the porosity networks identified microscopically and will be further examined in the next paragraphs.

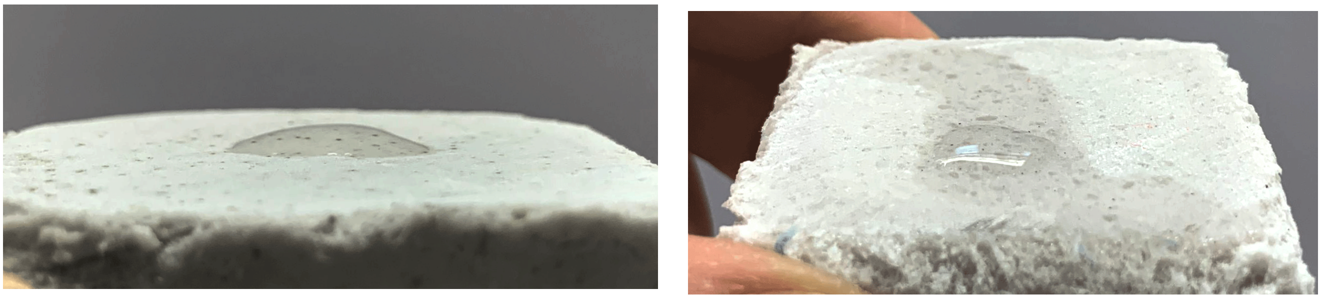

Figure 63. TS10 (on left) identifying by the 2nd attempt that the water is forming a high contact angle & TS07 (on the right) monitoring its low contact angle, however without observing it absorbed during the test.

Figure 62. TBS08 (on the left) & TC13 (on the right) showcasing similar behavior of absorbing the water immediately, with different dispersion effects.

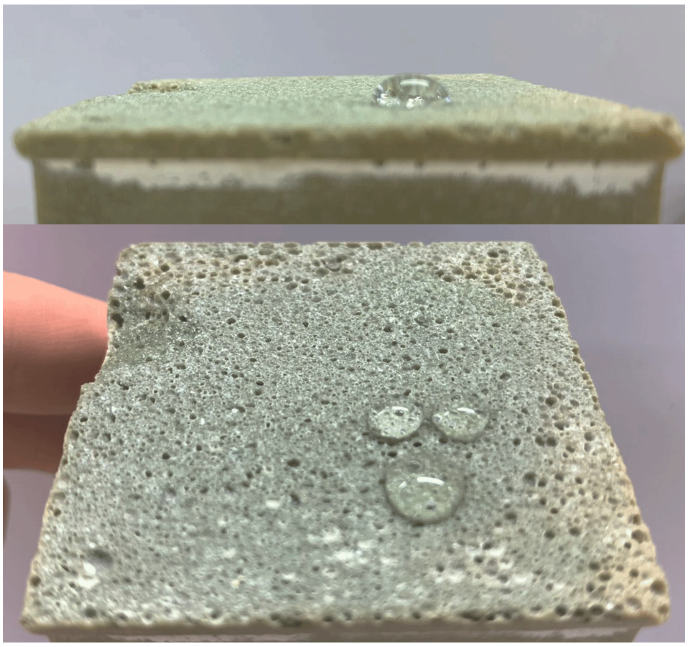

Figure 64. Highest contact angle observed, on a sample produced by T. Bristogianni, out of foaming Borosilicate glass.

| | Recipe Description | 1st attempt | 2nd attempt | Contact Angle | Observation |
|---|---|---|---|---|---|
| **TC01** | Cyclon mix*, no foam. additive, 840°C, slow cool | x | x | low | droplet did not get absorbed |
| **TC04** | Cyclon mix* + $CaCO_3$ (10%), 840°C, slow cool | x | - | low | water got soaked immediately, droplet did not remain on the surface to monitor the angle, therefore it is estimated that it was low. |
| **TC05** | Cyclon mix* + C + $CaHPO_4$, 840°C, slow cool | x | - | low | sample is not equally comparable due to its half-cut size. However, the droplet formed a low contact angle and it was not immediately absorbed. |
| **TC06** | Cyclon mix* + C + CaHPO4, 960°C, slow cool | x | x | low | even though large pores led the water immerse, so contact angle was difficult to be defined, light reflected in these pores showed the formation of a regular meniscus, proving positive results. |
| **TS07** | SLS float powder + C + $CaHPO_4$, 960°C, slow cool | x | - | low | holding the specimen straight, the droplet was shaping a low contact angle, even though it was not getting absorbed. |
| **TBS08** | SLS float powder + Borosilicate cullet + C + $CaHPO_4$, 790°C | x | - | low | similar results with TC04, with lower water dispersion |
| **TC09** | Cyclon mix* + C + $CaHPO_4$, 790°C | x | x | low | similar results with TC01 & TC05, angle seems below 90° |
| **TS10** | SLS float powder + C + $CaHPO_4$, 790°C | x | x | high | surface gets wet probably because of pores, however light reflected onto the droplet shows a contact angle close to 90° |
| **TC11** | Cyclon mix* + $CaCO_3$ (3%), 840°C | x | - | low | similar results as TC04, there was no need for 2nd attempt |
| **TC12** | Cyclon mix* + $CaCO_3$ (5%), 840°C | x | - | low | similar results as TC04, there was no need for 2nd attempt |
| **TC13** | Cyclon mix* + $CaCO_3$ (10%), 840°C | x | - | low | similar results as TC04, there was no need for 2nd attempt |
| **TBS15** | SLS float powder + Borosilicate cullet + $CaCO_3$ (5%), 840°C | x | - | low | similar results with TBS08, but less quicker absorption |
| **TS16** | SLS float 2 particle sizes + $CaCO_3$ (5%), 840°C | - | - | - | cannot be tested due to its irregular shape, however it seems highly permeable |
| **TBS18** | SLS float powder + Borosilicate cullet + $CaCO_3$ (5%), 790°C | x | - | low | similar results with TBS08 & TBS15, with higher water dispersion |

Table 9. Results of monitoring the contact angle on the specimens by simply using a pipette to drop water.

* refer to Appendix_Table 1 for exact chemical composition. Cyclon is a by-product of the bottle- recycling industry, containing SLS glass heavily contaminated.

### 3.3.2.2. Permeability test

This test was designed in order to arrive to some quick conclusions about the potential of the different porosity structures checked microscopically, by comparing the performance of the samples' permeability. Its set-up is well-described both in the diagram included in the paragraph of the experimental process (Figure 43) and the following photographs in Figure 65.

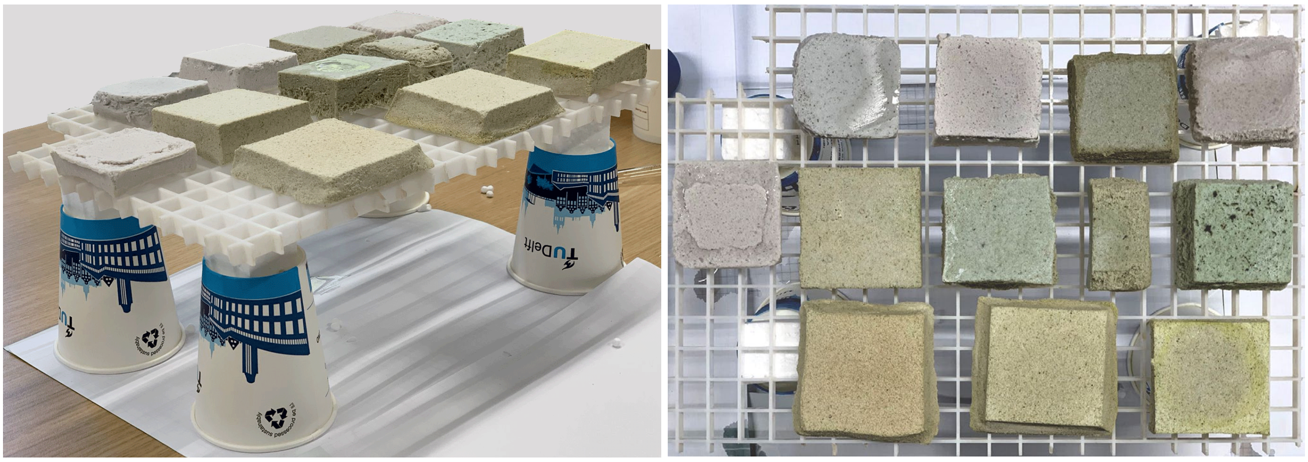

Figure 65. Experimental set-up to test how permeable is the microstructure, by dropping 1-5 ml of water onto the surface of the slated samples and measuring the time, while monitoring the effect of the results.

As it is seen in the Table 10, the experiment was conducted by dropping specific amounts of water and measuring the time that the water was absorbed from the surface, as well as checking its effect on the backside of the sample. The polished surface was used for the first contact with the water, since in the outer one the structure is altered due to the mould reaction. Depending on the absorption capability that was inspected at that moment, the amount of the dropped water varied, indicating already a difference in the potential. While, the droplet-falling time was aimed to take place within the first minute of the examination.

Particular interest showcased the behaviour of the different types of porosity. In detail, the most expected results were validated, concerning the microscopically observed closed-porosity, mainly in TS07 that the water remained on the surface for the whole duration of the experiment. In contrast to the previous, high potential was revealed in the samples TC04, TC11-TC13 composed by the Cyclon mix and $CaCO_3$ in different temperatures and percentages. Having the Porosity type 03 (granules) as it was analyzed in the paragraph of microstructure, the performance of TC13 is depicted in the Figure 66 where the water appeared to disperse along the sample in both axes, vertically and horizontally. Among these, at TC11 and TC12, corrosion was observed by change in the particles' colour both at the edges of the sample, but also at the outline of the area in contact with water ( Figure 67) leading to the conclusion that their mixture reacted with water and therefore, already rendered inappropriate for biofouling.

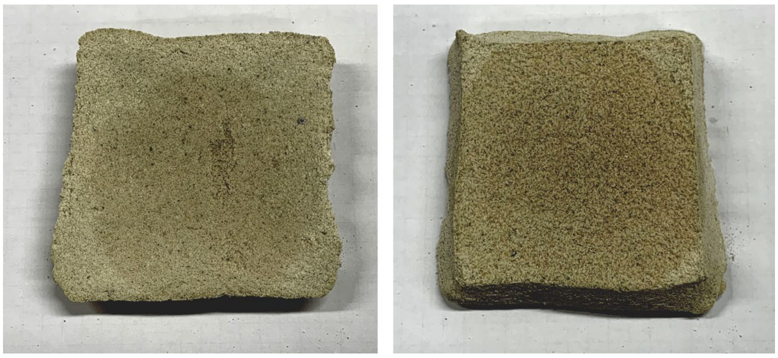

Figure 66. Photographs of sample TC13, a Cyclon mix with 10%wt $CaCO_3$, showing the stain of the dispersed absorbed water from the polished surface towards the opposite one.

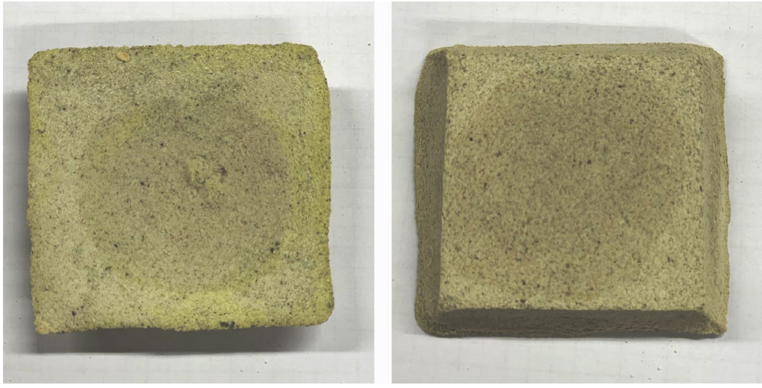

Figure 67. Photographs of sample TC12, made from Cyclon mix together with 5%wt of $CaCO_3$, depicting the corrosion from water only on the surface which also has reacted with the mould. However, the water in comparison with sample TC13 has slightly limited dispersion.

| | Recipe description | Water (ml) | Time (min) | Permeable | Observation |
|---|---|---|---|---|---|
| **TC01** | Cyclon mix*, no foam. additiv., 840°C , slow cool | 1 | 10 | + | indication for vertical open-network after a long time |
| **TC04** | Cyclon mix* + $CaCO_3$ (10%), 840°C, slow cool | 5 | 10 | +++ | water dispersion, only the 4 edges were not wet |
| **TC05** | Cyclon mix* + C + $CaHPO_4$, 840°C, slow cool | 1 | 10 | - | sample is not equally comparable due to its half-cut size. After a long time there were moisture signs on the cut-side revealing shallow vertical connection |
| **TC06** | Cyclon mix* + C + $CaHPO_4$, 960°C, slow cool | 1 | 15 | + | partial absorption mainly due to large pore-openings, moist opposite surface on the one edge, showing diagonal connection |
| **TS07** | SLS float powder + C + $CaHPO_4$, 960°C, slow cool | 1 | 10 | - | Signs for closed porosity- water remained on the surface during the whole experiment |
| **TBS08** | SLS float powder + Borosilicate cullet + C + $CaHPO_4$, 790°C | 5 | 5 | +++ | absorbing at a slower pace, moisture signs on the side surfaces |
| **TC09** | Cyclon mix* + C + $CaHPO_4$, 790°C | 1 | 15 | + | sample was wet mainly from the sides after such a long time, that the initial wet surface had dried |
| **TS10** | SLS float powder + C + $CaHPO_4$, 790°C | 1 | 10 | - | water remained on the surface for a long time |
| **TC11** | Cyclon mix* + $CaCO_3$ (3%), 840°C | 5 | 3 | ++ | among all the cyclon & CaCO3 recipes, it had the smallest dispersion, corrosion is observed |
| **TC12** | Cyclon mix* + $CaCO_3$ (5%), 840°C | 5 | 1 | ++ | high corrosion observed at the non-treated surface |
| **TC13** | Cyclon mix* + $CaCO_3$ (10%), 840°C | 5 | 1 | +++ | the most water absorbent with highest water dispersion |
| **TBS15** | SLS float powder + Borosilicate cullet + $CaCO_3$ (5%), 840°C | 5 | 5 | +++ | highly absorbent with high dispersion, even though its thickness was the thinnest |
| **TS16** | SLS float 2 particle sizes + $CaCO_3$ (5%), 840°C | - | - | - | cannot be tested due to its irregular shape, however it seems highly permeable |
| **TBS18** | SLS float powder + Borosilicate cullet + $CaCO_3$ (5%), 790°C | 5 | 3 | - | the most absorbent among the borosilicate & SLS samples with high dispersion. |

Table 10. Results from the permeability quick set-up to assess the potential of the created recipes.
*Cyclon mix contains SLS glass, heavily contaminated, since it is a by-product of the bottle-recycling.

Additionally, positive remarks were noted regarding the Borosilicate and Soda-lime mixtures TBS08 & TBS15 with different additives, that both of them absorbed the maximum amount of dropped-water and showcased quick results, but not extremely rapid to imply a relation with abrupt evaporative trends. Proof of this is depicted both in Figure 68 and Figure 69, where it is shown how the water is absorbed and dispersed simultaneously.

Figure 68. Photograph of sample TBS08, where the darker-coloured areas are moist from the dropped water, showing how permeable the material is.

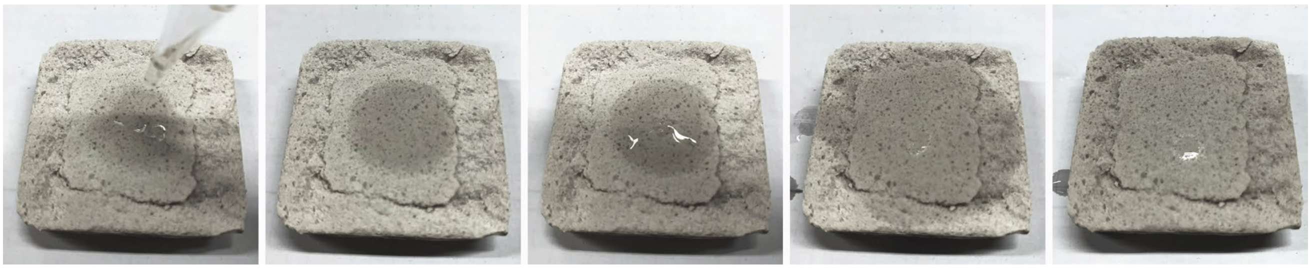

Figure 69. Timeframe from testing the sample TBS15, showcasing the low contact angle and therefore, high potential for water absorption along the whole thickness of it.

Apart from the previous findings, the rest of the samples had either a great or a small delay in taking in the water, affecting the amount that was chosen to drop in each case. Such an example, was TC09 which needed a lot of time in absorbing only 1 ml and when it did, the initially-wet surface had already starting to become dry, while the rest of the surfaces were really moist, revealing a potential dispersion in small depth along the sides of the sample, rather than a vertical one (Figure 70). Another case constitutes the specimen TC06, which also presented one of the longest absorption timings, illustrated on Figure 71, where it is obvious from the moist sides that only the larger pores of the polished surface transferred the water along its thickness, while the rest of it must be characterized mainly from non-permeable porosity.

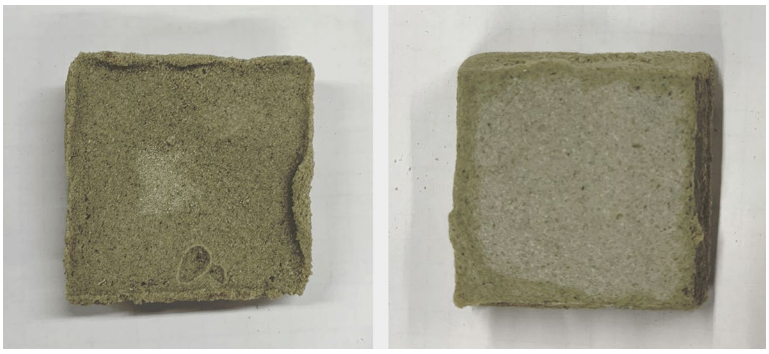

Figure 70. Dispersion effect along the surrounding sides of the sample TC09, implying that its vertical network is not fully permeable.

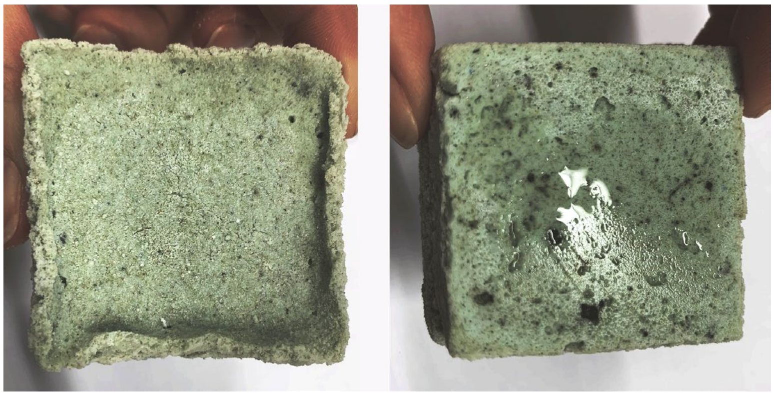

Figure 71. Sample TC06 showcasing similar effect with TC09, however, only the wider pore sizes seem to transfer the water into the sample.

### 3.3.2.3. Water Saturation

The water saturation test is one of the most important indicators that illustrate the maximum capacity of the sample to absorb water. For this reason, in the testing process it was deemed necessary to initially conduct the samples' sinking, because with drying measured right after, it was already evident which recipe had the largest capacity and was worth to explore even further, meaning also that there was a higher percentage of open porosity.

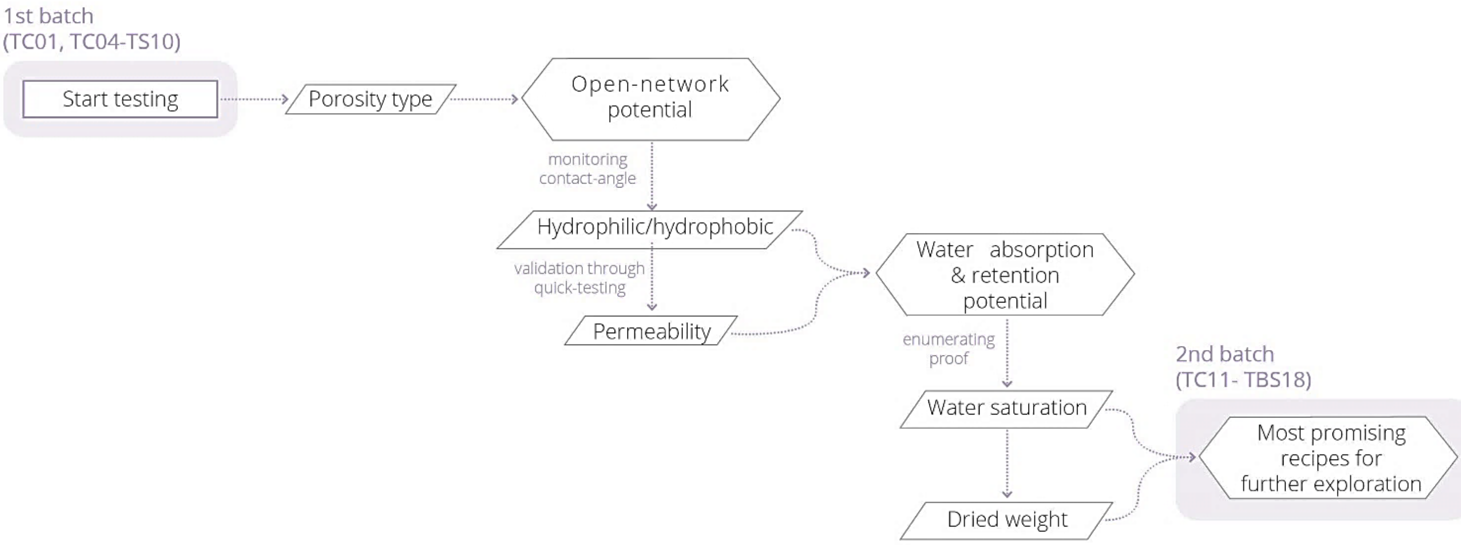


Figure 72. Flowchart illustrating the testing process as a methodology for choosing the parameters to be tested (Ingredients – Temperature – Heating schedule). Results from quick testing are used as an input for the next experimentations, while the rest of the testing process continues for validation and further exploration.

Thus, by observing the results of the first batch (TC01, TC04 - TS10) with the methodology, presented in the Figure 72, the choice of the next batch's recipes and parameters to be tested is proved. As seen in the Chart 2, TC04 with its distinguishing microstructure type (Figure 51), presents by far the highest saturation level, however during the whole experimental process it exhibited a very brittle behaviour with subtracting material left every time upon touching. Whereas, the samples created with different ratios of the foaming agent ($CaCO_3$ in 3%, 5% & 10%) presented a better structure against brittleness as the agent percentage decreased, which was also reflected proportionally in the saturation levels. During the submerging of the samples, the corrosion of samples TC11 & TC12 was not so evident, as right after saw-cutting.

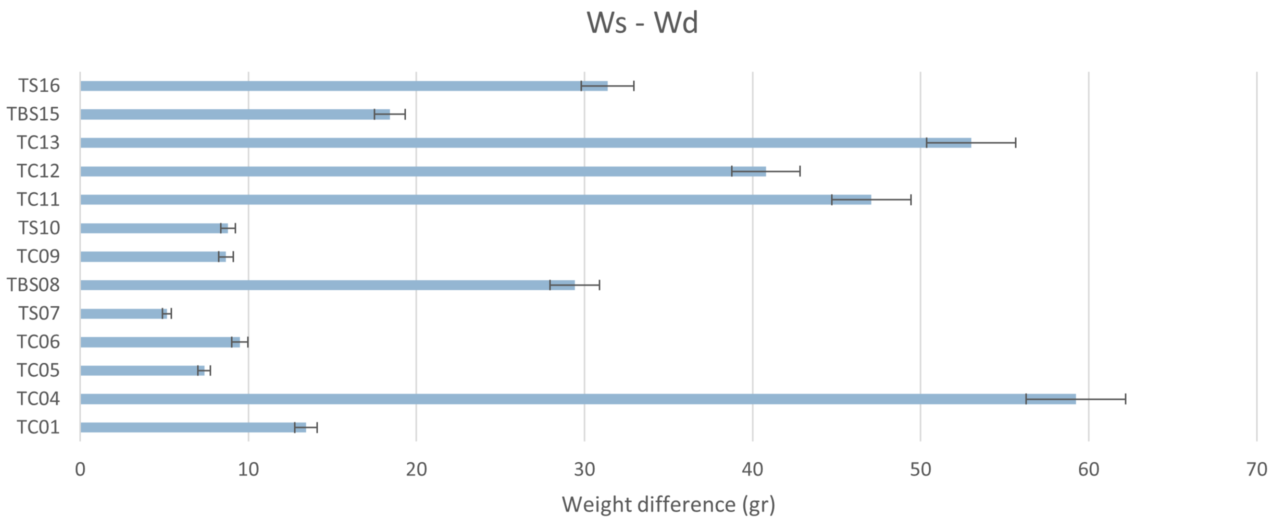


Chart 2. Comparative analysis of the saturation level of the cubic-shaped samples.

Great interest holds the recipe with the different-sized of Soda-lime glass cullets (powder + crushed), that presented the highest porosity and surface roughness, due to the reaction with the agent when foaming, and this is also linked to the saturation test results. Together, the Borosilicate mixtures with Soda-lime powder showcase the third best performance, indicating their monitoring significance in the next steps of the testing process.

Finally, the rest of the samples composed of the recipe analysed in Table 6, present similar measurements. These mixtures were formed based on the promising example of König et al., 2020, that was mostly investigated under different foaming temperatures and heating schedules, but yet the microscopic results regarding high propability for closed-pores were also verified by the lowest rates of water-saturation. Whilst TS07 was using Soda-lime glass as the main ingredient similarly to the literature example, among all the specimens it showcased the worst performance, rendering that higher temperatures for open-porous foams are not beneficial.

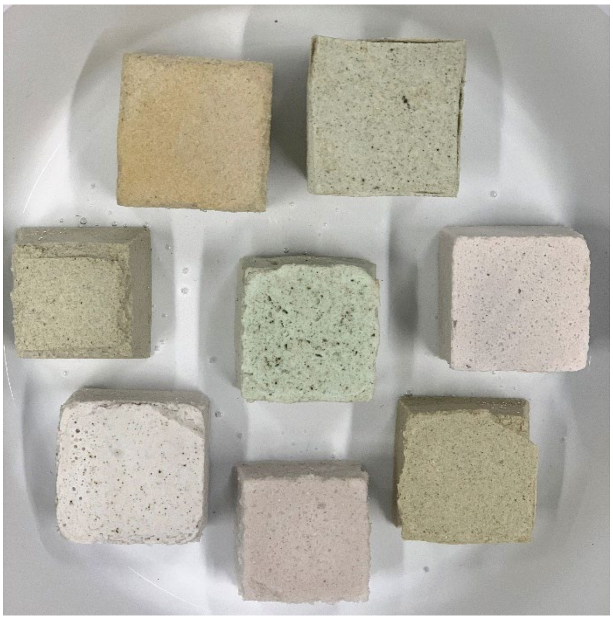

Figure 73. Specimens (TC01, TC04-TC06, TS07, TBS08, TC09, TS10) submerged into the water for 24hours to measure their weight after reaching their full-water saturation point.

### 3.3.2.4. Water Absorption rate

In general, the test of water absorption rate, verified the inspections and results that were already obtained about porosity from the microscopic images. However, the main question remained regarding the Porosity Type 2 & 3 (Figure 51), whether they absorb water and at what rate to finally offer concrete answers about the bioreceptivity potential for the materials. Encouraging was the evidence, that from the beginning of the test, the weight measurements were different from the initial one ($W_0$), characterizing the materials without only closed-pores as water-absorbent. Since the nature of the hydrophilic / hydrophobic surface was a major obstacle for the goal of this research oriented on manufacturing the right porosity type and hydraulic properties for microorganisms' colonization.

The experimental set-up as depicted in the Figure 74, presented some limitations, even though the samples were carefully positioned onto the scale after being gently dried with a cloth, it was observed that there were leaving traces of water on the scale. This fact, proves that the measurements gathered include a human error and the reported weight of the absorbed weight was varying by ±0.20gr.

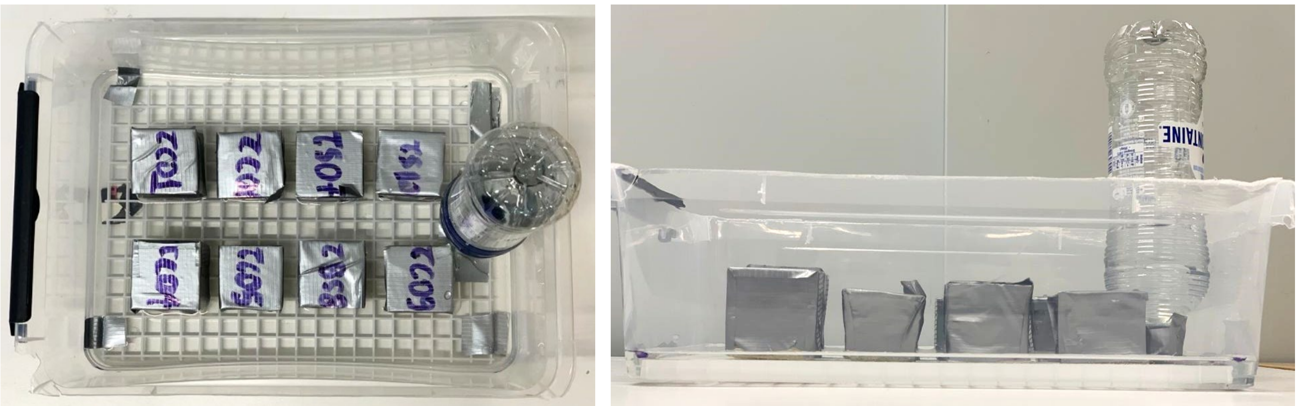

Figure 74. Experimental set-up for testing the water absorption rate. Image Source: Own (29/04/2022).

Regarding the results, illustrated in the Chart 3, a general trend is observed of the curve rising abruptly from the first measurements, while later values increase ranging 0,01 - 0,1, forming a very slow pace, that is shown as an almost straight line in the chart. Although this implies that the samples absorb water almost equal to their capacity from the very first minutes, it is not yet examined if they dry as quickly. Whilst, it is encouraging that the absorption continues to take place during the next 8 hours that the measurements are being gathered, with the last values reaching identical numbers at the very end. The two recipes that distinguish from the first batch of samples (TC01, TC04-TS10) are clearly shown both in the water absorption curve and the water saturation levels (Chart 2). Since, the adsorption in all the samples follows a similar path, reaching in the first few minutes values closer to the ones of the fully-saturated specimens, the results of these two tests coincide.

In addition, during the experiment the reported rate clearly validated the porosity results of firstly TS07, which was by far the least porous with closed-cellular structure. Whereas, the samples TC05, TC06, TC09 and TS10, mixed with the same foaming agents (refer to Table 6), present similar values in the water-saturation levels and absorption rate. Proving that, the tested additives for creating an open-pore structure did not react at their full extent as intended, leaving denser elements with higher closed-porosity ratios. A vertical section should also prove this, shedding light on the variety of the pore structure in height, creating short open-network paths closer to the upper surface, as illustrated in Figure 57.

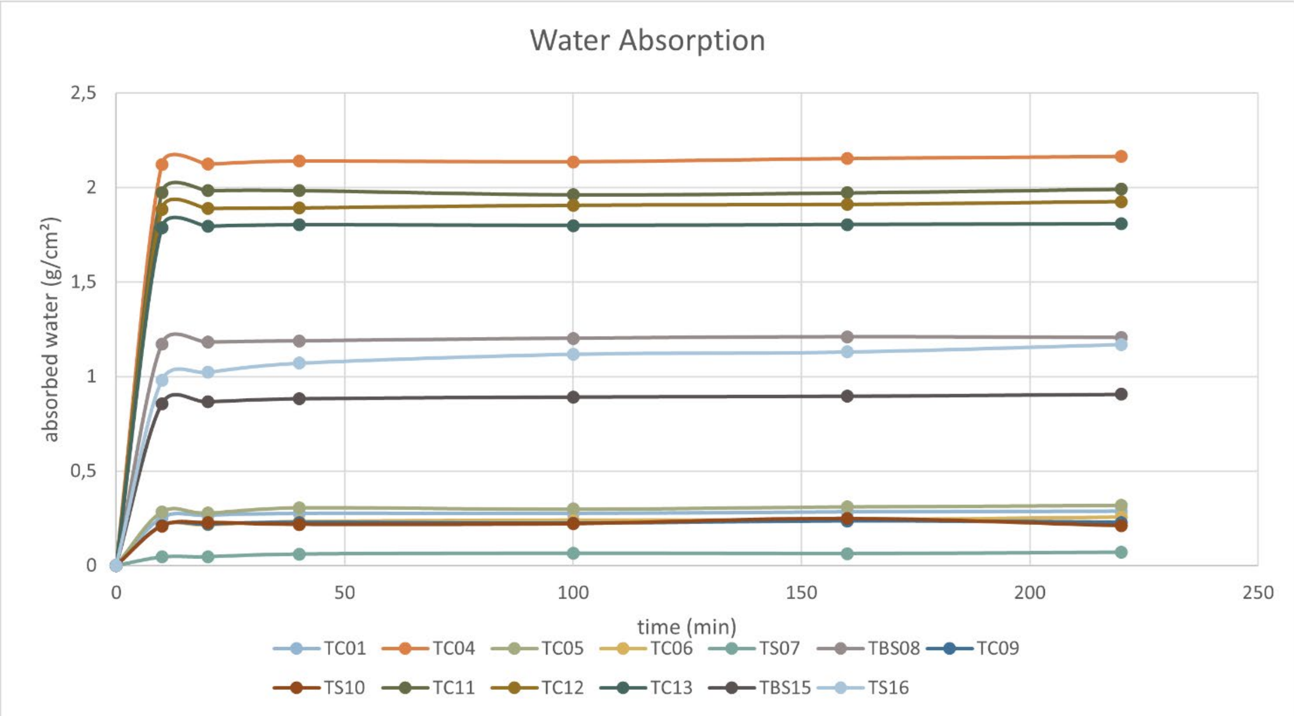


Chart 3. Water absorption curves for all the cubic-shaped specimens. Measurements taken after the shown time-period were excluded because they did not portray any specific difference.

Regarding the next batch of 5 samples created based on the results of the first measurements, it can clearly be concluded that their adsorption performance strikes better levels for all the recipes (TC11-TC13, TBS15 & TS16). While the Cyclon mixes present very similar properties, they are exactly the opposite of what was expected based on the microstructure analysis. Since TC13 is composed from exactly the same recipe as TC04, which until now has the highest saturation level, a matching performance was anticipated to score the highest and being followed in this sequence by TC12 & TC11. On the contrary, TC11is the highest of the three, succeeded by TC12 and then, TC13. This outcome is supported by the phenomenon of capillary rise. Since, the size of residual porosity of the samples is reversely analogous to their absorption performance, water is easier sunk into the smaller-sized pore network of TC11 that contains the lower percentage of foaming agent, rather than the more permeable TC13.

As far as TBS15 and TS16 are concerned, their performance still scores in satisfying levels comparing to the other samples. Nonetheless, the extremely large pore-sizes recorded on the surface of TS16 raise attention about its evaporative performance that is going to be analysed in the next paragraph. While, TBS15 depending on its compressive strength performance, that needs validation during the next experiments, might constitute a good compromise between the hydraulic properties and brittle behaviour.

Surprising was the fact, that in a few examples the weight measurements during the absorption rate testing, exceeded the water-saturation ones. A possible explanation can be attributed to the entrapped air inside the specimens that existed during the 24hours-sinking and prevented to showcase the full capacity. For this reason, the test of water saturation was repeated after the absorption rate, presenting values closer to the ones indicated in the absorption curve.

To further analyse and compare the test results with other papers and materials, an attempt was made to calculate the Water Absorption Coefficient (WAC) and Initial Rate of Absorption (IRA) from the presented Chart 3. According to Lubelli B. et al. (2021), the first is calculated from the slope of the linear part of the absorption curve, as illustrated in Chart 4, while the second one is the absorbed water during the first minute per unit of area. Although this information is gathered in Table 11, WAC is not fully comparable to the paper of Lubelli B. et al. for example, due to their different measurement units. Nonetheless, from the comparison obtained for IRA, the glass foam samples of this research that present the highest potential have scored with by far larger values, than the ones analysed of the chosen bricks (B2- 3.91, B8-0.20) for the testing of the bioreceptive masonry wall. This, reveals that the glass foam's behaviour vary greatly from bricks, absorbing from the first minutes almost its maximum capacity, whereas clay bricks optimized for water retention reach their saturation levels at a much lower pace. Such an outcome, can only act negatively if this happens also during the evaporation test, leading to the result that the investigated material cannot retain water for longer periods when compared to already developed products for bioreceptive applications.

| | TC01 | TC04 | TC05 | TC06 | TS07 | TBS08 | TC09 | TS10 | TC11 | TC12 | TC13 | TBS15 | TS17 |
|---|---|---|---|---|---|---|---|---|---|---|---|---|---|
| IRA (Kg/m² min) | 2,388 | 21,092 | 2,613 | 1,953 | 0,4 | 11,753 | 2,132 | 2,16 | 19,423 | 18,608 | 17,692 | 5,58 | 7,2 |
| WAC (gr/cm² min) | 0,025 | 0,212 | 0,028 | 0,021 | 0,004 | 0,117 | 0,021 | 0,021 | 0,197 | 0,189 | 0,179 | 0,086 | 0,098 |

Table 11. Samples properties regarding water absorption. Reported values on WAC & IRA.

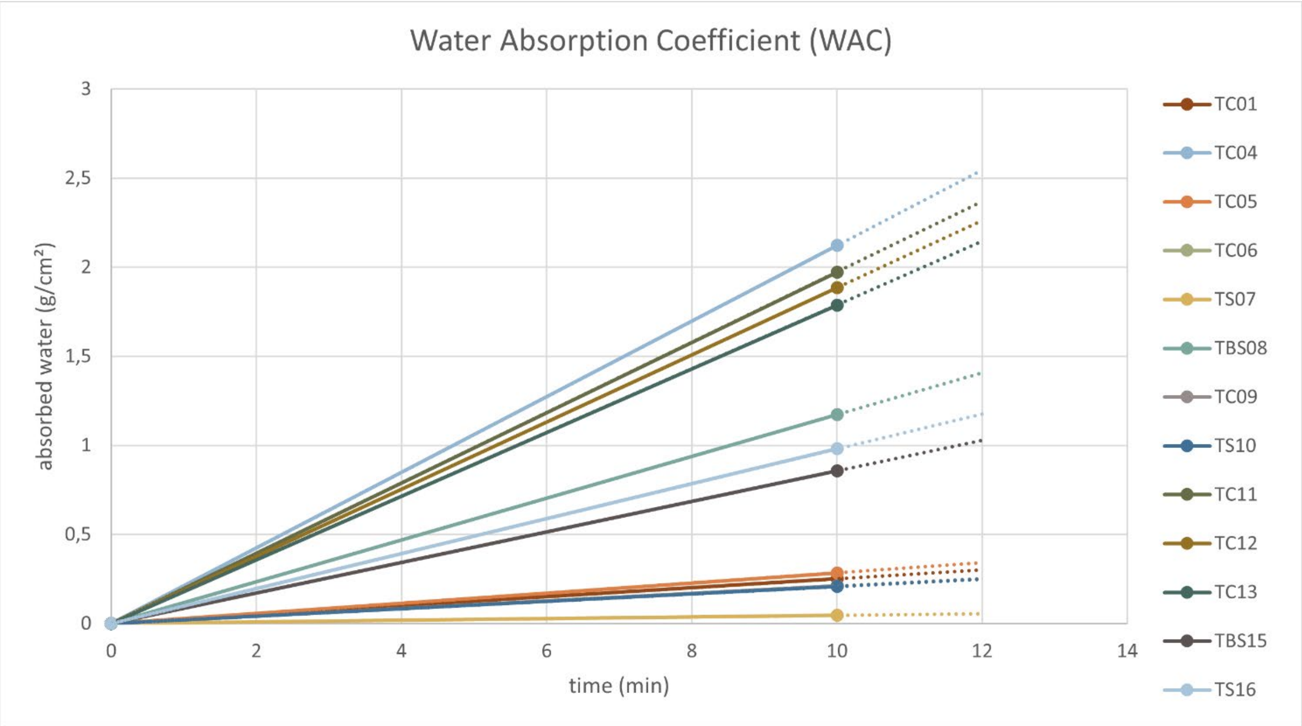


Chart 4. Isolated linear part of the absorption curve to measure WAC.

### 3.3.2.5. Evaporation rate

Equally important to measuring the absorbing capacity is to reveal the rate that the material gets dried again. Since, it is mentioned in the first chapters analysing the material conditions for primary bioreceptivity, that microorganisms thrive onto materials that can be kept moist for longer, or even better they can retrieve water from them, in order to survive during drought periods of time.

During the test, in which the set-up is depicted in Figure 75, the samples as described in the experimental process paragraph, were covered from all sides, leaving the drying to take place only from one. The measurements in this case, were not recorded as frequently as in the absorption test, in which the first 8 hours were the most critical. Because, in this experiment duration is more crucial to reveal the point in time that the samples approach the levels of their dried weight.

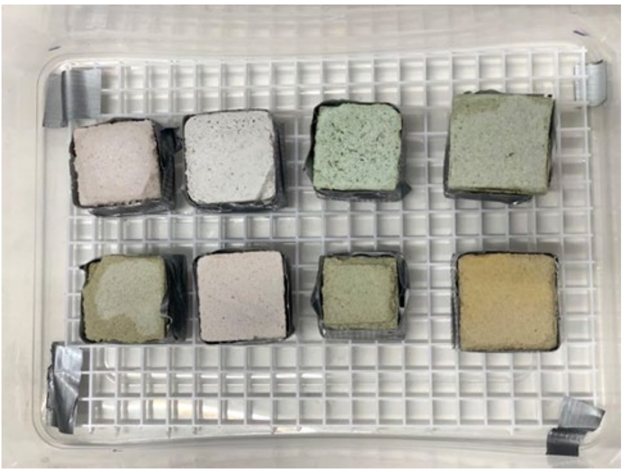

Figure 75. 1st batch of samples during the evaporation-rate testing. Uncovered surfaces have already started drying, from most of the specimens, except TC04 & TBS08. Image Source: Own.

Assessing the test results illustrated in Chart 5, the behaviour of the specimens which showcased the greatest potential in the previous experimentations appears to be really promising, when compared with the rest of the produced glass foams. Specifically, the highest performing specimens are: TC04, TC13 & TBS08, followed by TC11 and TC12. Their scoring can be also related to the highest adsorption capacity that they resulted when measuring their saturation levels, however it should be noted that their benefit is focused on the fact that their evaporation curve rises gradually. Hence, these satisfactory results of a lower evaporation rate, compared with the rest of the produced glass foams, indicates positive evidence identified from their studied porosity and better absorption performance, for further exploration.

On the contrary, the rest of the samples – apart from TBS15 – show an abrupt increase reaching close to their highest point in the first measurements, and then a stable path is monitored. The reason for such a behaviour can be attributed either to the existence of a superficial open pore-network, or to large pores that lead to rapid evaporation, almost all the absorbed amount, which from Chart 3 can be inferred that took place in the first 30 minutes. Therefore, these series of material models are deemed unsuitable for applications that demand water retention. Their recipe and way of foaming did not reach the desired porosity network that combines both coarse and fine-shaped pores connected.

The un-anticipated curve presented by TC01 can be justified from the findings of Chart 1. Although its porosity was characterized with clustered pores containing low percentages of connectivity, the smallest size of them, compared to the rest of the samples with the lowest-scored performance, proved the importance of fine-sized pores in contrast to large coarse ones.

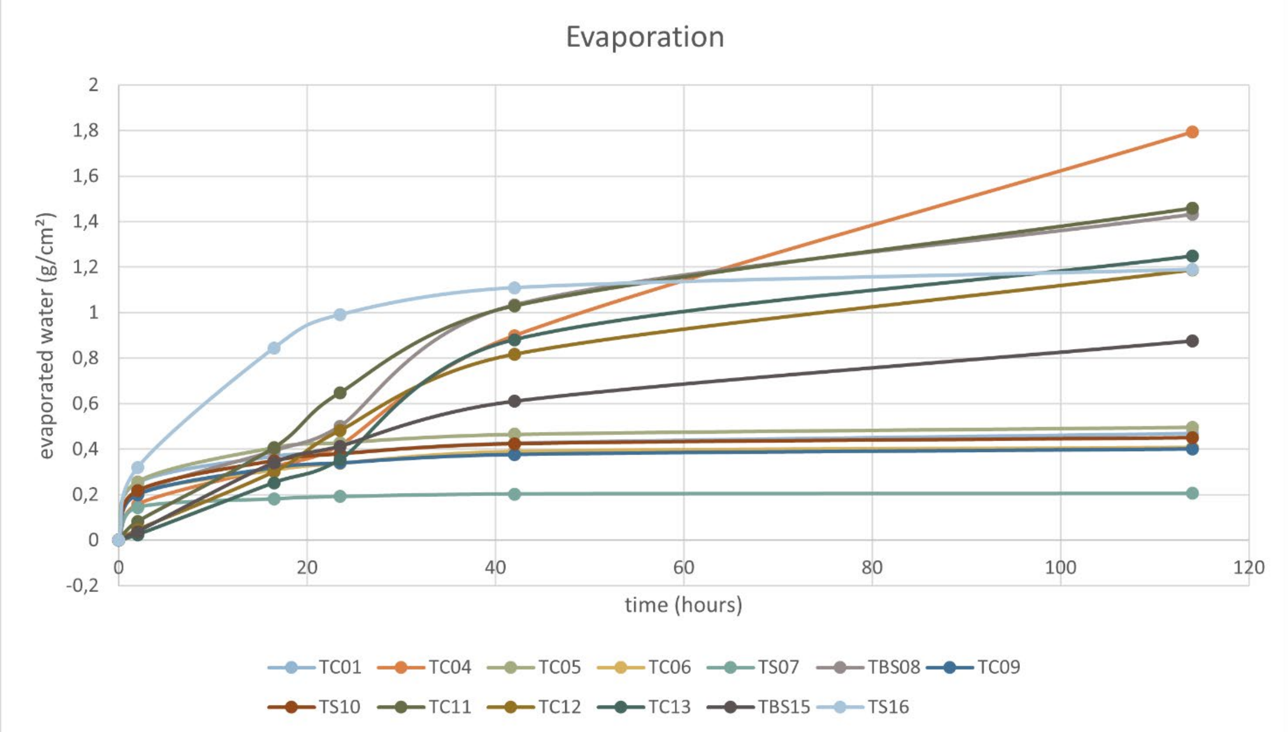


Chart 5. Evaporation rate curves formed from measurements taken during one-week period.

### 3.3.3. Frosting resistance

To achieve a holistic investigation in the time constraints of this thesis, a test checking the durability against frosting was explored regarding the capabilities and limitations of the produced experimental samples. Since water-absorbing porous materials are under examination, the aim of this step of the experimental process is to give a rough indication, whether the specimens are proved worthy of exploring further, or they are deemed completely inappropriate to withstand environmental conditions.

To answer this, all specimens were inserted to a freezer located at microlab in the Building of Civil Engineering in TU Delft, for 24 hours initially, at -5 °C. After this test-cycle there were no alterations either in the surface or in the touch of even the most brittle of the glass foams. For this test, the status of absorbed water should not be relevant, as the outdoor conditions can be unpredictable. However, it should be mentioned that the sequence that this test was conducted and reported is after the evaporation rate assessment. Therefore, even though the amount of retained water was at low levels, samples were not in a fully-dried condition, in order to check the effect of freezing water inside the porous network of the material. Exception to the previous is only the sample TBS18, which was being measured for its absorption performance at the point of insertion to the freezer, since it was created at a later stage than the rest.

For this reason, the test was repeated in the water-saturation state for all the samples and inserted in the freezer at a lower temperature than previously, at -12 °C, similarly for 24 hours. In this case, noteworthy for the open porous structure, is the formation of ice on the upper surface of most of the specimens, proven by the photographical documentation presented in Appendix_Table 5. Although more formed ice was observed on top of the ones with the higher water absorption capacity, no cracks or stress signs were detected.

Despite this positive general outcome, decomposing material particles upon friction were noticed as the ice was melting in the most porous samples especially of Porosity Type 03 & 04 (Figure 51 & Figure 52).

With repetitive frosting cycles, this effect should be measured in order to determine with accuracy the samples' resistance. In addition, with different loading conditions, the resistance to frosting which is based on the tensile strength of the material, might have been even lower, thus this should be a point for further examination depending the application that the material is being developed for. Since the current samples have already been characterized as brittle, the primary goal of monitoring which microstructures are not robust enough to endure extreme environmental conditions was achieved by all of them.

### 3.3.4. Compressive Strength

For the compressive strength assessment, a triad of the most promising recipe, concluded from the previous tests, was chosen to be tested. Even though, the current research is at such an early experimental stage, the results regarding their mechanical properties were deemed important to be analysed, in order to draw holistic conclusions about, not only the material's hydraulic performance, but also the weakening points for further exploration. Since, high brittleness was already been exhibited from the initial tests, as far as strength performance is concerned high values were not awaited.

For this reason, 8872 linear fatigue testing system by Istron (Figure 76) was used for measuring the maximum load applied on the samples until the moment of plastic deformation. The device in microlab, TU Delft was set accordingly to record at least 2 measurements of the maximum force applied per quarter of second, due to the level of the awaited results. Although this test was held only as a reference of strength, a statistical analysis should also be taken into consideration, to obtain concrete answers, because there are many factors playing an important role on such a measurement.


Figure 76. (from left to right) a) Compressive strength test set-up, b) cracks of permanent deformation appeared in the specimen TBS21 under the maximum load of 3,14 kN, c) apparent material residue after testing. Image Source: Own.

During the test, the three samples presented similar behaviour, despite the slight difference of the resulted maximum load applied. Specifically, the first reaction of the tested glass foam to compression was a small amount of particles starting to fall off, creating a sand-like film near the testing area as seen in Figure 76. This effect became more evident as the load was increasing, until the formation of cracks along the specimens' section, splitting it into pieces, that were varying in sizes per each sample (Appendix_Table 4).

It is worth to mention, that even though the same recipe was being tested the first cube, which withstood the smallest load, had the less brittle behaviour according to the findings represented in Chart 6. Since the curve after the first convex point representing the occurrence of the first crack, does not follow such an abrupt path compared to the samples TBS20 & 21, showing their higher prompt to breakage. Apart from the possible range in microstructure, the longer testing period aiming to record more accurate results due to unknown performance by the time, forms an additional explanation leading to this alteration in the deformation curves. What's more, the linear part of the curves before the maximum deformation, showcases certain fluctuations that can be attributed to the gradual material loss, which was observed taking place firstly on the corners of the cube.

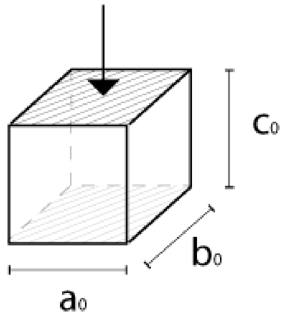


Figure 77. Diagram illustrating the specimens' measurements in relation to the applied force-surfaces.

| Sample | $a_0$ [mm] | $b_0$ [mm] | $c_0$ [mm] | Testing time (s) | $P_{max}$ [Kn] | dL at $F_{max}$ [mm] | $\sigma_{max}$ (MPa) | Characterization based on deformation curve |
|---|---|---|---|---|---|---|---|---|
| TBS19 | 48,5 | 42 | 49 | 311,45 | 2,7 | 1,54 | 1,33 | Moderate Ductile |
| TBS20 | 48 | 42 | 49 | 213,66 | 3,25 | 1,31 | 1.61 | Brittle |
| TBS21 | 48,5 | 44 | 49 | 167,75 | 3,14 | 1,22 | 1,47 | Brittle |
| Mean | - | - | - | - | 3,03 | 1,36 | 1,47 | - |

Table 12. Test results regarding maximum load applied and relative deformation per specimen.

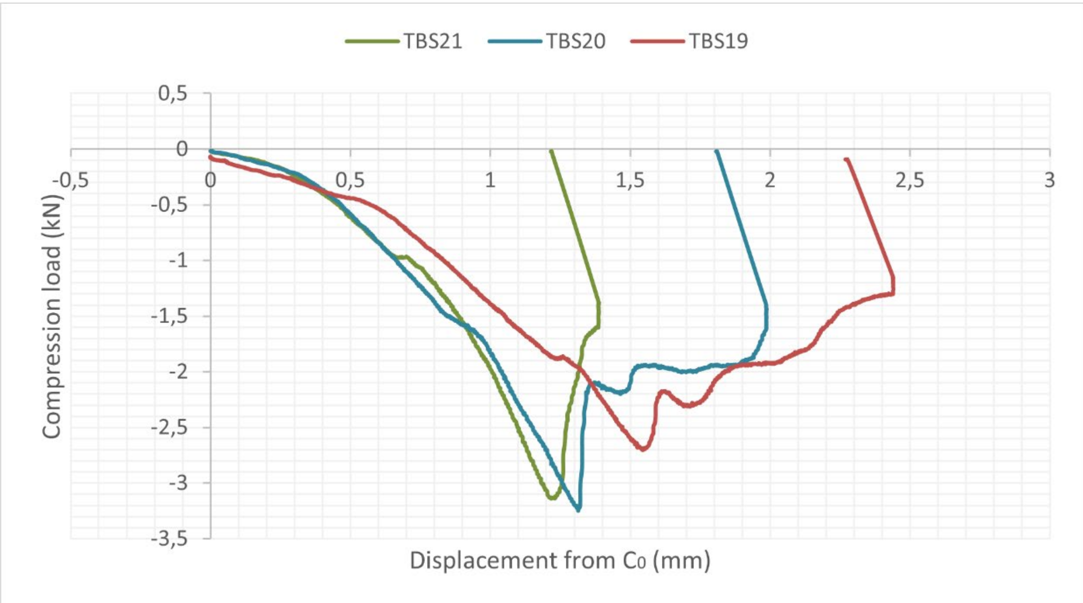


Chart 6. Load – displacement graphs for the three specimens of the same recipe [SLS powder (float glass) + Borosilicate cullet + carbon + CaHPO4, 790°C (2hrs), fast cool to anneal. point (1hr)]. Test conducted on 07/06/2022 together with Maiko van Leeuwen, using Istron 8872, in microlab, TU Delft.

It must be noted that even before conducting this test, the testing triad presented considerable differences in their brittle behaviour from the original sample that scored high in the previous hydraulic properties assessments. Since, the heating schedule and the main recipe ingredients between the samples TBS19-21 & TBS08 were similar, the possible explanation might lie on the sizing of the SLS powder or even the mixture proportions of the previous with the Borosilicate cullet, taking into account the human error. The timings that the specimens were produced were distant, and the powder used in the triad was produced from sieving crushed SLS float glass and milling it afterwards for 4 s, as explained also in Figure 42. Checking the more brittle tested specimens, in contrast to TBS08, the powder used in the latter must have been more refined, leading to better particle-bonding in 790 °C, which was one of the lowest foaming temperatures tested. Therefore, if such an incident had not taken place, the expected values for the compressive strength would be even higher, which is a very positive indication when compared with other materials, derived either from the literature regarding bioreceptivity of from other building applications.

The test findings of the chosen recipe to test -SLS powder (float glass) + Borosilicate cullet + carbon + $CaHPO_4$, 790°C (2hrs), fast cool to anneal. point (1hr)- reported in the Table 12, with respect to the maximum force and the point of permanent deformation, show a mean compressive strength of 1,47MPa. Such a low value, needs further consideration depending on the specific building or product application. In further detail, the difference between the aforementioned obtained value and other examples analysed in literature is depicted in Chart 7. Even though the information gathered reflect values from different materials, which under no circumstances can be effectively compared between them, it offers an overall guide about the recent state-of-art research in the field and the desirable outcome that can be set for further research.

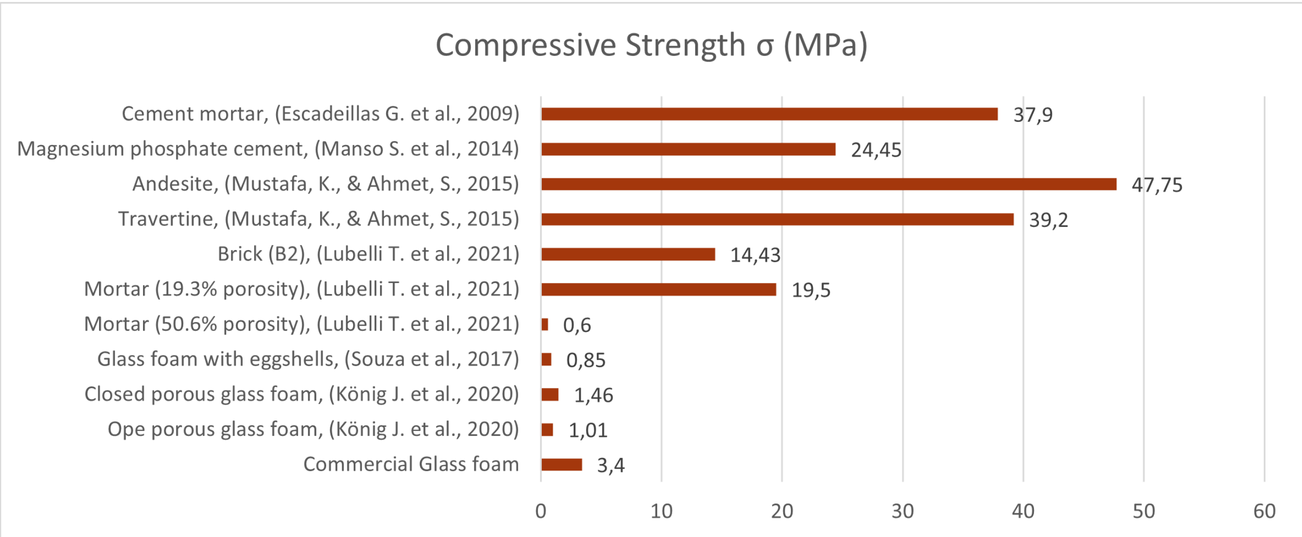


Chart 7. Data collected regarding other materials' values studied in literature review, either for their bioreceptive performance or for their glass-foam structure.

### 3.3.5. Moss growth

Figure 78. Photograph taken during the 4th week of the experiment, showing the lower placement of the tiles, near the mist sprinkler.

The last phase of the experimental series is included in the report as part of the process, even though during the time constraints, the results cannot be thoroughly analysed. This argument is based on the fact that, botanical and ecological knowledge would be beneficial in studying the growth rate or the reasons for limited or even no growth presented. In general the application of the specific type of moss 'tortula murallis', which was retrieved from the outer surfaces of the Faculty of Architecture, in TU Delft, as indicated in the photographs Figure 83, was based on developed techniques that Veeger M. (2021) has presented in his thesis. The steps are documented in Figure 52 and the moss type depicted in Figure 82.

For the experiment, two tiles, sized approx. 10 x 10 cm, were placed in the Botanical garden of Delft, in a tropical environment without any maintenance or fertilizer for the duration of 6 full weeks. The greenhouse conditions were very moist, since there were mist sprinklers spraying the space every 5-10 minutes. Despite the unfavourable time period during May and June, due to warmer weather that raised the temperatures above 20 – 25 degrees inside the greenhouse space, the specimens did not receive direct sunlight and were kept moist during the whole testing time. What's more, to ensure the best conditions possible regarding shadow and water, they were placed near the floor level on a ceramic step, in close proximity with the sprinklers, as seen in Figure 78.

The recipes that were chosen, while conducting the experiments for water absorption, were firstly TC04 (Cyclon* + $CaCO_3$ (10%), 840°C, slow cool) that presented the highest potential among all the specimens in every test conducted related to its hydraulic properties, resulting in the sample TC14, and secondly the recipe of TBS08 (SLS float powder + Borosilicate cullet + C + $CaHPO_4$, 790°C) that was the second one in scoring from the first batch of the samples, producing the tile TBS17 Even though the decision for these samples was made from early on, by looking into the hydraulic properties test findings these were the most promising samples, out of different glass waste sources.

Figure 80. Moss identified as species Tortula muralis, gathered from the Faculty of Architecture to be applied on the samples.

Figure 79. Tortula muralis as the chosen moss for testing onto the bio-host glass tile.

In the Appendix_Table 6 is presented a chronological photographical report from almost every week, demonstrating the progress regarding the bio-growth. It is obvious that during the first two weeks at least, the moss powder sticked on top of the natural glue had dried. As the critical time passed, against all the odds, during the fourth week the first evidence of life was observed. In the next visit to the greenhouse, all doubts regarding the type of the observed microorganism were erased, as the first green moss stems started to appear. However, this desirable evidence was noted firstly on the sample of TC14, whereas the TBS17 did not have clear signs, or as brightly green-coloured as the previous.

Due to the short testing period, together with no previous literature review or experiment supporting the fact that microorganisms can host a material like the produced one, the results of this experimental step were very doubtful. This evidence however, proves the theory that microorganisms can host every material in the right environmental conditions, and that the material developed specifically for this phenomenon, is successful. While gathering information and measured values related to material properties, such as pH level and chemical consistency to derive conclusions prior to testing, if the material can be colonized, such positive findings can already elucidate the answer that indeed the produced glass-foam out of waste sources meets all the relative bioreceptive conditions and can be further analysed for validation and experimented for urban applications.

## 3.4. Experimental Limitations

The analysis of the limitations for this research was deemed extremely important, since the goal is to provide a tool for further research on upcycling glass waste, by taking advantage material bio-colonization. In general, the constraints during this work can be divided in two categories, the ones that are mainly addressed to inaccessible laboratory and experimenting equipment that would have led to totally different conclusions, and the rest being identified as part of the conducted process contributing to the specific results.

To begin with, the very first choice of experimenting with glass foams was followed, not only because of the potential of incorporating many waste sources into this method, but also based on the fact that only foaming in a heating furnace was available, instead of compacting cullet for sintering. In addition, the furnace used in the Stevin-II lab in the tested programs reached its maximum capability for cooling down (-200°C/hour) the temperature, right after the dwell time for foaming. As a result, for higher cooling rates the result would be the same as these would not be possible to be reached.

Regarding the testing of the samples, porosity could not be investigated with accurate methods as discussed in literature, using either a mercury intrusion porosimeter, or a pycnometer for measuring the density and comparing it with the apparent density, or even a scale for measuring the samples inside the water following the way, which Lubelli B. et al. (2021) executed for the tested bricks. What's more, Scanning Electron Microscopy was unavailable for the precise investigation of the samples' pore network. The current method by analysing digital microscopic images may have led to more inspections and assumptions on the specimens' microstructure than desired for a scientific experimental analysis.

Except for the previous, the following obstacles posed constraints on the current results. Specifically, by looking into the cut surface under the microscope, certain porosity types and coloured-particles implied that the mixtures had not been totally been mixed together. Homogenizing the mixture manually instead of using a machinery with 10mm balls, such as the one mentioned in the literature review (König et al., 2020) has potentially affected the result of all the specimens, either by not aiding the chemical reactions to take place, or by creating bigger pores in the size of agglomerated particles instead of fine pores. Last but not least, parallel lines on the surface like the ones indicated in the Figure 81, were produced together with colour contamination, by the process of cutting them with the saw cutter. Thus, the microscopic results have slightly been affected, when aiming to identify pore connections and the type of the network.


Figure 81. Cut and polished surface of sample TS10, microscopic image in stitching mode, Image Source: Own.

## 3.5. Conclusions

To recall the appropriate microstructure, derived from the analysis of both the literature review, together with a microscopical analysis of other materials that have inherent capillary porosity, presented in Appendix_Figure 1-6, an open-pore structure is sought, combining coarse as well as fine shaped-pores, promoting the instant water absorption to aid primary bioreceptivity. After the analysed experiments in this chapter, concrete evidence has been revealed, towards the manufacturing of glass-foams with the ability to be colonized.

Regarding the heating schedule findings closely-related to the material science, in favour of the aforementioned pore structure, it can be concluded that overall, higher temperatures, aid the mixture to be enriched with pores of various sizes and distributions depending on the particle size of the mixture – both main ingredient and foaming agent –. Although the set of the top temperature is described as high, the value of 960°C, that was studied can already be considered as the upper limit for the discussed foaming method. Short cooling times, by accelerating the transition of the mixture from a viscous liquid to a porous solid, allow its pores created by both chemical reactions and residual porosity, to freeze and maintained. Reverse outcomes, produced by low cooling rates, due to higher pore kinetics result in a denser material, because the formed pores that have not stabilized yet, grew and coalesce creating larger irregular pores, leading also to uneven distribution.

As far as the recipe ingredients are concerned, by looking merely into the most open-pore structure with the most promising hydraulic performance, the Cyclon mix showcased great interest as a raw material. The high level of contaminants in its mixture, clearly proved to be beneficial for the experiment, but for further development, it is crucial to control their level of reaction, in order to predict the way particles are bonded, because in the produced samples, the greatest range of pore sizes and shapes was observed. Leading to the conclusion, that the inclusion of Borosilicate glass into the recipe, as a glass waste source with high crystallization tendency is very promising for the set criteria and needs to be further studied.

With respect to the tested foaming additives, samples with $CaCO_3$ proved to have a higher brittle behaviour, regardless their main ingredient, compared to the ones that contained carbon black and $CaHPO_4$. What's more, their microstructure was not resembling to a typical glass foam, since the release of $CO_2$, as the only gas product from the chemical reaction, was expected to form porosity out of gas-bubbles, which was not inspected at all in the microscopical analysis. On the contrary, the revealed structure was based on the partial fusing of different-sized granules contained in the mixture. However, in the conducted tests regarding permeability and water absorption the potential of this microstructure was immediately identified and explored further both in increased cooling rates, different temperatures and lesser dwelling times at the top temperature.

Therefore, out of the four identified types of microstructure the most promising was proved to be Type 3 & 4, based on the phenomenon mentioned above. To this, great contribution has another variable that was briefly explored, because its potential was revealed at a late state of the experiments, in regards of the combination of different sizes in the mixture's particles, such as small-cullet (200-2000μm) and powder (20-250μm). Specifically, by delving deeper into the samples with the highest performance in the conducted tests, that persistently remained the same (TC04, TC11-13, TBS08), it can be concluded that in glass foams porosity obtained from the residual voids of the mixture's granule sizes is more favourable for the desired microstructure, than gas bubbles. The latter, examined in the microscopical images obtained both in the horizontal sections and the vertical from TC05, when their pore walls are not closed, form open networks of limited depth range in their majority, especially when they coalesce and result in bigger clusters. Related to this observation, further experimental analysis should be conducted in the vertical section of the glass foams to provide more insight, extremely useful for the sizing of proposed products out of designed mould shapes for product applications.

Combining these findings with the bio-growth types, it could be suggested that porosity Type 03 & 04 can serve applications with primary and secondary bioreceptivity since their water absorption capabilities are increased. Whereas, samples included in Types 01 & 02, that require higher strength and robustness, represented by the closed-porosity network, could be further explored and used in products for tertiary bioreceptivity that is based on the accumulation of dust and soil on the increased surface roughness.

The overall rating of the samples based on their hydraulic properties, is presented in Figure 82, and depicts the already discussed results along with certain comments derived either from the tests, or during the testing process. All the low-scoring samples are linked to porosity Type 01 & 02, linked to either high percentages of closed-pores or larger-sized ones formed out of clusters, that evaporate rapidly. The prevailing recipes, regardless the observations for their brittle behaviour were chosen to be tested for moss growth, in which they both succeeded, during the 6-weeks testing period.

Higher green growth and evident moss stems were demonstrated in the sample TC14, that was based on the recipe of TC13 ( Cyclon mix* + 10% $CaCO_3$, 840°C), in contrast to TBS17 out of TBS08 (SLS float powder + Borosilicate cullet + C + $CaHPO_4$, 790°C). However, its brittle behaviour and larger impact of the frosting test, by material falling-off upon touch, deprived its testing for compressive strength, since it is regarded unsuitable for building applications as it is. Thus, steps for further research should be focus in overcoming these obstacles, by not mitigating at a great extent its current performance.

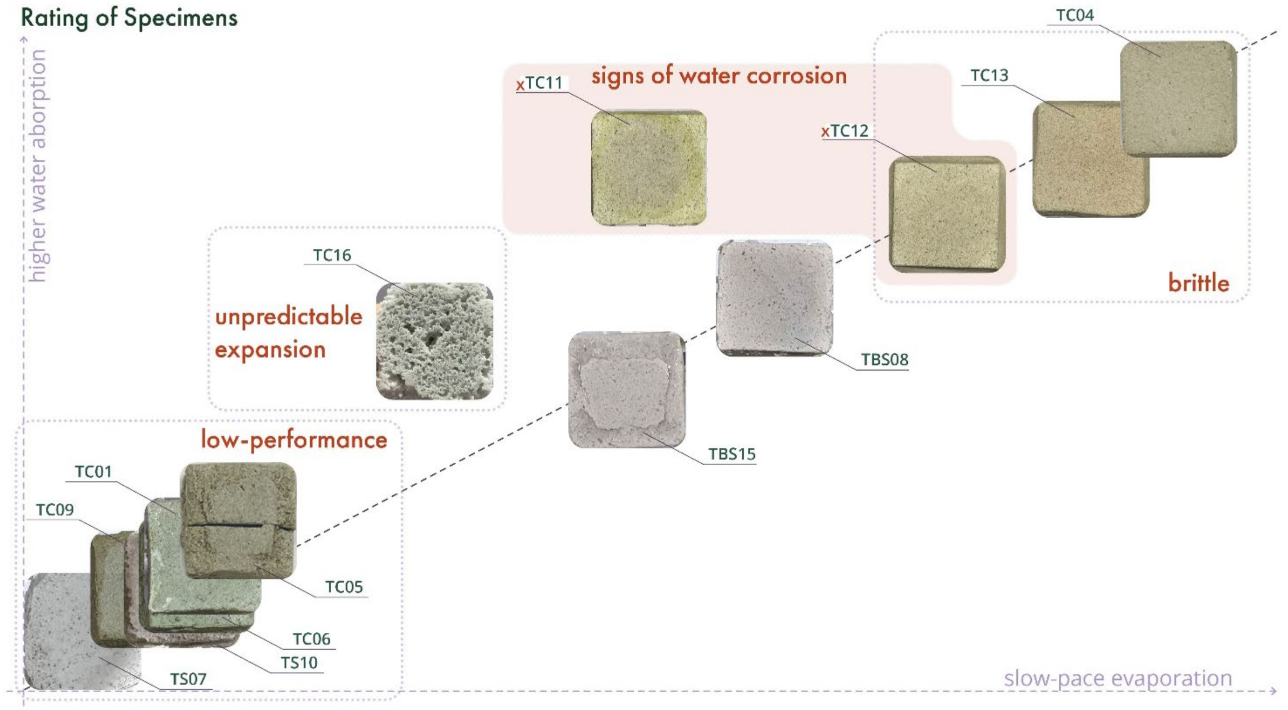


Figure 82. Diagram illustrating the findings of all the conducted tests, together with observations made along the process.

Based on the findings of this research, to further explore the potential of Cyclon mix, the first testing parameter should be a higher foaming temperature. Specifically, this should not be set above of 960°C, as the potential formation of cracks during annealing is critical, in combination with rapid cooling, which benefits the open-pore structure. What's more, the choice of foaming additives is regarded as a key element in this mixture, since tests containing carbon black and calcium hydrogen phosphate did not present encouraging results regarding porosity, in contrast to their very low brittle behaviour. The educated guess out of the recipes tested, would be to proceed with the sample TC11 (Cyclon mix* + 3% $CaCO_3$, 840°C), due to its high water absorption performance and stronger bonds revealed in the microscopic images by the least containing amount of foaming agent. Once its residual voids on the microstructure become from larger-sized to smaller-sized, but maintain its density, potentially the brittle fracture will not be of the same extent.

For the Borosilicate mixture with SLS float powder, that is currently regarded as the most promising recipe, representing the best compromise of the values obtained in the Table 14, recommendations for further analysis could focus on testing the cullet and powder size combinations. This, could aim to improve even more the compressive strength for ensuring the viability of the material for market applications. To obtain higher strength values, more refined glass powder in higher percentages than the ones used could be tested in foaming temperatures that do not exceed 840°C, with fast cooling.

Finally, one last recommendation related to the ingredients is the exploration of the eggshells into the mixture. Due to time constraints, this was not feasible in this research, but positive evidence from the literature review correlated to the nutrients needed for plants, could be a solution to optimize bioreceptivity, while incorporating higher waste percentages in upcycled products.

Related to the experimental process followed, the designed small testing set-ups prove to be of a great value to quickly assess the potential of an idea that has not been tested before. Hence, when bioreceptivity is aimed to be incorporated in contemporary solutions in our urban environment and upcoming biobased or other materials are the subject of investigation for their hydraulic properties, such testing workflow can set a guide for the first steps of the research. Then, depending on the depth of the analysis, more high-tech testing methods can be used for validation and scientific results based on accurate porosity measurements, combined with strength tests.

| Samples | Recipe description | Density | Porosity Type | Pore Size | Max Adsorption (per unit area) | IRA (Kg/m² min) | WAC (gr/cm² min) | Evaporation rate (after 1 week-per unit area) | Frosting durability | Brittle Fracture Tendecy |
|---|---|---|---|---|---|---|---|---|---|---|
| TC01 | Cyclon mix*, no foam. additiv., 840°C , slow cool | 2,13 | Type 02 | 215,5 | 0,3 | 2,388 | 0,025 | 0,47 | +++ | - |
| TC04 | Cyclon mix* + $CaCO_3$ (10%), 840°C, slow cool | 2,22 | Type 03 | 479,3 | 2,18 | 21,092 | 0,212 | 1,8 | + | --- |
| TC05 | Cyclon mix* + C + $CaHPO_4$, 840°C, slow cool | 2,12 | Type 02 | 383,3 | 0,32 | 2,613 | 0,028 | 0,5 | ++ | -- |
| TC06 | Cyclon mix* + C + $CaHPO_4$, 960°C, slow cool | 1,67 | Type 02 | 996,3 | 0,25 | 1,953 | 0,021 | 0,4 | +++ | - |
| TS07 | SLS float powder + C + $CaHPO_4$, 960°C, slow cool | 1,82 | Type 01 | 583,4 | 0,09 | 0,4 | 0,004 | 0,2 | +++ | + |
| TBS08 | SLS float powder + Borosilicate cullet + C + $CaHPO_4$, 790°C | 2,09 | Type 04 | 316,8 | 1,26 | 11,753 | 0,117 | 1,43 | ++ | - |
| TC09 | Cyclon mix* + C + $CaHPO_4$, 790°C | 2,25 | Type 02 | 154,3 | 0,25 | 2,132 | 0,021 | 0,4 | +++ | - |
| TS10 | SLS float powder + C + $CaHPO_4$, 790°C | 2,45 | Type 01 | 701,2 | 0,23 | 2,16 | 0,021 | 0,45 | +++ | -- |
| TC11 | Cyclon mix* + $CaCO_3$ (3%), 840°C | 1,71 | Type 03 | 185,8 | 2.02 | 19,423 | 0,197 | 1,46 | + | --- |
| TC12 | Cyclon mix* + $CaCO_3$ (5%), 840°C | 1,66 | Type 03 | 170 | 1,94 | 18,608 | 0,189 | 1,2 | + | --- |
| TC13 | Cyclon mix* + $CaCO_3$ (10%), 840°C | 1,54 | Type 03 | 117 | 1,83 | 17,692 | 0,179 | 1,25 | + | --- |
| TBS15 | SLS float powder + Borosilicate cullet + $CaCO_3$ (5%), 840°C | 1,88 | Type 04 | 143,4 | 0,92 | 5,58 | 0,086 | 0,88 | ++ | -- |
| TS16 | SLS float 2 particle sizes + $CaCO_3$ (5%), 840°C | 1,52 | Type 04 | 721,6 | 1,1 | 7,2 | 0,098 | 1,19 | +++ | - |
| TBS18 | SLS float powder + Borosilicate cullet + $CaCO_3$ (5%), 790°C | 1,77 | Type 04 | 931 | 1,03 | 8,4 | 0,104 | 1,26 | + | --- |

Table 13. Measurements' Results for the tested samples.

*Cyclon mix contains SLS glass, heavily contaminated, since it is a by-product of the bottle-recycling.

# 4. Manufacturing the meso-scale

When aiming to design for bioreceptivity, every urban surface and item that is in contact to the outdoor environment can host biological colonization. This, creates a double potential, by rethinking and redesigning existing products of the market and another one by designing differently the surrounding surfaces.

Certain guidelines for designers are going to be presented in the next paragraph, focusing on optimizing any kind of surface or product for bio-film growth. Such principles define the design, regardless the product, while they also let the product to adapt to a new material. Hence, they can be expressed in different ways, producing an array of options that should be examined in a case-by-case study. For this reason, a number of existing applications are going to be presented as recommendations, showcasing the methodology of analyzing their requirements, combined with the bioreceptive guidelines, in order to provide a framework for the next steps towards their manufacture out of bio-host glass.

## 4.1. Design Guidelines for optimum biofilm growth

Even though designing in favour of  bioreceptivity – rather than against – is a fairly new subject, certain projects that were analysed in the literature review section, offer already some useful insights, which are tested along experimental work in TU Delft.

Starting from a macro scale to zoom into the micro one, the conditions described in Fig 5 & 6, in the first chapters are further explored through design. Therefore, when it comes to define general guidelines, which can be applied in every bioreceptive application, two main aspects have to be addressed through every design. The first, is connected to water and maximizing its ways of capturing it and distributing along the whole surface, while the second is affiliated with the microorganisms themselves (Figure 83).

Apart from the surface roughness that is a material prerequisite and is connected to porosity, design comes to play also an important role by enhancing the effects of a non-smooth surface. Anchorage of the microorganisms' cells, as well as their protection from harsh wind and extensive solar exposure are the immediate benefits of creating these pockets or otherwise surface grooves. These are necessary to be engraved horizontally, otherwise they lose their main advantage of enabling biological organisms to stick onto of the surface. Furthermore, it must be mentioned that horizontal recesses should not capture excess water, due to the hindering effect this will have to the organisms growth. Thus, under no circumstances should the water flow be discontinuous.

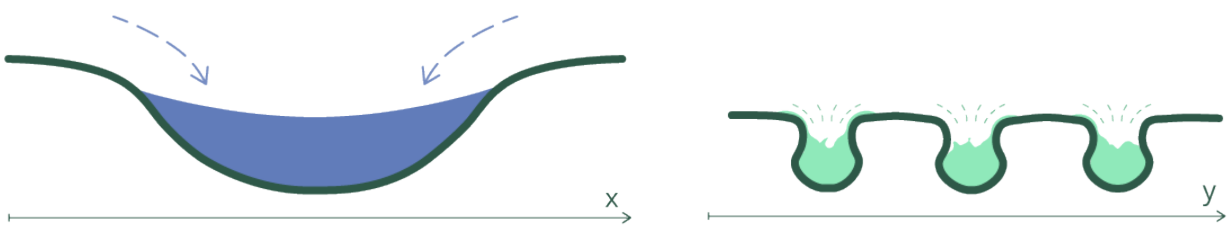


Figure 83. Diagrams expressing main design principles regarding bioreceptivity, emphasizing that these formations should take place in different directions. The left diagram showing the importance of directing water, therefore corresponds to a horizontal section, while the image on the right depicting a pocket-formation for the anchorage of microorganisms and capturing water in a vertical section. Image Source: Own.

For this reason, Kazi (2020) in her thesis experimented with designing the optimum surface geometry for bio-growth, where reported as the most successful evidence of moss growth in her samples, the area of grooves that followed the water flow and were sculpted with horizontal pockets (Figure 88).

Figure 85. Panel 2 after 12 weeks of culturing in the greenhouse of the Botanical Garden in Delft. Image Source: Kazi, 2020.

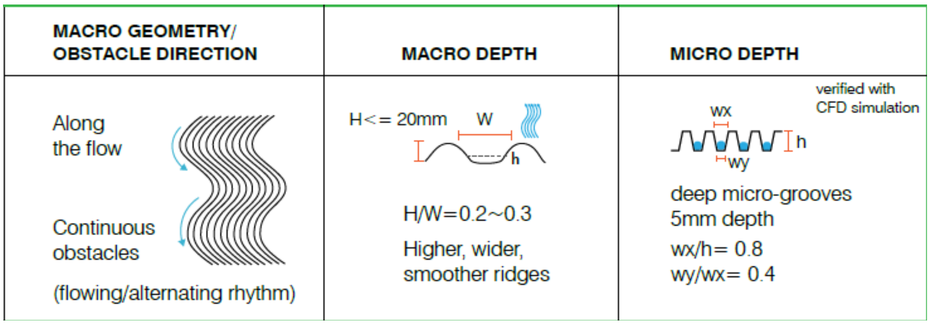


Figure 84. General guidelines for surface geometry from macro to micro scale. Image Source: Kazi, 2020.

In Figure 87 the discussed principles are illustrated. Firstly, combining the bigger scale of the surface, the water movement is directed in an organic flow instead of a straight line to exploit it in an increased area, cutting its speed in order to be better absorbed by the material. Then, in the micro scale of the surface, by zooming in the engraved texture, the suggested geometry for the moss adherence, is supported by a CFD analysis conducted by Kazi (2020), presented in Figure 86 & Figure 87.

The CFD analysis, justifies thoroughly the choice of the specific section with the dents and even their dimensions, after having analysed larger and smaller gaps. The main objective of this was to not let unfavourable conditions created by high wind velocities and cause nutrients loss or even microorganisms' detachment.

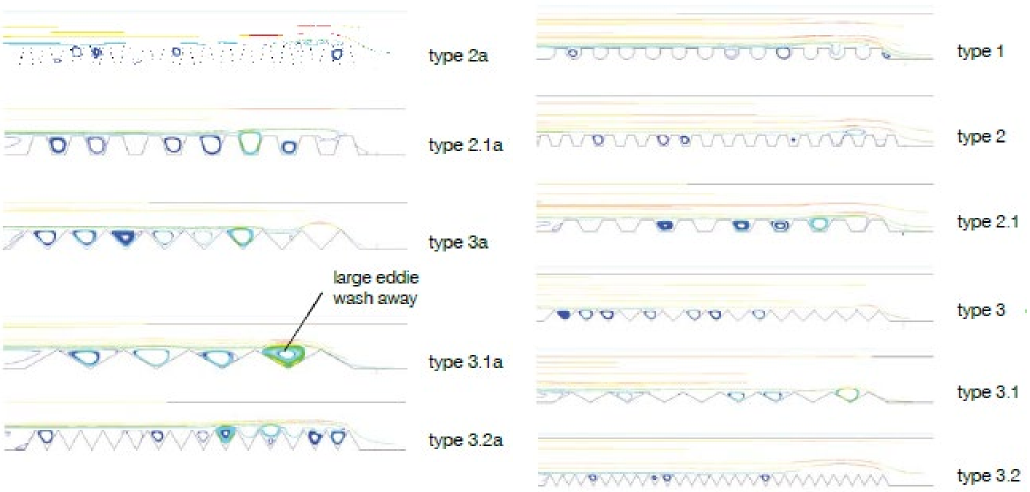


Figure 86. Streamline vertex diagram of CFD Simulations for micro-grooves geometry, inlet velocity set to 5m/s. Out of these tested formations, every time the best ones proceeded to the next detailed stage for simulations, by changing the section of the grooves.

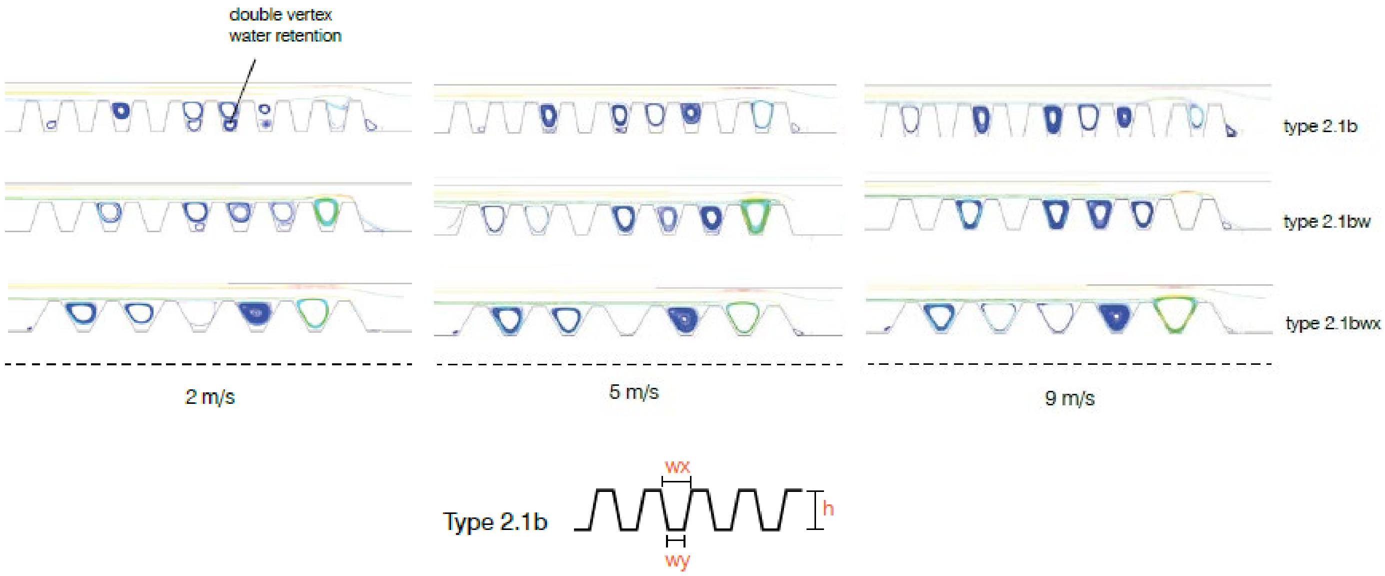


Figure 87. Streamline vertex diagram of CFD Simulations, with three different inlet velocities (from left to right): 2, 5, 9 m/s, illustrating the effect of altering the width of the groove geometry. The final geometry that is proved to work best for both water circulation and retention is the type 2.1b.

## 4.2. Existing applications for bioreceptive products

For the next steps, to illustrate the way a new material transforms to a product application, the link to the product requirements is studied, to offer an overview of the relative specification tests needed. The general flow of such an engineering process is presented in Figure 88, focusing mainly on the appropriate inputs and outputs to reach a satisfactory and well-informed result by any kind of designer.

In brief, the starting point in this case is the material requirements based on the product application each time. Only through this, a specific array of tests and experiments will be able to determine the exact material recipe and manufacturing process matching the needed material properties. An example is studied in the next paragraphs. Then, the achieved material properties along with the bioreceptive conditions for this application, can form the product specifications for optimum bio-growth. Finally, according to the design demands and the boundary conditions regarding size and maintenance, a holistic input is shaped, for the best design to emerge as the final output. Other criteria related to the involved stakeholders can take part in this final decision that may differs per case study.

This theoretical approach was chosen to outline the needed methodology designed to explicitly match the material experimentations with the application's requirements, without having reached the last. By doing this, out of a series of product recommendations, for the mere purpose of showcasing the great potential of this upcycling material, points for further testing become explicit for every researcher or stakeholder that aims to develop a specific aspect or part of this research. The analysed steps aim to elucidate the material's unique way of treatment, supported by small experimental findings concerning the actual manufacturing implementation, such as the mould design or surface treatments.

Thus, a set of application as recommendations are illustrated in Figure 89, created by the aforementioned described process.

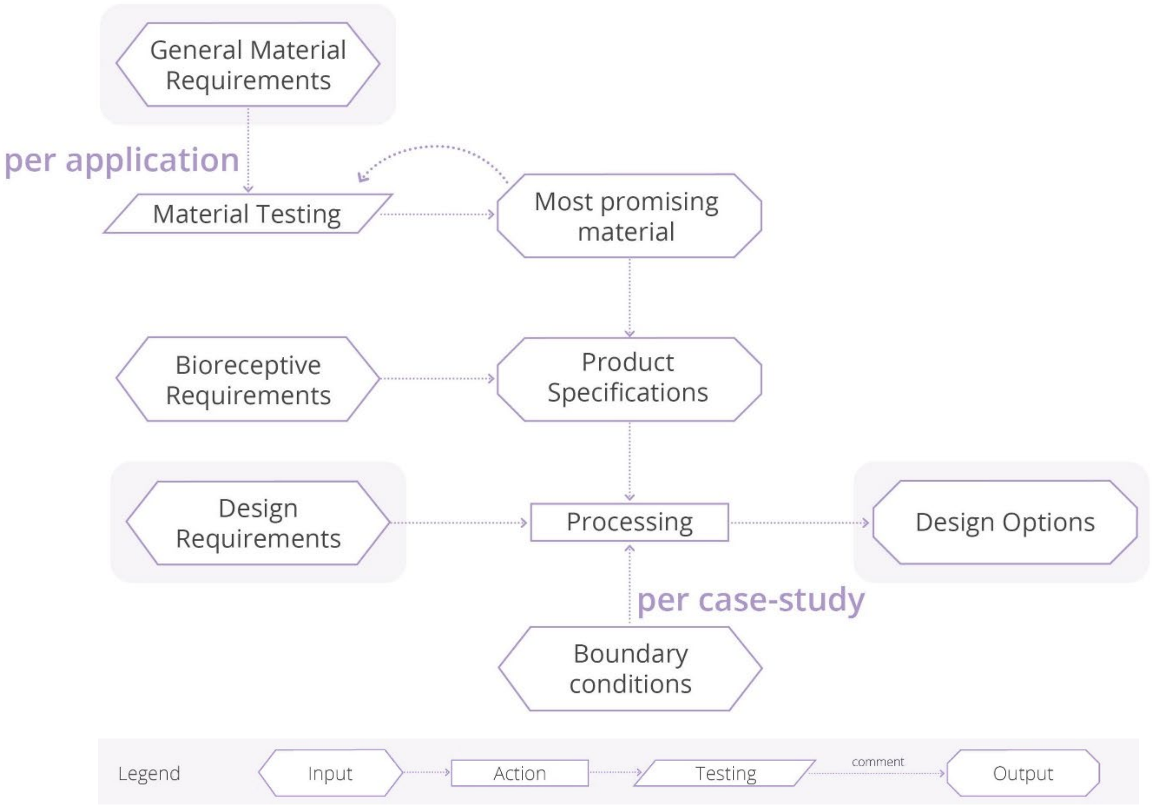


Figure 88. Engineering process for testing the upcycling bio-host glass and every new material to the design needs and bioreceptivity guidelines, to create a market application by adjusting the design according to the boundary conditions of each case study. Image Source: Own.

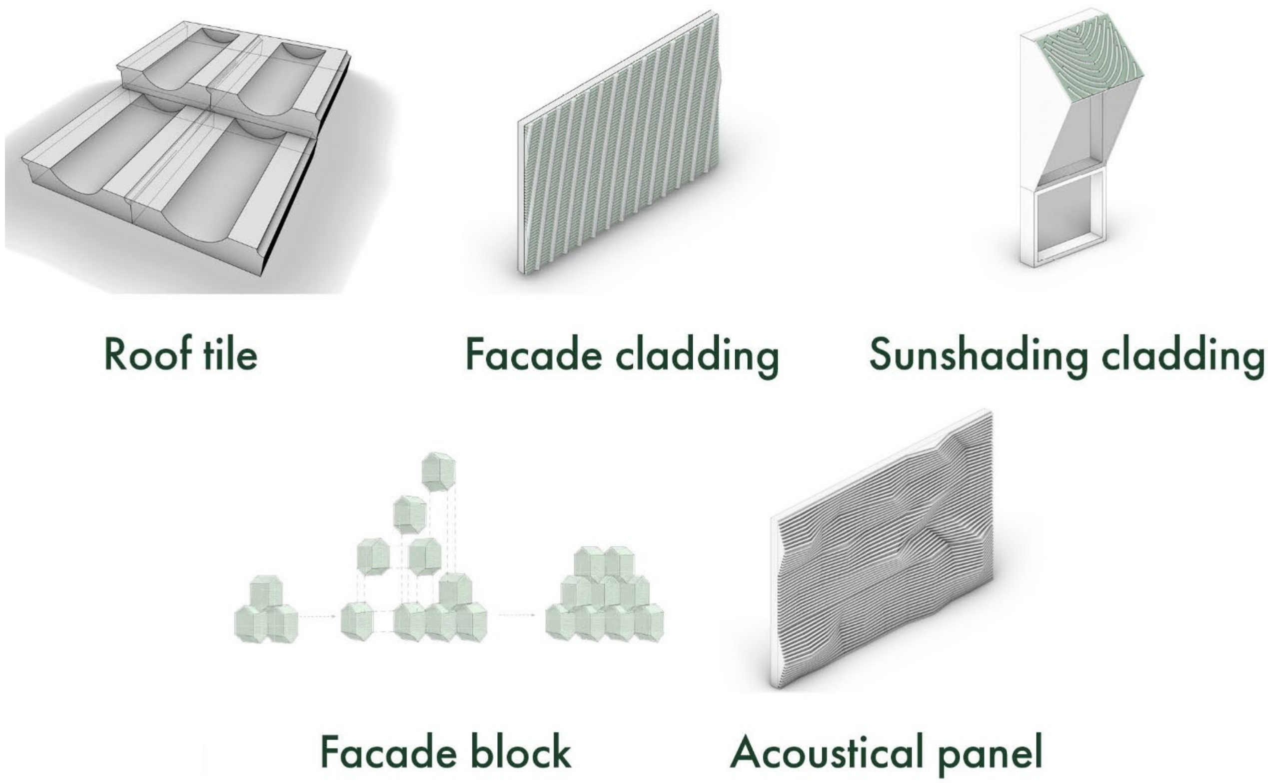


Figure 89. A set of recommendations defining the start of an application catalogue with schematic illustrations to demonstrate the potential of different products that the material can be modified to form. Image Source: Own.

### 4.2.1. The case of a roof tile

Part of the building envelope and traditional architecture, the roof tile comprises an exemplary case study to investigate the different conditions and adjustments for bio-host glass to be applied. Delving into the material needs, in order to highlight a set of properties for further experimentation, a first analysis of the required tests is presented in Figure 90. Since during this research, only the compressive strength analysis, together with a rough estimation for brittle behaviour and frosting susceptibility, are the only conducted tests accompanying the porosity and hydraulic performance investigations, it would be impossible to give a concrete answer regarding which mixture would match a roof tile product.

For this reason, the decision process towards manufacturing is analysed, identifying possible limitations and points for further exploration. To continue with, the specific design guidelines (Figure 91) should be taken into consideration, in absolute relation with the bioreceptive conditions regarding the geometry design, depicted in Figure 83 & 75. Afterwards, by analysing the previous inputs, regarding the desired material properties and the distinctive design requirements, a product specifications tag related to the tertiary type of bioreceptivity is deemed as the most competitive and feasible solution, based on the material findings until now. Due to the high demand for durability towards extreme environmental conditions and strength, because of large potential loads, a specimen with increased surface roughness, low porosity and therefore high strength values should be created. This set of properties, justifies why a highly-porous and water absorbent material is not chosen, since its strength performance would be low with potential brittle behaviour. Hence, in another application that the demands are different, another produced sample could constitute a satisfactory match.

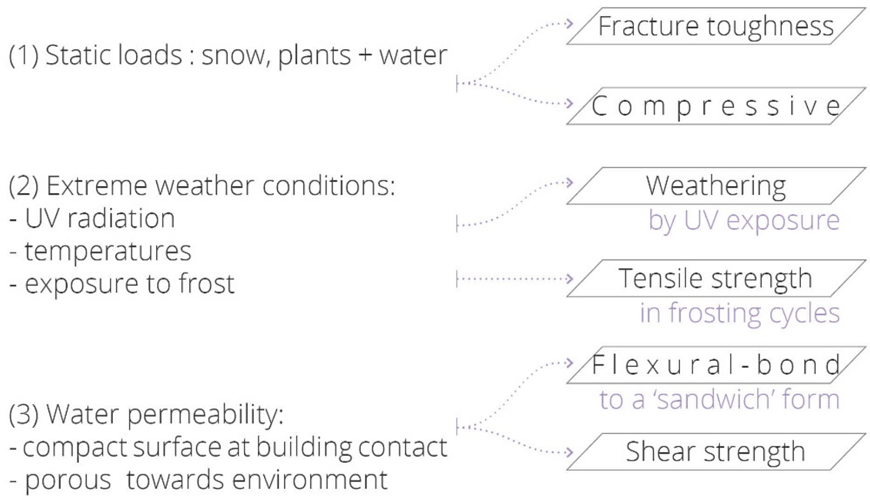


Figure 90. Identified critical points for the material based on the application's demands and the series of needed testing to provide the answers for the allowable product's specifications, adjusted for bioreceptivity. Image Source: Own.

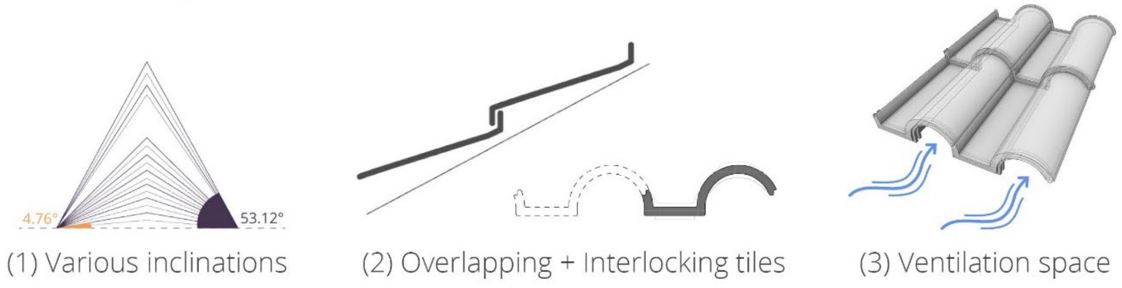


Figure 91. Diagram describing the primary set of design guidelines for roof tiles, forming the final input together with the boundary conditions for designing the product. Image Source: Own.

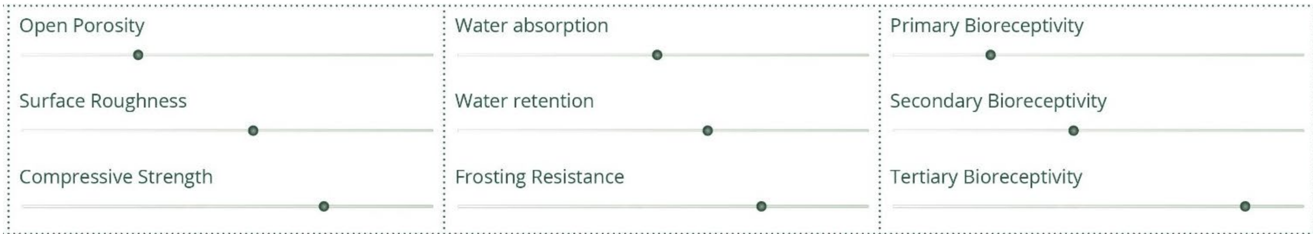


Figure 92. Product specifications for a roof tile calibrated for the specific needs of bioreceptivity in this application. Image Source: Own.

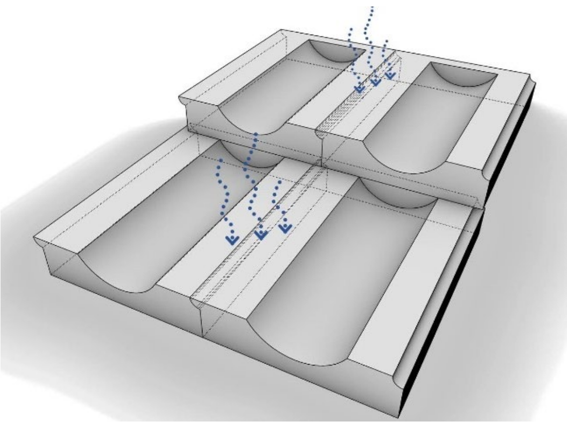

Taking the aforementioned into account, a schematic design is presented in Figure 93, by creating concave coves in sequence to not pose any obstacles, but direct the water flow. What's more, such a geometry by reversing the traditional form creates more volume for the material to retain water, mainly in the thicker parts, but also to allow for a porosity gradient when touching the building roof. Regarding its overlapping and interlocking design further improvement is needed, along with additional investigation for the adding mass impact.

Figure 93. Schematic design option representing the bioreceptive principles applied on a roof tile.

A first suggestion for material testing regarding this product could be the one presented in Figure 94. Specimen TT02, even though it was not included in the hydaulic properties testing due to its evident closed-porosity, presents the maximum surface roughness of all the produced samples. In addition, because of its foaming experimentation without any additives, it does not showcase brittle behaviour, therefore with such evidence it constists an option for further examination for its durability and strength. Similarly, TC06 scoring low for its water absorption and retention due to its large-sized pores, it also showcases great surface roughness. To assess accurately its potential, more information are needed regarding its vertical section. Since, this was one of the few specimens that presented a typical closed-porous network for glass-foams in the pore walls between the larger coalesced ones. As a result, this leads to lower density which is beneficial for the roof tile, and it can be assumed that because of the gas-bubbles pores its vertical section could showcase a gradient of porosity, that could be applied in an experimentation combined with a glass pane to create a complete compact and impermeable surface on the side in contact with the building. Last but not least, TBS08 can be assumed that out of the mixtures containing Borosilicate glass might score the best in compressive strength, since it obtained one of the lowest scores of the most promising samples in water absorption.

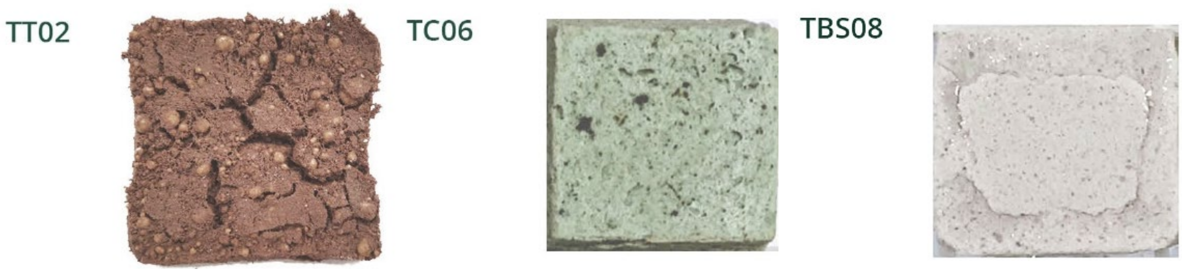


Figure 94. First set of samples selected for further testing to meet material requirements for roof tiles.

The above samples merely indicate a suggestion to present the reasoning behind selecting the material that best fits the product specifications. Although extensive experimentation would be needed to reach to the final stage for launching such a product especially regarding bio-fouling, the obtainement of testing models with different material properties and good absorbing performance is already extremely valuable and promising.

Similarly, the outcome for a façade tile and an acoustical panel are presented in.Figure 95 The matching samples out of the produced pallette of this thesis, pose a suggestion for which recipe could be further experimentally explored for the actual market application. This, was done based on each product's engineering criteria.

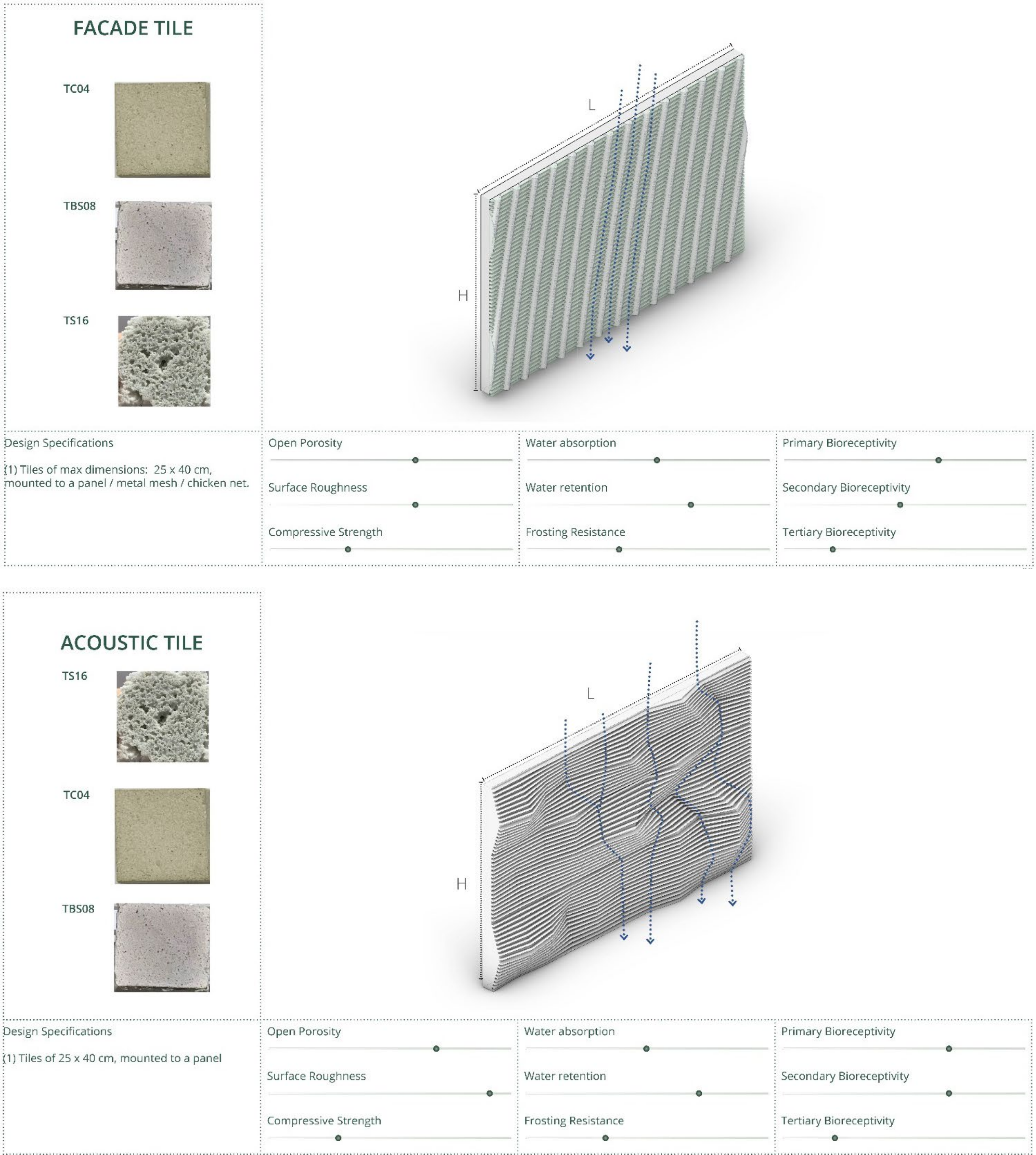


Figure 95. Boards for the recommendations of a façade and an acoustical tile, showcasing the different demands for material and bioreceptive properties, matching accordingly with the most relative specimens, created in this thesis.

## 4.3. Prototype experimentation

Despite the fact that, a final material is not chosen among the produced samples, the most promising mixtures analyzed in the conclusions of the previous chapter, were selected to test their behavior on an organic-patterned mold surface of a tile. The tile's dimensions are approximately 5x5 cm and its pattern repetitive that per 2 tiles, can form a uniform seamless pair, once its tapered sides are cut or polished.

Sample TBS22 that was firstly sorted out for further experimentation, as it was highlighted to form the best compromise between hydraulic properties and strength performance, when compared with the rest, presented an outstanding result in Figure 97 with such an intricate geometry.

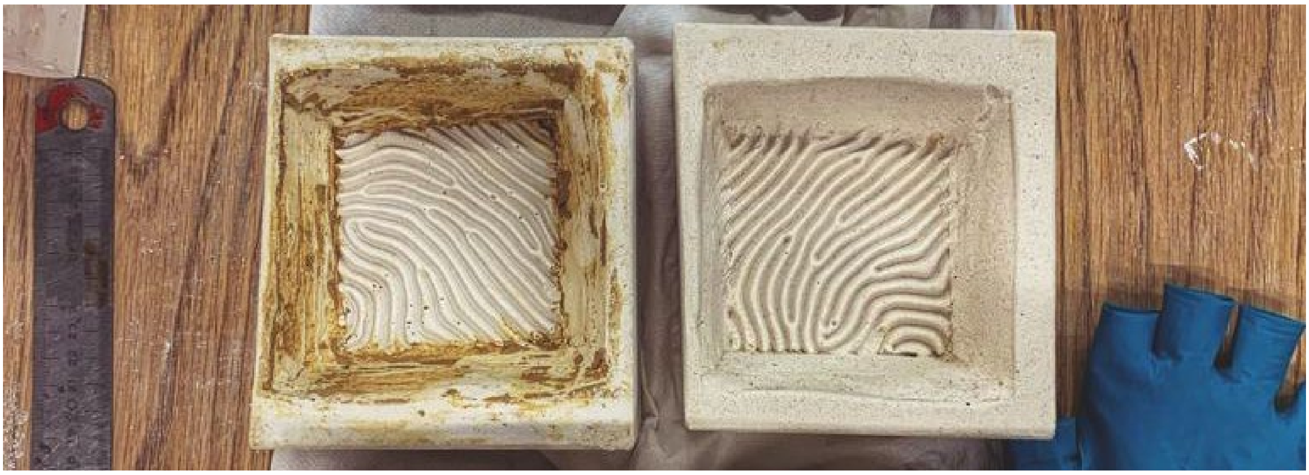

Figure 96. Image of two moulds, -one with clay traces of the inverted 3d-printed shape stabilized for pouring of the crystal cast mixture and the other cleaned- captured while bio-host glass mixtures were being demoulded after foaming. Image Source: Own.

Figure 97. Sample TBS22 depicted to showcase the detail of the formed surface, in contact to the mould, to monitor the level of mould reaction. Image Source: Own.

Due to the findings of the previous tests and the general high brittle trend in the samples, it was not expected such a firm shape on thin material protrusions. However, the reaction with the mold is evident, rising many questions on how this could be overcome, since this is the surface to be used for the microorganisms' colonization.

A potential solution that needs additional experimentation in a representative number of samples for accuracy, is the one described in Figure 98. In detail, the proposed geometry of microgrooves from Kazi

(2020), is used as a starting point since it matches the tested pattern in the tile, but a scaled version mainly in the depth of the grooves, so as to provide extra height that can be subtracted afterwards during polishing, in order to reveal the mixture's desired surface with porosity. Specifically, the difference between the cut-polished and the untreated surface in contact with the mould are seen in Figure 99. Therefore, a way of tackling this effect must be tested.

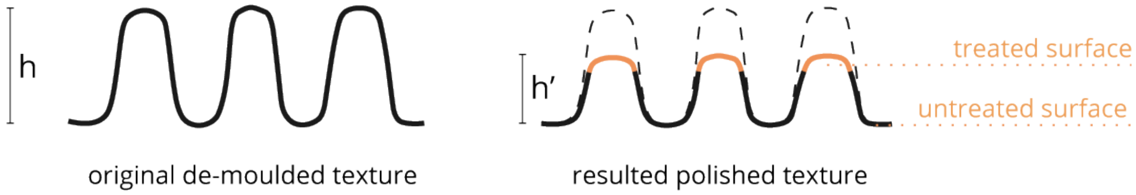


Figure 98. Diagram illustrating the original and obtained texture in section, after attempting to polish the tile shown in Figure 97. Image Source: Own.

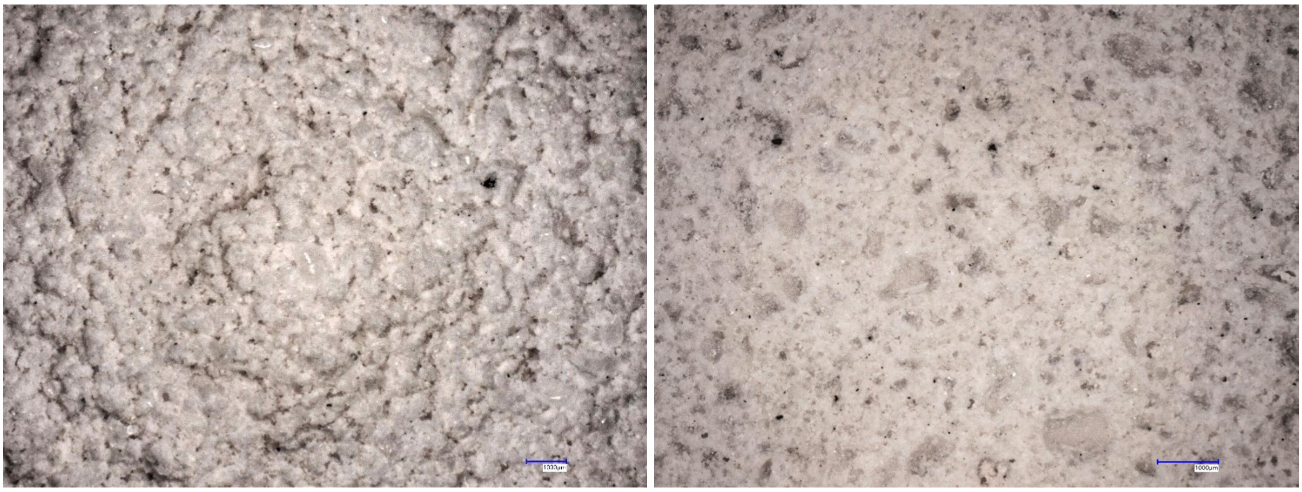

Figure 99. Microscopic images of TBS08, taken with digital microscope (VHX-7000 series, Keyence located at the Faculty of Architecture), with different scales (x20, x30), illustrating the main difference in texture and consistency of the surface in contact with the cystal-cast mould (left), and the cut and polished one. It is obvious that in the right one the texture of the glass foam is revealed by taking advantage the existing pore-network, while on the other one (left) there is a crust formed with mould particles also combined with closed pores formed during foaming, that blocks the connected network, which is the goal of this research. Image Source: Own.

## 4.4.Conclusions

The analysis of this chapter elucidates the next steps of the material exploration towards the application research and modification for product manufacturing. Even though the results presented in regards of the application catalogue are merely suggestions, these examples are needed to demonstrate the great variety that glass foams can serve by achieving the desired material specifications. Therefore, the promising evidence presented in the previous chapter, can be realized only in combination with the application catalogue to offer the spectrum of directions bio-host glass could follow.

By taking into consideration the analysis of the further material testing needed illustrated for the case of a roof tile, the goals for a material researcher are set regarding the range of values that need to be achieved. Undoubtedly, roof tile is one of the most challenging applications for a porous-water absorbent material, concentrating many problems to tackle, therefore the material properties compromise will be sought in different aspects than the application of a façade or an acoustical tile.

Taking further the bioreceptive principles that Kazi (2020) developed in her thesis, these should be adjusted for the manufacturing process of bio-host glass. Therefore, from the exploration of foaming the most promising recipe from the experimental analysis, in the mold with the organic pattern illustrated in Figure 97, certain conclusions can be derived. Firstly, to fully exploit the desirable hydraulic potential of the material, the need of removing the crust formed by the mold reaction becomes an important topic for further research. Secondly, depending on the brittle behavior of the final material the sizing of the micro and macro grooves, suggested in the bioreceptive design principles, should be tested to prevent failure upon application.

# 5. Designing the macro-scale

## 5.1. Data-driven design

Focusing on the macro-scale of a bioreceptive design, certain environmental data have to be taken into account and inform the final shape for the maximum performance per location. In Figure 103, the decision-making process of a designer is depicted, by outlining which type of data and choices are primarily needed in each step towards the formation of the final design.

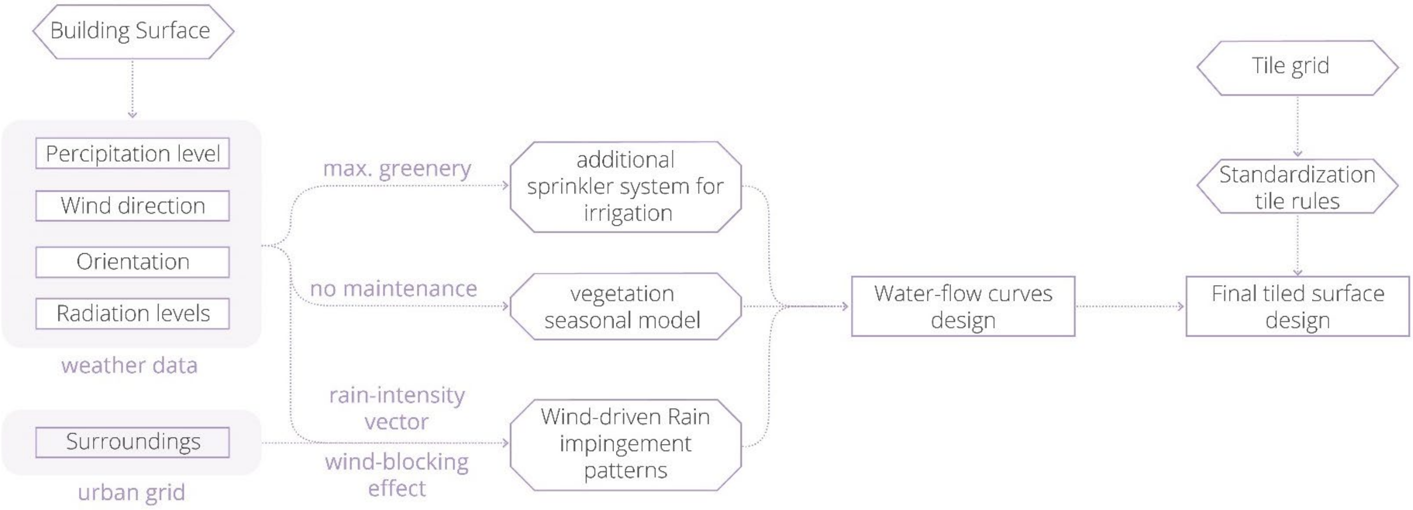


Figure 100. Decision flowchart regarding the general design of a surface in the urban environment, based on the bioreceptive design guidelines, regardless the final application product. This process can be applied both for roof , façade or acoustical tiles.

The reason for choosing rainfall and principle wind direction, to be one of the major inputs depending on the orientation of the surface, is merely to provide the highest water content to every part of the design. Since, a standard surface design that is repeated regardless the weather analysis, might result to partial bio-growth taking place only where the water flow is abundant, as it is already observed in building surfaces under pipe leakages or in roofs underlying the rainfall runoff route (Figure 6).

Especially in the Netherlands and in other locations where it is very windy, the rain falling onto urban surfaces is greatly affected. For this reason, the first step towards the design of a bioreceptive façade, is to analyze the relative climate data, as depicted in Figure 104, in order to form the wind-driven rain impingement pattern, based on a computational fluid dynamics simulation (cfd analysis), the rain levels

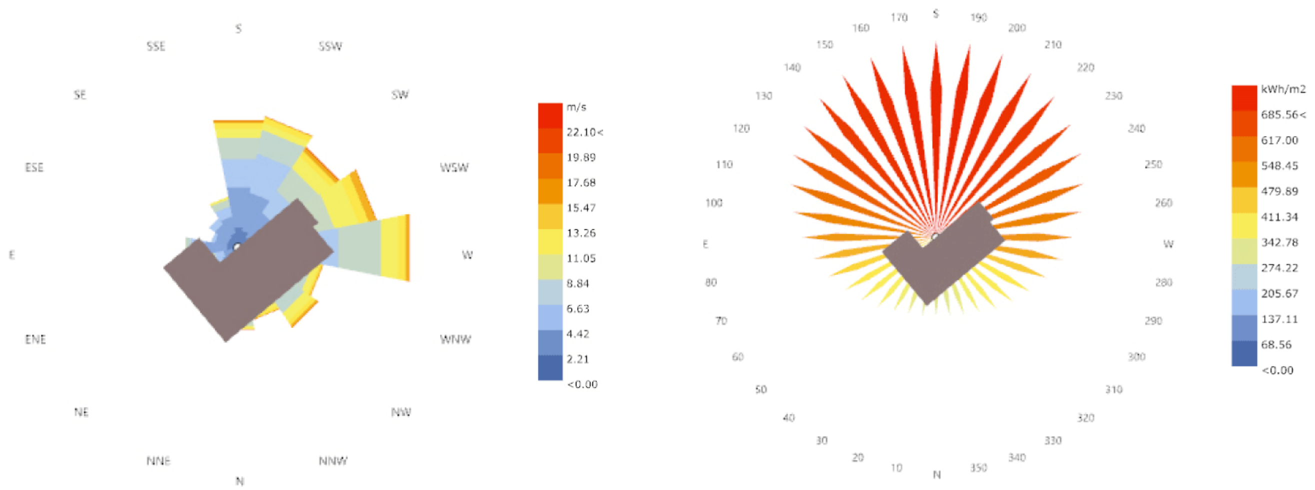


Figure 101. Wind rose (left) & radiation annual analysis (right) from the Montevideo tower in Rotterdam. South is oriented at the top. From these two diagrams, it is shown that the principle wind direction is the SW, while the radiation levels are important in combination with an analysis of the microorganisms' light needs.

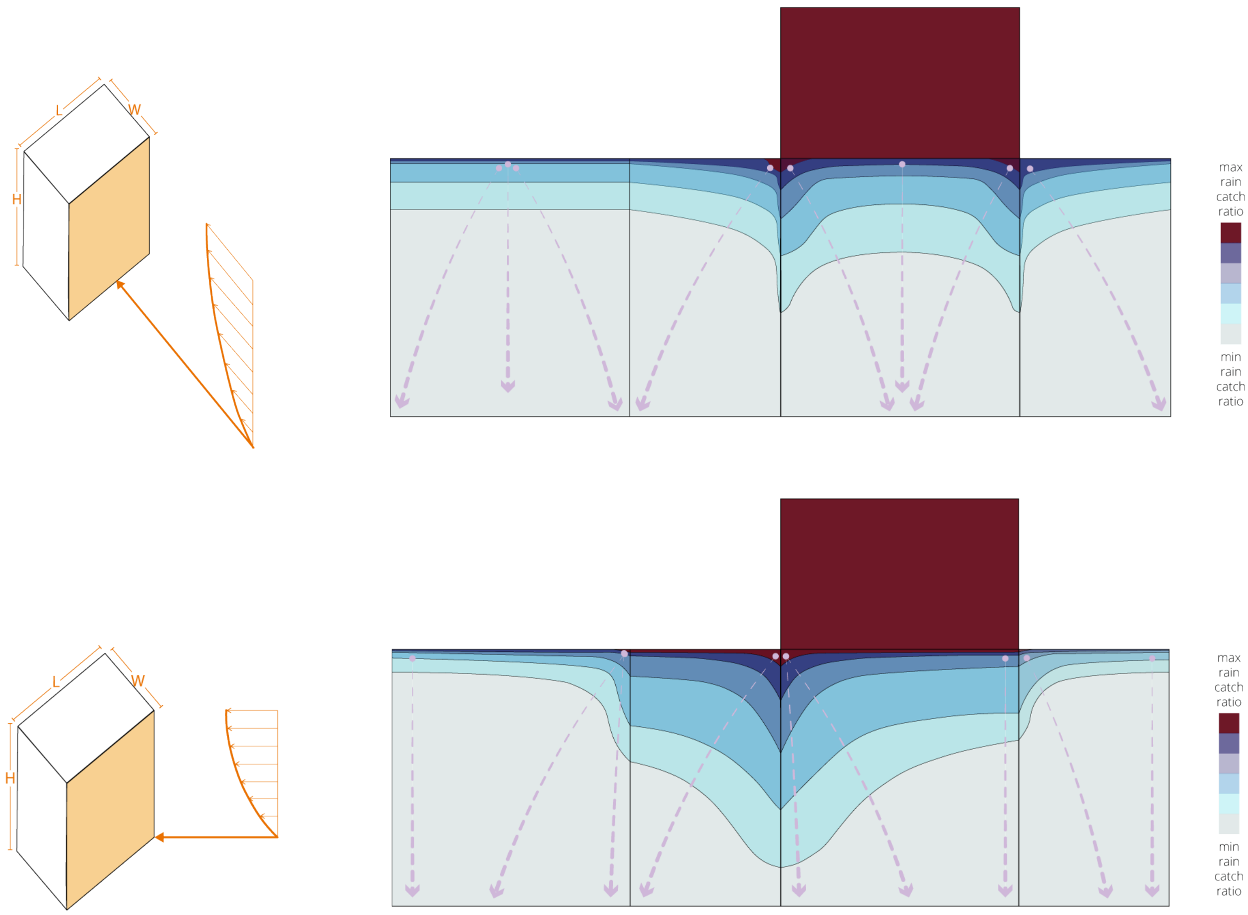


Figure 102. Wind-driven rain impingement pattern formed for the case of principle wind, for the simplification of a stand-alone building, firstly falling onto the façade's centre (upper diagram) and secondly on the building's corner (lower diagram). The arrows in the unfolded elevations, symbolize the main direction that the meso-scale curves should direct the water, with alternating flows to ensure a slow velocity for the best absorption conditions.

and semi-empirical methods. Two examples of the wind-driven rain impingement patterns are developed for the Dutch climate conditions in Figure 105, where the principle wind is directed perpendicular to the façade or on the corner of the building. Similarly, every different incident angle of the rain trajectory can be simulated according to the produced cfd analysis of the buildings. Then, depending on the rain levels of the area, the exact maximum water amount can be calculated for each zone of the different catch ratios. This process is further analyzed in Appendix, part C and illustrated in Appendix_Figure 16 – 18.

Therefore, this methodology should be followed for taking advantage the material's potential to the fullest, or a completely different path could be followed in the hands of the designer, such as implementing an artwork with the designed ridges, by stirring the moss growth. However, in each chosen method the advantages and disadvantages should be weighted according to sustainability rules.

For the specific goal of this thesis, it should be mentioned, that the rainwater runoff analysis studies the phase before the raindrop impact onto the building, while the properties of surface cladding material determines the raindrop behavior in the second phase at and after the contact with the building (Appendix_Figure 19). During this, the raindrop can splash, bounce, adhere, spread and be absorbed, form a water film, runoff, evaporate or create moisture along the wall itself (Blocken B. et al., 2013). Precisely this part is the subject under investigation, surface roughness, surface tension and porosity network of the micro-scale of the material are the principal factors which define the amount of absorbed water, aiming to reveal the maximum levels for biofilm growth. Thus, together with the principles for bioreceptive design shaping the meso-scale of the material's surface geometry in each application, a holistic approach for maximum growth is achieved.

## 5.2. Tile standardization

In the following Table 14 an attempt for creating standard-tiles is presented, resulted from the simple replication of the bioreceptive principles, to provide abundant customized solutions with a finite number of mould-shapes. With the presented 11 tile-forms, inspired from the input of Figure 105, the verticality of the water with alternating the flow direction is achieved, based on the analysis of wind-driven rain impingement patterns, covering the needs of facades located in the Netherlands.

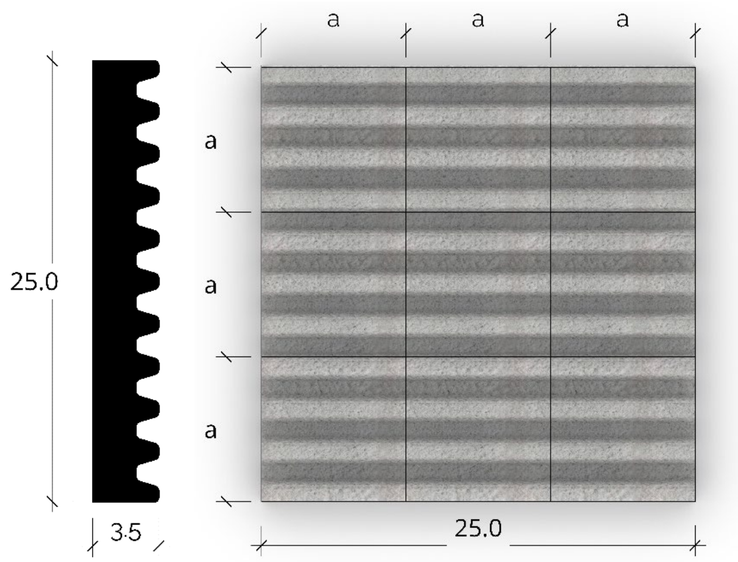


Figure 103. The case-study tile at its initial design phase with only the microgrooves engraved for microorganisms' anchorage and the division

The dimensions and the scale of the grooves are shown in Figure 103. For the standardization of the meso-scale towards a feasible macro-design, the logic is to divide the x and y axis into thirds, where every time the water-flow curve starts in the middle of this third. Then, the curve itself as seen in the images of the Table 14, follows either a straight profile or a curved one, defined by the location of the endpoint, that it can be located in the consecutive third, or the next one. Towards reaching the tile edge, the designed curves become more linear, in order to avoid the creation of pointy edges when the tiles are combined. Similarly, their curvature aims to create a continuous flow that will not create any areas that the water could potentially be accumulated. Due to their size, only linear macro-grooves can be combined in one tile more than one time, as seen in C02e1728 & C03e172839.

Although the possibility that the design can become even further tailor-made remains, suggesting a tile of such a small size (25 x 25 cm), aiming to cover facades that may size at an extreme case even 90 x 20 m, means that around 30000 tiles will be needed for only one surface. Hence, the demand that the design of this extremely large amount of tiles cannot be unique, is highlighted. It should also be mentioned, that this proposal is put into absolute effect, once the moulds are not produced with the same technique as it was done during this thesis (refer to 3.2.3), because their re-use is not feasible.

| | | | |
|---|---|---|---|
| 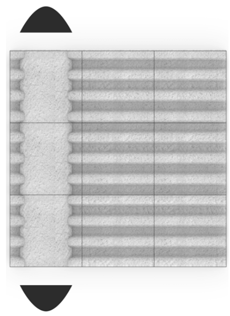 C01e17 | 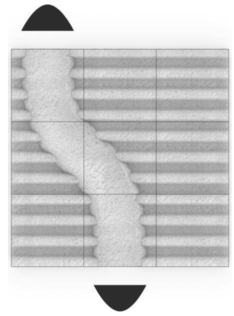 C01e18 | 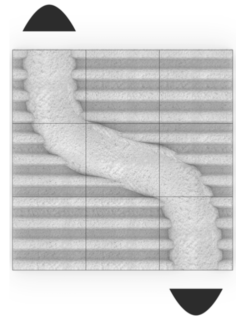 C01e19 | 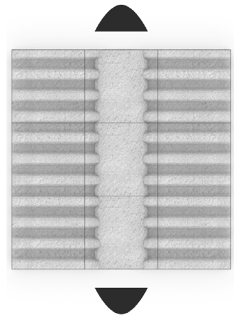 C01e28 |
| 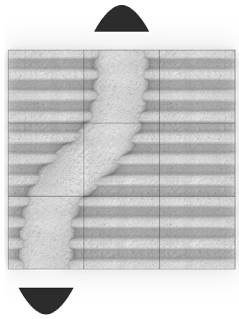 C01e27 | 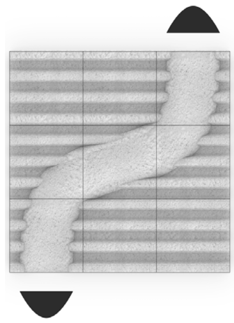 C01e37 | 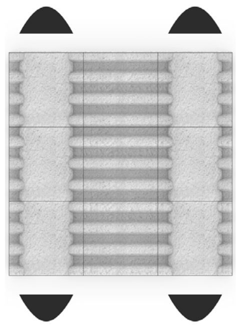 C02e1739 | 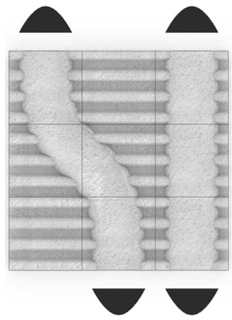 C02e1839 |
| 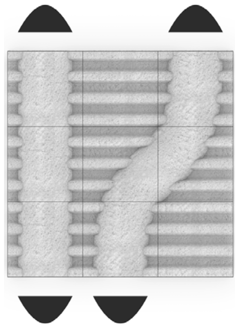 C02e1738 | 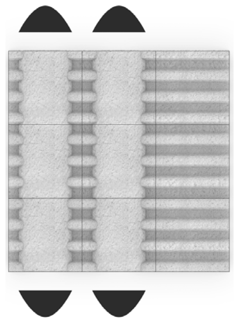 C02e1728 | 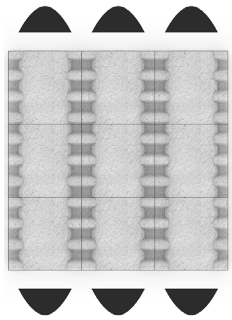 C03e172839 | |

Table 14. Standardizing the 'fluid' design, with specific number of different mould-tiles. The coding of the designs symbols C : curve – 01: number of curves on the tile – e: endpoints – 17: the clockwise numbered thirds , if more curves are apparent, then these will appear consecutively starting from the left one, moving the right with the maximum number of three curves.

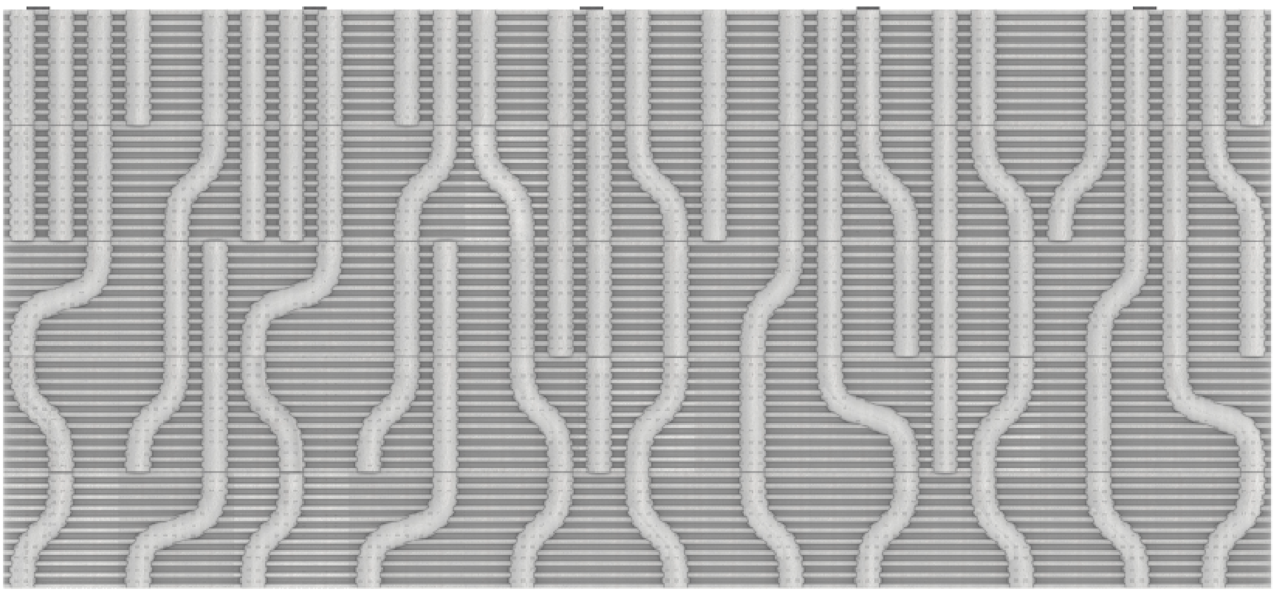

Figure 104. Façade fragment of 2,75 m length by 1,25 m height, as a design example of combining the standardized tiles.

## 5.3. Assembly process

### 5.3.1. Assembly criteria

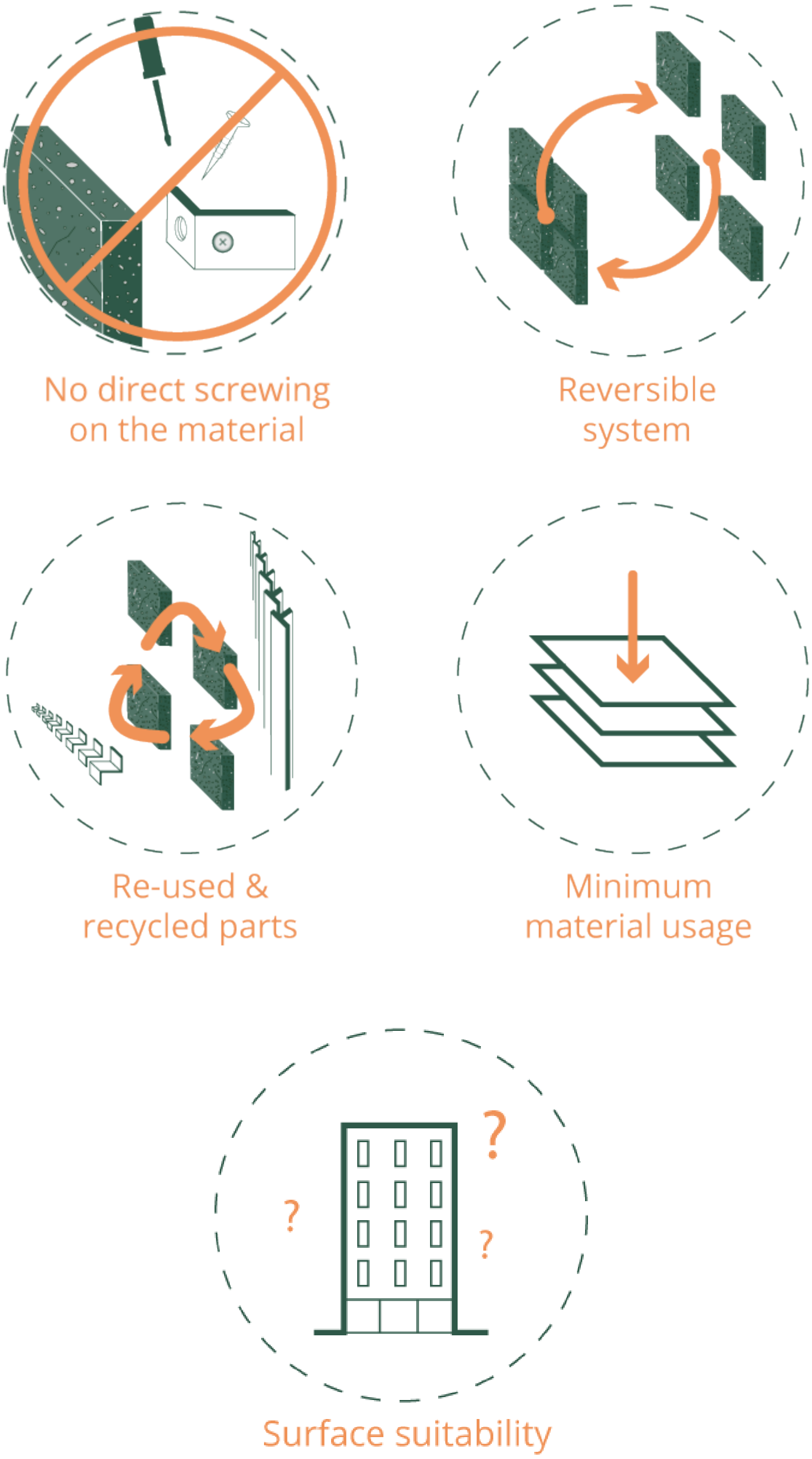


Figure 105. Set of criteria for choosing the right assembly system, specifically defined for the material of bio-host glass and its possible product applications.

### 5.3.2. System types

## Standard cladding supporting system
Rail connection

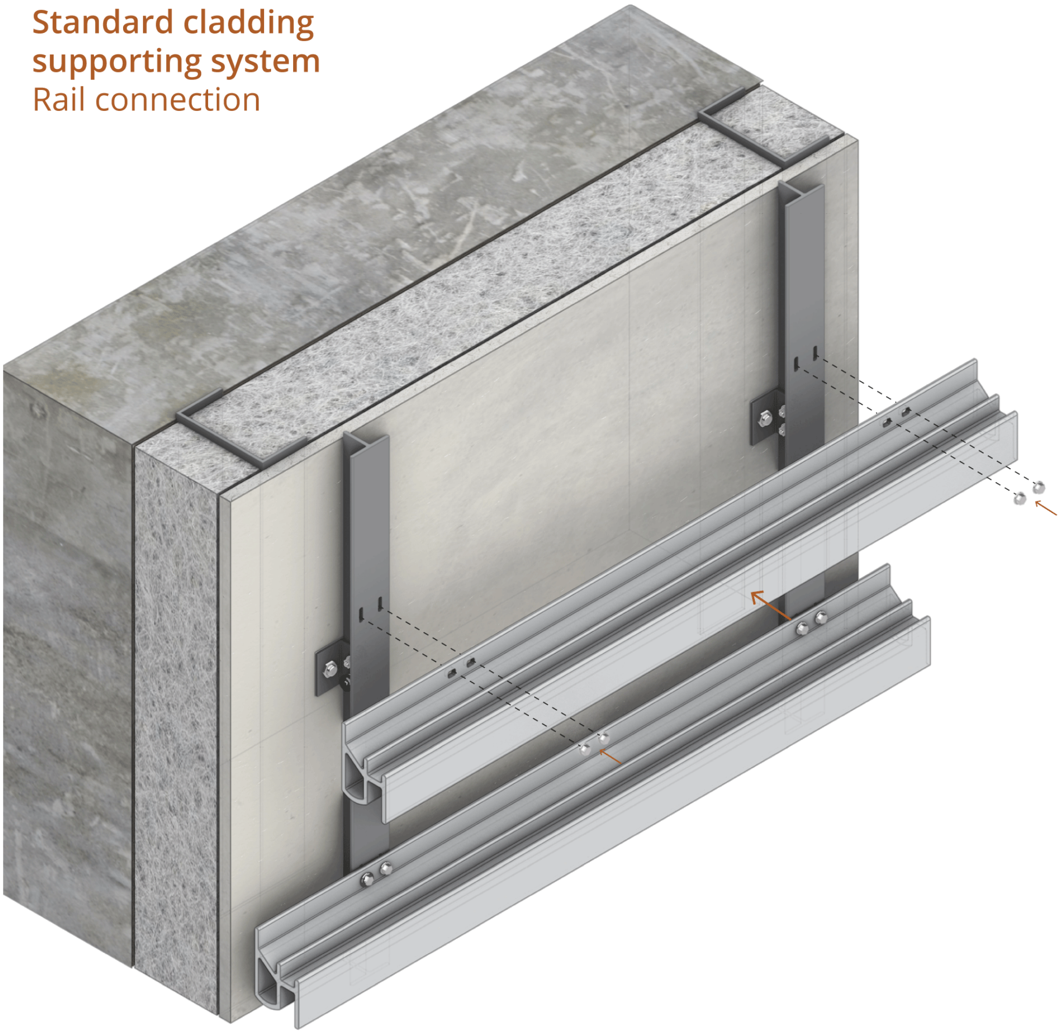

Figure 106.

Attaching and supporting system for standard façade cladding, having a profile as a horizontal guide, offering the advantage of less material usage from the vertical 'T-shaped' guides, regardless the tile sizing.

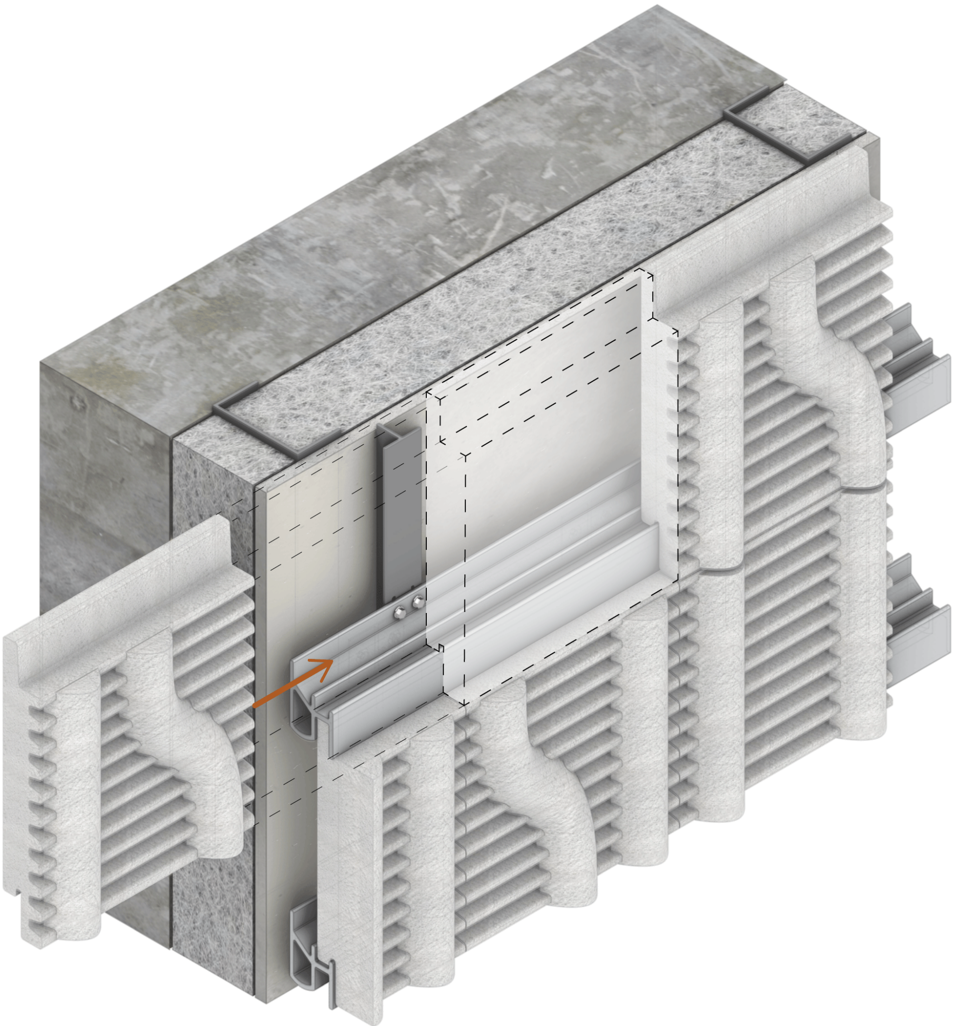

Figure 107.

Frame during the assemblance of the glass-foam tiles on a façade by sliding their matching profiles that interlocks. In case of a failure the whole row should be disassembled.

**Standard cladding supporting system**
Vertical framework
& dual grip connection

Figure 108.

Representation of the assembly process for a standard cladding system consisting of a supporting bracket attached to the exterior wall, vertical framework connected to it and finally dual grip connections

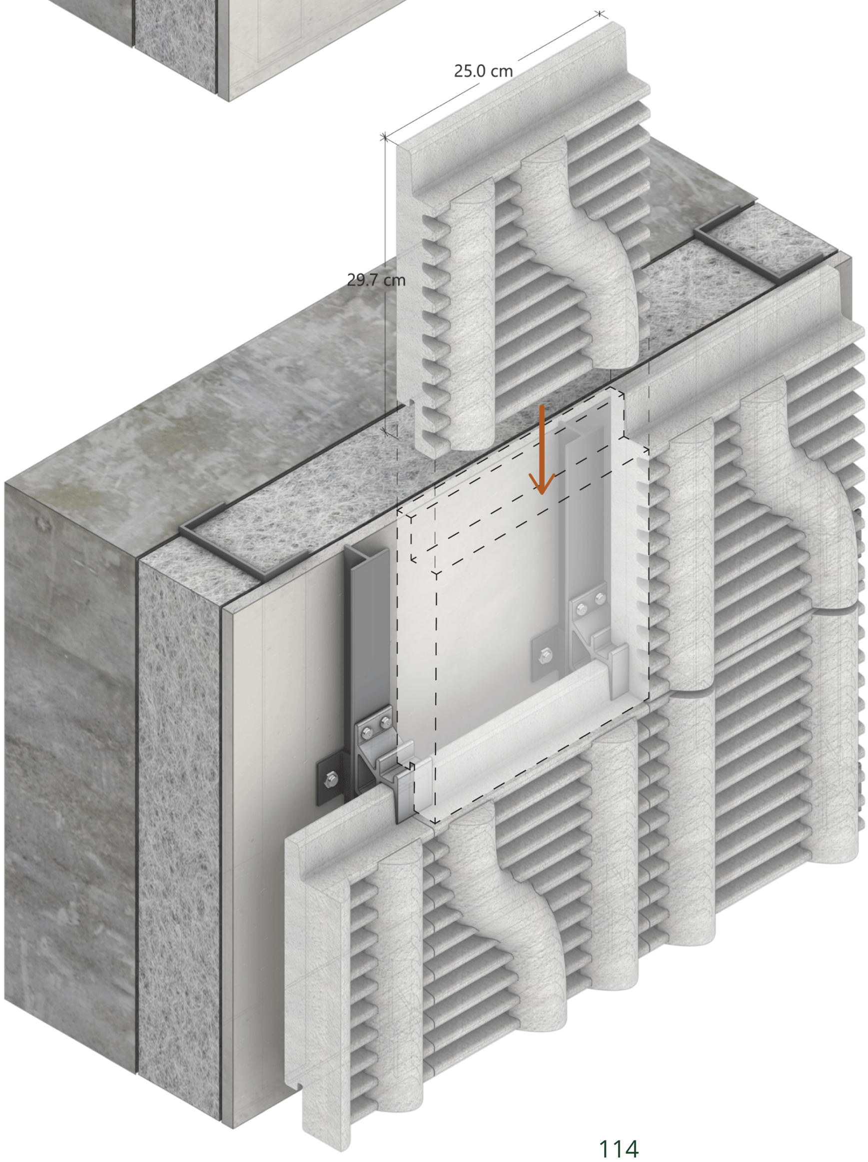


Figure 109.

Frame showing the placing of the bio-host tiles. For this system the mould shape needs to be adjusted at the edges to interlock with the grip connection.

**Lego-like connection system**
Vertical profile carrying
interlocking connections

Figure 110.

Attaching and supporting system for standard façade cladding, having a profile as a horizontal guide, offering the advantage of less material usage from the vertical 'T-shaped' guides, regardless the tile sizing.

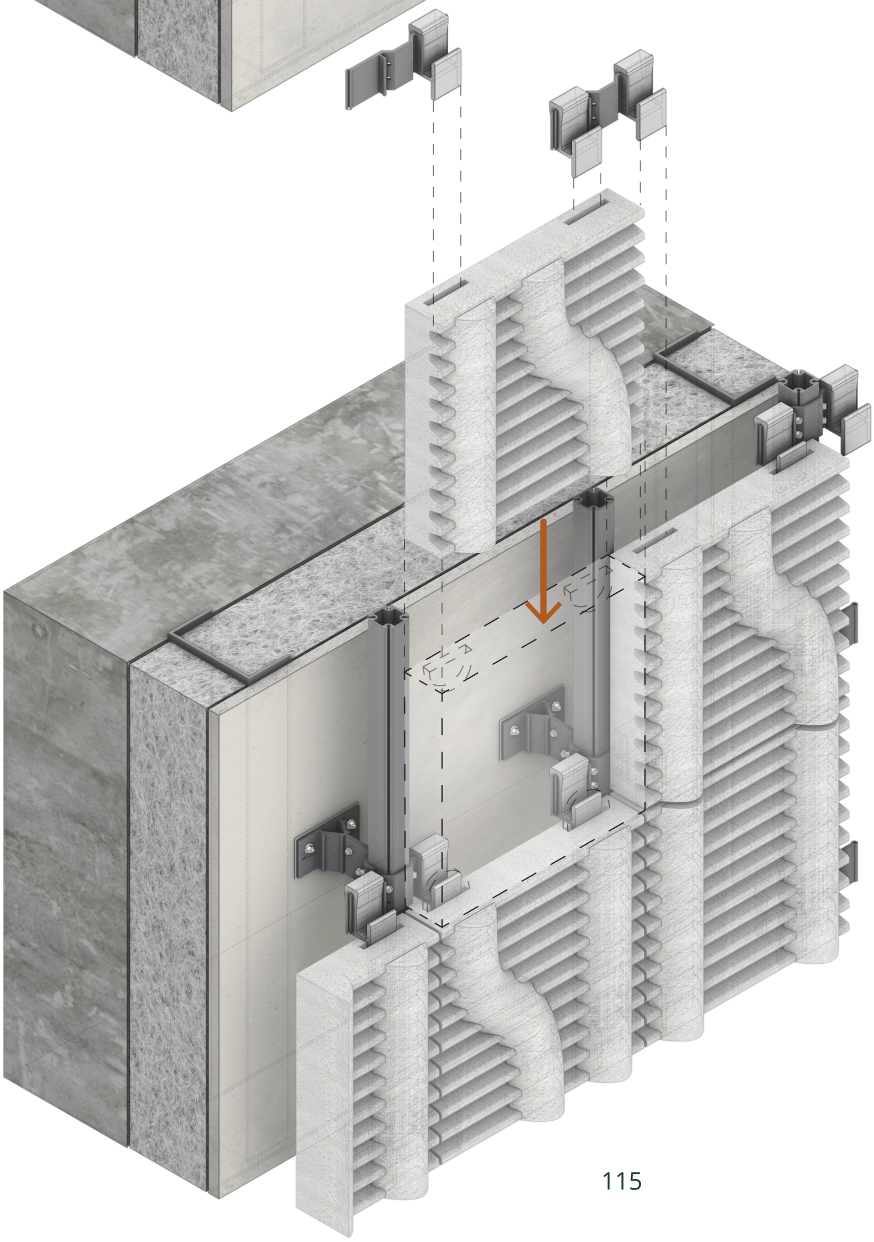

Figure 111.

Frame illustrating the sequence of placing the glass-foam tiles on the cladding system. The precision slots, made in the tiles prior to the assembly, are matched with the interlocking components.

## 5.4. Vision applied in TU Delft campus

Figure 112. Impression of the Mekelweg, in TU Delft campus and the application of many different products, out of bio-host glass,

## 5.5. Conclusions

The design illustrated in Table 14 is a result of a simplification of the bioreceptive design principles presented in Figure 83 for the purposes of standardization, which is a step of utmost importance for the manufacturing process. Even though the result showcased in the scale of Figure 104, as an example of the combinatorial game of 11-tile designs, is not representative of covering a whole building façade, these tile shapes should be further explored. The result is only the first attempt made during the time constraints of this thesis to showcase the material's potential by highlighting the important steps of the process. For this reason, the rigidity and bulkiness of the product represented in the zoomed in scales, is replaced by an organic design, mimicking natural and fluid patterns in the impressions created for the application in the TU Delft campus. Taking into consideration the 3d-printing technique with sand, for creating more complex or customized molds, great design variety could be achieved that could be further explored for the bio-growth results

In a similar way, the cross-section of the tile became even thicker than initially proposed, for certain assembly methods studied in this chapter. Interlocking edges integrated in the mold design, or precision slots made afterwards with a saw cutter, for the Lego-like connection inspired by the company BILDA are decisions that increase the thickness of the product, in order to ensure its integrity. However, even such suggestions are based on educated guesses that need further testing. For instance, if experimentations prove that the product's facture limits permit screwing or bolting on it, the adaptation of the tile to the existing assembly systems could be reconsidered.

The suggested size of 25 x 25 cm that responds to a tile was chosen based on the current knowledge derived from the material's behavior in the series of testing. The main concern focuses on the current brittleness, while also the limitations of the manufacturing of the glass foam and the dimensions of the heating furnaces for its foaming have been taken into account. However, due to circularity purposes and ease for disassembly, the current assembly systems for façade cladding proposed in this section, result in a mismatch to the sizing of the tile and the original standard panel sizes in the market, that these mechanisms are designed for. Consequently, regarding the aspect of material usage and less attachment parts requiring fixing between them and to the building on site, the size of the tile should be further developed, in order to reveal its upper limit. In other words, existing façade cladding systems are not fully exploited, if for the bio-host tile there are demanded at least the double guides to reach its 25 x 25 cm size, in contrast to standard panel sizes of 60 x 40 cm and larger, that for example, exist already in the market of terracotta or stone.

Keep in mind that the manufacturing parameters, especially the relation of temperature and time have to be experimentally explored, since bigger mold sizes have different effects when foaming. The critical points from the material science perspective are the probable alterations in the porosity network that might be caused from the larger distances from the mold walls, which in the experiments conducted of the 5 x 5 cm samples were small and did not present such a phenomenon. This assumption should be definitely explored further, even when the right heating schedule regarding the annealing time has been defined for larger tile samples. Knowledge based on the current evidence, implies the difference in the microstructure network in the vertical axis, due to the bubbles' upward movement when foaming, however the temperature in larger-sized or just deeper molds can be reached in different timings, resulting also in a horizontal pore-gradient. This gradient implying also the sample's disproportion, will probably be radial from smaller or closed pores at the edges to bigger ones closer to the center. This, could lead even to the formation of cracks, caused by the higher stresses formed if rapid cooling follows, or just make the center of the tile more vulnerable to external loads. Because, for the same amount of dwell time at the top temperature, the edges in contact with the mold will have reached the top temperature earlier, making the mixture less viscous for longer period, giving more time to both the bubble-pores and the residual particle-porosity to coalesce and move upwards, which is an undesirable effect for the aimed pore network.

# 6. Discussion

The endeavour of aiming to engineer the microstructure of a glass foam for the right amount of open porosity, dependent upon a number of variables, that even the same set could result in a slightly different outcome each time tested, was already challenging from the beginning. However, the developed material, even though in a primitive experimental state, has achieved notable results within the goals set at the beginning of this research related to bioreceptive criteria and sustainable manufacturing processes.

From the literature review, touching such a novel topic that currently raises a lot of attention for other construction materials, such as concrete, mortars and stone, the limited sources from mainly lab experimental work, posed a great obstacle to identify the desired values that need to be obtained. Not to mention, that comparing the most promising sample with the aforementioned materials optimized for bio-growth, entails many assumptions, since there is not a specific guideline nor the same method applied for testing these materials, being also in an experimental level.

Therefore, it can be supported that from the knowledge gained by studying microscopic images of materials with inherent capillary porosity, like mortars and clay, the resulted promising porosity type 04, presents a lot of similarities. Notwithstanding the different manufacturing method that these materials are produced, their porosity networks are formed by the residual porosity between their particles of the initial mixture. Due to the strong bonds that characterize the pore walls of the glass foam, it could be stated that when compared to mortars or concrete, its weathering resistance longtermly could be higher, once its surface brittle behaviour is overcome.

Regarding, its compressive strength as analysed in the paragraph 3.3.4, the obtained values, even if certain recommendations are incorporated and the samples undertake larger forces, the strength will still remain at low levels when compared with concrete or stone. Currently, they can be compared with porous mortars and other similar materials in experimental phase, leading to the conclusion that in order to achieve better outcomes a great deal of research has to be carried out, regarding the pore network and its potential. These findings, together with the first indicators gathered for frosting resistance, justify completely the choice of developing a façade tile as the most probable design application with the minimum demands for compressive strength. However, since the most promising recipe for primary bioreceptivity was tested for its compressive strength, the rest of the samples supported to serve also other applications that demand higher strength and less water absorption for tertiary bioreceptivity, remain unexplored.

Hence, with the current research on this new topic, only the surface is scratched of the immense potential of re-thinking existing products under the lens of bioreceptivity. Introducing glass waste that is currently not even recyclable back into the building industry as a raw material, outlines the most important reason that bio-host glass compared to the other bioreceptive materials, should become the most upcoming, based on the fact that life can grow on it.

## 6.1. Research results

The market niche for bioreceptive applications, as a solution for retrofitting of buildings or infrastructural constructions, has already been identified and only a few ventures like Respyre and Quay walls have started their first steps in developing bioreceptive products out of concrete or mortars, rendering the potential of this concept huge.

Even though the research focus was to investigate the potential of the glass foam microstructure, to meet the criteria of bioreceptivity by obtaining inner porosity that absorbs water and retains it, a series of promising applications by re-thinking existing products was also outlined as recommendations. To this, the methodology for a designer that works with bio-host glass is also presented, by illustrating how the bioreceptive design guidelines can be applied to the recommended applications until their realization and building implementation. This whole process, whilst its critical points regarding the sizing of the modules that require further studying, already highlights the simplicity of the needed design, as the objective is to provide just a porous substrate that will be finally covered fully out of greenery in the optimum conditions. The increased difficulty of this multi-objective topic lies on the aspect of the material science.

Recalling the posed research question, together with the literature review and the experimental analysis, the ways of producing porosity in glass were thoroughly investigated. Having set from the starting point, one of the main criteria of this thesis to be the incorporation of unexploited glass waste into the new material's ingredients, glass foaming was chosen as the manufacturing method to be explored. Despite the revealed obstacles along the process of transforming the glass foam, from an insulating product with absolute moisture resistance and low thermal conductivity to a water absorbent one, positive evidence has been achieved not only regarding its hydraulic performance but also its bio-hosting ability.

Regarding the revealed types of glass foam microstructure, the initial hypothesis supported in the literature review, that increasing porosity favors microorganisms' material colonization was also proved from the conducted experiments. Since, the moss growth was observed on the sample with the maximum water absorbance capacity, developed out of Cyclon mix with calcite as a foaming additive (10% wt), foamed at 840°C, with slow cooling. However, to meet the market's demand, this recipe needs further testing to overcome the observed brittle behavior along with certain corrosion incidents.

For this reason, the best compromise of material properties and bioreceptive potential, out of the developed recipes was the mixture TBS08, out of Soda-lime float glass powder (50% wt) with Borosilicate cullet (50% wt), carbon black and calcium hydrogen phosphate ($CaHPO_4$), foamed at 790 °C with fast cooling. The successful performance of its type of microstructure (04), is attributed to the high tendency of Borosilicate glass to crystalize, as this phenomenon is suggested in the literature that produces open pores, as well as to its mixing with refined SLS powder, resulting in better glass particle connections with more refined pores. Therefore, its porosity network, from the residual porosity of the mixing of powder with small-sized cullets, resulting to droplet dispersion once it touches its surface, showcases a very positive outcome for the set goals of this research.

Thus, by following all the steps for the development of a new material, aiming to stir bio-growth, a holistic methodology is outlined in this research. From the micro- to the meso- and finally to the macro-scale, the seeds are planted with encouraging evidence, that glass foams constitute a novel solution for hosting bioreceptivity and let it grow.

## 6.2. Points for further research

During this whole experimental process, the outcome of every analyzed step was drawing conclusions that pose recommendations for further research, especially for such a topic that has not been researched before. Specifically, the greatest of these is the work presented in the applications catalogue. Contrary to what is expected from a material research, to first invent the material, and afterwards determine its purpose, the reverse is more meaningful to be applied in this case. The match of the applications' needs to the material properties' outcome, leads to the weakening points that need to be further researched and experimented, depending on the chosen product to be developed. with to identify the weakening points for further research.

Overall, regarding the point that the material development reached, next steps of testing would focus on ameliorating the brittle behavior and therefore compressive strength. What's more, the ideal sizing of a tile in relation to the heating schedule, mold reaction and incorporation of the bioreceptive design principles needs further exploration.

Last but not least, the method followed for producing the glass foam samples could also be improved in terms of sustainability, regardless the fact that landfilled glass waste is investigated to be upcycled. Since, there is energy consumption for the use of furnaces in high temperatures, but also the cyrstalcast molds used, cannot be re-used. A Life Cycle Assessment (LCA) (R.C. da Silva et al., 2021) could elucidate not only the production method for glass foams, but also determine what happens when bio-host glass is disassembled from the construction.

# 7. Reflection

The starting point of this research has been on providing new market applications for glass waste that currently remains unutilized. To do this, bioreceptivity was chosen as an upcoming trend to serve the means to this purpose. Therefore, out of the proposed graduation topics a new one was formed by combining some existing concepts developed to promote sustainability in the construction industry. On the one hand, testing methods to re-introduce material waste and especially upcycle glass is of utmost importance, since currently there is a linear process prevailing from the manufacturing of glass products – apart of bottles – until the end-of-life usage of a product, that gets landfilled. On the other hand, bioreceptivity as a phenomenon benefits greatly the urban environment in a bigger scale by creating a better microclimate against climate change effects, while also takes advantage a natural phenomenon in materials that is now considered to be negative.

The experimental research approach that was followed, had been based at a great extend on literature findings and used them as a starting point for testing. I feel that the process could not have been followed in a different way, since the topic and the set goal was to complex to be fully-achieved in this short-period of time. The research question is answered holistically by the conclusions of this study, not by a final product or material that one may expect, but with a designed methodology based on the findings already achieved by now, and specific aspects for further research and experimentation that could consist many different graduation topics or even one PhD thesis.

Specifically, the variables that had to be considered are immense and only revealed to me, when I had delved into the topic, by combining knowledge found in the literature from different fields of expertise. Due to the topic's novelty, only through the guidance of my mentors, I managed to focus my thinking on defining a strategy for dealing with this specific topic and determine its engineering and design requirements. Thus, its relevance with the Building Technology track is absolute because it combines both the methodological thinking for engineering by analyzing a problem and identifying the specific inputs and outputs that have to be generated to reach to the desired solution, or define the steps towards your goal.

What's more, from the problem statement the main inspiration was to take advantage of certain criteria that lead to bioreceptive performance, such as porosity and non-transparency, that for any other application derived from glass would pose a major flaw, therefore the topic's contribution to the scientific world can be identified in multiple aspects, no matter its size. Firstly, by addressing the development of a new material, new experiments held during the time of this graduation, offer findings for innovation, in the same way that I was investigating evidence by unsuccessful experiments that would serve the purpose of porosity and crystallization in recycling glass, in order to achieve open-porous glass foams, which are exactly the opposite than the current industry offers. Secondly, extensive information was collected from published lab-experiments that other researchers have already conducted, in order to define, not only the testing process for such a phenomenon, but also the desired values for material properties that would serve as exemplary results to be achieved in my work.

A proof of the aforementioned is the fact that, this work already offers a guideline for young researchers participating in Bucky Lab studio having bioreceptivity as the main topic. Although the desired range for the material properties, optimized for bio-colonization, could not been accurately defined, the collected information enabled me to deeply understand porosity as a material process and search for ways to achieve the right pore network for optimum water behavior. It is an undeniable fact that, until now there has not been any research in the field about manufacturing such properties, but only enhancing the ones that are already described as inherent.
All the above, offer insight also to the societal relevance, to which greatly contributes even the formed topic itself highlighting extremely contemporary problems of the construction industry and suggests a competitive solution, once it is achieved.

However, to accomplish the execution of an idea that has not been done or researched before entails great difficulties and challenges. For this specific topic investigating material properties, climatic conditions and natural phenomena related to our urban environment, such problems may would have been easier to tackled if more experts, - apart from the mentors - could offer their insight on the topic. Despite the fact that not only did I try to take advantage of talking with other researchers, but also promoting to them my work and the difficulties that I encounter, this contact was not enough at the first steps of the research, mainly due another outbreak of corona. A potential result of this, would be the need of extensive experimentations and testing, in order to achieve the goal of my graduation topic and conclude to a final material. However, this act would entail an ethical dilemma regarding the consumption of huge amounts of material for mold casting and energy for heating the samples. Towards this, working closely with Telesilla Bristogianni my mentor both in the topic and in the lab, the samples produced were minimized and their results examined carefully, for the purpose of assessing with scrutiny the next experiments, so as to avoid superfluous work for the scope of this research.

Overall, what I learned is that regardless of the experimental results, it is of utmost importance to report every step with scrutiny and provide all the knowledge you have gained that can be taken advantage for further research and exploration. For this reason, I chose to also work on building a catalogue of potential applications for bio-host glass before it is even created or tested, by highlighting the engineering steps and requirements towards their manufacture. Due to the limited time frame of this graduation topic, specific variables could be further explored, thus the designed applications will already constitute a solid basis on the general specifications for the new material. This fact illustrates a vast potential for bio-host glass, since this material emerges out of current industrial waste and replaces existing products with enhanced ecological benefits related to climate change mitigation tactics.

# 8. Glossary

Upcycling: term referring when a new material value is created from waste, either through reuse, regeneration, recycling, and/or repurposing. Source: https://materialconnexion.com

Closed-loop recycling: the process in which the product, for example the glass or the glass cullet is being used as a raw material for the generation of a recycled product. *Source: Lebullenger, R. (2012). Mousses de verre issues du recyclage : Quelques exemples d'études et applications, ISCR Expertise Conception & Synthesis of Molecules & Materials. https://www.slideserve.com/nico/recyclage.*

Open-loop recycling: the process in which the product at its end-of-life is used only as an additive or a matter to transform before re-using, therefore the product gets downcycled losing its value as a raw material. *Source: Lebullenger, R. (2012). Mousses de verre issues du recyclage : Quelques exemples d'études et applications, ISCR Expertise Conception & Synthesis of Molecules & Materials. https://www.slideserve.com/nico/recyclage.*

Coalescence effect: depending on the soacking time of a concrete mixture, or the heating time when foaming for example, pores tend to become unified forming bigger ones. This results in a material of a higher density. *Source: wikipedia*

Carbonation: the state of having carbon dioxide gas dissolved in a liquid. The process usually involves carbon dioxide under high pressure, when the pressure is reduced, the $CO_2$ is released from the solution as small bubbles. In the literature, it is referred that this process takes time to happen naturally when concrete is produced and by this, the pH is reduced, forming a friendlier environment for microorganisms to develop.

Water capillarity, Capillary action, Capillarity, Capillary motion, Capillary effect: describes the process that a liquid flows in a narrow space, such as a tube, while gravity or other external forces do not interfere. This happens, because of intermolecular forces among the water and the surrounding solid wall boundaries. When the tube is adequately small, surface tension among the liquid and container wall and forces that cause the liquid particles to adhere together, force the liquid to move forward (Wikipedia).

Moss: non-vascular, flowerless plants belonging to the group of bryophytes, forming dense green mats, usually located in damp or shady locations. Individually, they are composed of simple leaves with only one cell thickness, attached to a stem that may be branched or unbranched (Britannica).

Cyanobacteria: are an ancient group of photosynthetic microbes, generally developing in inland waters, affecting the water quality, while they also grow in biofilms forming a firm crust on porous substrates (W.F. Vincent, in Encyclopedia of Inland Waters, 2009).

Heterotrophic organisms: microorganisms (yeast, moulds & bacteria) that feed from organic carbon nutrients (Wikipedia)

Autotrophic organisms: microorganisms that produce their own food either by using inorganic substances and transform them into organic nourishment, or from sunlight (Wikipedia).

Phototrophic organisms: mainly bacteria, whose energy to develop derives from light and their carbon sources come from carbon dioxide (CO2) (Wikipedia).

Vermiculite: hydrous phyllosilicate mineral, that when heated showcases considerable expansion. One of its main uses is as a substrate for seed germination (Lubelli et al., 2021).

Mucilage Sheet: is a 'thick, gluey substance produced by nearly all plants and some microorganisms', generally serves for the storage of water, food and seed germination (Wikipedia).

Fly Ash: mainly coal residuals, comprised from fine particles of burned fuel. Main elements included are silicon dioxide ($SiO_2$) in both amorphous and crystalline phase, aluminium oxide ($Al_2O_3$) and calcium oxide (CaO) (Wikipedia).

Bottom Ash: is the part of the ash that falls to the bottom of the boiler's combustion chamber. The compound together with fly ash, is also known as coal ash (Wikipedia).

Hydrophilic surfaces: from ancient Greek, 'water-loving', surfaces that attract water molecules, due to their electrical charging from oxygen atoms or hydroxyl groups (Giorgio Torraca, Porous building materials, materials science for architectural conservation, 1981, ICCROM 2005).

# 9. Bibliography

Aisar, A., Katoh, Y., Katsurayama, H., Koganei, M., & Mizunuma, M. (2017). Effects of convection heat transfer on Sunagoke moss green roof: A laboratory study. *Energy and Buildings*, *158*. https://doi.org/10.1016/j.enbuild.2017.11.043

Anagni, G. M., Bristogianni, T., Oikonomopoulou, F., Rigone, P., & Mazzucchelli, E. S. (2020). *Recycled Glass Mixtures as Cast Glass Components for Structural Applications, Towards Sustainability* Challenging Glass Conference, https://doi.org/10.7480/cgc.7.4482

Anderson, M., Lambrinos, J., & Schroll, E. (2010). The potential value of mosses for stormwater management in urban environments. *Urban Ecosystems*, *13*, 319-332. https://doi.org/10.1007/s11252-010-0121-z

Barberousse, H., Lombardo, R. J., Tell, G., & Couté, A. (2006). Factors involved in the colonisation of building façades by algae and cyanobacteria in France. *Biofouling*, *22*(2), 69-77. https://doi.org/10.1080/08927010600564712

Bernardo, E., Scarinci, G., Bertuzzi, P., Ercole, P., & Ramon, L. (2010). Recycling of waste glasses into partially crystallized glass foams. *Journal of Porous Materials*, *17*(3), 359-365. https://doi.org/10.1007/s10934-009-9286-3

*Bioreceptive concrete for liveable cities*. https://www.ams-institute.org/urban-challenges/resilient-cities/bio-receptive-concrete-liveable-cities/

Blocken, Bert & Carmeliet, Jan. (2006). The influence of the wind-blocking effect by a building on its wind-driven rain exposure. Journal of Wind Engineering and Industrial Aerodynamics. 94. 101-127. 10.1016/j.jweia.2005.11.001.

Bristogianni, T., Oikonomopoulou, F., Barou, L., Veer, F. A., Nijsse, R., Jacobs, E. A. M., Frigo, G., Durmisevic, E., Beurskens, P., Lee, J., & Rutecki, K. (2019). Re^3 glass a reduce/reuse/recycle strategy. *Spool, 6(2 #5)*, 37-40. https://doi.org/10.7480/spool.2019.2.4372

Bristogianni, T., Oikonomopoulou, F., Justino de Lima, C., Veer, F., & Nijsse, R. (2018). *Cast Glass Components out of Recycled Glass Potential and Limitations of Upgrading Waste to Load-bearing Structures* International Conference on Architectural and Structural Applications of Glass, https://doi.org/10.7480/cgc.6.2130

Bristogianni, T., Oikonomopoulou, F., Lima, C. J. D., Veer, F., & Nijsse, R. (2018). Structural cast glass components manufactured from waste glass: Diverting everyday discarded glass from the landfill to the building industry. *Heron*, *63(1/2)*, 57-102. http://resolver.tudelft.nl/uuid:f4e41fb0-13b3-4f70-9195-fea304e3f06e

*Building Greener Cities with Poikilohydric Living Walls*. UCL. Retrieved 10/01/2022 from https://www.ucl.ac.uk/bartlett/architecture/about-us/innovation-enterprise/building-greener-cities-poikilohydric-living-walls

Burszta-Adamiak, E., Fudali, E., Kolasińska, K., & Łomotowski, J. (2019). A pilot study on improve the functioning of extensive green roofs in city centers using mosses. *Przegląd Naukowy Inżynieria i Kształtowanie Środowiska*, *28*(1), 118-130. https://doi.org/10.22630/pniks.2019.28.1.11

Croce, S., & Vettorato, D. (2021). Urban surface uses for climate resilient and sustainable cities: A catalogue of solutions. *Sustainable Cities and Society*, 103313. https://doi.org/10.1016/j.scs.2021.103313

da Silva, R. C., Puglieri, F. N., de Genaro Chiroli, D., Bartmeyer, A., Kubaski, T., Tebcherani, S. (2021). Recycling of glass waste into foam glass boards: A comparison of cradle-to-gate life cycles of boards with different foaming agents. *Science of The Total Environment, 771.* https://doi.org/10.1016/j.scitoten.2021.145276

D'Orazio, M., Cursio, G., Graziani, L., Aquilanti, L., Osimani, A., Clementi, F., Yéprémian, C., Lariccia, V., & Amoroso, S. (2014). Effects of water absorption and surface roughness on the bioreceptivity of ETICS compared to clay bricks. *Building and Environment*, *77*, 20-28. https://doi.org/10.1016/j.buildenv.2014.03.018

DeBrincat, G., & Babic, E. (2018). *Re-thinking the life-cycle of architectural glass* (Construction flat glass recycling, Issue Viability study & value report).

Dubosc, A., Escadeillas, G., & Blanc, P. J. (2001). Characterization of biological stains on external concrete walls and influence of concrete as underlying material. *Cement and Concrete Research*, *31*, 1613–1617. https://doi.org/10.1016/S0008-8846(01)00613-5

Escadeillas, G., Berton, A., Blanc, P., & Dubosc, A. (2007). Accelerated testing of biological stain growth on external concrete walls. Part 1: Development of the growth tests. *Materials and Structures/Materiaux et Constructions*, *40*. https://doi.org/10.1617/s11527-006-9205-x

Escadeillas, G., Bertron, A., & Blanc, E. R. P. (2009). Accelerated testing of biological stain growth on external concrete walls. Part 2: Quantification of growths. *Materials and Structures/Materiaux et Constructions*, *42*(7), 937-945. https://doi.org/10.1617/S11527-008-9433-3

Fedorov, A. G., & Pilon, L. (2002). Glass foams: formation, transport properties, and heat, mass, and radiation transfer. *Journal of Non-Crystalline Solids*, *311*(2), 154-173. https://doi.org/10.1016/s0022-3093(02)01376-5

Fedosov, S. V., Bakanov, M. O., & Nikishov, S. N. (2018). KINETICS OF STRUCTURAL TRANSFORMATIONS AT PORES FORMATION DURING HIGH-TEMPERATURE TREATMENT OF FOAM GLASS. *International Journal for*

*Computational Civil and Structural Engineering*, *14*(2), 158-168. https://doi.org/10.22337/2587-9618-2018-14-2-158-168

Fernandes, H. R., Ferreira, D. D., Andreola, F., Lancellotti, I., Barbieri, L., & Ferreira, J. M. F. (2014). Environmental friendly management of CRT glass by foaming with waste egg shells, calcite or dolomite. *Ceramics International*, *40*(8, Part B), 13371-13379. https://doi.org/https://doi.org/10.1016/j.ceramint.2014.05.053

Ferrándiz-Mas, V., Bond, T., Zhang, Z., Melchiorri, J., & Cheeseman, C. R. (2016). Optimising the bioreceptivity of porous glass tiles based on colonization by the alga Chlorella vulgaris. *Science of the Total Environment*, *563-564*, 71-80. https://doi.org/https://doi.org/10.1016/j.scitotenv.2016.04.023

FEVE, T. E. C. G. F. (2021, 25 November). *Record collection of glass containers for recycling hits 78% in the EU*. Retrieved 27/12/2021 from https://feve.org/glass_recycling_stats_2019/

Francis, R. A. (2010). Wall ecology: A frontier for urban biodiversity and ecological engineering. *Progress in Physical Geography: Earth and Environment*, *35*(1), 43-63. https://doi.org/10.1177/0309133310385166

Gaylarde, P., Englert, G., Ortega-Morales, O., & Gaylarde, C. (2006). Lichen-like colonies of pure Trentepohlia on limestone monuments. *International Biodeterioration & Biodegradation*, *58*(3-4), 119-123. https://doi.org/10.1016/j.ibiod.2006.05.005

Giulia, T. A. (2018). *RECYCLED GLASS MIXTURE AS CAST GLASS COMPONENTS FOR STRUCTURAL APPLICATIONS TOWARDS SUSTAINABILITY* Politecnico di Milano].

Guiamet, P. S., Soto, D. M., & Schultz, M. (2019). Bioreceptivity of archaeological ceramics in an arid region of northern Argentina. *International Biodeterioration & Biodegradation*, *141*, 2-9. https://doi.org/10.1016/j.ibiod.2018.10.003

Guillitte, O. (1995). Bioreceptivity: a new concept for building ecology studies. *The Science of the Total Environment*, *167*(1–3), 215-220. https://doi.org/10.1016/0048-9697(95)04582-L

Guillitte, O., & Dreesen, R. (1995). Laboratory chamber studies and petrographical analysis as bioreceptivity assessment tools of building materials. *Science of the Total Environment*, *167*(1-3), 365-374. https://doi.org/10.1016/0048-9697(95)04596-s

Hall, C., & Hoff, W. D. (2003). *Water Transport in Brick, Stone and Concrete* (Second ed., Vol. 25). CRC Press - Taylor & Francis Group. https://doi.org/10.1520/CCA10518J

Hesky, D., Aneziris, C. G., Groß, U., & Horn, A. (2015). Water and waterglass mixtures for foam glass production. *Ceramics International*, *41*(10, Part A), 12604-12613. https://doi.org/https://doi.org/10.1016/j.ceramint.2015.06.088

Hubálková, J., Voigt, C., Schmidt, A., Moritz, K., & Aneziris, C. G. (2017). Comparative Phenomenological Study of Fracture Behavior of Ceramic and Glass Foams under Compressive Stress Using In Situ X-Ray Microtomography. *Advanced Engineering Materials*, *19*(9), 1700286. https://doi.org/10.1002/adem.201700286

Hujova, M., Monich, P. R., Sedlacek, J., Hnatko, M., Kraxner, J., Galusek, D., & Bernardo, E. (2020). Glass-Ceramic Foams from Alkali-Activated Vitrified Bottom Ash and Waste Glasses. *Applied Sciences*, *10*(16), 5714. https://doi.org/10.3390/app10165714

Jurado, V., Miller, A. Z., Cuezva, S., Fernandez-Cortes, A., Benavente, D., Rogerio-Candelera, M. A., Reyes, J., Cañaveras, J. C., Sanchez-Moral, S., & Saiz-Jimenez, C. (2014). Recolonization of mortars by endolithic organisms on the walls of San Roque church in Campeche (Mexico): A case of tertiary bioreceptivity. *Construction and Building Materials*, *53*, 348-359. https://doi.org/10.1016/j.conbuildmat.2013.11.114

Kaufman, M. (2016). *A Feasibility Growth Study of Native Mosses Associated with Self-Sustaining Flora on Vertical Infrastructure*

König, J., Lopez-Gil, A., Cimavilla-Roman, P., Rodriguez-Perez, M. A., Petersen, R. R., Østergaard, M. B., Iversen, N., Yue, Y., & Spreitzer, M. (2020). Synthesis and properties of open- and closed-porous foamed glass with a low density. *Construction and Building Materials*, *247*, 118574. https://doi.org/https://doi.org/10.1016/j.conbuildmat.2020.118574

Lebullenger, R. (2012). *Mousses de verre issues du recyclage : Quelques exemples d'études et applications*, ISCR Expertise Conception & Synthesis of Molecules & Materials. https://www.slideserve.com/nico/recyclage

Lubelli, B., Moerman, J., Esposito, R., & Mulder, K. (2021). Influence of brick and mortar properties on bioreceptivity of masonry – Results from experimental research. *Construction and Building Materials*, *266*. https://doi.org/10.1016/j.conbuildmat.2020.121036

Matteucci, E., Scarcella, A. V., Croveri, P., Marengo, A., Borghi, A., Benelli, C., Hamdan, O., & Favero-Longo, S. E. (2019). Lichens and other lithobionts on the carbonate rock surfaces of the heritage site of the tomb of Lazarus (Palestinian territories): diversity, biodeterioration, and control issues in a semi-arid environment. *Annals of Microbiology*, *69*(10), 1033-1046. https://doi.org/10.1007/s13213-019-01465-8

Miller, A. Z., Sanmartín, P., Pereira-Pardo, L., Dionísio, A., Saiz-Jimenez, C., Macedo, M. F., & Prieto, B. (2012). Bioreceptivity of building stones: A review. *Science of the Total Environment*, *426*, 1-12. https://doi.org/10.1016/J.SCITOTENV.2012.03.026

Mondo, A. D., Pinto, G., Carbone, D. A., Pollio, A., & Natale, A. D. (2018). Biofilm architecture on different substrates of an Oculatella subterranea (Cyanobacteria) strain isolated from Pompeii archaeological site (Italy). *Environmental Science and Pollution Research*, *25*, 26079-26089. https://doi.org/10.1007/s11356-018-2643-5

Municipality of Rotterdam. (2013). *Rotterdam Climate Change Adaptation Strategy* (Rotterdam.Climate.Initiative: Climate Proof, Issue. M. o. Rotterdam. www.rotterdamclimateinitiative.nl

Mustafa, K., & Ahmet, S. (2015). Impact of the surface roughness of stones used in historical buildings on biodeterioration. *Construction and Building Materials*, *80*, 279-294. https://doi.org/10.1016/j.conbuildmat.2015.01.073

Oikonomopoulou, F. (2019). *Unveiling the third dimension of glass: Solid cast glass components and assemblies for structural applications* [Doctoral, Delft University of Technology]. https://doi.org/10.7480/abe.2019.9

Ottelé, M. V. A. P. M. (2021). Exploring the Possibility of Using Bioreceptive Concrete in Building Façades. *JOURNAL OF FACADE DESIGN & ENGINEERING*, *9*(1), 73-86. https://doi.org/10.7480/jfde.2021.1.5527

P. Sanmartín, D. Noya-Pintos, E. Fuentes, & Pozo-Antonio, J. S. (2021). Cracks in consolidants containing TiO2 as a habitat for biological colonization: A case of quaternary bioreceptivity. *Materials Science and Engineering: C*, *124*, 112058. https://doi.org/10.1016/j.msec.2021.112058

Perini, K. (2021). Greening the Building Envelope. In (pp. 401-414). https://doi.org/10.1007/978-3-030-59328-5_21

Perini, K., Castellari, P., Giachetta, A., Turcato, C., & Roccotiello, E. (2020). Experiencing innovative biomaterials for buildings: Potentialities of mosses. *Building and Environment*, *172*, 106708. https://doi.org/https://doi.org/10.1016/j.buildenv.2020.106708

Ponstein, Y. H. S. (25 May 2021). *Climate adaptive cities: can we make Amsterdam cooler with moss walls?* Amsterdam Institute for Advanced Metropolitan Solutions. Retrieved 05/01/2022 from https://www.ams-institute.org/news/climate-adaptive-cities-can-we-make-amsterdam-cooler-with-moss-walls/

Prieto, B., & Silva, B. (2005). Estimation of the potential bioreceptivity of granitic rocks from their intrinsic properties. *International Biodeterioration & Biodegradation*, *56*(4), 206-215. https://doi.org/10.1016/j.ibiod.2005.08.001

*Respyre | Advanced Bioreceptive Technology*. Living-lab. Retrieved 05/01/2022 from https://www.living-lab.nl/experiments/respyre

Samoilenko, V. V., & Tatarintseva, O. S. (2013). Role of recipe and technological factors in foam glass formation. *Glass and Ceramics*, *70*(5-6), 205-207. https://doi.org/10.1007/s10717-013-9543-4

Sanmartín, P., Miller, A. Z., Prieto, B., & Viles, H. A. (2021). Revisiting and reanalysing the concept of bioreceptivity 25 years on. *Science of the Total Environment*, *770*, 145314. https://doi.org/10.1016/j.scitotenv.2021.145314

Siddika, A., Hajimohammadi, A., & Sahajwalla, V. (2022). Stabilisation of pores in glass foam by using a modified curing-sintering process: sustainable recycling of automotive vehicles' waste glass. *Resources, Conservation and Recycling*, *179*, 106145. https://doi.org/https://doi.org/10.1016/j.resconrec.2021.106145

Somayeh, S., Jeffrey, A., E., G. M., Tracy, I., & Dennis, M. (2017). Fungal bioreceptivity of Japanese tissue papers treated with plant dyes, watercolours, and acrylic paints in paper conservation. *Studies in Conservation*, *62*(2), 104-113. https://doi.org/10.1080/00393630.2015.1137132

Souza, M. T., Maia, B. G. O., Teixeira, L. B., de Oliveira, K. G., Teixeira, A. H. B., & Novaes de Oliveira, A. P. (2017). Glass foams produced from glass bottles and eggshell wastes. *Process Safety and Environmental Protection*, *111*, 60-64. https://doi.org/https://doi.org/10.1016/j.psep.2017.06.011

Tanaca, H. K., Dias, C. M. R., Gaylarde, C. C., John, V. M., & Shirakawa, M. A. (2011). Discoloration and fungal growth on three fiber cement formulations exposed in urban, rural and coastal zones. *Building and Environment*, *46*(2), 324-330. https://doi.org/10.1016/j.buildenv.2010.07.025

Toreno, G., Isola, D., Meloni, P., Carcangiu, G., Selbmann, L., Onofri, S., Caneva, G., & Zucconi, L. (2018). Biological colonization on stone monuments: A new low impact cleaning method. *Journal of Cultural Heritage*, *30*, 100-109. https://doi.org/https://doi.org/10.1016/j.culher.2017.09.004

Torraca, G. (1982). *Porous Building Materials: Materials Science for Architectural Conservation*. ICCROM. https://books.google.nl/books?id=oFbdAAAAIAAJ

Veeger, M., Ottelé, M., & Prieto, A. (2021). Making bioreceptive concrete: Formulation and testing of bioreceptive concrete mixtures. *Journal of Building Engineering*, *44*, 102545. https://doi.org/10.1016/j.jobe.2021.102545

Velden, M. v. d. (2020). *The increased thermal performance of a structural cast glass brick wall* Delft University of Technology]. http://resolver.tudelft.nl/uuid:d230d385-5734-4b5e-97b8-e544004d652d

Zhang, Z., MacMullen, J., Dhakal, H. N., Radulovic, J., Herodotou, C., Totomis, M., & Bennett, N. (2013). Biofouling resistance of titanium dioxide and zinc oxide nanoparticulate silane/siloxane exterior facade treatments. *Building and Environment*, *59*, 47-55. https://doi.org/https://doi.org/10.1016/j.buildenv.2012.08.006

The source of all the images that is not mentioned, is own.

# Appendix

| Chemical Elements | Cyclon (%(m/m)d.s.) | Maltha Glasstof | Black Glass Sibelco | Fiber Glass Sibelco |
|---|---|---|---|---|
| $SiO_2$ | 48,1 | 69,7 | | |
| $B_2O_3$ | - | - | | |
| $P_2O_5$ | 0.16 | 0,2 | | |
| $Al_2O_3$ | 1,52 | 2,4 | | |
| $GeO_2$ | - | - | | |
| $Na_2O$ | 6,34 | 11,6 | | |
| PbO | 0,04 | 0,05 | | |
| $K_2O$ | 0,66 | 0,7 | | |
| CaO | 9,98 | 11,8 | | |
| BaO | 0,07 | 0,02 | | |
| MgO | 0,95 | 1,6 | | |
| ZnO | 0,03 | 0,08 | | |
| $Fe_2O_3$ | 0,5 | 0,7 | | |
| $Na_2SO_4$ | - | | | |
| $SO_3$ | 0,32 | 0,3 | | |
| $TiO_2$ | 0,12 | 0,2 | | |
| $Cr_2O_3$ | 0,06 | 0,07 | | |
| NiO | n.a. | 0,008 | | |
| CuO | 0,01 | 0,04 | | |
| SrO | 0,02 | 0,02 | | |
| $ZrO_2$ | 0,02 | 0,02 | | |
| Cl | 0,3 | 0,4 | | |
| $V_2O_5$ | n.a. | - | | |
| MnO | - | 0,04 | | |
| $SnO_2$ | - | 0,009 | | |
| $Rb_2O$ | - | 0,003 | | |
| Samples | TC01, TC04 (+Ca 30%) | | TT02 | TT03 |

Appendix_Table 1. Concentrated XRF Analysis of glass waste mixtures used as a raw material for the samples' composition, conducted by 3Me, Ruud Hendrikx, with a Panalytical Axios Max WD-XRF spectrometer and data evaluation was done with SuperQ5.0i/Omnian software.

## Samples Photographical documentation

| TT02 | TT03 |
| --- | --- |
|  | 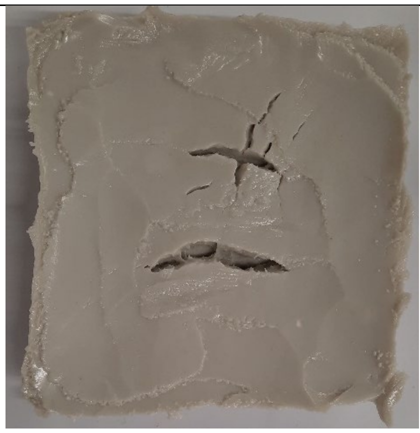 |
| 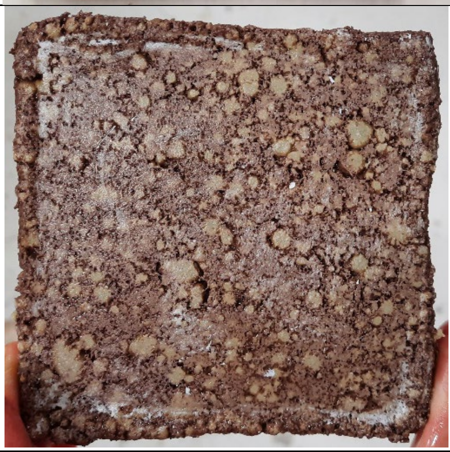 |  |

| TC01 | TC04 | TC05 |
| --- | --- | --- |
|  |  | 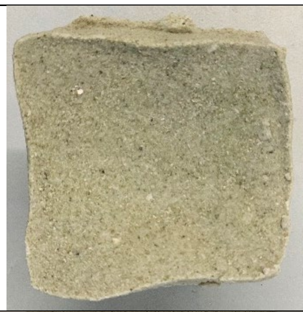 |
|  |  |  |

| | | |
|---|---|---|
|  |  |  |
| Not available | Not available |  |
| TC06 | TS07 | |
| 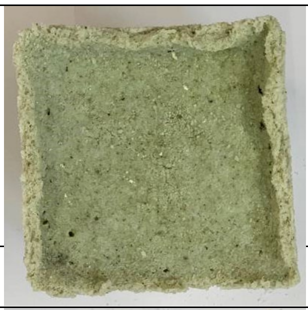 |  |  |
|  |  | 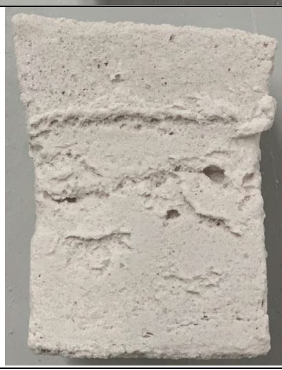 |
|  |  | Not available |
|  |  |  |

| TC09 | TS10 | TC11 |
| --- | --- | --- |
|  |  |  |
|  |  |  |
|  |  | |
| | |  |
| TC12 | TC13 | TC14 |
|  |  |  |

| | | |
|---|---|---|
|  |  |  |
| | 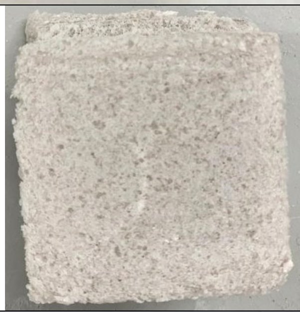 | Not available |
|  |  | Not available |
| TBS15 | TS16 | TBS17 |
| 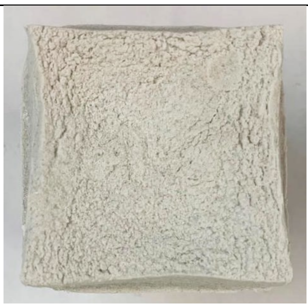 |  | 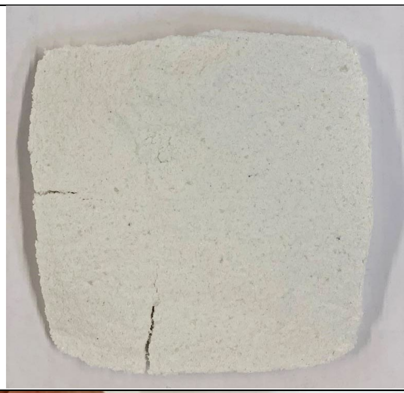 |
|  |  |  |

| | | |
|---|---|---|
|  |  | Not available |
|  | 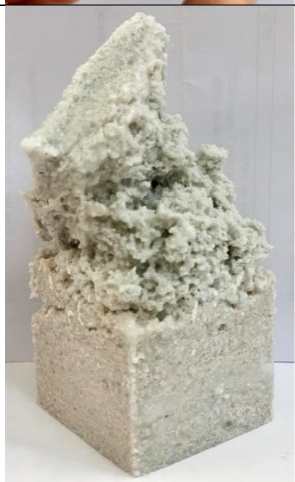 | Not available |
| TBS18 | TBS19 | TBS20 |
|  |  |  |
| TBS21 | TBS22 | TBS23 |
|  |  | TBC |
| |  | |

Appendix_Table 2. Photographical documentation of all the samples, in the order that were produced for all the analysed tests described in chapter 3. For each sample either cube or tile (from top to bottom) is presented: (a) top side of the mould, (b) side-view, (c) cut-surface, (d) perspective image. Image Sources: T. Bristogianni for samples: TC01, TT02, TT03, TC04, for the rest: Own.

## Microscopical analysis

| TC01 | TC04 | TC05 |
| --- | --- | --- |
|  | 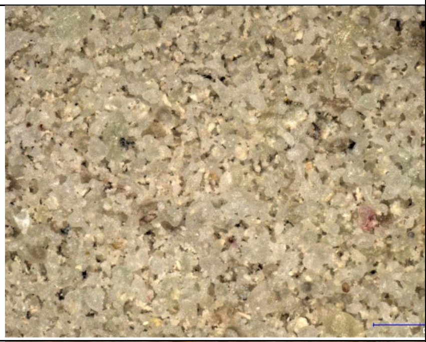 |  |
| 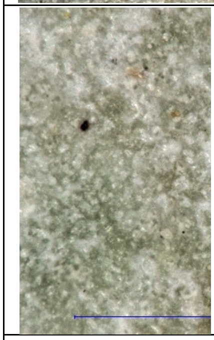  |  | 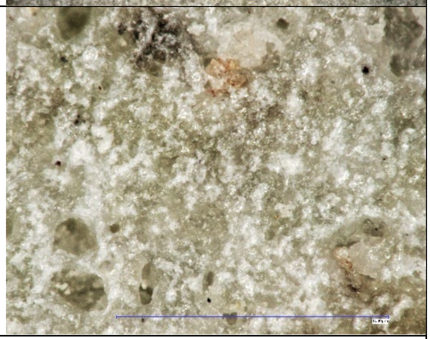 |
| **TC06** | **TS07** | **TBS08** |
|  |  | 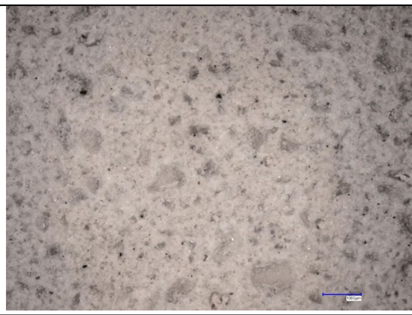 |
|  | 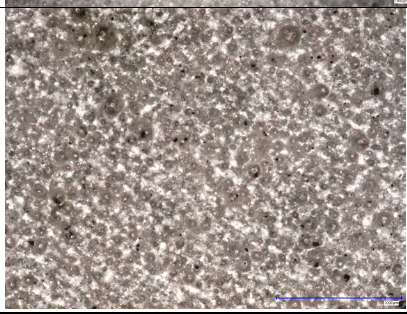 |  |
| **TC09** | **TS10** | **TC11** |
|  | 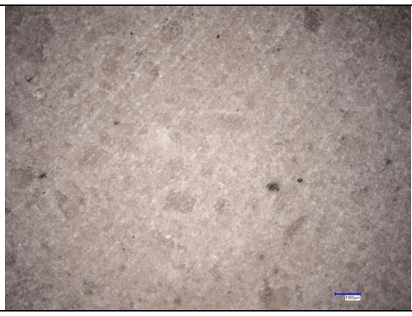 |  |

| | | |
|---|---|---|
| 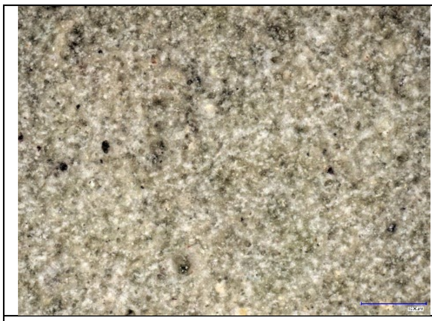 | 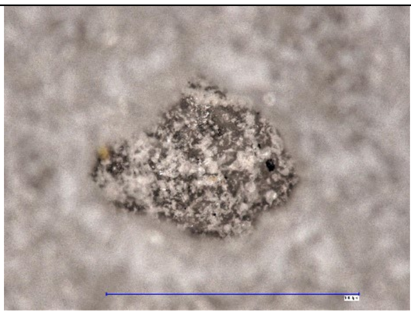 | 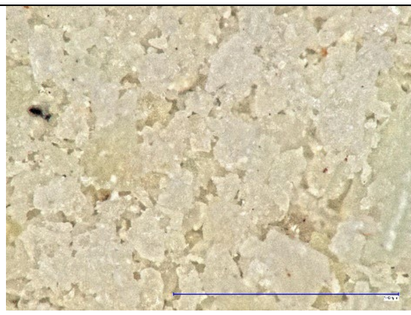 |
| TC12 | TC13 | TBS15 |
|  |  |  |
| 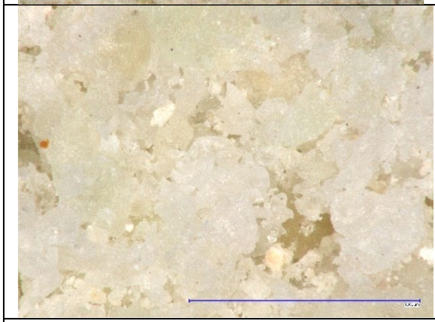 |  | 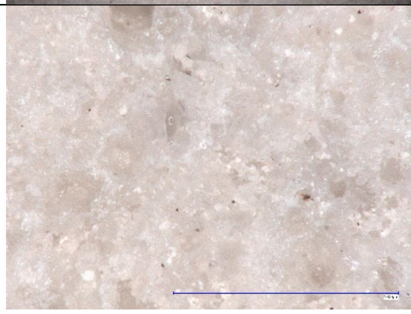 |

| TS16 | TBS18 |
|---|---|
|  | 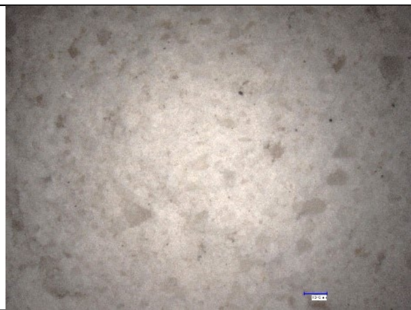 |
|  |  |

Appendix_Table 3. Microscopical documentation of all the cubic samples produced for testing their porosity & hydraulic properties. Samples of a tile shape and the ones used for compressive strength were excluded from the image analysis of the digital microscope (VHX-7000 series, Keyence located at the Faculty of Architecture). Image Source: TC01-TS10: captured with the aid of T. Bristogianni, rest: Own.

## Compressive Strength Results & Photographical documentation

Three specimens of the same recipe and heating schedule -SLS powder (float glass) + Borosilicate cullet + carbon + $CaHPO_4$, 790°C (2hrs), fast cool to anneal. point (1hr) - were tested in the Istron , recording their deformation and maximum load applied ($F_{max}$).

| | Before | After |
|---|---|---|
| TBS19 | 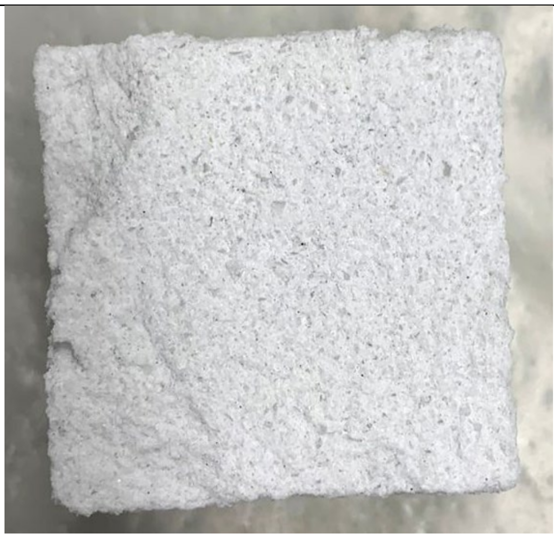 |  |
| |  |  |
| TBS20 |  | 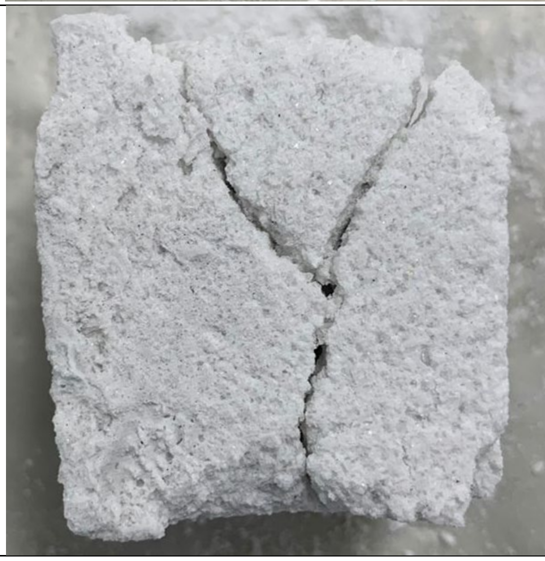 |

| | | |
|---|---|---|
| |  | 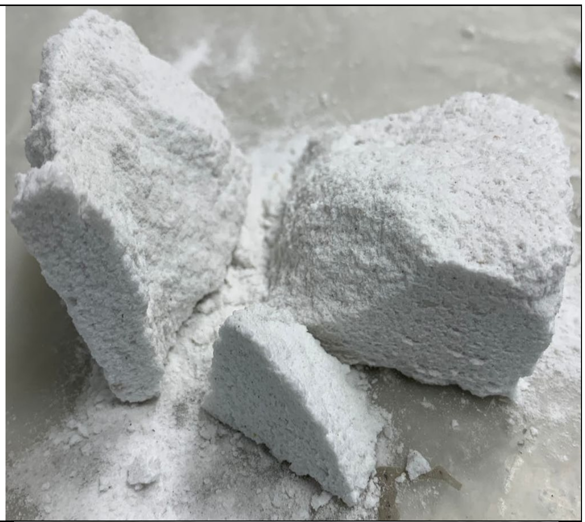 |
| TBS21 | 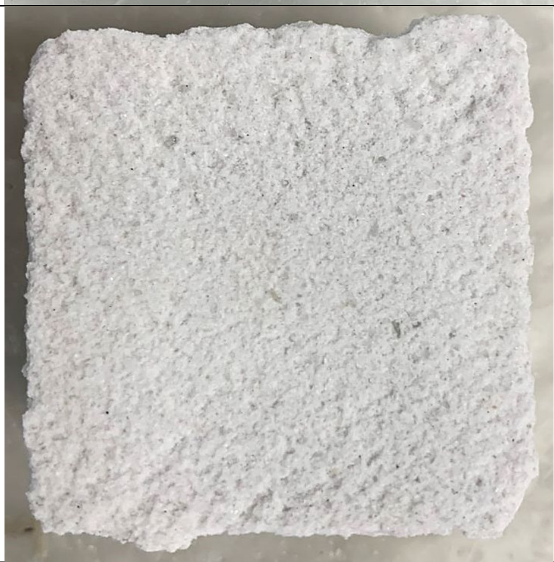 | 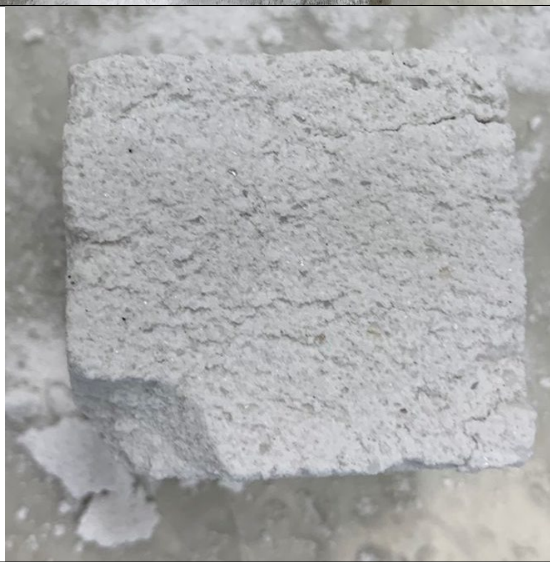 |
| |  |  |

Appendix_Table 4. Photographical documentation of the three samples (TBS19-21) tested in Istron 8872, with the help of Maiko van Leeuwen, in microlab, TU Delft.

## Results from frosting at -12 for 24hrs, at saturation point

| | | |
|---|---|---|
| TC01 | TC04 | TC05 |
|  |  |  |
| TC06 | TS07 | TBS08 |
|  |  |  |
| TC09 | TS10 | TC11 |
|  |  |  |
| TC12 | TC13 | TBS15 |
|  | 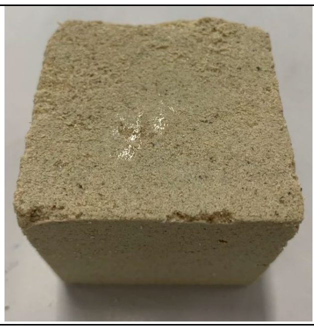 |  |
| TS16 | TBS18 | |
| 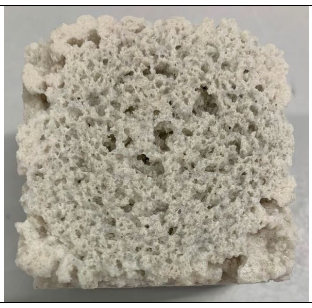 |  | |

Appendix_Table 5. Photographical documentation of the samples right after they were taken out of the freezer. The formation of ice has already started melting, without any apparent damages, apart from the fact that the initial brittle samples, were even more brittle when frozen. When the samples came to room temperature, no evidence of failure was detected.

## Results from moss-growth test

| | TBS17 | TC14 |
|---|---|---|
| $3^{rd}$ of May (formation) |  |  |
| $11^{th}$ of May ($2^{nd}$ week) |  |  |
| $24^{th}$ of May ($3^{rd}$ week) |  |  |
| $1^{st}$ of June ($4^{th}$ week) |  | 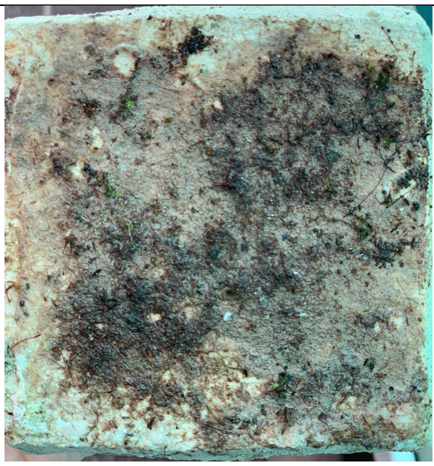 |

Appendix_Table 6. Photographical report of the samples positioned in the botanical garden in greenhouse 6, in Delft. The samples showed signs of life from the $3^{rd}$ week, while in the $4^{th}$ on the sample TC14 the greenery was more evident.

## Bioreceptive experimentations of other materials under the microscope

In this section, images produced by the author in the digital microscope as part of other projects' research are cited, aiming to reveal the difference in microstructure of other material production methods with inherited porosity, compared to foaming that the right pore-network for bioreceptivity is engineered.


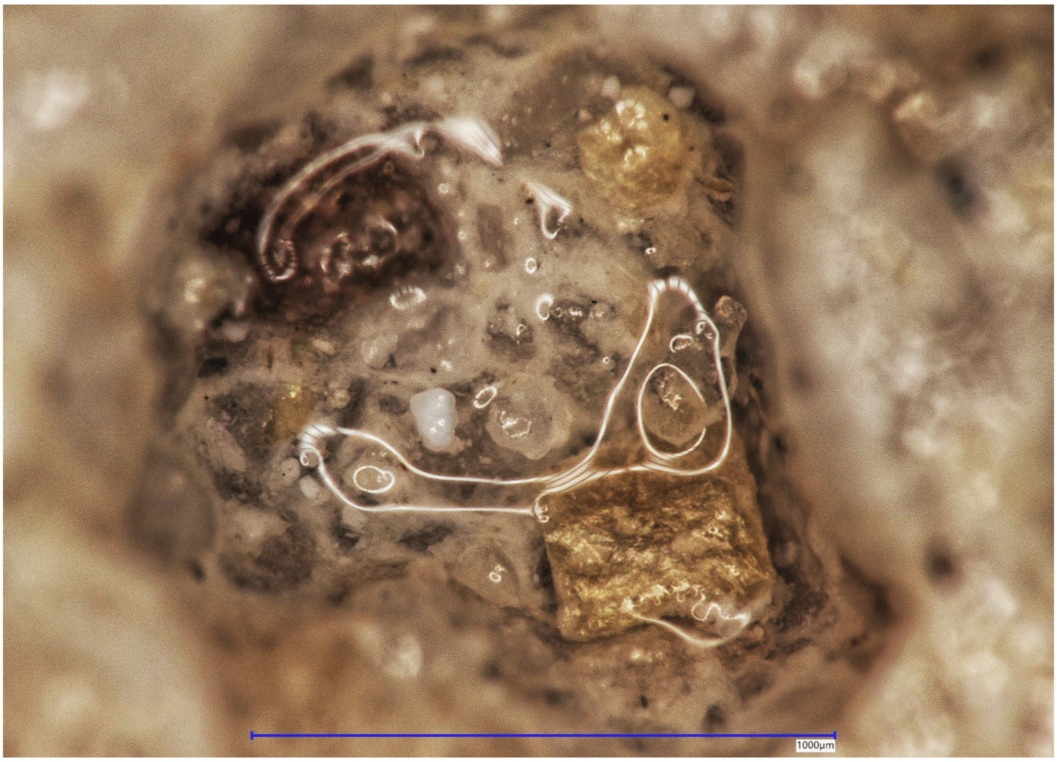


Appendix_Figure 1. Microscopic images taken on 03/05/2022, from a mortar optimized for bioreceptivity produced by Dimitrios Ntoupas as part of his thesis. The mixture contains natural hydraulic lime, with thin sand grains (0.08-1) & vermiculite, while the image was taken right after the sample was being tested for water absorption rate, therefore the reflection is caused by water and not from the material. Despite this, the porosity is obvious between the aggregate and the sand grains, especially in the lower image focusing inside a pore where irregular voids around pebbles are evident and covered in water film.

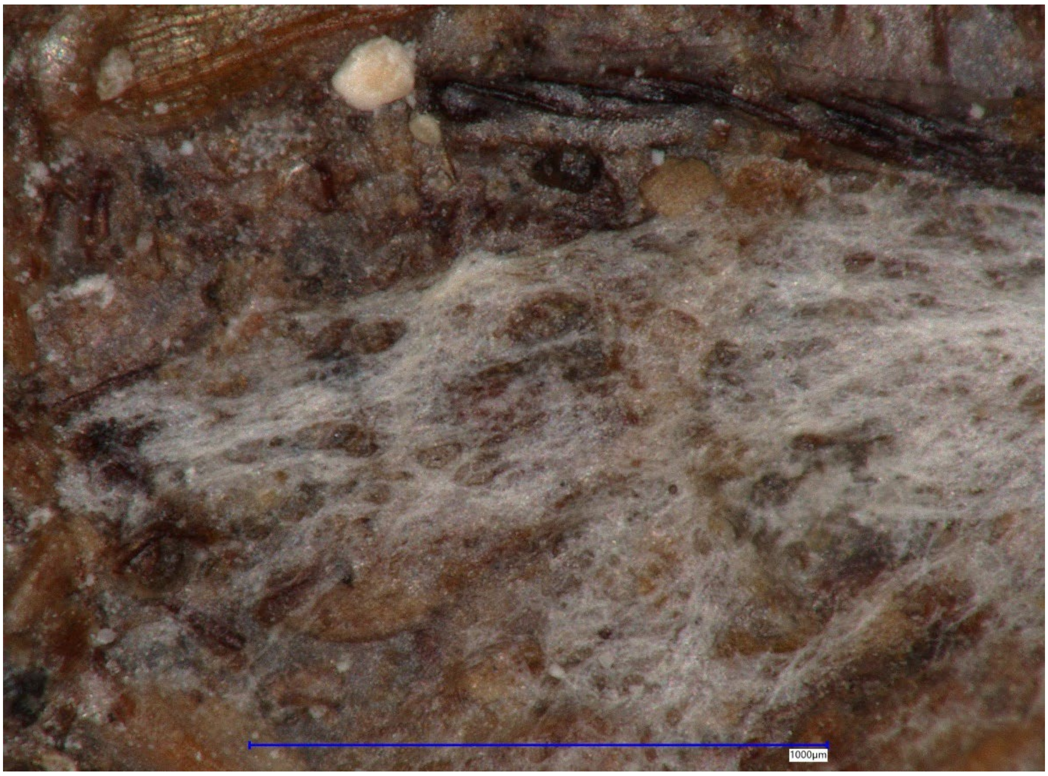


Appendix_Figure 2. Fungi formation during moss-growth test conducted by Dimitrios Ntoupas on the mortar mixture presented in Appendix_Figure 1. Potential reasons for this phenomenon, are the extreme lack of sunlight and samples-sealing from natural ventilation.

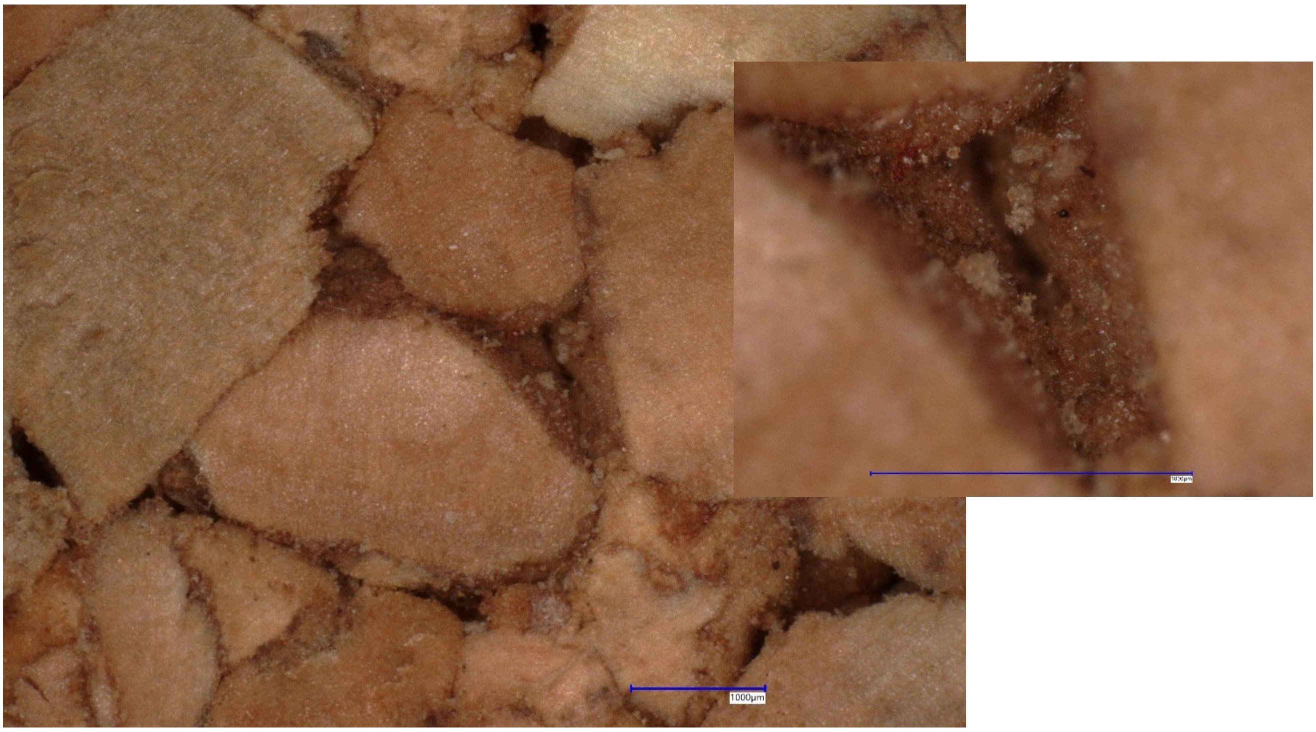


Appendix_Figure 3. Microscopic image taken on 04/05/2022, from a kitchenware cork under investigation by Hartmann N. during Bucky lab course. As cork particles are bonded by its natural resin, produced under pressure, pores identified to be connected to the outer surface, are greatly affected by the particle size


Appendix_Figure 4. Microscopic image taken on 04/05/2022, from a thinner kitchenware cork than the one analysed in Appendix_Figure 3, under investigation by Hartmann N. during Bucky lab course. From these two different particle-sized corks, it can be concluded that larger particles have the potential to form larger pores by the remaining voids of their irregular shapes. However, it is highly unlikely that these voids will be connected in greater depth. In general, when focusing only to porosity, a better-connected pore-network was observed in cork products with smaller-sized particles. In the case that bioreceptivity is examined for this material, extensive exposure to water can lead to the dissolve of its particles, and render it unsuitable.

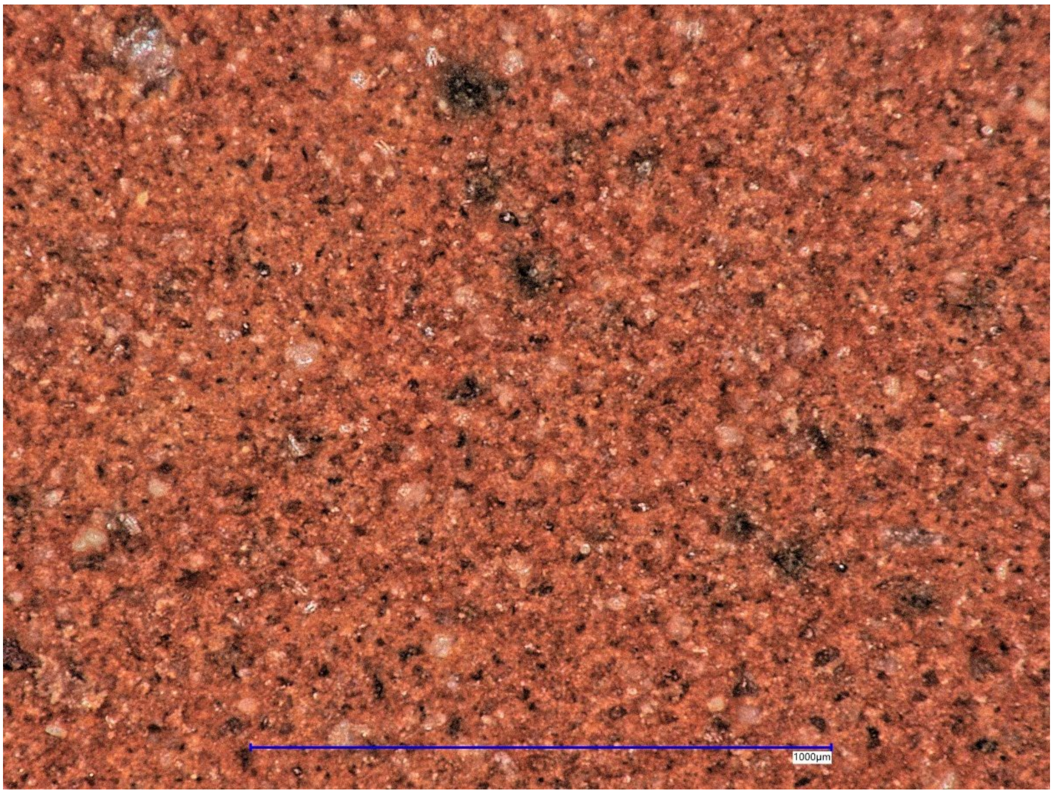


Appendix_Figure 5. Microscopic image taken on 04/05/2022, from a commercial roof tile that was sandblastered by Kalkhoven T. during Bucky lab course. Even though, the material was surface-treated to reveal its inherited porosity, the image taken at the maximum scale of the digital microscope (x200), shows how compact is the product, rendering it unsuitable for primary bioreceptivity, or modifying its hydraulic properties by only degrading its outer crust. Depending on the environmental conditions and water content, the growth of algae and bacteria could be supported.

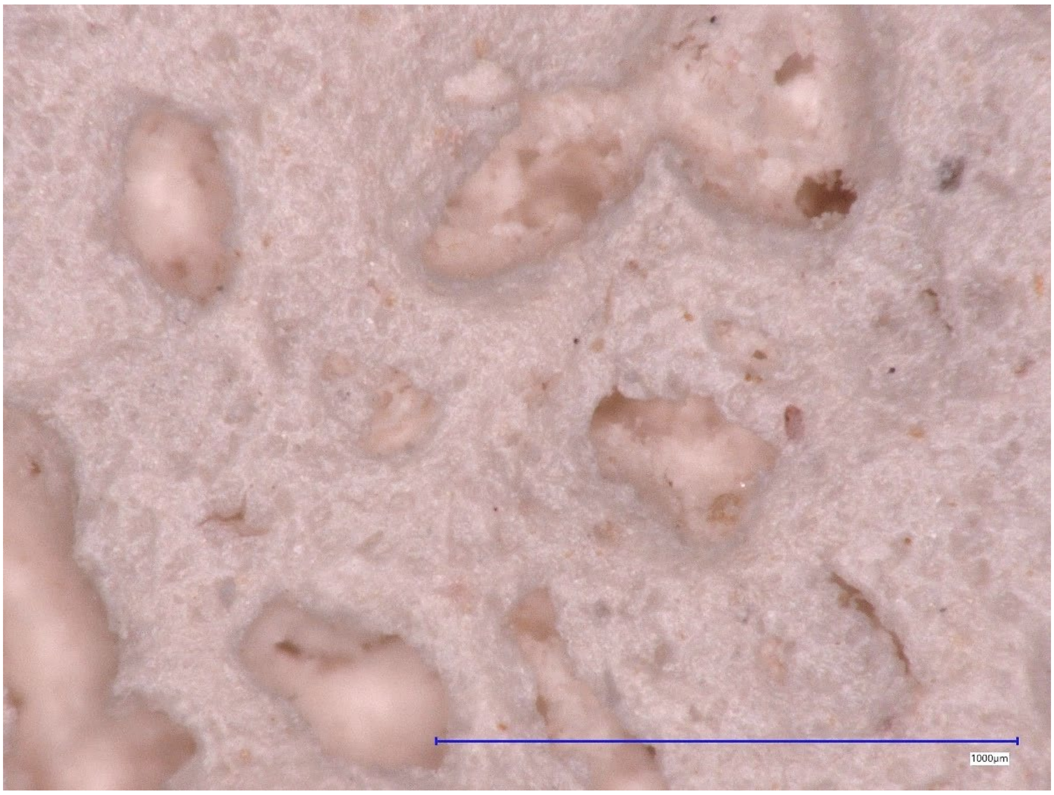


Appendix_Figure 6. Microscopic image taken on 09/06/2022, commercial clay sample treated on the surface with coffee beans produced during Bucky lab course by Verhaagen B., V. , D. , Paszek W.. The chosen manual treatment has increased the surface roughness of the commercial product, by revealing the network of residual porosity underneath the outer layer, in which particles are bonded by water-mixing covering all the pores, but cracks.

## A. Porosity

Porosity is a material property occurring naturally, for materials like rock, brick and concrete because of their forming process and their chemical composition effects. When their particles bind together either due to pressure or chemical reactions, a considerable residual porosity is left. Only by examining microscopically can we derive conclusions about the material porosity, which from the images in Appendix_Figure 7 & 2 is obvious that various materials have completely different porosity image. The pore system can be irregular, while the pore sizes can have a wide range. In these materials it is usually observed that the volume of the voids does not exceed the 35 per cent of the total one, mainly because the original size of their particles that were either compacted, cemented or sintered, remained the same, leaving the pore space observed to be the rudimentary relation to the original geometry.

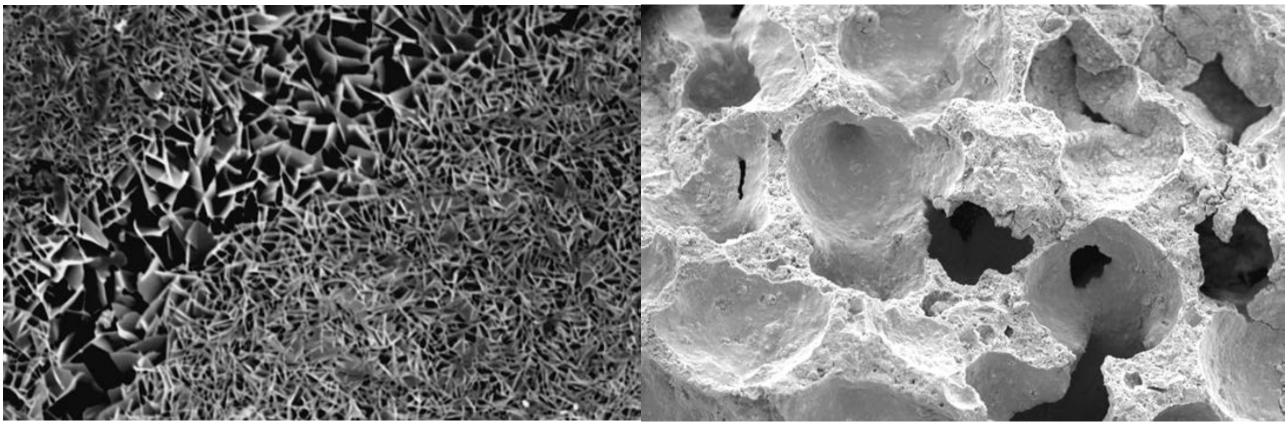

Appendix_Figure 7. From left to right: a) High magnification view of microstructure of AAC material with bulk density 450kg DIA m-3_linear mesopore filled with crystalline tobermorite running between regions of microporosity. Scale bar 20μm. SEM image by Andrea Hamilton. b) Low magnification view of the coarse structure of a fracture surface of AAC showing aeration pores. Scale bar 0.5 mm. SEM image by Andrea Hamilton.

Images Source: Fig 1.3, page 23, (Hall & Hoff, 2003).

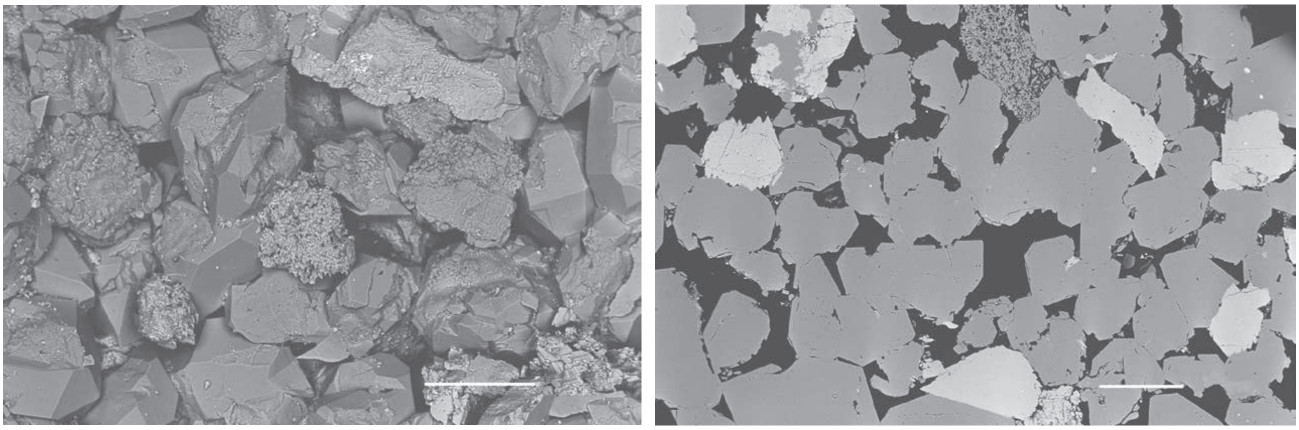

Appendix_Figure 8. Clashach sandstone coarse structure in a fracture surface packaged grains of 0.2-0.5 mm in diameter electron micrographs by Francis Clegg.

Image Source: Fig 1.1, page 21, (Hall & Hoff, 2003).

There is one major difference between these three materials: stone, brick and concrete. Specifically, for the stones, their grains which have been compacted or pressurized, still hold their mineral identity. While, the hydrated cement, the initial particles forming the new material, lose their original identity, as the water binds them together through a series of chemical reactions.

There are certain ways to generate higher porosity in materials. One of these, is to produce aerated or foamed materials with gas bubbles into a paste before hardening or during firing. These type of materials present a very different type of microstructure, as it is obvious in the Appendix Figure 2 with the autoclaved aerated concrete (AAC), forming approximately large, spherical pores. If bubbles do not coalesce, then the foam generated will have a stable microstructure by segregated pores. Another way for creating higher levels of porosity is through the addition of fibres, or wool.

To define if a material has open or closed porosity, or in other words connected or disconnected pores, it requires to know the production method. In general, voids created by gas bubbles, form closed pores that are not connected with each other, whereas compacted or sintered particles may have only some parts that are isolated from the rest. However, for the transportation of liquids and gases within the material, what is crucial is to identify the kind of pores that are or aren't connected to the boundary surface. Thus, isolated disconnected pores are considered to count in the solid matrix, since it is often intricate to detect them from the outside (Hall & Hoff, 2003).

### Porosity & Temperature dependence:

In uniform porous materials without internal stresses, the ratio of the pore volume to the bulk volume is constant, nonaligned with changes in temperature. Since, the thermal expansivity is dependent from the matrix material.

### Porosity & Stress dependence:

The volume fraction porosity is getting lower by applying compression loads. However, because the change in porosity receives most of the strain, it is also analogous to the change of the total volume ΔV (Hall & Hoff, 2003).

## B. Water distribution in pores

In water, there is a tendency to have a shape with the most economical form, such as a sphere, due to the surface molecules that are attracted to the inside from the hydrogen bonds with the rest of the water molecules, forming the drop.

When touching a surface, the shape of the drop is formed by the force attracting the water molecules to the solid. This force can be estimated, by measuring the contact angle (Appendix_Figure 9). For liquids other than water, the contact angle is always small, mainly because of the low surface tension, instead of strong attraction between solid and liquid (Torraca, 1982).

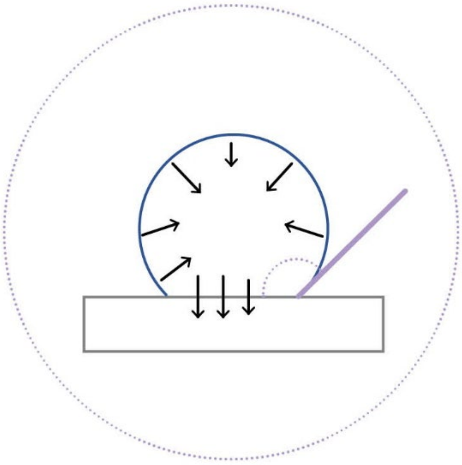

Appendix_Figure 9. Diagram illustrating the measurement of the contact angle of the liquid to the surface, when there is a low attraction between the solid and the liquid and the surface tension of the droplet is stronger
Image Source: Own.

In the case, that the water is inserted into the porous network of the solid, the attraction of the liquid towards the pore walls is expressed by the meniscus shape formed (Appendix_Figure 10). In this case, the molecular attraction of the water, drives the centre of it inwards.

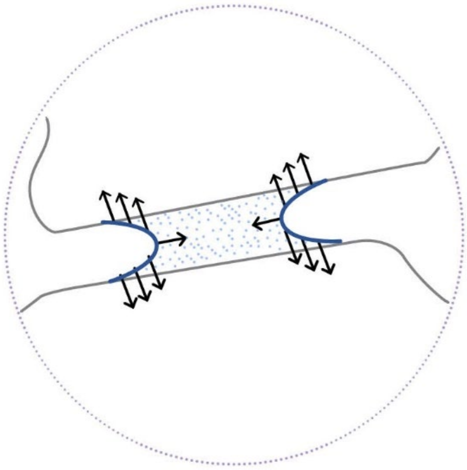

Appendix_Figure 10. Diagram illustrating the typical meniscus shape of water inside a pore and its centre drawn inwards.
Image Source: Own.

For the water to travel into the porous media, the capillary suction matters. Specifically, capillary pores or capillaries are named the very small pores – from latin, meaning hairlike. Once the attraction to the pore walls is stronger than the water -to-water attraction, then water will be sunk into them. The suction force is dependent on the nature of the pore surface and the pore size. In general, smaller pores create stronger forces, proven by capillary rise (Appendix_Figure 11).

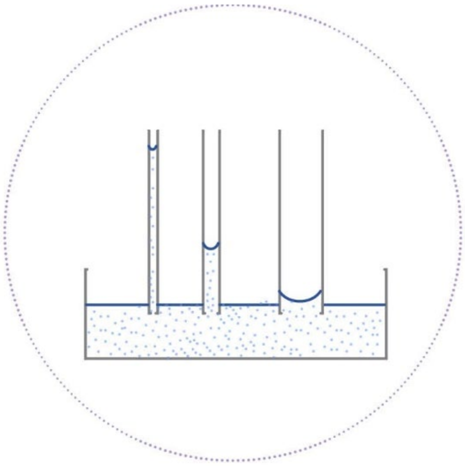

Appendix_Figure 11. Diagram showing how smaller diameter pores are able to transfer the liquid further, by rising.
Image Source: Own.

It is stated that, in the case that the water content is not equal to saturate the material, then it moves inside the material so that the lowest possible energy state is achieved. An example of this is illustrated in Appendix_Figure 12, for clarity. It is important to stress out, that the behaviour of the water in non-hydrophilic surfaces, which are named hydrophobic, is completely different. Because of their neutral charge, attributed to the existence of carbon and hydrogen atoms, such surfaces do not attract water. Therefore, water molecules are attracted between each other, leading to large contact angles and water film is not formed on the surface (Appendix_Figure 13).

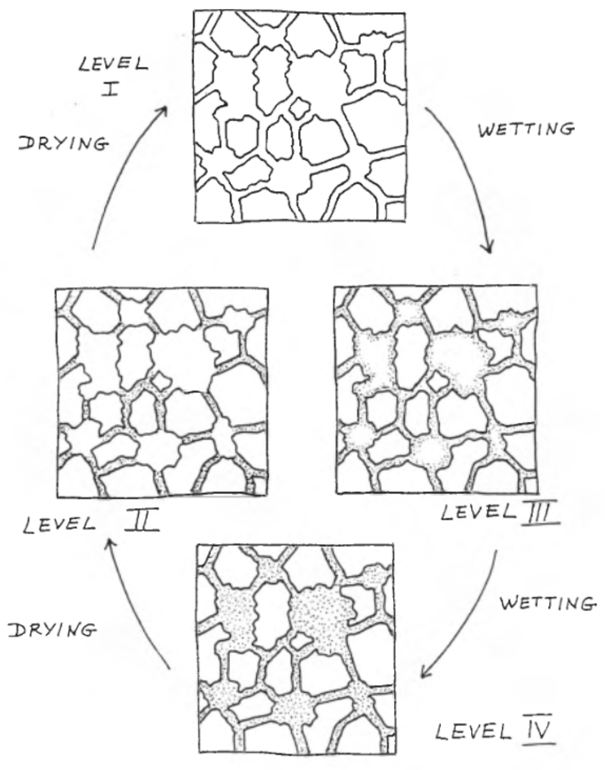


Appendix_Figure 12. Diagram illustrating how the water moves inside a porous hydrophilic body.
Image Source: page 10, Torraca, 1982.

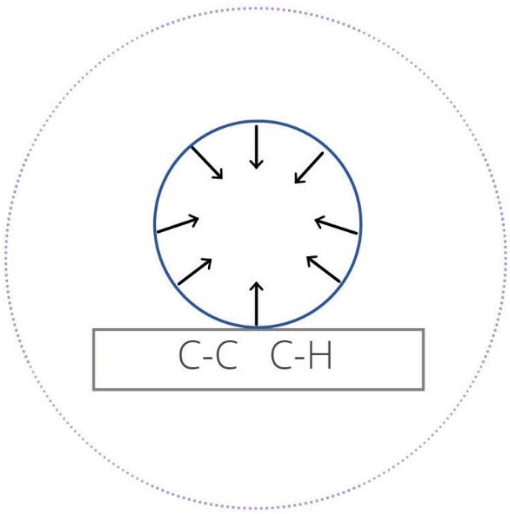


Appendix_Figure 13. Diagram showing the water drop maintaining its spherical shape, without being absorbed by the hydrophobic solid.
Image Source: Own.

A result of this, is the opposite of the capillary suction since there is no attraction of the water molecules to the pore surfaces. In addition, an inverted meniscus is formed, almost indicating that the water is being pushed out from the pore (Appendix_Figure 14).

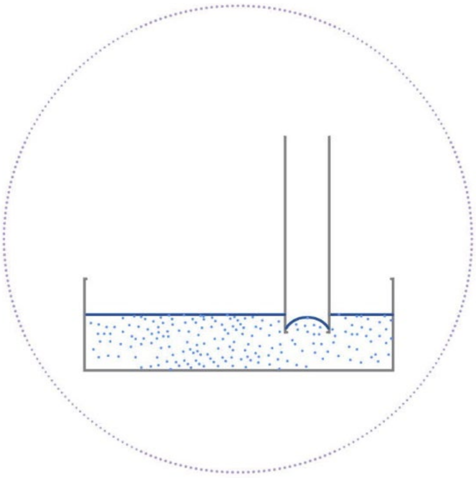

Appendix_Figure 14. Diagram showing how water does not exhibit capillary rise on hydrophobic surfaces, an inverted meniscus is formed and there is no suction observed.
Image Source: Own.

## C. Wind-driven rain impingement pattern

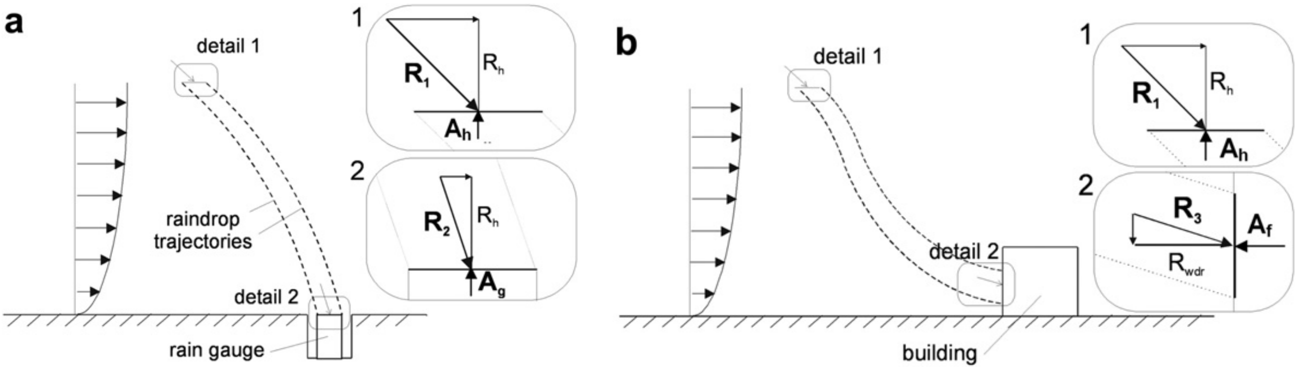


Appendix_Figure 15. Wind direction and speed altering the rainfall in different conditions. (a) when there is homogeneous wind, the raindrop trajectories are parallel, (b) while when falling on a building they are not because in different heights the wind speed alters. Image Source: Blocken B. et al. (2013).

When studying the rainwater runoff on vertical facades in order to elucidate the potential of each surface for the application of bioreceptive materials, certain weather data are needed, since until now a tool or a ready-to-use plugin for this analysis does not exist. Firstly, the wind direction influence the trajectory of the incoming rain (Appendix_Figure 15), while the wind speed together with either the building geometry or the urban surroundings define the wind-blocking effect. In further detail, obstacles found along the wind route disturb and alter its flow pattern. For instance, in the case of a stand-alone building the upstream wind-speed would slow down because of the building itself, whereas in a dense urban setting, a computational fluid dynamics (CFD) analysis would be required to provide the needed information. The aforementioned wind-blocking effect is the reason, that a vertical façade might not be fully wet equally at all parts, or it does not receive more rain in the upper parts because of the higher wind speed, contrary to what many believe. This phenomenon varies greatly, depending on the dimensions of the surface and the nearby buildings. To illustrate this, four different cases are examined by Blocken B. et al. (2013) to showcase the impact of different façade-sizes and their wind-driven rain impingement pattern, derived from the wind analysis and the precipitation levels, in Appendix_Figure 16 - 18.

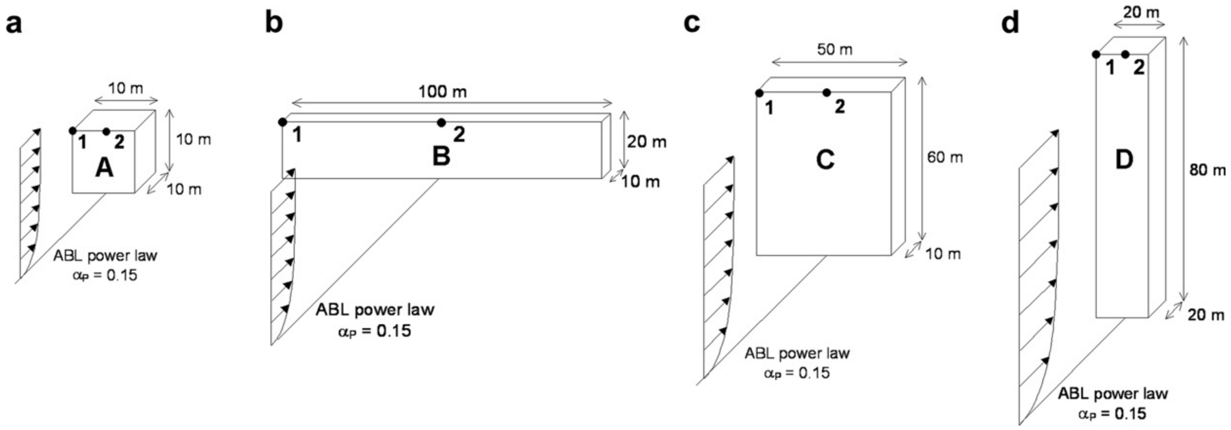


Appendix_Figure 16. Different volumetric case studies to analyse the wind-blocking effect. (a) low-rise cubic building, (b) wide medium-rise building slab, (c) high-rise building slab, (d) tower building. Image Source: Blocken B. et al. (2013).

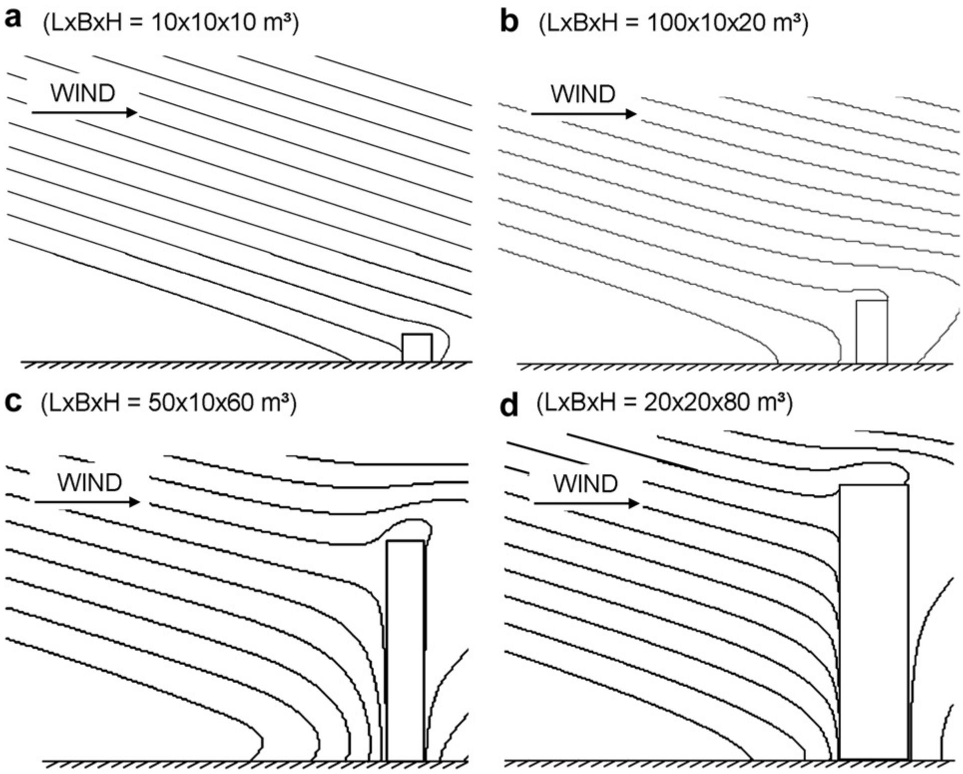


Appendix_Figure 17. Wind flow pattern in the four different case studies, formed by rain trajectories of 1mm diameter raindrops, with a wind speed of 10m/s. Image Source: Blocken B. et al. (2013).

What's more, to the impingement patterns also building geometries, façade detailing with cornices and ornated sills, or parapets etc. play an important role both to the way of that the water film forms and the runoff patterns (Blocken B. et al., 2013).

Apart from the impinging of Wind-driven rain intensity and towards the façade material, the impact of the wall when a raindrop falls governs the behavior of it after touching the surface. The complex behavior includes many phenomena, illustrated in Appendix_Figure 19, that all-together define the way a surface wets and dries. In this part, the bioreceptive cladding layer with its material properties come to play an important role. Therefore, the following equation reveals the aforementioned impact, affected also by the raindrop diameter, velocity and impact angle (Blocken B. et al., 2013).

$$V_{drop} = V_{splash} + V_{evap} + V_{abs} + V_{adh} + V_{runoff}$$

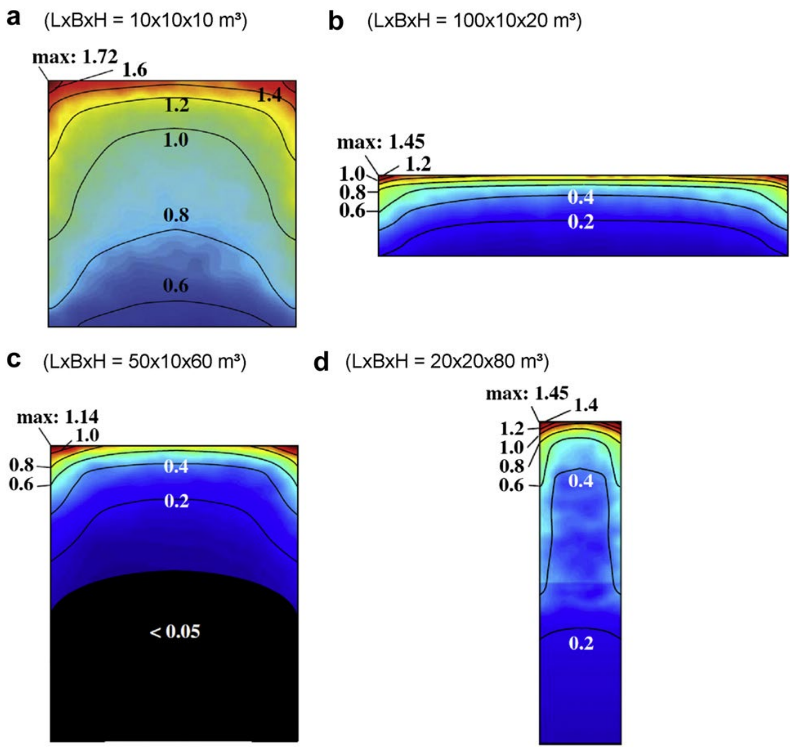


Appendix_Figure 19. Catch ratio patterns along the analysed façade of the different building configurations, taking into account similar conditions as in Appendix_Figure 16. Image Source: Blocken B. et al. (2013)

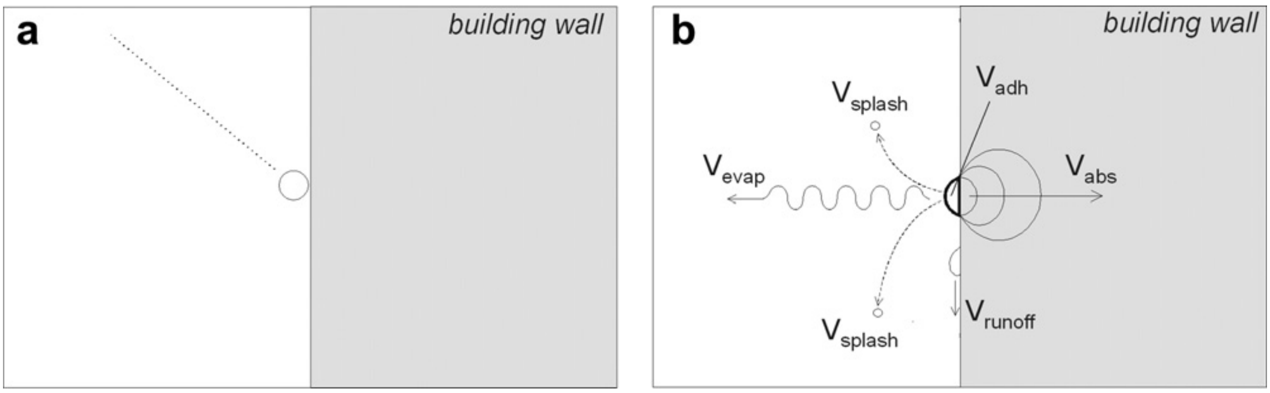


Appendix_Figure 18. Diagram illustrating the separate phases of the wind-driven rain analysis. (a) defining the wind-driven rain intensity and pattern, (b) wall response at the raindrop. Image Source: